

**LIFE HISTORY AND CARBON ECONOMIC TRADE-OFFS ADAPTING AN ANNUAL
PLANT ACROSS A CLIMATE GRADIENT**

by

Marnin David Wolfe

B. S. in Biology, Eckerd College, 2006

Submitted to the Graduate Faculty of
the Kenneth P. Dietrich School of Arts and Sciences, Department of Biological Sciences,
in partial fulfillment of the requirements for the degree of
Doctor of Philosophy in Ecology and Evolution

University of Pittsburgh

2013

UNIVERSITY OF PITTSBURGH
KENNETH P. DIETRICH SCHOOL OF ARTS AND SCIENCES

This dissertation was presented

by

Marnin David Wolfe

It was defended on

August 30, 2013

and approved by

Tia-Lynn Ashman, PhD, Professor, Biological Sciences

Susan Kalisz, PhD, Professor, Biological Sciences

John Stinchcombe, PhD, Associate Professor, University of Toronto

Brian Traw, PhD, Assistant Professor, Biological Sciences

Dissertation Advisor: Stephen Tonsor, PhD, Associate Professor, Biological Sciences

Copyright © by Marnin David Wolfe

2013

**LIFE HISTORY AND CARBON ECONOMIC TRADE-OFFS ADAPTING AN
ANNUAL PLANT ACROSS A CLIMATE GRADIENT**

Marnin D. Wolfe, PhD

University of Pittsburgh, 2013

Understanding the mechanisms behind adaptation to different climates is key to understanding the prevalent phenomenon of local adaptation in plants. Variation among sites in seasonal patterns of temperature and precipitation is thought to select functional strategies that work locally but not range-wide. These strategies tend to involve the concerted evolution of suites of traits including life history, acquisition and allocation resources. I studied adaptive differentiation due to climate in *Arabidopsis thaliana*. I examine natural genetic variation in this genome-sequenced species, because it provides insight into the functional ecology of annual plants generally, while providing context for future research on adaptation genetics. I investigated plants collected along an altitudinal gradient where hot, dry low contrasts cold, wet high elevation climates. Heating and drying in a growth chamber during reproduction favored plants from low elevations where conditions are most similar to the experiment. I found that stress avoidance traits like earlier flowering and faster fruit ripening were advantageous in this setting. Subsequently, I focused on how variation in the lifespan-dependent balance between carbon income and investment adapt plants across the climate gradient. Leaves generally fall along a continuum between short lives with rapid photosynthesis and long lives with slow photosynthesis, a pattern known as the worldwide leaf economic spectrum. Under seasonal hot, dry growth chamber conditions simulating low elevation climate, I demonstrated for the first time natural variation in an economic spectrum at the rosette level. Low elevation plants had short-lived economies compared to plants from colder, wetter locations. I then considered the

whole plant including photosynthetic inflorescences, which were previously ignored. I discovered that earlier flowering led to a majority of the whole plant economy depending on the contribution of the inflorescence. Plants as a whole exhibited the same trade-offs observed at lower levels of organization, with inflorescence-centric life adapting plants for avoidance of spring stress. My work supports the general hypothesis that avoidance of stress at low elevation, which requires a fast life, is traded off with a strategy of delay and tolerance associated with winter in high altitude populations, leading to local adaptation.

TABLE OF CONTENTS

PREFACE	XZI
1.0 INTRODUCTION	1
2.0 ADAPTATION TO SPRING HEAT AND DROUGHT IN N.E. SPANISH ARABIDOPSIS THALIANA	8
2.1 SUMMARY	8
2.2 INTRODUCTION	9
2.3 MATERIALS & METHODS	13
2.3.1 Collections	13
2.3.2 Planting	14
2.3.3 Growth conditions	15
2.3.4 Trait measures	16
2.3.5 Climate data	18
2.3.6 Statistical analysis	19
2.4 RESULTS	22
2.4.1 Principal component analysis of the climate gradient	22
2.4.2 Principal component analysis of trait space	23
2.4.3 Evidence for local adaptation, trait-elevation and trait-climate associations	23

2.4.4	Selection under heat and drought during reproductive phase.....	24
2.5	DISCUSSION.....	25
3.0	ADAPTIVE DIVERGENCE OF <i>ARABIDOPSIS THALIANA</i> ROSETTE ECONOMIC SPECTRUM ACROSS A TEMPERATURE AND PRECIPITATION GRADIENT.....	49
3.1	SUMMARY.....	49
3.2	INTRODUCTION	50
3.3	MATERIALS & METHODS	53
3.3.1	Collection	53
3.3.2	Planting.....	54
3.3.3	Seasonal climate conditions	54
3.3.4	Sampling design	55
3.3.5	Statistical analysis.....	56
3.4	RESULTS	59
3.5	DISCUSSION.....	62
4.0	ADAPTIVE SHIFTS IN WHOLE PLANT ECONOMY FROM ROSETTE TO INFLORESCENCE ACROSS A CLIMATE GRADIENT IN <i>ARABIDOPSIS</i> <i>THALIANA</i>	89
4.1	SUMMARY.....	89
4.2	INTRODUCTION	90
4.3	MATERIALS & METHODS	95
4.3.1	Collection	95
4.3.2	Planting.....	95

4.3.3	Dynamic Growth Chamber Cycle.....	96
4.3.4	Sampling Design	98
4.3.5	Trait measurements at each sampling point	98
4.3.6	Other traits measured	100
4.3.7	Estimating Return on Investment (Relative Lifetime Carbon Gain)	100
4.3.8	Estimating Functional Lifespan	101
4.3.9	Rosette Economic Spectrum Traits from Chapter 3	102
4.3.10	Statistical Analysis.....	103
4.3.10.1	Test for rosette, inflorescence and whole plant economic spectra.....	103
4.3.10.2	Relationships among rosette, inflorescence and whole plant economic spectra	105
4.3.10.3	The association between plant economics and bolting time.....	105
4.3.10.4	Test for climate associated adaptive variation.	105
4.3.10.5	Assessing the fitness effects of plant economic variation.....	106
4.4	RESULTS	107
4.4.1	Functional lifespan model results.....	107
4.4.2	Whole plant economic spectra.....	108
4.4.3	Relationships among rosette, inflorescence and whole plant economic spectra.	109
4.4.4	The association between plant economics and bolting time	109
4.4.5	Test for climate associated adaptive variation.....	110
4.4.6	Assessing the fitness effects of plant economic variation	110

4.5	DISCUSSION	111
5.0	CONCLUSION	134
	APPENDIX A	138
	APPENDIX B	144
	APPENDIX C	154
	APPENDIX D	159
	BIBLIOGRAPHY	183

LIST OF TABLES

Table 2.1: Univariate results for <i>Arabidopsis thaliana</i> population-mean trait values regressed on climate PC1 scores.....	32
Table 2.2: Full AIC-selected best models of phenotypic selection on N. E. Spanish <i>Arabidopsis thaliana</i>	33
Table 2.3: Locations, elevations and climates of the 16 sites in northeastern Spain from which the studied <i>Arabidopsis thaliana</i> genotypes originated. Longitude and latitude are reported in decimal degrees. Elevation is reported in meters above sea level (m.a.s.l.). Nineteen variables from the BIOCLIM dataset (http://www.worldclim.org) are reported; temperature in degrees celsius and precipitation in millimeters. Isothermality is $(\text{BIO2} / \text{BIO7}) * 100$ (Hijmans et al. 2005).	34
Table 2.4: Eigenvector coefficients of first principal component resulting from a PCA of the value 19 bioclimatic variables at 16 study populations of <i>Arabidopsis thaliana</i> in NE Spain.....	35
Table 2.5: Principal Component Scores of each population of <i>Arabidopsis thaliana</i> for the first principal component of trait space plus the first and second principal components of climate space.....	36
Table 2.6: Eigenvector coefficients of first principal component resulting from a PCA of the population means for each trait of <i>Arabidopsis thaliana</i>	37

Table 2.7: Population-mean trait values for N.E. Spanish *Arabidopsis thaliana*. 38

Table 2.8: Pearson product moment correlation matrix for N.E. Spanish *Arabidopsis thaliana*.
Bold-faced = $p < \text{Sequential Bonferonni corrected critical value}$. ** $p < 0.0001$, * $0.0001 < p < 0.05$ 39

Table 3.1: Tests of life-history cohort, climate-of-origin and interaction effects on rosette economic and related traits. Analyses of covariance results are presented for rosette economy PC1 scores, each rosette economic trait, the summed fruit length and age at bolting. F-tests and corresponding P-values are reported for each of the following model factors: Life History Cohort (fixed effect), Climate PC1 (covariate) and the interaction. Model p-value and r-square are also reported. Each row represents an independent analysis on the trait indicated. Analyses were performed on within-cohort population mean trait values so in all cases $n=32$ 67

Table 3.2: Relationship between summed fruit length and rosette economy. Here we test for the effect of life history cohort (fixed effect) and within cohort genotype score on rosette economy PC1 (covariate) on summed fruit length (fitness). Both the summed fruit length and rosette economy PC1 score were standardized to mean = 0 and variance = 1 prior to analysis. Selection coefficients (β) and standard errors on the parameter estimates (SE) are presented along with p-values for the t-test ($h_0: \beta = 0$). Additionally, the F-tests and corresponding p-values for each model factor are reported as well as the overall model statistics. $N=64$ 68

Table 3.3: Results from two parameter exponential nonlinear regression models fit to each genotype in both germination cohort are provided here for rosette per-mass photosynthetic rate versus time. In addition to the parameter estimates, standard errors, 95% confidence intervals, and significance tests are provided for each parameter. Pseudo r-squares are provided as a measure of each models fit. 69

Table 3.4: Results from regression models fit to each genotype in both germination cohort are provided here for rosette mass per area versus time. In addition to the parameter estimates, standard errors, 95% confidence intervals, and significance tests are provided for each parameter. Pseudo r-squares are provided as a measure of each model's fit. Three parameter logistic functions are fit in (A) and two parameter exponential functions are reported in (B)..... 71

Table 3.5: Results from two parameter logistic nonlinear regression models fit to each genotype in both germination cohort are provided here for the proportion of living rosette leaves versus time. In addition to the parameter estimates, standard errors, 95% confidence intervals, and significance tests are provided for each parameter. Pseudo r-squares are provided as a measure of each model's fit. 74

Table 3.6: Basic descriptive statistics within and across cohorts for rosette per-mass photosynthetic rate and rosette mass per area at bolting, rosette lifespan, age at bolting and summed fruit length. 76

Table 3.7: Genotype mean trait values within each cohort for rosette per-mass photosynthetic rate and rosette mass per area at bolting, rosette lifespan, age at bolting, summed fruit length and score on rosette economy PC1..... 77

Table 3.8: Population mean trait values within each cohort for rosette per-mass photosynthetic rate and rosette mass per area at bolting, rosette lifespan, age at bolting, summed fruit length and score on rosette economy PC1..... 79

Table 3.9: Genotype mean correlation matrix for rosette per-mass photosynthetic rate and rosette mass per area at bolting, rosette lifespan, age at bolting and summed fruit length. In each cell, the top row represents the Pearson product-moment correlation coefficient, the middle row includes

the p-value for the two-tailed test of the hypothesis that the correlation is zero and the bottom contains the sample size..... 80

Table 3.10: Rosette economy PCA results. Each column contains information for one of the three principal components. Each row of the first subsection contains the loading for an individual variable onto each of the three PCs. The second subsection contains eigenvalues, 99% significance thresholds and variance explained for each PC..... 81

Table 3.11: Daily high and low temperatures, day length, water table height and total daily water supply (in grams) per pot for each week of the experiment. Standard errors are given for temperature data as they represent averages from multiple sites and years based on data logger data. The actual growth chamber program did not incorporate the temperature variance reported below..... 82

Table 3.12: The week, plant age and growth chamber conditions for each sampling time point is shown for both fall and spring germinated cohorts. Additionally, the pot types sampled at each time point are listed (see Appendix A.3 in Supporting Information for details). 83

Table 4.1: Carbon economy variable list by plant module. Details on the measurement or calculation of traits are provided. Carbon economy traits are grouped based on the plant module they represent rosette, inflorescence and the whole plant. Within each plant module traits are further grouped based on the aspect of plant carbon economy they describe; either resource investment (cost) or return on investment (income). Return on Investment is subdivided into traits measuring the lifetime return, the duration of return (lifespan) and the rate of return. 118

Table 4.2: Results from 3-parameter Gaussian function regression of whole plant net photosynthesis on plant age for each genotype. In addition to the parameter estimates, standard

errors, 95% confidence intervals, and significance tests are provided for each parameter. Pseudo r-squares are provided as a measure of each models fit..... 120

Table 4.3: Results from 3-parameter Gaussian function regression of rosette net photosynthesis on plant age for each genotype. In addition to the parameter estimates, standard errors, 95% confidence intervals, and significance tests are provided for each parameter. Pseudo r-squares are provided as a measure of each models fit. 121

Table 4.4: Results from 3-parameter Gaussian function regression of inflorescence net photosynthesis on plant age for each genotype. In addition to the parameter estimates, standard errors, 95% confidence intervals, and significance tests are provided for each parameter. Pseudo r-squares are provided as a measure of each models fit..... 122

Table 4.5: Eigenvalues, proportion variance explained and significance threshold for rosette, inflorescence and whole plant carbon economy PCAs. * denotes PC's with eigenvalues > threshold..... 123

Table 4.6: Loadings onto PC1 from three separate PCAs of rosette, inflorescence and whole plant economic traits. 124

Table 4.7: Results from univariate regressions of plant carbon economy traits onto home climate PC1 scores. Each regression was conducted independently on the population means for the traits listed on each row. Dependent variables were standardized (mean = 0, standard deviation = 1). Regressions are sorted by the economy measured (i.e. rosette, inflorescence, whole plant). For each regression, the parameter estimates \pm the standard error are provided followed by the t-test, p-value and r² describing the model fit. Descriptive statistics (mean, standard deviation, minimum and maximum values) for each dependent variable are also provided. Significant models are in bold. 125

Table 4.8: Analysis of fitness effects. Standardized (mean = 0, std. dev. = 1) summed fruit length was regressed on genotype mean scores for rosette and inflorescence economy PC1. Parameter estimates $\beta \pm$ one standard error is provided with significance tests. Overall model F-value, p-value and r2 are also presented. N=32..... 126

Table B1: Results for 28 response variable of a general linear model testing the fixed effect of fertilizer treatment, the covariate effect of elevation-of=origin and the interaction of the two. Factor F- and P-values are provided as well as the model r-square and p-value.....152

Table C1: Loadings for each of 19 bioclimatic variables and elevation onto the first principal component from two separate analyses. In the first analysis, 10,000 locations across Eurasia were randomly sampled for the variables listed. In the second analyses as is explained in Chapter 2, the values for each variable at 16 *A. thaliana* collection sites are analyzed. The percentage of multivariate variance accounted for by the first PC is also listed.....156

Table C2: Scores along the first PC of climate space from two separate analyses are present here. Scores along PC1 for the Eurasian and N.E. Spanish climate were calculated based on the loadings as described in the text.....157

LIST OF FIGURES

Figure 2.1: Map of the sixteen <i>Arabidopsis thaliana</i> collection sites used in this study. Colors indicate elevation going from low to high as follows: Green to brown to white.....	40
Figure 2.2: Eigenvector plot of the loadings of 20 climate variables onto the first and second principal component of climate space that describe conditions in 16 N. E. Spanish <i>Arabidopsis thaliana</i> populations. Each arrow represents a vector of loadings. Direction of each arrow represents the relationship of a variable to climate PC1 and PC2 and the length of the vector represents the strength of that relationship. Clusters of similar variables e.g. Precipitation are bracketed and labeled to help summarize results.....	41
Figure 2.3: Eigenvector plot of the loadings of 12 traits onto the first and second principal component of trait space for N. E. Spanish <i>Arabidopsis thaliana</i> . Each arrow represents a vector of loadings. Direction of each arrow represents the relationship of a variable to trait PC1 and PC2 and the length of the vector represents the strength of that relationship.....	42
Figure 2.4: Scatter plot and least squares regression of <i>Arabidopsis thaliana</i> population scores on the first PC of trait space (vertical axis) on population scores on PC1 of climate space (horizontal axis). P-value for the slope parameter estimate and r-square of the regression line are also presented.	43

Figure 2.5: Scatter plot and least squares regression of *Arabidopsis thaliana* population-means for each trait (vertical axis) on the elevation of origin (horizontal axis). The line is only shown if $P < 0.10$. Equations for each fitted line, p-values for the slope parameter estimates and r^2 statistics are also provided..... 44

Figure 2.6: Experimental conditions *Arabidopsis thaliana* genotypes were exposed to. Daily minimum and maximum temperatures in degrees Celsius (a). number of hours of light per day (b). Water availability expressed as grams supplied per day (c). 45

Figure 2.7: Field conditions for low elevation populations of N.E. Spanish *Arabidopsis thaliana*. Daily minimum and maximum temperatures in degrees Celsius (A). Daily temperature range in degrees Celsius (B). Plant height temperature data from field loggers placed at three low elevation sites (BAR, COC and RAB) over multiple years. BAR data are from 2009-2011, COC and RAB data are from 2010-2012. Data are averaged across sites and years within days. 46

Figure 2.8: Eigenvalues from PCA of *Arabidopsis thaliana* population values for 19 bioclimatic variables (black line). The gray dashed line represents the lower 99% confidence interval on the null hypothesis for eigenvalues based on 5000 randomizations. 47

Figure 2.9: Eigenvalues from PCA of *Arabidopsis thaliana* population means for 12 measured traits (black line). The gray dashed line represents the lower 99% confidence interval on the null hypothesis for eigenvalues based on 5000 randomizations. 48

Figure 3.1: Rosette economy PCA results. Eigenvalues for a PCA of three rosette economic traits (AM, RMA and RL) are plotted against the upper 99% limit of the distribution of eigenvalues under the null hypothesis of random correlation structure (A). Eigenvector coefficients (loadings) of the 3 rosette economic variables onto the first PC of trait space (B). The sign of each loading

indicates whether trait values increase or decrease with increasing scores on rosette economy PC1 and also indicates the relationship between each trait pair. 84

Figure 3.2: Trait vs. Climate Plots. Scatter plot and least squares regressions of population-means for each trait (vertical axis) on the climate PC1 score for that population (horizontal axis). Filled circles and solid regression lines represent the results for the Fall germinated cohort while open circles and dashed regression lines are for the Spring germinated cohort. R-squares are presented for each individual regression line within each plot. Climate PC1 is the result of a PCA of population values of 19 BIOCLIM variables and Elevation originally published in Wolfe & Tonsor *in press*. High values of climate PC1 represent high elevation sites that are cold and wet overall while low values are low elevation sites with hot, dry climatic conditions..... 85

Figure 3.3: Rosette economy predicts fitness (summed fruit length). Scatter plot and least squares regressions of genotype-means within the spring (open circles, dashed regression lines) and fall (closed circles, solid regression lines) germinated cohorts. The vertical axis represents a fitness component related to total seed number (summed fruit length) while the horizontal axis represents each genotype's score on rosette economy PC1. High values of the predictor variable represent "slow-type" economics; long rosette lifespan, high rosette mass per area and low rosette photosynthetic rate at bolting. Low values of rosette economy PC1 represent "fast-type" rosette economies. R-squares are presented for each individual regression line within each plot. 86

Figure 3.4: Genotype mean scatterplot matrix for rosette per-mass photosynthetic rate and rosette mass per area at bolting, rosette lifespan, age at bolting and summed fruit length. 87

Figure 3.5: The dynamic growth chamber cycle simulating a low elevation N.E. Spanish seasonal climate is shown here. Daily high and low temperatures in centigrade (A), day lengths in hours

(B) and daily water supply in grams per pot (C) are plotted by week. Standard errors bars for the temperature cycle represent variance in field temperature data (averaged across sites and years) and do not represent thermal variance in growth chamber conditions. 88

Figure 4.1: Conceptual model of rosette and inflorescence carbon economy. Illustrated here is our conceptual framework for understanding whole plant carbon economy. Plant carbon economy is determined by the balance between resource investment (cost) and return on investment (income), which is a function of rate and duration of income. Total rosette photosynthesis rises until a peak near the time of bolting. Upon bolting, a period of photosynthetic carbon gain by the inflorescence begins and the plants life ends when the inflorescence has fully senesced. In this scheme, the whole plant’s lifespan is allocated between rosette and inflorescence with a period of functional overlap, which hinges on the age at bolting. The inset lists carbon economic indicators quantified in this study according to the aspect of economy they measure (i.e. resource investment). 127

Figure 4.2: Examples of lifetime photosynthetic carbon gain data and models. Here we compare line plots of lifetime carbon gain for an early bolting, low elevation genotype RAB4 (A) to the high elevation, late bolting genotype PAN5 (B). We also compare Gaussian functions fit to each genotypes carbon gain curve for the rosette and the inflorescence separately (C, D). We place a narrow vertical bar through the age at bolting in each plot. 128

Figure 4.3: Rosette, inflorescence and whole plant carbon economy PCA results. Correlatings between PC scores and the original variables (loadings) are presented in this horizontal bar plot. Panels A-C show loadings for rosette, inflorescence and whole plant economy PC1 respectively. The sign of each loading indicates whether trait values increase or decrease with increasing scores on the corresponding PC and also indicates the relationship among the traits in each

analysis. Panel D shows scree plots for the analyses summarized in panels A-C. In each scree plot, eigenvalues are plotted against the upper 99% limit of the distribution of eigenvalues under the null hypothesis of random correlation structure. Eigenvalues that are greater than the threshold represent meaningful axes for summarizing carbon economy..... 129

Figure 4.4: Scatterplot matrix for whole plant, rosette and inflorescence economy PC1 scores. 95% confidence ellipses are shown and pearson product-moment correlation coefficients and corresponding p-values are inset in each panel. N = 32. 130

Figure 4.5: Regression of rosette, inflorescence and whole plant economy PC1 scores on age at bolting (days since sowing). The equation for the best fit line along with corresponding p-value and r^2 are inset in each panel. N = 32. 131

Figure 4.6: Associations between carbon economic spectra (A-C) plus age at bolting (D) and summed fruit length (E) and home climate PC1 scores. r^2 and p-value are provided at right.... 132

Figure 4.7: Regression of summed fruit length on whole plant (A), inflorescence (B) and rosette economy PC1 (C) plus age at bolting (D). r^2 and p-value are presented, n = 32..... 133

Figure B1: Least squares means for the fertilizer effect estimated from a GLM with the model Trait = FERT + ELEVATION + FERT x ELEVATION + RACK. One standard error is shown above and below each LS mean..... 153

Figure C1: Map of Eurasian climate PC1 generated in ArcGIS 9.0 based on the loadings from a PCA conducted on a random sample of 10,000 locations across the region indicated. Warmer colors denote hotter, drier climates corresponding to the positive end of Eurasian climate PC1 while cooler colors indicate colder, wetter high latitude / altitude locations on the negative size of climate PC1.....158

PREFACE

Science requires collaboration and so do doctorates. I am entirely unable to do justice and pay homage to all the myriad teachers and other important influences that have helped me get to this point. Thank you all.

I would like to express my appreciation for the members of my committee: Drs. Brian Traw, Susan Kalisz, Tia-Lynn Ashman and John Stinchcombe (University of Toronto). Dr. Jeff Brodsky also deserves mention for his efforts as an early member of my committee and for generosity with his laboratory facilities and expertise. All of the members of my committee have been extraordinarily open and generous with their time providing constructive criticism and support every step of the way.

Most importantly, I wish to thank my advisor, colleague and friend Dr. Stephen Tonsor. I cannot adequately describe all of the ways in which Steve has inspired and mentored me. Steve is one of the best teachers, brightest minds and most curious souls that I have ever known. Steve makes science fun, makes time to help anyone willing to learn and maintains a passion and energy for science that I find remarkable. Furthermore, without his ingenuity, persistence and penchant for DIY science, much of the actual research I conducted would have been impossible. Thank you Steve!

I also could not have succeeded without a wonderful and diverse group of individuals that have variously made up the Tonsor lab throughout the years. My experiments could not have been possible without the help of several dedicated, hard-working lab managers including Jessica Dunn, Adam Sinder and Kali Theis. Thanks to Ellen York for sharing her knowledge and skill

with greenhouse and growth chamber operations. I have collaborated with a number of amazing undergraduate researchers including: Matt Simon, Tim Helbig, Jesse Raszewski and Brian Belsterling, Lisa Rain, Dusica Solic and Victoria Muntean as well as the talented post-baccalaureates Jackie Cameron and Keith Garmire.

Previous graduate students in the Tonsor lab including the now Drs. John Paul, Alicia Montesinos-Navarro and Tarek Elnaccash have been inspiring examples to me. Watching John Paul go through the process of publishing and defending his dissertation gave me a view of the light at the end of the tunnel. Alicia was always generous with her time and helped me plan some of my first experiments in the lab. Tarek deserves thanks most particularly here as he has been there for me throughout my time in the department as a friend and colleague. Tarek's limitless curiosity and meticulous mind has vastly improved the scope and quality of my research and science education. The brilliant Natalie Settles, master of fine art and artist in residence in the Tonsor lab also deserved huge credit. Natalie has generously given of her time and experience and has helped massively improve the quality of my science writing and speaking, I consider her a friend, colleague and also a mentor. I would also like to acknowledge Drs. Alison Hale and Maya Groner who attended lab discussion meetings and always offered valuable, constructive criticism. To the future generation of graduate students in the Tonsor lab, Nana Zhang and Paul Crawford, good luck, enjoy every minute!

The graduate students, faculty and post-doctoral researchers in the Ecology and Evolution program at U. Pittsburgh are a key part of making every graduate student successful and for that I thank them. The atmosphere of open communication, sharing of knowledge, resources, blood, sweat, tears, as well as beer and snacks that pervade the community of biologists in the Biological Sciences department is one of a kind.

I also wish to thank and express my love to my mother Pam, my father Ken and my younger brother Ari all of whom continue to encourage and support me. I am the man I am today thanks to them. I also owe thanks for setting inspiring examples of a life in the sciences and for providing priceless guidance through my long and continuing science education to my uncle Alan Wolfe and my grandfather William Wolfe. Furthermore, my grandfather Irving Moss will forever hold a place in my heart for igniting my curiosity and imagination throughout my childhood.

To Elizabeth Wolfe, my best friend and the love of my life. You always told me not to give up. I didn't. Thank you. Your support, your patience, your point of view, your passions and your humor, strengthens and lifts me up. I am honored, overjoyed and ever grateful to have you in my life.

Lastly, a special acknowledgement is deserved for my cat Dillinger, who has purred quietly in my lab as I wrote the vast majority of this dissertation.

Funding Sources

Funding was raised primarily by Dr. Stephen Tonsor from the National Science Foundation grants IOS 0809171 and IOS 1120383. Funding was also awarded to me via a Sigma Xi grant-in-aid-of-research.

1.0 INTRODUCTION

Life is difficult. No species is perfect. All populations and lineages are constrained in their adaptability (Antonovics 1976; Blows & Hoffmann 2005). Every genotype and individual has a finite set of conditions under which it can survive and reproduce (Hutchinson 1957, Chase & Liebold 2003). While these statements are obviously true if you consider whether a fish could fly or a bird breathe under water, as these are extreme cases of developmental and biophysical constraint (Smith et al. 1985), in most cases the mechanisms that enable and the factors that constrain adaptive evolution are unclear (Anderson et al. 2011; MacColl 2011).

In plants, local adaptation and among population adaptive differentiation within species is common, particularly along environmental gradients (Clausen et al. 1940; Antonovics 1976; Endler 1986; Linhart & Grant 1996; Hereford 2009; but see Leimu & Fischer 2008). The mechanisms that result in these phenomena are clearly important. Indeed, adaptation to variation in environment is a key process defining distribution edges (Mayr 1947; Kirkpatrick & Barton 1997; Sexton et al. 2009) as well as range and niche sizes (Paul et al. 2009). Adaptive divergence can be a crucial step resulting in speciation (Mayr 1947; Ackerly 2003). Furthermore, understanding the history of adaptive evolution in plants, particularly across climate gradients will be crucial for anticipating adaptive responses or lack thereof as the climate changes in the coming centuries (Visser 2008; Hoffmann & Sgrò 2011; Anderson et al. 2012).

In general, adaptive divergence is thought to occur when there are selective differences between environments that place conflicting demands on plant form and function leading to a trade off in fitness among environments (Endler 1986; Kawecki & Ebert 2004; Westoby & Wright 2006). When resources (including time) are limited (almost always) plants must allocate among functions such that some functions must be traded for others (Bloom et al. 1985; van Noordwijk & de Jong 1986; Stearns 1989). Adaptive divergence will therefore occur when allocation patterns are heritable and differently selected among sites (Stearns 1989). Researchers in the last half-century have identified patterns in the combinations of plant traits that are associated with particular environments or niches (Grime 1977). These patterns of trait correlation can be interpreted in terms of how they alter plant form and function and either increase or decrease fitness under a given selection regime (Murren 2002; Pigliucci 2003; Westoby & Wright 2006).

For example, plants tend to trade off current versus future survival and reproduction based on the relative allocation of meristems and biomass between reproductive and vegetative functions (Geber 1990; Bonser & Aarssen 1996; Bonser & Aarssen 2006). Plants inhabiting harsh environments such as exceptionally hot, cold or dry locations tend to allocate more to vegetative function typically associated with adaptive stress tolerance. In contrast, plants that instead allocate relatively more to reproductive function are usually associated with disturbed habitats or other environments that select for maximizing early reproduction (Grime 1977). Despite these general patterns, the genetic mechanisms by which adaptive divergence of integrated suites of traits emerge and optimize plants for different environments is poorly understood (Anderson et al. 2011).

A new frontier in understanding the mechanisms of adaptation has emerged in the last half century and is picking up steam at a tremendous rate. Thanks to affordable high throughput sequencing, expression profiling, exponential increases in computing power and numerous other advances in molecular biology, the mechanisms of inheritance are finally being revealed in detail (Feder & Mitchell-Olds 2003; Stearns & Magwene 2003; Tonsor et al. 2005; Straalen & Roelofs 2006; Ungerer et al. 2008; Mitchell-Olds et al. 2008). Quantitative geneticists can now sequence large numbers of loci across large populations of wild and domestic species and are beginning to identify the specific genetic polymorphisms underlying variation in key plant traits (Straalen & Roelofs 2006; Hudson 2007; Zhu et al. 2008; Atwell et al. 2010). Yet our understanding of how gene function influences phenotype comes mostly from human-induced lesions of the genome resulting in impaired or nulled gene function (Bolle et al. 2011).

In order to understand gene function in the context of adaptation, we must identify natural genetic variations in gene function that influence phenotype (Tonsor et al. 2005; Mitchell-Olds et al. 2008). Furthermore, we must study the functional ecology and adaptive evolution of model organisms (Anderson et al. 2011). In the dissertation that follows, I examine patterns of natural genetic variation and covariation in suites of key ecologically important traits related to life-history timing, physiology, morphological investment, and fitness in the plant genetic model organism, *Arabidopsis thaliana*. I conduct a series of growth chamber experiments, in which genotypes collected along a temperature and precipitation gradient in N.E. Spain are examined. In so doing, I provide insight into adaptive trade offs in plant form and function that result from adaptation across a climate gradient.

In chapter two, I conduct a preliminary study of adaptive divergence along a climate gradient using N.E. Spanish *A. thaliana*. Low elevation populations of *A. thaliana* experience

relatively rapid warming and drying during their reproductive season. In contrast, high elevation sites must survive long, freezing winters but experience cool, moist spring growing conditions. I tested whether subjecting 48 lineages from across the climate gradient to spring heat and drought in a growth chamber favored plants from sites with hot, dry spring conditions. I examined the relative adaptive values of variation in 11 traits related to either tolerance or avoidance of stress. Lineages collected at low elevation were most fit and fitness scaled with climate of origin. Higher fitness was associated with earlier bolting, greater early allocation to increased numbers of inflorescences, reduction in rosette leaf photosynthesis and earlier fruit ripening. I hypothesized that the adaptive strategy of low elevation plants is stress avoidance through early flowering, but accompanied by a restructuring of the organism that adapts *A. thaliana* to low elevation Mediterranean climates. This chapter has been accepted for publication in *New Phytologist* with Dr. Stephen Tonsor as coauthor.

Across the entire plant kingdom, there is a trade off to which almost all leaves appear to conform. The worldwide leaf economic spectrum describes a trade-off between “fast” and “slow” return leaf tissues and is observed among nearly all plant species examined to date (Wright et al. 2004; Wright et al. 2005a; but see Farnsworth & Ellison 2007; Wright & Sutton-Grier 2012). Plants appear to trade off between leaves with high metabolic and photosynthetic rates per unit mass and a short lifespan (fast return) and leaves with low physiological rates but long lifespans (slow return). Differences among species in leaf economy appear to be adaptive and are often associated with gradients in temperature and precipitation. “Slow return” leaves are generally found in colder, drier northern climates (Reich et al. 1999; Wright et al. 2004; Wright et al. 2005b; Reich et al. 2007; but see Pensa et al. 2009). In chapters three and four, I follow up on the results obtained in chapter two and specifically address the role of carbon economic

strategy and its integration in life history in adaptation across the N.E. Spanish climate gradient. In both chapters, I utilize data from a yearlong growth chamber study in which I simulated the hot, dry climate of low elevation populations based on field temperature logger data. I grew replicates of 32 genotypes (two from each of 16 populations) and measured traits of interest at multiple time points during the growing season. This allowed understanding of how plant carbon economy and life history events were integrated.

In chapter three, I tested for and found a rosette carbon economic spectrum among N.E. Spanish populations of *A. thaliana*. I hypothesized that since the rosette has a discrete lifespan (all leaves die in concert) linked to age at bolting (Vasseur et al. 2012) that factors that cause variation in lifespan would result in variation in overall rosette economy. I measured three economic traits (rosette lifespan, photosynthesis and mass per area) in a growth chamber experiment. I germinated plants under both fall and spring conditions simulating hot, dry seasons at one extreme of the climate gradient. I found a rosette economic spectrum, which is correlated with climate of origin such that plants from hot, dry sites show faster return economies. Additionally, I found that spring germination produced faster economies than fall, regardless of climate, indicating plasticity in rosette economy. Finally, I show that the faster return economic strategy of low elevation plants was favored in this experiment. This work advances our understanding of the role of plant economic constraints in adaptive evolution. This work will be submitted for peer review and publication in the journal *Ecology Letters*.

In chapter four, I expand on the idea of a rosette economic spectrum. Previous research in the Tonsor lab indicated that on average the green stems, leaves and fruits of the inflorescence contribute the majority of photosynthetic carbon gained by *A. thaliana*, but the proportion contributed varies widely across stock center ecotypes (Earley et al. 2009). I therefore measured

carbon economic traits related to the inflorescence (e.g. photosynthetic rate per gram, mass per unit length, lifespan) specifically as well as the whole plant (e.g. lifespan, photosynthetic rate, total mass) in addition to the rosette. I compare rosette, inflorescence and whole plant-level carbon economies to each other and to the single leaf worldwide spectrum. I hypothesized that the inflorescence might offer an alternative and bolting time independent (compared to the rosette) dimension of whole plant carbon economy. However, I found that rosette and inflorescence carbon economies were actually negatively correlated, indicating that whole plant carbon economics were integrated around major allocation “decision” determined by the age at bolting. The whole plant’s carbon economy varied along a spectrum that matched the worldwide leaf economic spectrum and was correlated with climate of origin in my study system. Low elevation plants from hot, dry conditions had higher fitness (see chapter three) associated with their inflorescence-centric economies. Interestingly, inflorescence centric carbon economy actually corresponded to lower total mass and shorter overall lifespan, yet resulted in higher fitness. This chapter is in preparation for submission to the journal *Functional Ecology*.

In chapter five, I provide a brief synthesis of this dissertation and discuss the implications of the work. I conclude by emphasizing future avenues for research.

Throughout my dissertation I use the pronoun “we” acknowledging the work as collaboration with my advisor Dr. Stephen Tonsor that will be published as such. Throughout the work Dr. Tonsor provided critical commentary, editing, and was critical in advising me on the theoretical, analytical and logistical aspects of each experiment. Furthermore, Dr. Tonsor provided funding (see preface) supporting lab work via the National Science Foundation. The primary goals, conceptual framework, analyses, SAS code, and writing are my own. Plant

growth and maintenance as well as phenotyping was a coordinated effort often times shared by all members of the Tonsor lab.

2.0 ADAPTATION TO SPRING HEAT AND DROUGHT IN N.E. SPANISH

ARABIDOPSIS THALIANA

2.1 SUMMARY

The extent to which a species' environmental range reflects adaptive differentiation remains an open question. Environmental gradients can lead to adaptive divergence when differences in stressors among sites along the gradient place conflicting demands on the balance of stress responses. The extent to which this is accomplished through stress tolerance vs. stress avoidance is also an open question. We present results from a controlled environment study of 48 lineages of *Arabidopsis thaliana* collected along a gradient in NE Spain across which temperatures increase and precipitation decreases with decreasing elevation. We tested the extent to which clinal adaptive divergence in heat and drought is explained through tolerance and avoidance traits by subjecting plants to a dynamic growth chamber cycle of increasing heat and drought stress analogous to low elevation spring in NE Spain. Lineages collected at low elevation were most fit and fitness scaled with elevation of origin. Higher fitness was associated with earlier bolting, greater early allocation to increased numbers of inflorescences, reduction in rosette leaf photosynthesis and earlier fruit ripening. We propose that this is a syndrome of avoidance through early flowering accompanied by restructuring of the organism that adapts *A. thaliana* to low elevation Mediterranean climates.

2.2 INTRODUCTION

More than half a century of research on adaptation in plants has shown that local adaptations are relatively common (Clausen et al. 1940; Linhart & Grant 1996; Leimu & Fischer 2008). Adaptive differentiation occurs when selection varies and requires conflicting optimization of plant form and function at different sites (Endler 1986, Kawecki & Ebert 2004). Especially given accelerating anthropogenic climate change (Parmesan 2006; Bradshaw & Holzapfel 2006), it is necessary to improve our understanding of the functional bases of local adaptations (Feder 2007; Mitchell-Olds et al. 2008; Anderson et al. 2011, 2012). One classic and powerful approach to understanding historical and future adaptation is the study of trait divergence along environmental gradients (Endler 1986) and this approach has been used successfully in studies of clinal variation in plant traits including leaf physiology and morphology (Martin et al. 2007), above and belowground carbon-nutrient balance (Freschet et al. 2010), phenology and architecture (Petrů et al. 2006). In this study we examine how a suite of life history, physiological and allocation traits provide an integrated adaptive response to increasing heat and drought during the reproductive season in an annual plant.

Range-wide studies of the model plant *Arabidopsis thaliana* (Brassicaceae) provide an excellent system for clinal studies of geographically varying adaptation and their genetic bases in annual plants (Mitchell-Olds 2001; Tonsor et al. 2005; Mitchell-Olds & Schmitt 2006; Wilczek et al. 2009; Fournier-Level et al. 2011; Ågren & Schemske 2012; Fournier-Level et al. 2013; Grillo et al. 2013). A broad suite of differentiated traits is emerging in studies of adaptation across *A. thaliana*'s latitudinal range. These include variable freezing tolerance (Hannah et al. 2006; Zhen & Ungerer 2008), vernalization requirements (Hopkins et al. 2008), responses to light quality (Stenoien et al. 2002), heat shock protein expression (Tonsor et al. 2008), growth rate (Li et al.

1998), seed dormancy and season of germination (Montesinos-Navarro et al. 2012; Kronholm et al. 2012) and age at onset of flowering (Stinchcombe et al. 2004; Wilczek et al. 2009).

Populations in northeastern Spain occur across an altitudinal range from near sea level at the Mediterranean coast to near tree line (~2200 m.a.s.l.) in the Pyrene Mountains. Along this gradient, low elevation sites are hotter and drier overall compared with high elevations. Low elevations experience temperatures above freezing for most of the fall and winter, but a relatively short spring reproductive period with rapid warming and drying. In contrast, high elevations experience periodic below-freezing temperature and snow cover during the winter, but have a relatively prolonged, cooler and wetter spring reproductive period (Montesinos et al. 2009; Montesinos-Navarro et al. 2011).

Importantly, genetic analyses indicate that the populations in this region are genetically distinct from surrounding regions and are likely descended from a common ancestor (Pico et al. 2008). There are two possible evolutionary genetic causes that could result in clinal trait variation. The first is historical colonization of high and low elevation sites by genetically distinct ancestors followed by spread from both ends towards mid-elevations and a subsequent isolation by distance-driven clinal pattern. . Since we do not detect isolation-by-distance among these populations and gene flow is very low (Montesinos et al. 2009), trait-environment covariation must therefore result from a response to a gradient in natural selection (Montesinos-Navarro et al. 2011).

Shifts in the timing of life history transitions appear to be an important mechanism of adaptation across this climate gradient (Montesinos et al. 2009; Montesinos-Navarro et al. 2011). Temporal duration of seed primary dormancy, sensitivity of seeds to induction of secondary dormancy by high temperatures (Montesinos-Navarro et al. 2012), probability of germinating in

fall vs. spring, and age at bolting (Montesinos Navarro et al. 2011) vary with climate of origin in our study populations. Under the constant cool, moist, mid-elevation conditions used in Montesinos-Navarro et al. (2011) late bolting high- and mid-elevation plants exhibited the highest seed production.

High temperatures and low water availability are important stresses for virtually all plants (Parmesan 2006; Wahid et al. 2007) and water availability and temperature have been proposed as determinants of the geographic range limits of *A. thaliana* (Hoffmann 2002; Hoffmann 2005). Therefore, in this study we test for adaptive divergence associated with variation in traits hypothesized to play a role in adaptation to hot, dry conditions. The climate gradient from the Mediterranean coast to near tree-line in the Pyrenees compresses much of *A. thaliana*'s range-wide climate gradient into a logistically manageable distance (see results). In particular, the coastal conditions are near the southern environmental limit for *A. thaliana*. The sites of the coastal populations are especially strongly differentiated from the inland, higher altitude by a rapidly warming and drying spring (Montesinos et al. 2009). We therefore focus particularly on clinal variation expressed under conditions of increasing temperature and decreasing water availability during the reproductive period. We can assess functional significance under our experimental conditions by quantifying the link between fitness and clinally varying traits. Additionally, we can use these relationships to generate hypotheses about fitness consequences of functional variation in the field.

Plants facing drought and increasing temperatures during the reproductive period potentially experience two forms of selection: for stress avoidance and/or for stress tolerance. Heat and drought stress during the spring reproductive season might accelerate *A. thaliana*'s developmental program leading to completion of the life cycle before conditions become

unsuitable, thus avoiding stress. Alternatively, *A. thaliana* populations under reproductive season stress might adapt their physiology, allocation strategy and morphology so as to complete the life cycle in spite of stress, thus tolerating it (Grime 1977). In this study, we investigate a suite of plant characters that are hypothesized to represent aspects of either avoidance or tolerance of spring heat and drought.

Clinal variation in photosynthetic parameters has yet to be investigated in *A. thaliana*. Variation in photosynthetic parameters might be expected to be associated with adaptation across the N.E. Spanish climate gradient for several reasons. First, in response to heat, plants may alleviate heat stress by opening stomata and increasing transpiration (Farquhar & Sharkey 1982). Alternatively, stomata may be closed for increased water use efficiency (WUE) (Kalisz & Teeri 1986; Chaves et al. 2002). Clinal variation in WUE might be expected to coincide with the previously observed cline in bolting time along the Spanish climate gradient (Montesinos-Navarro et al 2011) as age at bolting has been shown to correlate with WUE in *A. thaliana* (McKay et al. 2003). Finally, clinal variation in photosynthetic rates has been observed within- (Arntz & Delph 2001) and among- (Wright et al. 2004) species previously.

Montesinos-Navarro et al. (2011) observed clinal variation in allocation in which later-bolting high elevation plants produced larger rosettes but smaller root systems than did earlier-bolting low elevation plants. In the face of spring heating and drying, two opposing allocation patterns could hypothetically be beneficial. Plants fitting Grime's (1977) definition of ruderals would shift resources from vegetative to reproductive structures in the face of stress. In contrast, stress tolerant plants might show increased allocation to vegetative structures, potentially allowing continued survival in the spring (Grime 1977). At the leaf level, changes in dry mass allocation per unit area (specific leaf area; SLA) are known to vary clinally in *A. thaliana* (Li et

al. 1998) and other species with leaves from higher elevation or colder climates being thicker. In contrast, hot, dry spring conditions might favor plants with low-investment leaves as these have frequently been associated with shorter life spans thus possibly with stress avoidance (Wright et al. 2004; Levey & Wingler 2005).

We present results from a laboratory controlled environment study of multiple lineages collected from across an elevation gradient in NE Spain. We subjected the experimental population to warming and drying during the reproductive period placing plants under conditions similar to those in the field at the sites of origin of our low elevation populations. With this study, we accomplish the following aims: (1) we test for a correspondence between the elevation gradient across which the populations were collected and a major climate gradient. (2) We quantify the extent of adaptive divergence at the genotype level by testing in a common environment for correlations between trait values and elevation- and climate-of-origin. (3) We quantify the fitness effects under our experimental conditions of a suite of traits including: leaf-level gas exchange, specific leaf area, photochemical quantum efficiency of PSII, dry mass production of roots, rosettes and inflorescences, and the timing of bolting and fruit ripening under conditions of increasing spring heat and drought.

2.3 MATERIALS & METHODS

2.3.1 Collections

Seed collected from 16 sites along an elevation gradient in NE Spain (Figure 2.1) was propagated by single seed descent for at least two generations in a laboratory-controlled

environment to eliminate maternal effects and increase seed stock. Each collection site corresponds with a study population. Three genotypes per population were randomly selected (48 total) for inclusion in the present study.

2.3.2 Planting

Plants were grown in Ray Leach SC10 164 mL Supercell Conetainers (hereafter pots) (www.stuewe.com/products/rayleach.html) and arranged at a density of 24 pots per Ray Leach RL98 Tray (hereafter racks). Racks were placed in matching fiberglass bins. Pots were filled with Turface MVP fritted clay (<http://www.turface.com>). 1.5 mL of Nutricote was placed 10 cm below surface level. Nutricote encapsulated fertilizer releases equal daily quantities of nutrients for 100 days (NPK 13-13-13, Type 100, Arysta Life Science, New York NY). A 1 cm wide, 2 cm deep plug of Sunshine germination mix (<http://www.sungro.com>) was inserted at the surface of each pot. Prior to planting, seeds were surface sterilized via exposure to chlorine gas for three hours to avoid disease transmission. We planted five seeds per pot at the center of the germination mix plug and later thinned seedlings to one per pot.

Eight pots were planted per genotype. To allow sufficient time for measurement yet measure all plants at the same age, one replicate of each genotype was planted each day for eight days into sixteen bins (384 pots total). Planted bins were placed in the dark at 4°C and 100% relative humidity for four days to induce germination competency. After cold treatment, bins were transferred into two Conviron PGW36 growth chambers; eight bins each, for the remainder of the experiment.

2.3.3 Growth conditions

We created a dynamic growth chamber cycle in which temperature, day length and water availability changed over time. Our goal here was to provide key seasonal cues through which plants sense and respond to the environment thereby approximating key aspects of a fall-germinated, winter annual life history for the experimental plants. Most importantly for this study, during the simulated spring, we imposed a regime of increasing heat and drought stress. By doing this, we sought to determine whether the traits expressed by low versus high elevation plants were adaptive under reproductive phase heat and drought stress. Field conditions and therefore selective regimes undoubtedly differ from chamber conditions. Here, we ask whether plants collected along a gradient of seasonal patterns in heat and drought display fitness differences under our growth chamber conditions that are explained by genetically based patterns of trait variation. We use the combined associations between trait value, home climate and fitness to interpret the functional and adaptive significance of our results.

Our growth chamber cycle began with daily temperature ramping evenly from 14°C at lights on to 22°C at lights off and back to the minimum overnight. Daily maximum and minimum temperatures decreased by 2°C every eight days. On day 25, temperatures fell to a constant 5°C and were constant until day 45, when daily maximum temperature increased to 7°C, and then to 9°C and 11°C on days 49 and 53, respectively. On day 57, daily temperatures increased to a maximum of 26°C and a minimum 18°C. From day 57, for the remainder of the experiment (to day 125), maximum daily temperatures increased by 1°C and minimums by 0.5°C every four days to an ultimate daily maximum of 42°C and minimum of 26°C (Figure 2.6a). This produced a gradual increase in the daily temperature range similar to the progression of spring into summer in the low elevation population sites (Figure 2.7).

Initial day length was 12 hours, decreasing by 0.25 hours every four days, reaching a minimum of 10 hours on day 33, simulating day length at the winter solstice in NE Spain. From the solstice onward, day length increased at the same rate (0.25 hours every 4 days), reaching a maximum of 15 hours on day 113 (Figure 2.6b).

Water was supplied via an ebb-and-flood system (see Earley et al. 2009). Two modes of water control were imposed: water table height and watering frequency. A standpipe in one drain of each bin controlled the water table. Bins filled to standpipe height and remained filled for 45 minutes until a drain solenoid opened. Standpipe height was seven inches, and watering occurred twice daily until the beginning of simulated spring. In spring, water availability gradually declined to zero by reducing standpipe height to a minimum of 2.5" and reducing watering frequency to once daily, then every other day, until water supply was permanently discontinued. By weighing empty pots before and after watering at various standpipe heights, we express water availability in grams per watering (Figure 2.6c).

Light intensity was $150 \mu\text{M PAR m}^{-2} \text{s}^{-1}$ until day 45 when light increased by increments of $50 \mu\text{M PAR m}^{-2} \text{s}^{-1}$ every 4 days, reaching a maximum of $350 \mu\text{M PAR m}^{-2} \text{s}^{-1}$ on day 57.

Tray positions were rotated within each growth chamber every 4 days until day 85, when plants reached an advanced stage of flowering, making rotations impractical.

2.3.4 Trait measures

To measure differences in developmental timing, we recorded dates of germination, bolting and first-ripened fruit. We defined germination date as the day on which cotyledons were first visible, bolting as the date on which the first signs of primordial flower buds were visible, and ripening as the date on which we observed at least one fully yellow or brown fruit. From these

life-history transition dates, we derived two life-history traits: The number of days between germination and bolting (Time until Bolting) and the number of days between bolting and first ripened fruit (Bolting until Ripening).

We measured leaf traits on day 85 when all but one of the plants was flowering. At mid-day, two racks per day were transferred to a third Conviron PGW36 growth chamber set to 350 $\mu\text{M PAR m}^{-2} \text{ s}^{-1}$ and 32°C, the daily maximum temperature. We conducted gas exchange measurements to assess the capacity of the plants to photosynthesize under heat stress. The plants were acclimated for 30 minutes prior to measurements. Measures were conducted over eight consecutive days, giving one replicate per genotype per day. Thus measurements on each plant were conducted at the same age.

For each plant, we selected a recently expanded, fully green rosette leaf. One leaf was placed in the cuvette of a LI-6400 infrared gas analyzer (IRGA; LI-COR Biosciences, Inc., Lincoln NE) and allowed to equilibrate for five minutes while still attached to the plant. We took four measures of net carbon assimilation ($\mu\text{M CO}_2 \text{ m}^{-2} \text{ s}^{-1}$) and transpiration ($\text{mM H}_2\text{O m}^{-2} \text{ s}^{-1}$) over one minute. Measures were averaged for a single record of instantaneous CO_2 and H_2O exchange per leaf. WUE was calculated as the ratio of net carbon assimilation to transpiration.

We measured maximum PSII quantum efficiency using a PAM 2000 fluorometer (www.walz.com). We chose a second fully expanded rosette leaf per plant and dark-adapted it by placing it in a light-blocking leaf clip for five minutes. Immediately following dark-adaptation the baseline fluorescence (F_o) was measured. We then applied a saturating pulse of white light to determine the maximal fluorescence (F_m). The quantum efficiency of open PSII calculated as the ratio of variable fluorescence ($F_v = F_m - F_o$) to F_m (Baker 2008).

After gas exchange measurement leaves were excised, flattened under a pane of glass and photographed with an area standard. We measured leaf area using NIH ImageJ 64-bit version 1.44j (<http://rsbweb.nih.gov/ij/>). Finally, we dried the leaves at 70°C, and weighed them. Specific leaf area (SLA) was calculated as the ratio of fresh leaf area to dry mass.

When all plants had fully senesced (day 125) we partitioned the plants into rosettes, inflorescences and roots and dried them at 70°C for at least 7 days. As a fitness measure we used the summed fruit length, estimated as follows: Inflorescence branches were laid out on a table and the length of only the reproductive (fruit bearing) portions of each branch were measured with a PlanWheel XL™ (Scalex Corporation, Encinitas, CA). Next we estimated the density of fruits by counting the number of fruits along 10 cm of the primary inflorescence branch. Finally, we measured the length of five fruits to give an average fruit length. Fitness, or summed fruit length, is equal to the reproductive branch length times the fruit density (i.e. fruit number) times the average fruit length. Fruit length is tightly correlated with the number of seeds per fruit (Alonso-Blanco et al. 1999) and fruit number strongly predicts total seed number by itself (Mauricio & Rausher 1997) so summed fruit length is a good proxy for the total number of seeds. We also counted the number of basal inflorescence branches.

2.3.5 Climate data

We obtained temperature and precipitation data at each of the 16 collection sites from the BIOCLIM dataset described by Hijmans et al. (2005). This data set contains 19 biologically relevant climatic indices (Table 2.3) derived from monthly precipitation and temperature data for the period 1950-2000 (available at <http://www.worldclim.org>) and has a resolution of approximately 1 km²/grid cell.

2.3.6 Statistical analysis

We used principal components analysis (PCA) to produce orthogonal axes or principal components (PCs) that explain multivariate climate variance. We conducted the PCA on the correlation matrix of BIOCLIM values and the elevation above sea level at each of the 16 collection sites to produce indices that describe the major climate gradient(s) across which our populations are arrayed. We implemented randomization tests (Perez-Neto et al. 2003) to determine the number of meaningful climate axes (PCs). The distribution of PCs obtainable under the null hypothesis of climate variable independence was constructed by independently permuting the order of each BIOCLIM variable, then calculating principal components on the permuted data, repeated 5,000 times. By comparing the actual *n*th PC to the distribution of *n*th PCs from the 5,000 permutations, we obtained the probability of the actual *n*th PC value under the null hypothesis (SAS code available at <http://www.tonsorlab.pitt.edu>). By including elevation in the PCA we describe the overall multivariate relationship between climate and elevation and test the extent to which elevation can be treated as a proxy for climate.

Before analyses, we first removed variance from each trait accounted for by aspects of the experimental design, i.e., RACK, MEASURE DAY, and CHAMBER effects. We also tested for an interaction between CHAMBER and MEASURE DAY. We used SAS PROC GLIMMIX (version 9.3; SAS Institute Inc., Cary, North Carolina, USA) with RACK as a random effect nested in MEASURE DAY and the other factors as fixed effects. We added the grand mean for each trait to the residuals from this analysis and performed all subsequent analyses on these adjusted trait values.

One major aim of this study was to test for an adaptive cline in the multivariate phenotype associated with climate and elevation. Therefore, we conducted PCA on the

correlation matrix of the population means for 12 traits, thereby reducing the dimensionality of trait space to a few, orthogonal axes. As in the PCA of climate space, we used randomization (Perez-Neto et al. 2003) to determine the number of meaningful axes in the trait matrix. We then test whether among-population variation in climate predicts among-population variation in phenotype by regressing population-mean trait principal component scores on population-mean climate PC scores.

PCA produces ranked orthogonal vectors that reflect weighted combinations of variables based on the variables' covariances. While this is a powerful way to account for covariation and reduce the effective number of dimensions, the intuitive/biological interpretation of the regression of a trait PC onto a climate PC is difficult. Because of this, we also conducted univariate regressions of each trait on climate PC scores for visualization purposes. We also regressed population means for each trait on elevation and compared the predictive power of elevation to that of climate principal components. We used the SAS PROC REG (version 9.3, SAS Institute 2011) for the trait PC-climate PC, univariate trait-climate and trait-elevation analyses.

Finally, we tested hypotheses about natural selection under simulated low elevation spring heat and drought using a standard multiple-regression approach to quantifying phenotypic selection (Lande & Arnold 1983). We transformed all variables (including fitness) to the same scale with a mean of zero and standard deviation of one, allowing direct comparison of the strength and direction of selection among traits. Selection gradients therefore indicate the number of standard deviations increase in fitness per standard deviation change in trait grand mean. We tested for both linear and quadratic selection by regressing summed fruit length on both the traits and their squared values in the multiple-regression model. To satisfy the

regression assumptions we used log-transformed summed fruit length as the dependent variable in the estimation of p-values and r-squares. However, we present parameter estimates based on untransformed summed fruit length to facilitate biological understanding. We note that statistical tests for linear selection coefficients may correspond to more complex functions on the non-transformed scale. We have presented only the linear effects in the graphics of untransformed data.

Although multiple regressions provide a view of the relationship between a trait and fitness independent of other correlated traits, correlations among traits remain an important issue in the interpretation of apparent selection. This is in part because multiple regression estimates of selection gradients can suffer from multicollinearity wherein highly correlated traits act to some extent redundantly, inflating the variance explained but causing inaccuracy in our estimates of the effects for those traits (Mitchell-Olds & Shaw 1987). To aid in our interpretation of selection on and relationships among the traits measured, we used Akaike's Information Criterion (AIC) to determine the "best" model by rewarding added explanatory power but penalizing the inclusion of additional terms. This provided the simplest model for fitness with the least collinearity and thus, presumably, the best estimates of selection (Shaw & Geyer 2010). We used the SAS PROC REG (version 9.3, SAS Institute 2011) for all selection analyses.

To aid interpretation of selection analyses, we also calculate and present the phenotypic Pearson product-moment correlations. We employed a sequential Bonferonni correction to all p-values in the correlation matrix to compensate for the risk of false positive with multiple testing. We used the SAS PROC CORR (version 9.3, SAS Institute 2011) for all correlation analyses.

2.4 RESULTS

All pots contained germinated seeds. A small number of deaths or missing measurements resulted in a multivariate dataset (i.e. all observations with no missing values) of N=366 of the planned N=384 or 95% of the goal.

We detected significant CHAMBER, MEASURE DAY and CHAMBER x MEASURE DAY effects for many of the traits analyzed. All results reported below were obtained with the residuals from this model plus the trait grand mean.

2.4.1 Principal component analysis of the climate gradient

Randomization testing of the climate PCA eigenvalues detected two significant principal components (Figure 2.8), explaining 75% and 17% of the climate variation among our 16 collection sites respectively (Table 2.4, Figure 2.2). For climate PC1, eigenvector coefficients for all precipitation variables with the exception of Precipitation Seasonality (coefficient of variation in precipitation) were positive and varied from 0.21 to 0.25. Eigenvector coefficients for all variables that describe temperature variability (e.g. Annual Temperature Range) were positive but were smaller than the precipitation variables, ranging from 0.05 to 0.14. However, eigenvectors of variables that describe temperature during a particular time period (e.g. Max. Temp. of the Warmest Month) were negative, ranging from -0.20 to -0.26 (Table 2.4, Figure 2.2). Variables describing temperature variability (BIO2, BIO3, BIO4 and BIO7) loaded most strongly on climate PC2. Elevation loaded positively (0.24) onto climate PC1 but had an eigenvector of essentially zero on climate PC2 (Table 2.4, Figure 2.2). Climate PC1 and PC2 scores for each population are reported in Table 2.5.

2.4.2 Principal component analysis of trait space

There was a single, significant principal component (Trait PC1) in population mean trait space, explaining 71% of the variation (Figure 2.9). For Trait PC1, quantum efficiency, rosette mass, root mass, age at bolting, time from bolting to first ripe fruit, photosynthetic and transpiration rates had positive loadings ranging from 0.15 to 0.34. Summed fruit length, WUE, inflorescence mass, basal branch number and specific leaf area had negative loadings ranging from -0.26 to -0.33 on trait PC1 (Table 2.6, Figure 2.3). Table 2.5 contains Trait PC1 scores for each population.

2.4.3 Evidence for local adaptation, trait-elevation and trait-climate associations

Multiple regression of trait PC1 score on climate PC1 and PC2 scores explained 36% of the variance in PC1 ($n=16$, model p -value = 0.05). Climate PC1 showed significant positive relationship to trait PC1 while climate PC2 was not significant (Figure 2.4). The quadratic term was not significant so it was dropped from the model. Finally, we observe that the population BOS is an outlier in terms of its mean phenotypes relative to its elevation. For example, climate PC1 explains 56% of the variance in trait PC1 when BOS is excluded (not shown).

The population mean fitness in our simulated low elevation environment decreases by 590 mm (0.88 standard deviations) of summed fruit length per 1000 meters above sea level (m.a.s.l.) for the site of population origin. Elevation of origin explained 46% ($p = 0.004$) of among-population variation in summed fruit length (Figure 2.5). Population trait means and standard deviations are presented in Table 2.7.

Elevation of origin significantly predicted population means for all traits except specific leaf area ($p = 0.14$) and root dry mass. ($p = 0.74$). Maximum photosynthetic quantum efficiency ($F_v:F_m$) increased by 103% ($r^2 = 0.41$) per 1000 m.a.s.l. for the site of population origin. Net photosynthetic rate increased by 194% ($r^2 = 0.57$) and transpiration increased by 267% ($r^2 = 0.54$) per 1000 m.a.s.l. Instantaneous WUE decreased by 78% ($r^2 = 0.41$) per 1000 m.a.s.l. Rosette dry mass increased by 300 mg ($r^2 = 0.49$) while inflorescence dry mass decreased by 540 mg per 1000 m.a.s.l ($r^2 = 0.39$). Age at bolting increased by seven days and the time from bolting to the first ripened fruit increased by 1.4 days per 1000 m.a.s.l., explaining 50% and 22% of among-population variation, respectively. Plants produced eight fewer basal inflorescence branches ($r^2 = 0.63$) per 1000 m.a.s.l. (Figure 2.5). Scores along climate PC1 also significantly predicted population-mean trait values except quantum efficiency, specific leaf area, and root mass; days from bolting to fruit ripening was marginally significant (Table 3.1). The slopes describing the relationship between climate PC1 and trait values were significantly correlated with the slopes of the trait-on-elevation regressions ($r = 0.74$, $n = 12$, $p = 0.006$). Climate PC2 did not significantly predict any trait variable in univariate regression (results not shown).

2.4.4 Selection under heat and drought during reproductive phase

We detected significant linear selection on our suite of study traits (Table 2.2). Quadratic models did not significantly increase explanatory power and are therefore not presented. Most traits were correlated in this study (Table S6). Both the best-fit linear (hereafter “best”) model based on AIC and the full linear model explained 69% of the variance in fitness.

Both the full and best models indicated selection for earlier bolting ($\beta = -0.15$ and $\beta = -0.20$ respectively), with selection for faster fruit ripening detected only in the best model ($\beta = -$

0.07). In the best model, a standard deviation (six day) decrease in the age at bolting increases fruit production by 0.20 standard deviations, approximately 145 mm of fruit length. Age at bolting is nearly three times as important to fitness as time from bolting till ripening in both models tested. Age at bolting is the second most powerful predictor of fitness in both models after inflorescence mass and these traits are correlated.

In both models selection favored lower root mass ($\beta = -0.08$ full model and $\beta = -0.07$ best model). Rosette dry mass was excluded from the best model and was not significant in the full model. There was strong selection for greater inflorescence mass ($\beta = 0.62$ full model and $\beta = 0.61$ best model). A single standard deviation increase in inflorescence mass (721 mg) predicts a 0.61 standard deviation increase in summed fruit length (441 mm).

Among the leaf traits, significant selection was detected only for transpiration rate. Selection favored lower transpiration rate ($\beta = -0.12$ full model and $\beta = -0.11$ best model). A decrease in transpiration rate of one standard deviation ($6.5 \text{ mMols H}_2\text{O m}^{-2}\text{s}^{-1}$) is associated with an increase in fitness of approximately 800 mm of fruit length. In the best model, quantum efficiency, net photosynthesis and WUE are dropped, while specific leaf area is retained but remains non-significant.

2.5 DISCUSSION

To test the extent of adaptation to local climate, we grew plants from across an elevation gradient under dynamic growth chamber conditions that produced an accelerated winter annual life cycle and subjected plants to increasing heat and drought stress during the reproductive season, as is observed at low elevations in the field. We identified significant associations between climate

and 10 of the 12 traits investigated. Populations from low elevation coastal Mediterranean sites developed from germination to seed more quickly than those from high elevation. Low elevation plants had relatively more mass and time invested in inflorescence structures and less in vegetative growth and rosette photosynthesis.

The first principal component of climate indicated a gradient of increasing heat and drought with decreasing elevation (Figure 2.2). Interestingly, most regression analyses conducted with elevation as the independent variable performed better than those using climate PC1 scores. Indeed, elevation explained 54% of the variance in trait PC1 (not shown) while climate PC1 explained only 36% of trait PC1 variation (Figure 2.4). One explanation is that while elevation is accurately measured for each collection site, the climate data used are values averaged over 50 years interpolated from nearby weather station data (Hijmans et al. 2005) and do not account for local and micro-climatic site characteristics. There are other factors that may covary with elevation and contribute to clinally varying selection, including: soil, atmosphere and light environments. Additionally, there is a possible influence of the biotic community, which could vary in composition and phenology across the elevation gradient.

In this study, relative adaptedness to spring heat and drought scaled with elevation of origin, favoring low elevation phenotypes under the imposed warming and drying regime (Figure 2.5). Our findings form a complement with those of Montesinos-Navarro et al. (2011), who found, using the same study populations and an overlapping but not identical set of genotypes, that higher elevation plants out-produced low elevation plants when spring conditions were cool and wet. The clinal trait and fitness variation observed in this study indicate adaptive divergence due to differential selection among sites. It is however important to point out that in all cases, the direct agents of selection are not known and neither the conditions nor the developmental

sequences or phenotypes of the plants in our chambers perfectly match the conditions or phenotypes seen in the field. Our source populations exhibit repeated bouts of germination during favorable conditions from fall through spring in the field (Pico 2012). The life cycle can be as long as nine months or as short as 50-60 days (Pico 2012). Thus there is no one life cycle or set of seasonal conditions that most accurately describes the patterns of phenotype and selection in the field. Despite this variation in the early phases of the life cycle, all plants in low elevation populations experience spring heat and drought similar to that imposed in our chambers. It is also possible that the characters measured evolved due to indirect selection via correlated traits (Lande & Arnold 1983). With these caveats in mind, below we consider the relationship between traits, elevation and climate to better understand the phenotypic mechanisms underlying adaptive differentiation across the elevation gradient described above.

Low elevation plants exhibited characteristics consistent with avoidance of heat and drought stress during the spring reproductive season, including faster bolting and fruit ripening. Avoiding stress through shortening the vegetative phase and rapidly shifting resources to the reproductive structures is a key to the ruderal plant strategy described by Grime (1977) and has been observed in *Arabidopsis thaliana* and other species (e.g. Chaves et al. 2002; McKay et al. 2003; Griffith & Watson 2005; Heschel & Riginos 2005). We observed that genotypes from lower elevations bolted significantly earlier than genotypes from high elevation. This pattern of earlier bolting at hotter, drier low elevation sites is concordant with the range-wide pattern of earlier bolting at lower latitudes (Stinchcombe et al. 2004; Caicedo et al. 2004; Lempe et al. 2005; Wilczek et al. 2009). Earlier flowering was associated with functional shifts in the distribution of biomass among plant parts and in physiological rates.

Low elevation plants' distribution of dry mass reflects in part their earlier flowering time. Low elevation plants had smaller rosettes and larger inflorescences relative to those from high elevations (Figure 2.4, Figure 2.5). Initiation of primary rosette leaves ceases at bolting because the primary meristem activity transitions to inflorescence production. This ends or slows accumulation of biomass in the rosette, depending on leaf production by axillary meristems in the rosette short-shoot (Bonser & Aarssen 2001).

The advantage of earlier flowering in the field and its influence on the ratio of inflorescence to rosette may in part be due to the distinct thermal niches occupied by these organs. At rosette level radiated heat from the ground and the associated still air layer lead to significantly warmer conditions when compared to air at the inflorescence level above the ground (Geiger 1950). Thus early flowering may not just ensure earlier reproduction, but also successful carbon gain during warm, dry spring months and increasing carbon uptake capacity while avoiding further self-shading in the rosette. In support of this hypothesis, Earley et al. (2009) showed that on average, *A. thaliana* inflorescences contribute a greater proportion of lifetime carbon gain than rosettes. Earley et al. (2009) also found that the inflorescence had greater WUE than the rosette, which may be advantageous during a hot, dry low elevation spring. Future studies of lifetime carbon gain and water use by the rosette and inflorescence along climate gradients will provide important functional understanding of variation in flowering time.

Low elevation plants' greater inflorescence mass may be explained in part by their greater number of basal inflorescence-forming axillary meristems (Figure 2.5). This trait may also allow earlier increase in the number of fruits matured, since for n basal inflorescences, a

plant will produce n fruits more or less simultaneously at approximately the same age that a single inflorescence will ripen a solitary first fruit.

One final factor explaining the relationship between elevation and the distribution of aboveground dry mass is variation in senescence and re-allocation of rosette resources to the inflorescence. It is possible that maximum rosette mass is greater than the final rosette mass observed for early bolting plants. Earlier bolting may lead to earlier rosette senescence. The adaptive role of nutrient and carbon reallocation during senescence may be particularly important in environments where a rapid decrease in water availability can limit the ability of the plant to acquire nutrients from the soil, maximizing the importance of re-purposing of stored nutrients.

Leaves of low elevation plants had significantly lower $F_v:F_m$, carbon assimilation and transpiration rates and greater WUE than high elevation plants (Figure 2.5). McKay et al. (2003) found that earlier bolting genotypes of *A. thaliana* were less WUE as evidenced by decreased carbon isotope discrimination. Low elevation plants that bolt earlier produce much larger inflorescences both overall (Figure 2.5) and relative to the rosette (not shown). Inflorescences can contribute greater lifetime carbon gain while being more WUE than rosettes (Early et al. 2009). Thus, low elevation plants in this study may circumvent the expected trade-off between drought avoidance and tolerance mechanisms observed in McKay et al. (2003). This result is likely to be dependent on the timing of the measurements relative to the life history stage and the imposition of stress.

Our low values of gas exchange rates and $F_v:F_m$ among low elevation plants may indicate senescence of the measured leaves. This is in line with indications that low elevation conditions produce plants that develop more rapidly than their high elevation counterparts. The leaves we measured showed no visible sign of senescence at the time measurements were taken. However,

recent studies of the molecular and physiological underpinnings of senescence indicate that the process itself begins before visible signs appear (Balazadeh et al. 2008).

We conducted gas exchange measurements in late afternoon to assess the ability of experimental plants to photosynthesize under heat stress. Our results would not necessarily correlate with measurements taken earlier in either the daily or the developmental cycle. Nevertheless, our measures of gas exchange, WUE and quantum efficiency were all strongly related to the elevation of each population, indicating that measured or correlated unmeasured traits played a significant role in adaptation to the environmental gradient.

There was strong selection for high inflorescence masses (Table 2.2). This is expected, since the greater the inflorescence size, the greater the number of fruits borne. Additionally, there was selection for earlier flowering and shorter time until fruits ripen, which matches low elevation plants' life histories. Multiple-regression analysis indicates a much stronger relationship between inflorescence mass and fitness, when controlling for correlated traits like bolting time. Inflorescence mass is correlated with basal branch number ($r = 0.52$) and rosette dry mass ($r = -0.62$) neither of which are significant in the selection analysis (Table S6).

Inflorescence mass explained only 63% of the variance in fitness in a univariate regression (results not shown). Indeed, while low elevation plants produced the most fruit overall they also produced more fruit length per unit inflorescence mass (result not shown), i.e. exhibit greater mass use efficiency in the production of fruits under the conditions of this experiment. Given that inflorescences contribute significantly to lifetime carbon gain and have greater WUE than vegetative rosette tissue (Earley et al. 2009), they are likely to possess adaptive function above and beyond structurally supporting fruit production, further reflecting the advantage of conserving water via stomatal closure in the rosette while photosynthesizing in the inflorescence.

This study demonstrates variation in relative adaptedness of plants from across a climate gradient to heating and drying during the spring reproductive phase. Low elevation plants from NE Spain were able to maximize seed production given the short reproductive season we imposed because they bolted early and allocated more to reproductive relative to vegetative structures and because they ripened fruit more quickly. We propose that this is a syndrome of avoidance through early flowering accompanied by restructuring of the organism that adapts *A. thaliana* to low elevation Mediterranean climates.

Table 2.1: Univariate results for *Arabidopsis thaliana* population-mean trait values regressed on climate PCI scores.

Traits	Slope	r²	p-value
Quantum Efficiency	0.002	0.18	0.107
Net Photosynthesis	0.491	0.38	0.011
Transpiration	0.67	0.38	0.010
Water Use Efficiency	-0.048	0.29	0.031
Specific Leaf Area	-2.353	0.07	0.330
Root Mass	0.203	0.00	0.925
Rosette Mass	35.117	0.37	0.012
Inflorescence Mass	-64.113	0.30	0.028
Age at Bolting	0.724	0.29	0.033
Days from Bolting to Ripening	0.186	0.22	0.066
Number of Basal Branches	-0.966	0.51	0.002
Summed Fruit Length	-663.915	0.31	0.024

Each row represents a independent regression with the dependent variable indicated in the traits column. Slopes, r-squares and p-values of the slope parameter estimate are provided for each analysis in columns.

Table 2.2: Full AIC-selected best models of phenotypic selection on N. E. Spanish *Arabidopsis thaliana*.

Traits	Full Model		AIC-Selected Best Model	
	$\beta \pm SE$	P	$\beta \pm SE$	P
Quantum Efficiency	-0.05 \pm 0.04	0.30	---	---
Net Photosynthesis	-0.01 \pm 0.06	0.91	---	---
Transpiration	-0.12 \pm 0.06	0.03	-0.11 \pm 0.04	0.003
Water Use Efficiency	-0.03 \pm 0.04	0.38	---	---
Specific Leaf Area	-0.06 \pm 0.04	0.09	-0.05 \pm 0.04	0.15
Root Mass	-0.08 \pm 0.04	0.02	-0.07 \pm 0.03	0.02
Rosette Mass	0.02 \pm 0.05	0.97	---	---
Inflorescence Mass	0.62 \pm 0.05	< 0.0001	0.61 \pm 0.04	< 0.0001
Age at Bolting	-0.15 \pm 0.05	0.002	-0.20 \pm 0.04	< 0.0001
Days from Bolting to Ripening	-0.05 \pm 0.03	0.07	-0.07 \pm 0.03	0.01
Number of Basal Branches	0.05 \pm 0.04	0.26	---	---
	r^2 0.69		r^2 0.69	

Summed fruit length (fitness) regressed on phenotypic values of the traits listed in each row. To satisfy regression assumptions, p-values and model r-squares from regression with log-transformed summed fruit length are presented. All variables were standardized to mean = 0 and variance = 1 prior to analysis. Variable coefficients represented by --- were excluded from the best-fit model. Selection gradients (β) and standard errors on the parameter estimates (SE) are presented along with p-values for the t-test (ho: $\beta = 0$). Significant selection gradients are in bold.

Table 2.3: Locations, elevations and climates of the 16 sites in northeastern Spain from which the studied *Arabidopsis thaliana* genotypes originated.

Longitude and latitude are reported in decimal degrees. Elevation is reported in meters above sea level (m.a.s.l.). Nineteen variables from the BIOCLIM dataset (<http://www.worldclim.org>) are reported; temperature in degrees celsius and precipitation in millimeters. Isothermality is $(\text{BIO2} / \text{BIO7}) * 100$ (Hijmans et al. 2005).

POPULATION	ABBREV	Longitude	Latitude	Elevation (m.a.s.l.)	BIOCLIM Variables																		
					BIO1	BIO2	BIO3	BIO4	BIO5	BIO6	BIO7	BIO8	BIO9	BIO10	BIO11	BIO12	BIO13	BIO14	BIO15	BIO16	BIO17	BIO18	BIO19
					Annual Mean Temp.	Mean Diurnal Range	Isothermality	Temp. Seasonality (Std. Dev.)	Max. Temp. of Warmest Month	Min. Temp. of Coldest Month	Annual Temp. Range	Mean Temp. of Wettest Quarter	Mean Temp. of Driest Quarter	Mean Temp. of the Warmest Quarter	Mean Temp. of Coldest Quarter	Annual Precip.	Precip. Of Wettest Month	Precip. Of Driest Month	Precip. Seasonality (Coeff. Of Var.)	Precip. Of Wettest Quarter	Precip. Of Driest Quarter	Precip. Of Warmest Quarter	Precip. Of Coldest Quarter
Pineda de Mar	PIN	2.6591	41.6592	109	15	6.9	3	5.40	27	4.7	22.3	16	22.1	22.1	8.4	763	107	34	27	251	146	174	167
Rabos	RAB	3.0537	42.3781	110	15.1	8.1	3.4	5.36	27.8	4.1	23.7	16	22.1	22.1	8.5	617	91	24	29	207	111	129	138
Santa Pellaia	SPE	2.9162	41.9275	332	14.1	7.1	3.1	5.33	26.1	3.7	22.4	15.2	21	21.1	7.6	784	106	37	25	244	159	174	169
Barcelona	BAR	2.1278	41.4322	340	15.4	7	3.1	5.31	27.3	5.3	22	16.4	22.3	22.5	9	653	85	30	26	220	132	160	133
Hortsavinya	HOR	2.6202	41.6645	351	13.9	6.9	3.1	5.38	25.9	3.8	22.1	18.7	20.9	21	7.4	821	104	41	23	254	173	191	175
Arbucies	ARU	2.4941	41.8143	440	13.9	7.1	3.1	5.50	26.3	3.5	22.8	18.8	7.3	21.2	7.3	834	97	46	21	251	170	201	170
Cabo de Cruz	COC	3.1653	42.3263	519	13.9	7.9	3.4	5.27	26.3	3.3	23	14.9	20.8	20.8	7.5	688	95	29	26	222	130	147	155
Poblet	POB	1.0235	41.3526	597	12.1	8.8	3.5	5.78	25.9	0.8	25.1	13	5.9	19.8	5.2	680	77	30	24	205	137	154	137
Bossost	BOS	0.6913	42.7836	719	9.5	9.6	3.8	5.60	23.3	-1.9	25.2	11.4	3.5	16.7	2.4	987	102	65	14	284	216	252	218
Mura	MUR	2.0002	41.6757	836	12.1	7.4	3.2	5.52	24.8	2	22.8	17.1	5.6	19.5	5.6	760	87	41	23	231	141	197	141
Vilanova de Meia	VDM	1.0249	42.0292	912	9.2	8.8	3.5	5.77	23.2	-1.8	25	10.9	2.2	16.8	2.2	884	100	52	19	268	173	219	173
Albet	ALE	1.3187	42.4105	1163	8.5	8.5	3.5	5.64	22.1	-2.1	24.2	10	2.5	16	1.7	972	108	58	18	293	193	249	193
Bisanri	BIS	0.5334	42.4878	1397	4.4	7.5	3.2	5.43	17.4	-5.4	22.8	5.4	-1.4	11.8	-1.9	1220	131	81	13	347	271	282	274
Pallerols	PAL	1.2926	42.4312	1491	6.6	8.7	3.6	5.51	20.2	-3.9	24.1	8.1	0.7	13.9	-0.1	1070	115	70	15	311	236	248	236
Vielha	VIE	0.7606	42.6256	1538	5.1	8.1	3.4	5.43	18.2	-5.2	23.4	6.3	-0.8	12.3	-1.4	1192	127	80	13	342	266	276	270
Panticosa	PAN	-0.2310	42.7620	1664	4.3	8.5	3.6	5.29	17.4	-5.9	23.3	5.5	11.4	11.4	-2	1190	124	76	13	335	258	258	292
			Mean	782	11	8	3	5	24	0	23	13	10	18	4	882	104	50	21	267	182	207	190
			Standard Deviation	523	4	1	0	0	4	4	1	5	9	4	4	201	15	20	6	47	52	49	52
			Min	109	4	7	3	5	17	-6	22	5	-1	11	-2	617	77	24	13	205	111	129	133
			Max	1664	15	10	4	6	28	5	25	19	22	23	9	1220	131	81	29	347	271	282	292

Table 2.4: Eigenvector coefficients of first principal component resulting from a PCA of the value 19 bioclimatic variables at 16 study populations of *Arabidopsis thaliana* in NE Spain.

BIOCLIM #	Climate Variable Name	PC1	PC2
BIO1	Annual Mean Temp.	-0.26	-0.01
BIO2	Mean Diurnal Range	0.14	0.43
BIO3	Isothermality (BIO2/BIO7)*100	0.14	0.38
BIO4	Temp. Seasonality (Std Dev*100)	0.05	0.44
BIO5	Max. Temp. of the Warmest Month	-0.25	0.08
BIO6	Min. Temp. of Coldest Month	-0.25	-0.06
BIO7	Annual Temp. Range	0.10	0.50
BIO8	Mean Temp. of Wettest Quarter	-0.24	-0.03
BIO9	Mean Temp. of Driest Quarter	-0.20	-0.20
BIO10	Mean Temp. of the Warmest Quarter	-0.26	0.01
BIO11	Mean Temp. of Coldest Quarter	-0.26	-0.03
BIO12	Annual Precip.	0.25	-0.12
BIO13	Precip. Of Wettest Month	0.21	-0.28
BIO14	Precip. Of Driest Month	0.25	-0.08
BIO15	Precip. Seasonality (Coeff. Of Var.)	-0.25	-0.01
BIO16	Precip. Of Wettest Quarter	0.24	-0.16
BIO17	Precip. Of Driest Quarter	0.25	-0.13
BIO18	Precip. Of Warmest Quarter	0.24	-0.06
BIO19	Precip. Of Coldest Quarter	0.24	-0.16
n/a	Elevation of Origin	0.24	0.00
Percent Variance Explained		75%	17%

Table 2.5: Principal Component Scores of each population of *Arabidopsis thaliana* for the first principal component of trait space plus the first and second principal components of climate space.

POPULATION	ABBREV	Principal Component Scores		
		Trait PC1	Climate PC1	Climate PC2
Pineda de Mar	PIN	-4.16	-3.65	-1.76
Rabos	RAB	-4.18	-4.48	0.88
Santa Pellaia	SPE	-0.35	-2.92	-1.63
Barcelona	BAR	-1.83	-4.58	-1.20
Hortsavinya	HOR	-3.21	-2.71	-1.87
Arbucies	ARU	-1.02	-2.19	-0.68
Cap de Creus	COC	0.36	-3.28	-0.09
Poblet	POB	2.55	-2.00	3.73
Bossost	BOS	-3.60	2.61	2.63
Mura	MUR	2.04	-2.00	0.22
Vilanova de Meia	VDM	2.76	1.29	2.62
Albet	ALE	-1.11	2.31	1.25
Bisaurri	BIS	4.11	5.82	-2.25
Pallerols	PAL	0.62	4.26	0.62
Vielha	VIE	2.13	5.73	-1.19
Panticosa	PAN	4.88	5.79	-1.29

Table 2.6: Eigenvector coefficients of first principal component resulting from a PCA of the population means for each trait of *Arabidopsis thaliana*.

Traits	Trait PC1
Summed Fruit Length	-0.33
Water Use Efficiency	-0.30
Inflorescence Mass	-0.30
Number of Basal Branches	-0.28
Specific Leaf Area	-0.26
Root Mass	0.15
Days from Bolting to Ripening	0.16
Quantum Efficiency	0.29
Age at Bolting	0.31
Rosette Mass	0.33
Transpiration	0.33
Net Photosynthesis	0.34
Percent Variance Explained	71%

Table 2.7: Population-mean trait values for N.E. Spanish *Arabidopsis thaliana*.

POPULATION	ABBREV	Summed Fruit Length	Quantum Efficiency	Net Photosynthesis	Transpiration Rate	Water Use Efficiency	Specific Leaf Area	Root Mass	Rosette Mass	Inflor. Mass	Age at Bolting	Days from Bolting to Ripening	Number of Basal Branches
Pineda de Mar	PIN	1370	0.77	3.8	2.5	1.97	371	289	434	1813	57.2	19.4	13.5
Rabos	RAB	1265	0.77	4.6	3.4	1.66	344	212	320	1251	54.5	16.6	16.9
Santa Pellaia	SPE	783	0.79	8.3	7.8	1.40	283	329	577	1368	62.7	20.7	17.8
Barcelona	BAR	978	0.79	7.3	6.2	1.74	321	309	543	1661	59.9	17.8	12.7
Hortsavinya	HOR	1103	0.79	5.9	3.6	2.24	359	293	438	2013	60.3	19.8	12.5
Arbucies	ARB	854	0.79	6.9	6.5	1.57	321	302	575	1546	63.6	18.0	9.4
Cabo de Cruz	COC	596	0.80	9.4	8.0	1.50	317	283	721	1057	69.8	18.4	14.8
Poblet	POB	243	0.80	11.6	12.7	1.09	285	277	784	836	67.3	19.0	4.8
Bossost	BOS	1098	0.75	5.0	3.5	1.62	370	255	425	1455	57.5	18.3	11.8
Mura	MUR	234	0.80	10.3	9.5	1.24	311	322	774	880	68.0	19.1	3.7
Vilanova de Meia	VDM	94	0.80	11.8	10.1	1.27	354	335	963	540	69.7	20.1	3.8
Albet	ABT	947	0.80	8.3	6.6	1.69	358	279	508	1436	66.4	17.6	8.5
Bisaurri	BIS	87	0.80	12.7	14.1	1.13	272	320	1104	667	68.1	21.5	3.9
Pallerols	PAL	804	0.80	9.7	8.7	1.33	328	265	689	1338	65.5	22.6	7.5
Vielha	VIE	144	0.80	10.8	10.9	1.38	322	294	826	777	67.5	18.8	3.2
Panticosa	PAN	48	0.81	14.5	17.6	0.87	258	274	937	557	72.7	19.8	1.5
Grand Mean		667	0.79	8.9	8.3	1.48	323	290	664	1200	64.4	19.2	9.2
Standard Deviation		723	0.03	5.1	6.5	1.08	73	90	295	721	6.0	4.0	7.3
Units		mm	F_v / F_m	$\mu\text{Mols CO}_2 / \text{m}^2 \text{s}^{-1}$	$\text{mMols H}_2\text{O} / \text{m}^2 \text{s}^{-1}$	$\mu\text{Mols CO}_2 / \text{mMols H}_2\text{O}$	cm^2 / g	mg	mg	mg	days	days	number

Table 2.8: Pearson product moment correlation matrix for N.E. Spanish *Arabidopsis thaliana*. Bold-faced = $p < \text{Sequential Bonferonni corrected critical value}$. ** $p < 0.0001$, * $0.0001 < p < 0.05$.

	Summed Fruit Length	Quantum Efficiency	Net Photosynthesis	Transpiration Rate	Water Use Efficiency	Specific Leaf Area	Root Mass	Rosette Mass	Inflor. Mass	Age at Bolting	Days from Bolting to Ripening	Number of Basal Branches
Summed Fruit Length	1											
Quantum Efficiency	** -0.38	1										
Net Photosynthesis	** -0.52	** 0.45	1									
Transpiration Rate	** -0.51	** 0.37	** 0.73	1								
Water Use Efficiency	** 0.23	* -0.14	* -0.1	** -0.52	1							
Specific Leaf Area	** 0.23	** -0.32	** -0.35	** -0.46	** 0.23	1						
Root Mass	-0.08	* 0.18	0.06	0.08	-0.14	** -0.29	1					
Rosette Mass	** -0.61	** 0.44	** 0.49	** 0.54	** -0.27	** -0.33	** 0.32	1				
Inflorescence Mass	** 0.78	** -0.3	** -0.5	** -0.49	** 0.25	** 0.23	0.06	** -0.62	1			
Age at Bolting	** -0.61	** 0.53	** 0.56	** 0.53	** -0.22	** -0.3	* 0.16	** 0.67	** -0.58	1		
Days from Bolting to Ripening	* -0.18	* 0.12	* 0.13	* 0.13	-0.06	-0.05	* 0.13	** 0.26	* -0.15	-0.06	1	
Number of Basal Branches	** 0.49	** -0.37	** -0.41	** -0.39	* 0.18	* 0.15	0.00	** -0.5	** 0.52	** -0.56	-0.07	1

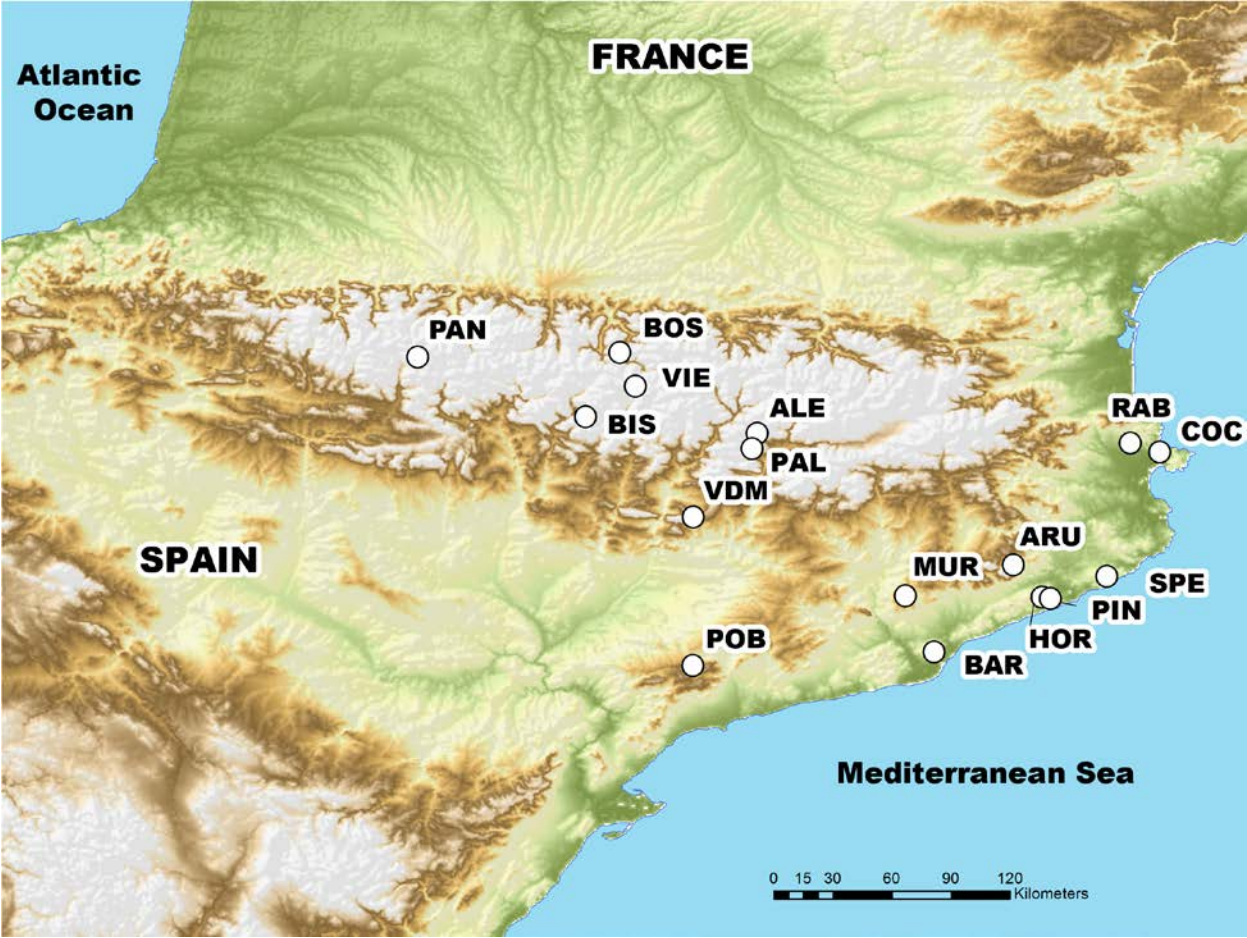


Figure 2.1: Map of the sixteen *Arabidopsis thaliana* collection sites used in this study. Colors indicate elevation going from low to high as follows: Green to brown to white.

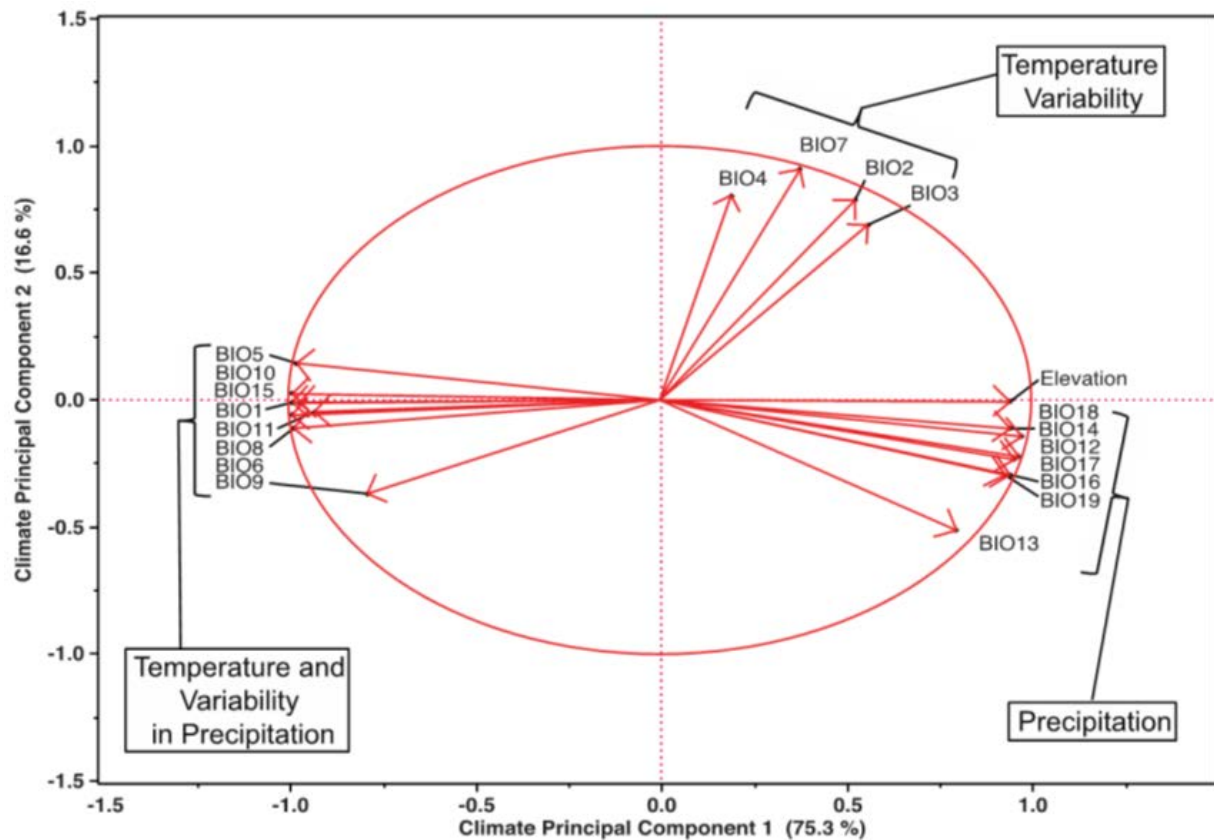


Figure 2.2: Eigenvector plot of the loadings of 20 climate variables onto the first and second principal component of climate space that describe conditions in 16 N. E. Spanish *Arabidopsis thaliana* populations. Each arrow represents a vector of loadings. Direction of each arrow represents the relationship of a variable to climate PC1 and PC2 and the length of the vector represents the strength of that relationship. Clusters of similar variables e.g. Precipitation are bracketed and labeled to help summarize results.

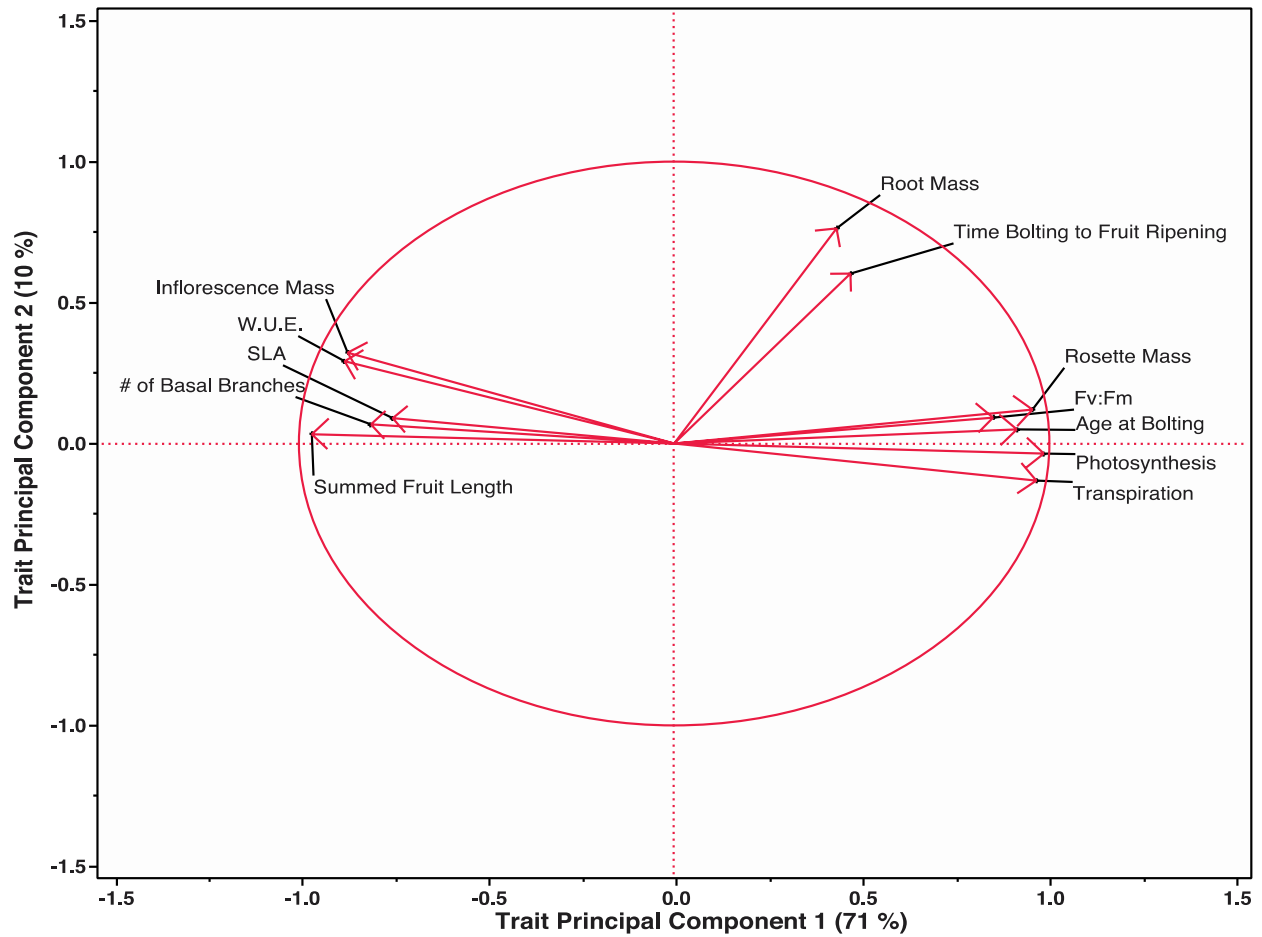


Figure 2.3: Eigenvector plot of the loadings of 12 traits onto the first and second principal component of trait space for N. E. Spanish *Arabidopsis thaliana*. Each arrow represents a vector of loadings. Direction of each arrow represents the relationship of a variable to trait PC1 and PC2 and the length of the vector represents the strength of that relationship.

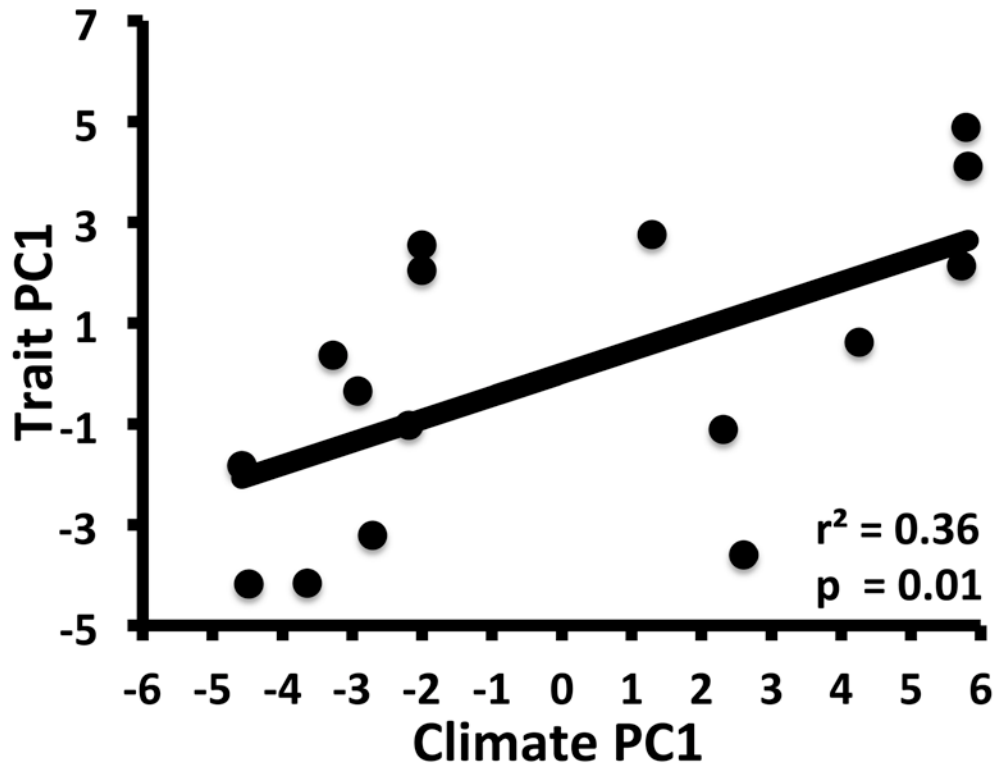


Figure 2.4: Scatter plot and least squares regression of *Arabidopsis thaliana* population scores on the first PC of trait space (vertical axis) on population scores on PC1 of climate space (horizontal axis). P-value for the slope parameter estimate and r-square of the regression line are also presented.

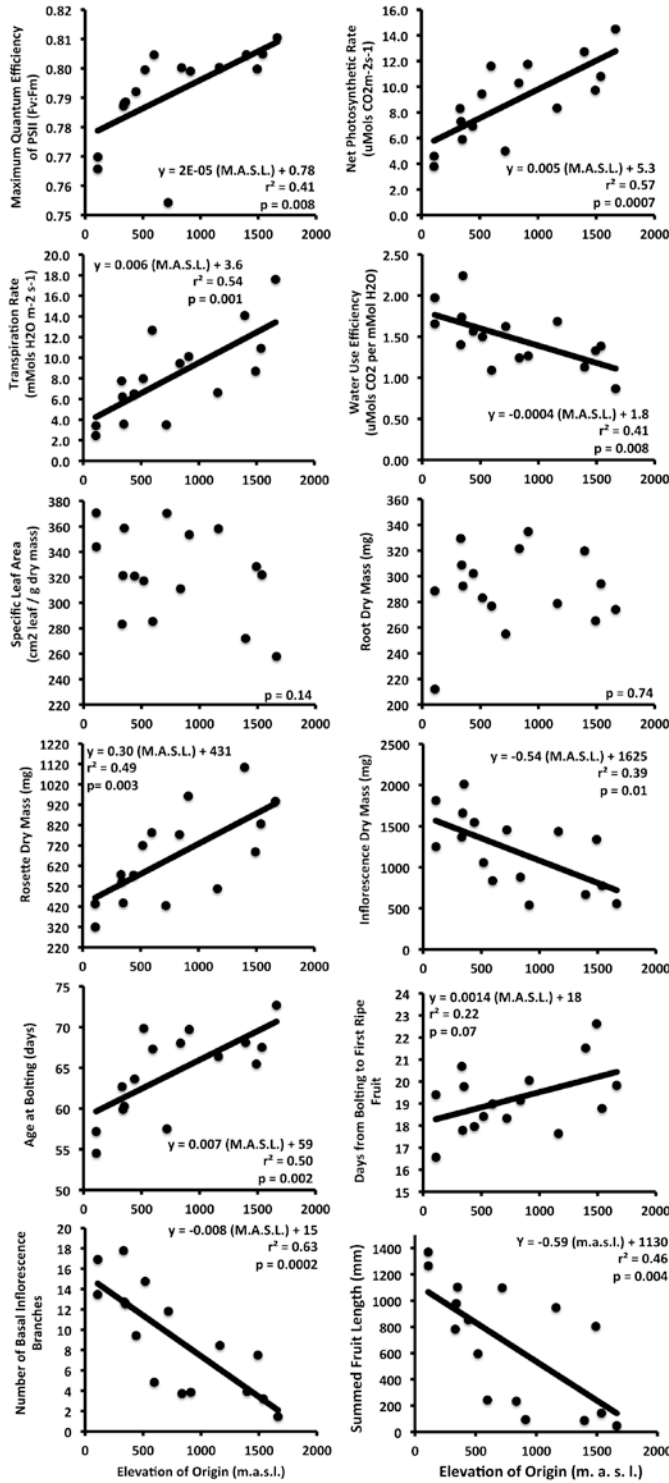


Figure 2.5: Scatter plot and least squares regression of *Arabidopsis thaliana* population-means for each trait (vertical axis) on the elevation of origin (horizontal axis). The line is only shown if $P < 0.10$. Equations for each fitted line, p -values for the slope parameter estimates and r^2 statistics are also provided

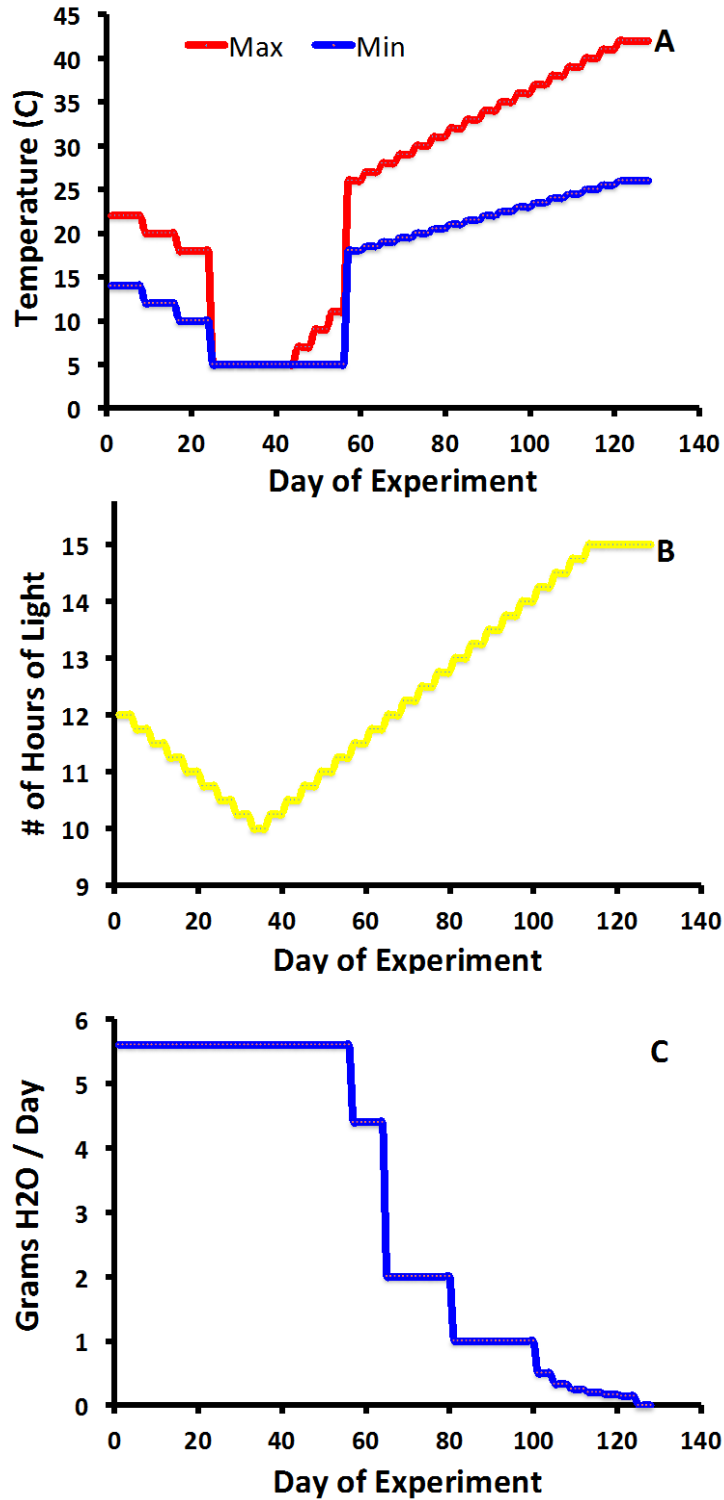


Figure 2.6: Experimental conditions *Arabidopsis thaliana* genotypes were exposed to. Daily minimum and maximum temperatures in degrees Celsius (a). number of hours of light per day (b). Water availability expressed as grams supplied per day (c).

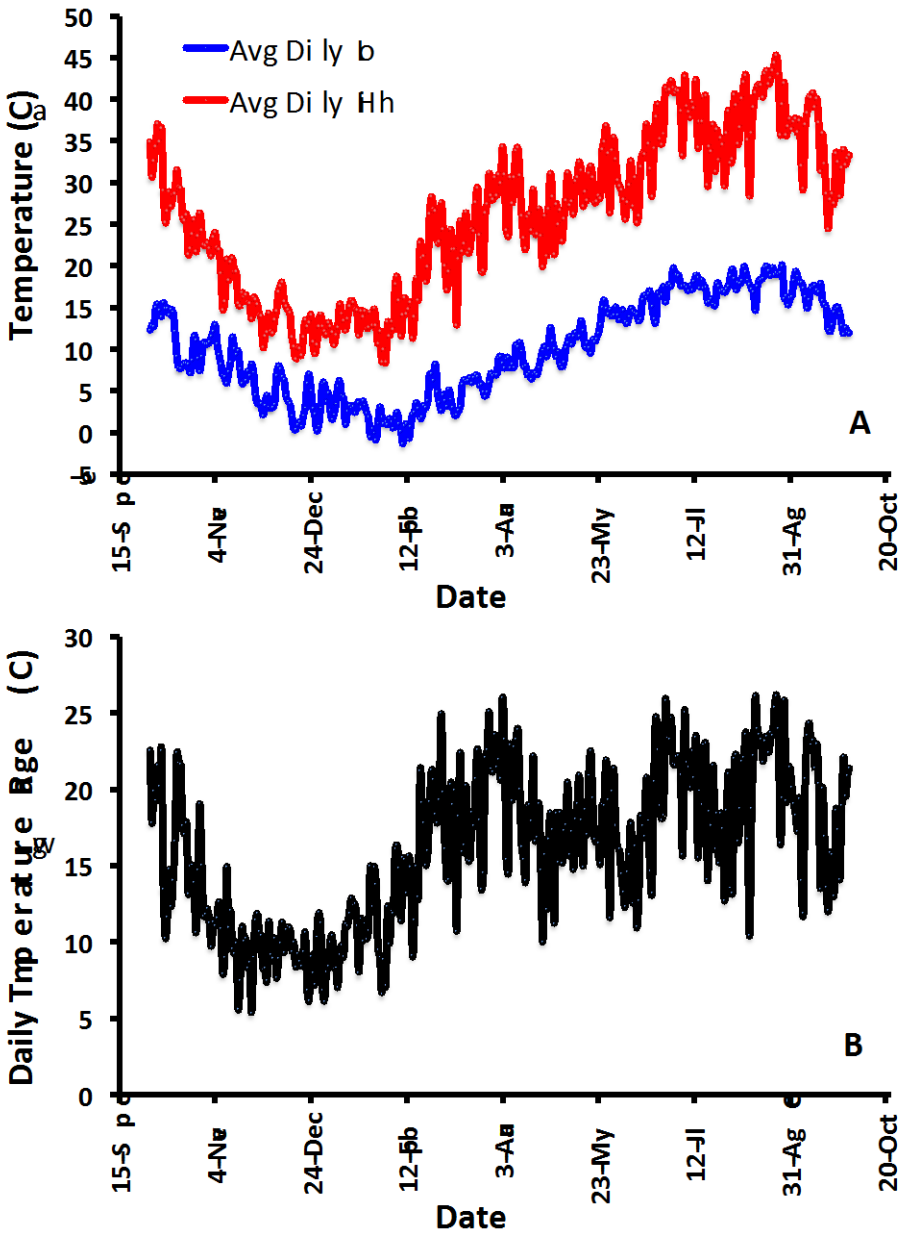


Figure 2.7: Field conditions for low elevation populations of N.E. Spanish *Arabidopsis thaliana*. Daily minimum and maximum temperatures in degrees Celsius (A). Daily temperature range in degrees Celsius (B). Plant height temperature data from field loggers placed at three low elevation sites (BAR, COC and RAB) over multiple years. BAR data are from 2009-2011, COC and RAB data are from 2010-2012. Data are averaged across sites and years within days.

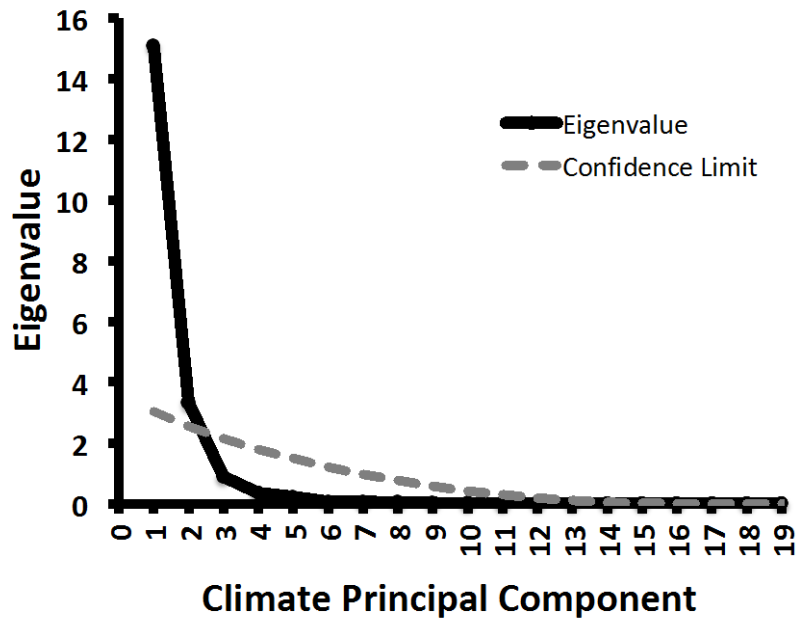


Figure 2.8: Eigenvalues from PCA of *Arabidopsis thaliana* population values for 19 bioclimatic variables (black line). The gray dashed line represents the lower 99% confidence interval on the null hypothesis for eigenvalues based on 5000 randomizations.

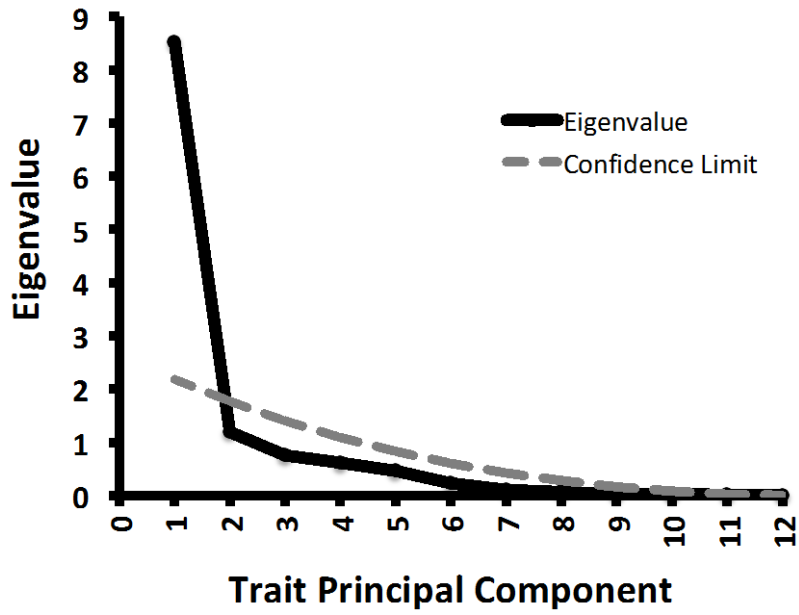


Figure 2.9: Eigenvalues from PCA of *Arabidopsis thaliana* population means for 12 measured traits (black line). The gray dashed line represents the lower 99% confidence interval on the null hypothesis for eigenvalues based on 5000 randomizations.

3.0 ADAPTIVE DIVERGENCE OF *ARABIDOPSIS THALIANA* ROSETTE ECONOMIC SPECTRUM ACROSS A TEMPERATURE AND PRECIPITATION GRADIENT

3.1 INTRODUCTION

The worldwide leaf economic spectrum represents a trade off between leaf traits optimized for resource acquisition versus conservation to which most plant species appear bound. We examine genetic variation in rosette carbon economy among *Arabidopsis thaliana* collected along a climate gradient. We measured three economic traits (lifespan, photosynthesis and mass per area) in a growth chamber experiment. We germinated plants under both fall and spring conditions simulating hot, dry seasons of one extreme of the climate gradient. We reveal a rosette economic spectrum, which is correlated with climate of origin such that plants from hot, dry sites show faster return economies. Additionally, spring germination produced faster economies than fall, regardless of climate, indicating plasticity in rosette economy. Finally, we show that the faster return economic strategy of low elevation plants was favored in this experiment. This work advances our understanding of the role of plant economic constraints in adaptive evolution.

3.2 INTRODUCTION

The worldwide leaf economic spectrum (LES hereafter) describes a trade-off between “fast” and “slow” return leaf tissues and is observed among nearly all plant species examined to date (Wright et al. 2004; Wright et al. 2005a; but see Farnsworth & Ellison 2007; Wright & Sutton-Grier 2012). Plants appear to trade off between leaves with high metabolic and photosynthetic rates per unit mass and a short lifespan (fast return) and leaves with low physiological rates but long lifespans (slow return). Differences among species in leaf economy appear to be adaptive and are often associated with gradients in temperature and precipitation. “Slow return” leaves are generally found in colder, drier northern climates (Reich et al. 1999; Wright et al. 2004; Wright et al. 2005b; Reich et al. 2007; but see Pensa et al. 2009). Variation in leaf economy has also been associated with post-fire regenerative ability (Saura-Mas et al. 2009), invasiveness (Penuelas et al. 2009), leaf litter decomposition rates (Cornwell et al. 2008), plant functional grouping (Wright et al. 2004; Wright et al. 2005 a, b; Reich et al. 2007), disease (Cronin et al. 2010), and can be used to parameterize global vegetation models (Wright et al. 2005a; Shipley et al. 2006a).

Trade-offs within species are thought to involve some combination of constraints imposed by the laws of chemistry and physics (Maynard Smith et al. 1985), as well as those imposed by selection and genetics (Antonovics 1976, Stearns 1989). The LES is thought to have arisen due to biogeographic (Heberling & Fridley 2012), biophysical (Shipley et al. 2006b; Blonder et al. 2011) and genetic constraints (Reich et al. 1999; Lusk et al. 2008; Blonder et al. 2011; Donovan et al. 2011; Vasseur et al. 2012). Cross-species clinal variation in LES associated with climate suggests adaptive divergence in the optimization of the balance between the fitness effects of LES component traits (Reich et al. 1999; Wright et al. 2004; Donovan et al. 2011).

Within species, very little is known about the extent of local differentiation in leaf economics. In a recombinant inbred line population (RIL) of the genetic model organism, *Arabidopsis thaliana*, Vasseur et al. (2012) found that variation along the LES was explained by antagonistic pleiotropy at a few loci. While important for gene discovery, a RIL population represents a very small proportion of the whole species gene pool. With the genes of only two genotypes being compared in a RIL population, it is not possible to make statistical associations between the divergent QTLs observed and hypothetical environmental causes of genetic differentiation. Thus while variation in leaf economics may be associated with local adaptive divergence in *A. thaliana*, the topic remains to be explored.

It seems likely that the same economics approach that has been applied to leaves can be fruitfully applied to the economics of plant parts in general (Freschet et al 2010, Vasseur et al. 2012). With its relatively simple architecture and short life cycle, natural populations of *A. thaliana* collected across a climate gradient in NE Spain make a good system to explore this approach. Here we extend understanding of the economics of the vegetative rosette in *A. thaliana* by testing for adaptive differences in rosette economics along a climate and elevation gradient in NE Spain.

Populations of *A. thaliana* in northeastern Spain occur across an elevation gradient from near sea level at the Mediterranean coast to near tree line in the Pyrenee Mountains. In this system, low elevation sites are hotter and drier overall compared to high elevation sites. The low elevation sites are above freezing for most of the fall and winter, with spring conditions suitable for growth and reproduction being relatively short with rapid warming and drying. In contrast, high elevation sites experience freezing and snow cover during the winter, but are cooler and

wetter during a more prolonged spring reproductive period (Montesinos et al. 2009; Montesinos-Navarro et al. 2011; Wolfe & Tonsor IN PRESS; see supplemental materials).

Bolting time and a number of other life history, growth and allocation traits have been shown to vary according to climate of origin in NE Spanish *A. thaliana* (Montesinos-Navarro et al. 2011; Montesinos-Navarro et al. 2012; Wolfe & Tonsor IN PRESS). Bolting time in *A. thaliana* is generally highly correlated with vegetative lifespan (Levey & Wingler 2005; Balazadeh et al. 2008; Vasseur et al. 2012). Low elevation populations from N.E. Spain exhibit adaptive early bolting and rapid seed production in spring conditions of rapid heating and drying (Wolfe & Tonsor IN PRESS). Since younger age at bolting time is associated with a shorter rosette lifespan, low elevation populations of *A. thaliana* in N.E. Spain exhibit younger age at bolting than high elevation populations, we hypothesized that “fast” return rosette economics would be found among low elevation plants and “slow” return economics would predominate among high elevation populations.

Studies of adaptive differentiation in *A. thaliana* on the N.E. Spanish climate gradient have largely focused on the winter annual life history; (Montesinos et al. 2009; Montesinos-Navarro et al. 2011; Wolfe & Tonsor IN PRESS but see Montesinos-Navarro et al. 2012; Pico 2012). Since reproduction occurs at the same time for both winter and spring annual *A. thaliana* (Pico 2012) a major consequence of fall vs. spring germination is in the total length of the life cycle. In the field at all sites plants are found germinating in both the fall and spring (Montesinos et al. 2009; Pico 2012). Further, in the laboratory all genotypes from N.E. Spain germinate some seeds under both simulated fall and spring germination cues (Montesinos-Navarro et al. 2012). We hypothesized that variation in rosette economic spectrum (RES) may occur both among life history strategies and among populations. We further hypothesized that the RES differentiation

among populations would be associated with climate of origin and that variation among life history types would be associated with length of life cycle, both explainable by the fast-return / slow return trade-off.

In this study, we examined the adaptive significance of variation in rosette economy in a growth chamber experiment that simulated the low elevation seasonal temperatures and late spring drought of N.E. Spain. In this experiment, genotypes from 16 sites along the climate gradient are germinated under both fall and spring conditions. We examined genetic variation in three key economic traits: rosette photosynthetic rate (PHOTO) and rosette mass per area at bolting (RMA), and rosette lifespan (RL). We hypothesized that the experiment's low elevation temperature regime would favor low elevation plants with fast return economies. In this study we accomplished the following aims: First, we tested whether rosette economy varies with elevation and climate of origin. Second, we determined whether rosette economy shifts depending on the season of germination. Finally, we test whether fitness covaries with climate of origin, favoring low elevation plants under low elevation conditions and whether clinal variation in rosette economy predicts genotype performance.

3.3 MATERIALS & METHODS

3.3.1 Collection

The rosette economy data presented in this paper are part of a study designed to measure seasonal growth curves for a number of ecologically important traits. Two genotypes were randomly selected from available seed stores from each of 16 different populations along a

climate gradient in N.E. Spain (Table 2.3). The genotypes have been donated to the Arabidopsis Biological Resource Center (ABRC). Information about the climate gradient and field collections is published elsewhere (Montesinos et al. 2009; Montesinos-Navarro et al. 2011; Montesinos-Navarro et al. 2012; Wolfe & Tonsor IN PRESS). Each genotype has experienced at least two generations of propagation by single seed descent in laboratory-controlled environments to minimize any possible environmental maternal effects.

3.3.2 Planting

We planted both fall and spring cohorts of the 32 experimental genotypes,. Eighteen replicate pots per genotype were germinated in the fall and 10 in the spring plantings. During each round of planting (fall and spring) we planted half of the replicates of each genotype on each of two consecutive days. The spring planting took place 20 weeks after the fall cohort was planted. After planting racks were placed in the dark at 4°C and 100% relative humidity for seven days to induce germination competency. After the cold treatment, racks were transferred into a Conviron PGW36 growth chamber for the remainder of the experiment. Additional details on the planting design and growth set-up can be found in Appendix S1 in Supporting Information.

3.3.3 Seasonal climate conditions

We imposed a dynamic growth chamber cycle in which temperature, day length and water availability varied over a 40-week period. We based the seasonal temperature cycle on field plant-height temperature data from multiple years at four low elevation sites. We also varied day length seasonally. Additionally, a late spring dry-down between weeks 34 and 40 was imposed.

Thus we created an archetype of a low elevation Mediterranean temperature regime, not representing any specific site or year. We conducted two plantings under the seasonal conditions outlined above. The first was under conditions corresponding to the fall (early October) and the second was 20 weeks later under spring conditions (late February). A detailed description of the creation and implementation of the seasonal growth chamber program can be found in Appendix S2.

3.3.4 Sampling design

The nine fall and five spring cohort measurement periods involved destructive sampling. At each time point two replicates of each genotype, one on each of two consecutive days, were sampled from the growth chamber (n=32 plants per day). This had the effect of thinning out growth chamber space as plants grew, minimizing light competition. All examinations of trait changes over time are done at the genotype means level.

At all except each cohort's final sampling date we measured whole plant photosynthesis. For plants with inflorescences, after whole plant measures were conducted, a measurement of inflorescences only was taken (see Earley et al. 2009). This allowed rosette gas exchange rates to be estimated by subtracting inflorescence from whole plant rates. Measures from plants with dead rosettes were not conducted and gas exchange was set to zero in these cases. Measurements commenced one hour after lights turned on in a separate growth chamber whose temperature matched that of the primary growth chamber. Gas exchange measures were made with a LI-6400 XT infrared gas analyzer (IRGA; LI-COR Biosciences, Inc., Lincoln NE) connected to a custom built four-cuvette array (Tonsor & Scheiner 2007; Earley et al. 2009; Tonsor et al. 2013). After

additional measurements rosettes were collected, dried for a week at 70°C and massed, allowing us to express rosette gas exchange rates on a dry mass basis.

After physiological measurements, we recorded the total number of live (TLLN and dead (TDLN) leaves. Rosette status was then calculated as the ratio ($TLLN / (TLLN + TDLN)$), or the proportion of rosette leaves that are alive (Proportion Live Leaves). After leaf counting, we severed each rosette from the root system at the soil surface, flattened under glass and photographed it with a 1cm² area standard obtaining a top down, projected rosette area using a pixel-counting macro (available upon request) in NIH ImageJ 64-bit version 1.47k (<http://rsbweb.nih.gov/ij/>). We then calculated the ratio of rosette dried mass to projected area (rosette mass per area or RMA hereafter). We estimated the summed fruit length, a proxy for total seed number (Wolfe & Tonsor *in press*). Summed fruit length is estimated by multiplying the total number of ripened fruits by the average fruit length. Finally, we conducted weekly censuses, recording age at bolting in days since sowing. Additional details on the sampling design and trait measurements conducted during this study are available in Appendix S3.

3.3.5 Statistical analysis

Our sampling design generated growth curves related to three key leaf economic traits (Rosette photosynthesis per mass, rosette mass per area and proportion live leaves) for each genotype in two germination cohorts. Our goal with the photosynthesis and rosette mass per area data was to estimate values for these two traits at bolting. Plant bolting provides a common developmental time point for comparing traits among genotypes (Vasseur et al. 2012). Trait values at bolting were not directly measured; instead we used nonlinear regression models to estimate the change

in trait values with age and used the intercept of this function with age at bolting to estimate trait value at bolting.

We note that Wright et al. (2004) analyze photosynthetic rates on both per mass and per area bases. While the correlation structure differs depending on the mode of standardization, the patterns were qualitatively similar at the single leaf level, worldwide (Wright et al. 2004). We therefore follow the previously published approach of Vasseur et al. (2012) in presenting per mass standardized photosynthetic rates.

For rosette per-mass photosynthesis we fit a two parameter exponential model: **PHOTO** = $\alpha * e^{(\beta * \text{Age})}$, where α and β are parameters to be estimated and age is in days since sowing. For rosette mass per area we fit a three parameter logistic function for each genotype: **RMA** = $\gamma / (1 + e^{(-\alpha * (\text{Age} * \beta)))}$. For a subset of genotypes, a logistic function would not converge because the growth curves did not reach a threshold or plateau phase prior to senescence. For these genotypes, we fit two parameter exponential functions as in the models of rosette per-mass photosynthesis.

The age at which 5% of rosette leaves remained alive was used to quantify rosette lifespan; at that point we considered the rosette dead. We first fit a two-parameter logistic function: **proportion live leaves** = $1 / (1 + e^{(-\alpha * (\text{Age} * \beta)))}$. We used each genotype's parameter estimates to solve for the age when the proportion of live leaves = 0.05.

We used the SAS PROC NLIN (version 9.3; SAS Institute Inc., Cary, North Carolina, USA) to carry out all nonlinear regressions. We fit the models described above for each genotype in each cohort and calculated model fit as the pseudo r^2 (pseudo $r^2 = 1 - (SS_{\text{Error}} / \text{Corrected } SS_{\text{Total}})$).

Principal components analysis of trait variation (PCA using SAS PROC PRINCOMP) for pooled fall and spring cohorts (n=64) were used to describe the multivariate correlation structure of rosette economy. Randomization tests determined the number of meaningful axes of rosette economy (Perez-Neto et al. 2003; Wolfe & Tonsor IN PRESS). The randomization approach compares the true eigenvalue of each PC to a distribution of eigenvalues obtainable under the null hypothesis that the traits are independent. This was done by independently permuting the order of each variable, then conducting a PCA on the permuted data, repeated 1,000 times. For each PC, if the real eigenvalue was greater than 99% of the null hypothesis distribution of eigenvalues that PC and its eigenvector were considered a significant dimension in multi-trait space (SAS macro program available at <http://www.tonsorlab.pitt.edu>). These will be referred to as “rosette economic PCs”.

In Wolfe & Tonsor (IN PRESS) we showed that 75% of the variation in climate among the 16 N.E. Spanish study sites could be described by the first principal component of a correlation matrix including 19 bioclimatic variables and elevation (Climate PC1 hereafter). Climate PC1 indicates that high elevation populations are relatively cold and wet while low elevation populations are relatively hot and dry (Figure 2.2). We used each population’s mean score on rosette economic PC1 as the dependent variable in a general linear model run in SAS PROC GLM to test for the fixed effect of life history cohort. In the same model, we included each population’s score on climate PC1 as a covariate and tested whether the climate-rosette economy relationship differed between life history cohorts as a difference in slope of the climate-rosette economy relationship between life history cohorts.

Finally, we analyzed the relationship between rosette economic variation and summed fruit length. We use standardized (mean centered, unit variance) genotype mean values of

summed fruit length as the dependent variable in an ANCOVA conducted using SAS PROC GLM. We tested for fitness differences associated with the fixed effect of life history cohort and included as a covariate rosette economy PC1 scores. We also tested for a difference in the fitness effects of economic variation between cohorts as an interaction term between life history cohort and rosette economic PC1 score.

3.4 RESULTS

All nonlinear models PHOTO converged successfully. In the fall cohort, pseudo r^2 ranged from 0.85 to 0.99 with a mean of 0.96. Spring cohort models had an average pseudo r^2 of 0.85 and ranged from 0.16 to 1.00. Parameter estimates were generally significant and visual inspection of the fitted models with insignificant parameter estimates indicate that they still fit the data well (Table 3.3). The logistic function we initially fit to RMA data converged in the majority of cases. All fall cohort models converged with pseudo r^2 ranging from 0.61 to 0.94 with an average of 0.86. All but seven spring cohort models converged and of those that did pseudo r^2 ranged from 0.55 to 1.00 and averaged 0.91 (Table 3.4a). The seven spring genotypes that did not converge for RMA were RAB17, RAB4, BAR4, COC7, VDM17, PAL12 and PAN1. In each case, the plot of rosette mass per area vs. age indicated that these genotypes never entered the deceleration and saturation phase that would have been fit by a logistic function. Instead, for these genotypes we fit a two-parameter exponential function. All seven exponential models converged and pseudo r^2 ranged from 0.64 to 0.95, averaging 0.87 (Table 3.4b). Finally, all models of proportion live leaves vs. age converged with pseudo r^2 ranging 0.83 to 1.00 (mean 0.98) in the Fall and from 0.92 to 1.00 (mean of 0.99) in the Spring (Table 3.5).

We estimated PHOTO and RMA at the age of bolting and rosette lifespan (RL, age when 95% of rosette leaves had died) using the parameter estimates from our nonlinear regressions. Estimated net rosette photosynthesis at bolting ranged from 1.1 to 144.6 and averaged 41.8 ($\sigma = 37.3 \text{ nM CO}_2 \text{ g}^{-1} \text{ s}^{-1}$) while rosette mass per area at bolting averaged 0.015 ($\sigma = 0.005 \text{ g cm}^{-2}$) across cohorts. Bolting ages ranged from 47 to 167.8 days ($\mu = 85.2, \sigma = 27.7$ days) while RLs ranged from 63 to 320.7 days ($\mu = 146.7, \sigma = 61.2$ days) (Table 3.6). Genotype mean trait values (Table S6) and population mean values (Table 3.8) are available in the data supplement.

We tested whether each of the three input traits (PHOTO, RMA and RL) were normally distributed across cohorts. Rosette photosynthesis deviated from normality significantly. To resolve this, we first removed a strong outlier data point (spring genotype PAN5). For this data point, the estimated photosynthetic rate at bolting is extremely low ($\sim 0.01 \text{ nmol CO}_2 \text{ g}^{-1} \text{ s}^{-1}$) which we judged to be unrealistic since all plants have green rosettes at bolting. This genotype, from the highest elevation, (1664 m.a.s.l.) and had the latest bolting date. The remaining values were \log_{10} transformed to obtain a normal distribution for the PCA and all subsequent plots and analyses.

As expected, the three rosette economic traits included in the PCA were highly correlated with each other and with age at bolting (Table 3.9, Figure 3.4). The first principal component (Rosette Economy PC1 hereafter) explained a significant proportion (76.2%) of multivariate genetic variation (Figure 3.1, Table 3.10). Rosette lifespan and rosette mass per area loaded positively onto rosette economy PC1 (0.56 and 0.60 respectively) while rosette photosynthetic rate loaded negatively (-0.56) (Figure 3.1, Table 3.10).

We tested whether cohort altered rosette economy and component traits, whether climate PC1 predicted rosette economy and whether germination season altered the climate-trait

relationships. To do this, we conducted analyses of covariance on rosette economy PC1 score, the three economic traits, age at bolting, and summed fruit length (Table 3.1). Cohort and Climate PC1 effects were significant except for photosynthetic rate at bolting while the interaction effects are significant only for summed fruit length (Table 3.1). Overall, a fall germinating life history and higher values of climate PC1 were positively associated with rosette economy PC1 (Figure 3.2a). Photosynthetic rate was not significantly related to climate PC1 nor was germination cohort (Figure 3.2b). Rosette mass per area was 37% greater in the fall cohort compared to the spring and rose by 51% across the range of climate PC1 values (Figure 3.2c). Rosette lifespan was on average 90 days longer in the fall-germinated cohort and rose 27% (34.9 days) with increasing values of climate PC1 (Figure 3.2d). Plants germinated in the fall were 314% more fecund than spring plants. In the fall cohort (but not the spring) summed fruit length decreased by 34% from the low to the high extremes of climate PC1 (Figure 3.2e). Plants germinated in the spring bolted on average 26.7 days earlier and in both life history cohorts plants from the lower extreme of climate PC1 bolted as much as 35 days earlier than those from the opposite climate extreme (Figure 3.2f).

Analysis of covariance indicated that summed fruit length is predictable based on life history cohort (Figure 3.2e, Figure 3.3, Table 3.1, Table 3.2). Further, we found that in both life history cohorts, a unit decrease in rosette economy PC1 score resulted in a 0.26 standard deviation (69 mm) increase in summed fruit length (Figure 3.3, Table 3.2). The combination of cohort differences and rosette economy differences explained 83% of the total variance in fitness in this study (Table 3.2).

3.5 DISCUSSION

In this study we quantified natural genetic variation in rosette carbon economy among *Arabidopsis thaliana* genotypes from along a climate gradient in Spain. We demonstrate that for the three rosette economic traits measured (lifespan, per mass photosynthesis and mass per area) the correlation structure is similar to that of the worldwide leaf-level economic spectrum of Wright et al. (2004) and the rosette-level economy demonstrated by Vasseur et al. (2012), forming a rosette economic spectrum. We found that climate of origin significantly predicted rosette economy such that low elevation plants from hot, dry Mediterranean sites show faster return, shorter lifespan economies. In addition, we show that, as hypothesized and in accordance with their shorter lifespans, spring-germinated have faster return rosette economies compared to fall-germinated plants. Finally, we link rosette economic variation to variation in fecundity (summed fruit length) under a simulated low elevation temperature regime, indicating that rosette economy is likely to have been under selection in the field.

Our rosette carbon economy traits differ from the single leaf measures of LES. *A. thaliana* is structurally organized in a nested hierarchy of units with the rosette being a photosynthetic unit one level up from that of the leaf. The identity of the rosette as a functional unit is strengthened by the observation that it has a discrete life span in which the leaves contained by the rosette die in concert (Lim et al. 2007; Balazadeh et al. 2008; Vasseur et al. 2012). We can match the LES traits with analogous traits at the rosette level and therefore expect that rosette economic spectrum will match that of the LES. When studying the LES, leaf photosynthetic capacity measures are typically used as indicators of the carbon revenue at any given time over its lifespan. Thus a leaf with a short lifespan can be a net carbon source by having higher assimilation rates. The analogous parameter of rosette carbon economy is the

rosette photosynthesis-lifespan relationship. Similarly, RMA in this study is the whole plant analogue of the single leaf mass per area (LMA), representing the structural carbon investment of the leaf over its lifespan (Diemer & Korner 1996; Shipley et al. 2006a). Rosette mass per area is determined by the LMA of its component leaves and the total number of leaves, i.e. leaf area index (Watson 1958), and the structural carbon content of petioles and the short shoot.

The economic traits measured in this study also differ slightly from Vasseur et al. (2012)'s study of RIL rosette economics in *A. thaliana*. In that study, whole plant rosette leaf mass per area was measured by detaching leaves from the short shoot, removing petioles and measuring total blade mass and area. Total leaf mass per area was therefore dependent on the same factors (e.g. cell size, wall thickness, number) as in prior LES studies (Reich et al. 1999; Vile et al. 2005; Shipley et al. 2006). However, Vasseur et al. (2012) as in this study, measured gas exchange on intact rosettes. Thus the photosynthetic rate estimates in both studies were affected by self-shading and plant architecture (Lake 2004). In contrast to Vasseur et al. (2012) we used projected rosette area for rosette mass per area and whole rosette dry-mass for per-unit mass photosynthesis. This approach comes closer to measuring both the total carbon cost and the carbon gain per unit investment. Ultimately, the differences in trait measurements between our and other economy studies are overshadowed by the fact that the economic trade-off between lifespan, structural investment and physiological rates are strongly manifested across studies.

We found that that plant economy varies not only between genotypes and populations but is also plastic, varying with the season of germination. Many studies in *A. thaliana* have addressed genotypic and environmental cues resulting in variation in germination season and subsequent adaptive value with little focus on other phenotypic characters (Donohue et al. 2005a, b; Korves et al. 2007; Wilczek et al. 2009; Metcalf & Mitchell-Olds 2009; Scarcelli & Kover

2009; Pico 2012). Among N.E. Spanish *A. thaliana* we find that fall and spring germination occurs at all sites across the climate gradient (Montesinos et al. 2009) and that all genotypes hedge their bets and germinate in both seasons (Montesinos-Navarro et al. 2012).

Here we find that all traits except PHOTO and including rosette economy PC1 differ according to germination cohort, supporting our hypothesis that spring germinated plants would exhibit fast return economies through shorter lives and lower rosette mass per area (Table 3.1, Figure 3.3). Changes in environment (i.e. growing season) can sometimes alter trait-trait scaling relationships in addition to overall trait means (Weiner 2004). Therefore, we used a Flury hierarchical analysis (not shown; see Phillips & Arnold 1999) to test for differences between cohorts in the economic correlation structure and found that the cohorts share PCs (same trait-trait relations along PC1) differing only in mean values and the magnitude of variation. This result is in line with Vasseur et al. (2012) who found little genetic variation off the main axis of the rosette economic spectrum. This may suggest either a physiological constraint (Blonder et al. 2011), or that one or a few tightly linked and pleiotropic alleles (Anderson et al. 2011) govern the trait-trait scaling of the RES.

In this study, we demonstrate genetically based clinal variation in rosette economy associated with home-site climate in N.E. Spain. Specifically, we found that low elevation plants from hot, dry Mediterranean sites exhibited fast-return economics (lower rosette economy PC1) compared to high elevation montane plants from cold, moist sites (Figure 3.2). This result is consistent with previous findings indicating that low elevation N.E. Spanish *A. thaliana* are adapted in having a minimal time *and* resource investment in vegetative structures hypothetically as a mechanism for avoiding spring reproductive season heat and drought stress (Montesinos-Navarro et al. 2011; Wolfe & Tonsor IN PRESS). Although fecundity did not vary with climate

of origin in the spring germinated cohort (Figure 3.2, Table 3.1), plants from hot-dry low elevation climates exhibited a fitness advantage in the fall cohort; a result that matches that of Wolfe & Tonsor (IN PRESS). Consistent with those results, in this study both fall and spring cohorts fast-return rosette economy was associated with higher fitness under this experiment's low elevation temperature and watering regime (Figure 3.3; Table 3.2). The cline we observe among populations cannot be easily matched to those of the worldwide clines in LES traits in part because leaf traits are differently modulated among functional groupings (Wright et al. 2005). For example, in deciduous species increased temperature extends leaf lifespan but decreases it for evergreens (Wright et al. 2004). Our example of clinal variation in rosette economy represents a specific example of adaptive divergence and is interpretable in the context of *A. thaliana* life history. In contrast, the clines in the LES depend on myriad factors including biogeography (Heberling & Fridley 2012) and plant functional groupings.

For traits to evolve trait variation must be heritable (Endler 1986). Heritable variation has previously been documented for single and pairs of leaf economic traits in natural populations but without specific reference to the LES (Donovan et al. 2011). Vasseur et al. (2012) contribute significantly to our understanding of LES and genetic basis through quantitative trait locus analysis, but examine a recombinant inbred line population whose parents differ in leaf traits but originate from disparate locations and therefore give us little guidance as to how much local or regional genetic variation might exist in this species. Our demonstration of naturally occurring regional genetic variation in rosette economy provides a key link in understanding the potential microevolutionary origins of the RES. Critically, by linking economic variation with geographic variation in climate we provide the first evidence of adaptive differentiation in RES within a species.

Our examination of rosette economy represents an important step forward in understanding evolutionary causes of variation in leaf and whole plant economics. Here the RES exists because populations evolve their way up and down this trade-off, optimizing the mix of positive and negative effects associated with the trade-off in their home environments. It is an open question whether in addition to contrasting selective regimes, genetic constraints and/or biophysical limitations account for the lack of deviation from the RES (Antonovics 1976, Stearns 1989; Reich et al. 1999; Shipley et al. 2006b; Blonder et al. 2011; Donovan et al. 2011). Future work must ask whether genetic crosses of disparate individuals can produce early bolting genotypes with long-lived rosettes that maintain high photosynthetic rates? Further, if genotypes occasionally arise naturally that do not conform to the rosette or single leaf economic spectrum, does natural selection result in their extinction? Future studies must leverage the power of quantitative genetics and functional genomics (e.g. Vasseur et al. 2012) combined with classical approaches to studying natural selection both in the field and in the lab (e.g. Lande & Arnold 1983; Wade & Kalisz 1990; Donovan et al. 2011) to answer these and other questions and to identify the ultimate source of observed within and among species economic trade offs.

Table 3.1: Tests of life-history cohort, climate-of-origin and interaction effects on rosette economic and related traits. Analyses of covariance results are presented for rosette economy PC1 scores, each rosette economic trait, the summed fruit length and age at bolting. F-tests and corresponding P-values are reported for each of the following model factors: Life History Cohort (fixed effect), Climate PC1 (covariate) and the interaction. Model p-value and r-square are also reported. Each row represents an independent analysis on the trait indicated. Analyses were performed on within-cohort population mean trait values so in all cases n=32.

Trait	Life History Cohort		Climate PC1		LH Cohortx Climate PC1		Model	
	F	P	F	P	F	P	r ²	P
Rosette Economic PC1	15.6	0.0005	7.0	0.01	0.1	0.82	0.45	0.0007
log ₁₀ (Net Rosette Photosynthesis)	2.4	0.13	3.5	0.07	1.0	0.33	0.20	0.1000
Rosette Mass per Area	9.0	0.006	9.0	0.006	0.1	0.8	0.39	0.0027
Rosette Lifespan	61.5	<0.0001	4.8	0.04	0.0	0.88	0.70	<0.0001
Summed Fruit Length	239.2	<0.0001	8.3	0.008	9.4	0.005	0.90	<0.0001
Age at Bolting	13.7	0.0009	12.4	0.002	0.4	0.54	0.49	0.0003

Table 3.2: Relationship between summed fruit length and rosette economy. Here we test for the effect of life history cohort (fixed effect) and within cohort genotype score on rosette economy PC1 (covariate) on summed fruit length (fitness). Both the summed fruit length and rosette economy PC1 score were standardized to mean = 0 and variance = 1 prior to analysis. Selection coefficients (β) and standard errors on the parameter estimates (SE) are presented along with p-values for the t-test ($H_0: \beta = 0$). Additionally, the F-tests and corresponding p-values for each model factor are reported as well as the overall model statistics. N=64.

Model Factor	F	P	Selection Coefficient \pm S.E.	T	P (Parameter $\neq 0$)
Rosette Economy PC1	17.9	<.0001	-0.26 \pm 0.12	-2.13	0.037
Life History Cohort	225.6	<.0001	2.11 \pm 0.14	15.02	< 0.0001
Economy X Cohort	0.54	0.4637	-0.11 \pm 0.015	-0.74	0.46
Model F	95.1				
Model P	< 0.0001				
Model r^2	0.83				

Table 3.3: Results from two parameter exponential nonlinear regression models fit to each genotype in both germination cohort are provided here for rosette per-mass photosynthetic rate versus time. In addition to the parameter estimates, standard errors, 95% confidence intervals, and significance tests are provided for each parameter. Pseudo r-squares are provided as a measure of each model's fit.

FALL GERMINATING COHORT														
		Alpha						Beta						
Elevation	Geno	Estimate	Std. Error	95% Confidence Intervals		t Value	Approx Pr > t	Estimate	Std. Error	95% Confidence Intervals		t Value	Approx Pr > t	Pseudo r-square
				Lower	Upper					Lower	Upper			
109	PIN6	1402.7	528.9	152	2653.5	2.65	0.0328	-0.0423	0.00931	-0.0643	-0.0203	-4.55	0.0026	0.92
109	PIN9	4899.5	2215.5	-339.3	10138.2	2.21	0.0627	-0.0727	0.0124	-0.1021	-0.0433	-5.85	0.0006	0.97
110	RAB17	3143.2	595.5	1735.1	4551.4	5.28	0.0012	-0.0532	0.00495	-0.0649	-0.0415	-10.75	<.0001	0.99
110	RAB4	5342.6	3434.3	-2778.2	13463.4	1.56	0.1637	-0.0736	0.0177	-0.1155	-0.0317	-4.16	0.0043	0.94
332	SPE5	2393.5	907.3	248	4539	2.64	0.0335	-0.0499	0.00976	-0.073	-0.0269	-5.11	0.0014	0.94
332	SPE6	4432.9	716.5	2738.8	6127.1	6.19	0.0005	-0.0645	0.00437	-0.0748	-0.0541	-14.75	<.0001	0.99
340	BAR4	1979.1	340.9	1173	2785.3	5.81	0.0007	-0.0481	0.0044	-0.0585	-0.0377	-10.93	<.0001	0.99
340	BAR9	1621.3	272	978.2	2264.5	5.96	0.0006	-0.046	0.00423	-0.056	-0.036	-10.86	<.0001	0.99
351	HOR16	2530.2	658.3	973.5	4086.9	3.84	0.0063	-0.0545	0.00683	-0.0706	-0.0383	-7.97	<.0001	0.98
351	HOR6	6632.8	1646	2740.6	10525.1	4.03	0.005	-0.0743	0.00684	-0.0905	-0.0581	-10.86	<.0001	0.99
440	ARB10	853.5	224.1	323.5	1383.4	3.81	0.0066	-0.0335	0.00603	-0.0478	-0.0193	-5.56	0.0008	0.94
440	ARB8	2332	284.1	1660.3	3003.6	8.21	<.0001	-0.0539	0.00319	-0.0615	-0.0464	-16.89	<.0001	0.99
519	COC14	2002.6	587.5	613.3	3391.8	3.41	0.0113	-0.0455	0.00739	-0.063	-0.028	-6.16	0.0005	0.95
519	COC7	1080	348.2	256.7	1903.2	3.1	0.0173	-0.0324	0.00731	-0.0497	-0.0151	-4.43	0.003	0.91
597	POB10	2861.7	896.7	741.3	4982.1	3.19	0.0152	-0.0528	0.00817	-0.0721	-0.0334	-6.46	0.0003	0.96
597	POB7	1515.5	298.3	810	2220.9	5.08	0.0014	-0.0416	0.00484	-0.053	-0.0302	-8.6	<.0001	0.97
719	BOSS	1283.6	455.9	205.5	2361.6	2.82	0.0259	-0.0354	0.0083	-0.055	-0.0158	-4.26	0.0037	0.90
719	BOS6	671.7	142.9	333.8	1009.7	4.7	0.0022	-0.0291	0.00464	-0.0401	-0.0182	-6.28	0.0004	0.95
836	MUR15	2788.4	968.6	498	5078.8	2.88	0.0237	-0.0576	0.00922	-0.0794	-0.0358	-6.24	0.0004	0.96
836	MUR17	1205.7	369.1	333	2078.4	3.27	0.0137	-0.0431	0.0076	-0.0611	-0.0252	-5.68	0.0008	0.94
912	VDM17	935.6	169.8	534	1337.1	5.51	0.0009	-0.0325	0.00412	-0.0422	-0.0227	-7.88	0.0001	0.97
912	VDM9	1028.7	396.6	90.9905	1966.4	2.59	0.0357	-0.0313	0.00864	-0.0517	-0.0109	-3.63	0.0084	0.85
1163	ALE10	1370.2	271.3	728.7	2011.6	5.05	0.0015	-0.0385	0.00475	-0.0497	-0.0272	-8.1	<.0001	0.97
1163	ALE12	1184.5	208.9	690.6	1678.4	5.67	0.0008	-0.0384	0.00423	-0.0484	-0.0284	-9.08	<.0001	0.98
1397	BIS11	3682.6	986.7	1349.4	6015.8	3.73	0.0073	-0.0635	0.00723	-0.0806	-0.0464	-8.78	<.0001	0.98
1397	BIS8	3037	1276.7	18.184	6055.9	2.38	0.049	-0.0581	0.0112	-0.0846	-0.0317	-5.2	0.0013	0.95
1491	PAL12	1623.2	383.6	716.2	2530.3	4.23	0.0039	-0.0433	0.00587	-0.0572	-0.0294	-7.37	0.0002	0.97
1491	PAL16	1432.2	399.1	488.5	2375.9	3.59	0.0089	-0.0451	0.007	-0.0616	-0.0285	-6.44	0.0004	0.96
1538	VIE3	926.4	310	193.4	1659.5	2.99	0.0203	-0.0346	0.00776	-0.053	-0.0163	-4.46	0.0029	0.90
1538	VIE6	1110.4	372.6	229.4	1991.4	2.98	0.0205	-0.0407	0.00819	-0.0601	-0.0213	-4.97	0.0016	0.92
1664	PAN1	1377.1	221.2	854	1900.2	6.22	0.0004	-0.0395	0.00389	-0.0487	-0.0303	-10.17	<.0001	0.98
1664	PAN5	928	135.6	607.3	1248.7	6.84	0.0002	-0.0338	0.00336	-0.0417	-0.0258	-10.04	<.0001	0.98

Table 3.3: Continued from previous page.

SPRING GERMINATING COHORT														
Elevation	Geno	Alpha						Beta						Pseudo r-square
		Estimate	Std. Error	95% Confidence		t Value	Approx Pr > t	Estimate	Std. Error	95% Confidence		t Value	Approx Pr > t	
				Lower	Upper					Lower	Upper			
109	PIN6	1885.1	1292.6	-2228.4	5998.7	1.46	0.2408	-0.0624	0.0189	-0.1225	-0.00228	-3.3	0.0456	0.93
109	PIN9	658	385.4	-568.4	1884.4	1.71	0.1863	-0.0458	0.0153	-0.0944	0.00278	-3	0.0576	0.92
110	RAB17	999.2	74.0379	763.5	1234.8	13.5	0.0009	-0.0447	0.00192	-0.0508	-0.0386	-23.25	0.0002	1.00
110	RAB4	835.3	348.7	-274.4	1945	2.4	0.0963	-0.0397	0.0106	-0.0733	-0.006	-3.75	0.0331	0.95
332	SPE5	110	157.2	-390.2	610.2	0.7	0.5345	-0.0119	0.0251	-0.0917	0.0679	-0.47	0.6679	0.16
332	SPE6	1333	281.1	438.4	2227.7	4.74	0.0178	-0.0665	0.00587	-0.0852	-0.0478	-11.33	0.0015	0.99
340	BAR4	1928.2	780.9	-557.1	4413.5	2.47	0.0901	-0.0694	0.0113	-0.1055	-0.0333	-6.11	0.0088	0.98
340	BAR9	1675	47.56	1523.6	1826.3	35.22	<.0001	-0.0545	0.000764	-0.0569	-0.052	-71.28	<.0001	1.00
351	HOR16	1006.4	554.5	-758.2	2771	1.82	0.1671	-0.0486	0.0145	-0.0949	-0.00244	-3.35	0.0441	0.93
351	HOR6	4563.6	389.8	3323.1	5804.1	11.71	0.0013	-0.0852	0.00246	-0.0931	-0.0774	-34.61	<.0001	1.00
440	ARB10	272.2	315.9	-733.3	1277.6	0.86	0.4523	-0.02	0.0247	-0.0986	0.0587	-0.81	0.4786	0.43
440	ARB8	5654.2	743	3289.7	8018.7	7.61	0.0047	-0.0904	0.00381	-0.1025	-0.0782	-23.69	0.0002	1.00
519	COC14	2656.1	1118	-902	6214.1	2.38	0.098	-0.0718	0.0119	-0.1096	-0.0341	-6.06	0.009	0.98
519	COC7	164.2	69.3419	-56.469	384.9	2.37	0.0987	-0.0272	0.00985	-0.0585	0.00416	-2.76	0.0701	0.91
597	POB10	333	165.9	-194.9	860.9	2.01	0.1383	-0.0225	0.011	-0.0576	0.0126	-2.04	0.134	0.83
597	POB7	228.8	75.5827	-11.714	469.4	3.03	0.0564	-0.0242	0.00747	-0.048	-0.00045	-3.24	0.0478	0.93
719	BOS5	649.2	93.5617	351.4	946.9	6.94	0.0061	-0.0323	0.0035	-0.0434	-0.0212	-9.23	0.0027	0.99
719	BOS6	4876.7	71.9034	4647.9	5105.6	67.82	<.0001	-0.0834	0.000424	-0.0847	-0.082	-196.67	<.0001	1.00
836	MUR15	395.3	298.4	-554.4	1345	1.32	0.2772	-0.0284	0.0178	-0.085	0.0282	-1.6	0.2089	0.77
836	MUR17	7700.1	1422	3174.7	12225.6	5.42	0.0124	-0.0887	0.00535	-0.1058	-0.0717	-16.59	0.0005	1.00
912	VDM17	32.2772	40.0363	-95.136	159.7	0.81	0.4791	-0.0108	0.021	-0.0775	0.056	-0.51	0.6433	0.18
912	VDM9	10846.6	865.5	8092.3	13600.9	12.53	0.0011	-0.0939	0.00233	-0.1013	-0.0865	-40.38	<.0001	1.00
1163	ALE10	159.7	159.7	-348.5	667.8	1	0.3911	-0.0138	0.0186	-0.073	0.0454	-0.74	0.5117	0.34
1163	ALE12	9860.7	1383.7	5457.1	14264.3	7.13	0.0057	-0.0899	0.00407	-0.1029	-0.077	-22.09	0.0002	1.00
1397	BIS11	342.4	201.6	-299.1	983.8	1.7	0.188	-0.0215	0.0128	-0.0624	0.0194	-1.67	0.1928	0.76
1397	BIS8	808.8	421.2	-531.6	2149.3	1.92	0.1506	-0.0355	0.0129	-0.0765	0.00559	-2.75	0.0708	0.91
1491	PAL12	577.7	159	71.8443	1083.6	3.63	0.0359	-0.0319	0.00667	-0.0532	-0.0107	-4.79	0.0173	0.97
1491	PAL16	4194.3	622.7	2212.7	6176	6.74	0.0067	-0.0695	0.00416	-0.0828	-0.0563	-16.71	0.0005	1.00
1538	VIE3	763.8	241.4	-4.5728	1532.2	3.16	0.0507	-0.0361	0.00786	-0.0611	-0.0111	-4.59	0.0194	0.96
1538	VIE6	388.9	233.8	-355.1	1133	1.66	0.1948	-0.0255	0.0138	-0.0693	0.0184	-1.85	0.1617	0.82
1664	PAN1	474.2	407.1	-821.4	1769.8	1.16	0.3283	-0.0294	0.0204	-0.0943	0.0356	-1.44	0.2455	0.72
1664	PAN5	34516.8	39827.1	-92231	161264	0.87	0.4499	-0.1353	0.0346	-0.2453	-0.0254	-3.92	0.0296	0.98

Table 3.4: Results from regression models fit to each genotype in both germination cohort are provided here for rosette mass per area versus time. In addition to the parameter estimates, standard errors, 95% confidence intervals, and significance tests are provided for each parameter. Pseudo r-squares are provided as a measure of each model's fit. Three parameter logistic functions are fit in (A) and two parameter exponential functions are reported in (B).

FALL GERMINATED COHORT																				
ALPHA							BETA					GAMMA								
Elevation	Geno	Estimate	Std. Error	95% Confidence		t Value	Approx Pr > t	Estimate	Std. Error	95% Confidence		t Value	Approx Pr > t	Estimate	Std. Error	95% Confidence		t Value	Approx Pr > t	Pseudo r-square
				Lower	Upper					Lower	Upper					Lower	Upper			
109	PIN6	0.0513	0.0283	-0.0179	0.1205	1.81	0.1195	0.0979	0.0485	-0.1108	0.3065	2.02	0.1811	0.0171	0.0014	0.0137	0.0205	12.19	<.0001	0.75
109	PIN9	0.0502	0.0188	0.00425	0.0962	2.67	0.0369	0.1129	0.039	-0.0548	0.2805	2.9	0.1014	0.02	0.00113	0.0172	0.0227	17.76	<.0001	0.88
110	RAB17	0.0315	0.0137	-0.0022	0.0651	2.29	0.062	0.0091	0.0132	-0.0477	0.0659	0.69	0.562	0.0166	0.00123	0.0136	0.0196	13.47	<.0001	0.85
110	RAB4	0.0683	0.0211	0.0166	0.12	3.23	0.0178	0.00824	0.0145	-0.0542	0.0707	0.57	0.6273	0.019	0.000819	0.017	0.021	23.25	<.0001	0.92
332	SPE5	0.0423	0.0151	0.00547	0.0792	2.81	0.0307	0.0246	0.0148	-0.039	0.0883	1.67	0.2376	0.0233	0.00141	0.0198	0.0268	16.5	<.0001	0.90
332	SPE6	0.0797	0.0389	-0.0155	0.1749	2.05	0.0864	0.0386	0.0354	-0.1136	0.1908	1.09	0.3891	0.0194	0.0013	0.0162	0.0226	14.95	<.0001	0.84
340	BAR4	0.0659	0.026	0.00231	0.1296	2.54	0.0443	0.0176	0.0301	-0.1119	0.1471	0.59	0.6173	0.0179	0.00105	0.0153	0.0205	17.02	<.0001	0.87
340	BAR9	0.0734	0.022	0.0196	0.1272	3.34	0.0156	0.0765	0.0168	0.0042	0.1488	4.55	0.045	0.0179	0.000753	0.0161	0.0198	23.81	<.0001	0.93
351	HOR16	0.1501	0.1266	-0.1598	0.46	1.19	0.2808	0.1022	0.0314	-0.0329	0.2373	3.25	0.0828	0.0194	0.00195	0.0147	0.0242	9.96	<.0001	0.61
351	HOR6	0.1086	0.0506	-0.0202	0.2274	2.05	0.0865	0.0855	0.0352	-0.0662	0.2372	2.43	0.1361	0.0187	0.00104	0.0162	0.0213	18.07	<.0001	0.87
440	ARB10	0.0412	0.0159	0.00232	0.0801	2.59	0.041	0.0844	0.1046	-0.3654	0.5343	0.81	0.5041	0.0191	0.00115	0.0163	0.022	16.69	<.0001	0.86
440	ARB8	0.0788	0.0211	0.0271	0.1305	3.73	0.0097	0.0591	0.028	-0.0613	0.1795	2.11	0.169	0.0166	0.000597	0.0152	0.0181	27.87	<.0001	0.94
519	COC14	0.0581	0.025	-0.003	0.1192	2.33	0.059	0.0779	0.0165	0.00669	0.1491	4.71	0.0423	0.0183	0.00117	0.0154	0.0212	15.62	<.0001	0.84
519	COC7	0.0456	0.0181	0.00126	0.09	2.52	0.0455	0.00392	0.0434	-0.183	0.1908	0.09	0.9364	0.0214	0.00137	0.018	0.0248	15.57	<.0001	0.87
597	POB10	0.0453	0.0231	-0.0112	0.1018	1.96	0.0977	0.0702	0.0255	-0.0894	0.1797	2.75	0.1104	0.0251	0.00219	0.0197	0.0304	11.48	<.0001	0.82
597	POB7	0.0452	0.0332	-0.0361	0.1265	1.36	0.2227	0.0591	0.0255	-0.0504	0.1687	2.32	0.1459	0.0239	0.00299	0.0166	0.0312	8	0.0002	0.68
719	BO55	0.0967	0.0383	0.00307	0.1903	2.53	0.0448	0.045	0.02	-0.0411	0.1311	2.25	0.1534	0.0157	0.000752	0.0139	0.0175	20.87	<.0001	0.86
719	BO56	0.0915	0.0661	-0.0702	0.2532	1.39	0.2153	0.1365	0.0703	-0.1658	0.4387	1.94	0.1915	0.0163	0.00139	0.0129	0.0197	11.73	<.0001	0.64
836	MUR15	0.0716	0.0335	-0.0103	0.1535	2.14	0.0762	0.0971	0.1467	-0.5342	0.7284	0.66	0.5762	0.021	0.0014	0.0176	0.0244	15.06	<.0001	0.84
836	MUR17	0.073	0.0295	0.00088	0.1452	2.48	0.048	0.0293	0.0125	-0.0246	0.0832	2.34	0.1441	0.0192	0.00107	0.0166	0.0219	17.91	<.0001	0.87
912	VDM17	0.0562	0.0209	0.00505	0.1074	2.69	0.0361	0.0122	0.0128	-0.0428	0.0671	0.95	0.4412	0.022	0.00131	0.0187	0.0252	16.71	<.0001	0.89
912	VDM9	0.0268	0.0149	-0.0096	0.0633	1.8	0.1215	0.0885	0.0245	-0.0171	0.1941	3.61	0.069	0.0241	0.00329	0.0161	0.0322	7.32	0.0003	0.82
1163	ALE10	0.0559	0.018	0.0117	0.1	3.1	0.0212	0.0253	0.0206	-0.0635	0.114	1.23	0.345	0.0202	0.00104	0.0177	0.0228	19.53	<.0001	0.91
1163	ALE12	0.0589	0.0147	0.0229	0.0949	4	0.0071	0.0389	0.026	-0.0728	0.1507	1.5	0.2727	0.0179	0.000677	0.0163	0.0196	26.47	<.0001	0.94
1397	BIS11	0.0858	0.0254	0.0237	0.148	3.38	0.0149	0.0627	0.0353	-0.089	0.2144	1.78	0.2174	0.023	0.000893	0.0208	0.0252	25.76	<.0001	0.94
1397	BIS8	0.046	0.0214	-0.0064	0.0984	2.15	0.0752	0.0962	0.0557	-0.1435	0.3358	1.73	0.2264	0.0234	0.00177	0.0191	0.0277	13.25	<.0001	0.83
1491	PAL12	0.0558	0.0151	0.0188	0.0928	3.69	0.0102	0.00999	0.0192	-0.0726	0.0926	0.52	0.6549	0.0174	0.000695	0.0157	0.0191	25.07	<.0001	0.93
1491	PAL16	0.034	0.0138	0.00012	0.0679	2.46	0.0494	0.0649	0.0135	0.00697	0.1227	4.82	0.0404	0.0205	0.00147	0.0169	0.0241	13.93	<.0001	0.87
1538	VIE3	0.0424	0.0132	0.01	0.0748	3.2	0.0185	0.0584	0.0156	-0.0086	0.1253	3.75	0.0642	0.0273	0.00148	0.0237	0.031	18.49	<.0001	0.92
1538	VIE6	0.0338	0.0132	0.00154	0.0661	2.56	0.0427	0.0638	0.0479	-0.1421	0.2697	1.33	0.3141	0.0281	0.00208	0.023	0.0332	13.52	<.0001	0.89
1664	PAN1	0.0439	0.0155	0.00596	0.0818	2.83	0.0299	0.0145	0.0182	-0.0636	0.0926	0.8	0.5082	0.0217	0.00127	0.0186	0.0248	17.11	<.0001	0.89
1664	PAN5	0.0557	0.0141	0.0212	0.0902	3.95	0.0075	0.0695	0.00946	0.0287	0.1102	7.34	0.0181	0.0241	0.000969	0.0217	0.0264	24.81	<.0001	0.94

Table 3.4: Continued from previous page.

								SPRING GERMINATED COHORT												
ALPHA								BETA				GAMMA								
95% Confidence								95% Confidence				95% Confidence								
Elevation	Geno	Estimate	Std. Error	Lower	Upper	t Value	Approx Pr > t	Estimate	Std. Error	Lower	Upper	t Value	Approx Pr > t	Estimate	Std. Error	Lower	Upper	t Value	Approx Pr > t	Pseudo r-square
109	PN6	54.7933	10.2273	29.768	79.8185	5.36	0.0017	37.4401	4.5498	17.864	57.0162	8.23	0.0144	0.011	0.000932	0.00699	0.015	11.8	0.0071	0.89
109	PN9	55.5794	7.0712	38.7767	72.8821	7.86	0.0002	48.7267	3.3397	34.3572	63.0961	14.59	0.0047	0.0133	0.000974	0.00909	0.0175	13.64	0.0053	0.96
110	RAB17	62.3637	11.011	35.4208	89.3066	5.66	0.0013	669.8	29574.3	-126578	127918	0.02	0.984	1.7392	452.1	-1943.7	1947.1	0	0.9973	0.95
110	RAB4	53.2914	4.677	41.8473	64.7355	11.39	<.0001	734.5	41734.9	-178836	180305	0.02	0.9876	2.4448	813.9	-3499.5	3504.4	0	0.9979	0.94
332	SPE5	69.3064	7.9676	49.8103	88.8025	8.7	0.0001	93.9171	52.7041	-132.9	320.7	1.78	0.2167	0.0325	0.0165	-0.0387	0.1037	1.96	0.1886	0.96
332	SPE6	57.2466	6.6616	40.9462	73.5469	8.59	0.0001	44.7227	13.3594	-12.758	102.2	3.35	0.0788	0.017	0.003	0.00404	0.0299	5.65	0.0299	0.85
340	BAR4	58.8152	6.3794	43.2053	74.425	9.22	<.0001	-4.541	33.9652	-150.7	141.6	-0.13	0.9059	0.0147	0.00475	-0.0058	0.0351	3.09	0.0907	0.81
340	BAR9	56.1002	4.3663	45.4162	66.7842	12.85	<.0001	45.511	2.5274	34.6364	56.3857	18.01	0.0031	0.0121	0.000523	0.00981	0.0143	23.05	0.0019	0.98
351	HOR16	46.4159	8.969	24.4695	68.3623	5.18	0.0021	41.1482	2.9752	28.3469	53.9495	13.83	0.0052	0.0112	0.000663	0.00833	0.014	16.85	0.0035	0.96
351	HOR6	54.5407	4.8611	42.646	66.4353	11.22	<.0001	41.563	4.4042	22.6132	60.5128	9.44	0.011	0.0115	0.000907	0.00757	0.0154	12.65	0.0062	0.93
440	ARB10	57.349	8.219	37.2378	77.4602	6.98	0.0004	38.5262	12.7854	-16.485	93.5372	3.01	0.0947	0.0125	0.00274	0.00072	0.0243	4.57	0.0448	0.55
440	ARB8	54.117	3.6309	45.2326	63.0014	14.9	<.0001	37.4202	5.7455	12.6991	62.1412	6.51	0.0228	0.0108	0.000821	0.00728	0.0143	13.17	0.0057	0.92
519	COC14	56.131	7.4577	37.8828	74.3793	7.53	0.0003	47.6319	2.4543	37.072	58.1919	19.41	0.0026	0.0144	0.000615	0.0117	0.017	23.39	0.0018	0.98
519	COC7	62.2657	8.2485	42.0824	82.449	7.55	0.0003	984.7	105651	-453596	455566	0.01	0.9934	0.418	152.1	-654	654.9	0	0.9981	0.64
597	POB10	72.3742	11.102	45.2087	99.5397	6.52	0.0006	54.4694	4.5217	35.0141	73.9248	12.05	0.0068	0.016	0.0011	0.0112	0.0207	14.53	0.0047	0.97
597	POB7	71.0184	15.9426	32.0081	110	4.45	0.0043	65.6564	8.1789	30.4655	100.8	8.03	0.0152	0.026	0.00215	0.0167	0.0352	12.06	0.0068	0.98
719	BO55	46.6677	4.6285	35.3422	57.9932	10.08	<.0001	47.0075	6.1772	20.4292	73.5858	7.61	0.0168	0.0129	0.00106	0.00836	0.0175	12.2	0.0067	0.96
719	BO56	44.757	8.4814	24.0037	65.5103	5.28	0.0019	42.0773	4.2618	23.7402	60.4144	9.87	0.0101	0.0127	0.00126	0.00732	0.0182	10.11	0.0096	0.90
836	MUR15	56.5679	6.9756	39.4992	73.6367	8.11	0.0002	57.3187	15.1094	-7.6919	122.3	3.79	0.063	0.0217	0.00617	-0.0048	0.0482	3.52	0.072	0.68
836	MUR17	54.5723	5.8499	40.258	68.8865	9.33	<.0001	88.454	28.7693	-35.331	212.2	3.07	0.0915	0.03	0.00889	-0.0082	0.0683	3.38	0.0776	0.98
912	VDM17	65.0281	6.9144	48.1091	81.9471	9.4	<.0001	607.8	40659	-174334	175549	0.01	0.9894	6.6987	3265.8	-14045	14058.2	0	0.9985	0.95
912	VDM9	90.842	21.0469	39.3421	142.3	4.32	0.005	48.6965	3.0654	35.507	61.8859	15.89	0.0039	0.0127	0.000736	0.00954	0.0159	17.26	0.0033	0.97
1163	ALI10	62.5193	5.9652	47.923	77.1155	10.48	<.0001	49.6187	24.6864	-56.599	155.8	2.01	0.1822	0.0117	0.00314	-0.0018	0.0252	3.73	0.0649	0.93
1163	ALI12	57.8155	4.3453	47.183	68.448	13.31	<.0001	47.2477	10.4221	2.4052	92.0902	4.53	0.0454	0.0128	0.00172	0.00537	0.0202	7.42	0.0177	0.92
1397	BIS11	56.7465	3.7338	47.6102	65.8829	15.2	<.0001	49.3418	7.0205	19.1349	79.5486	7.03	0.0196	0.0169	0.00179	0.0092	0.0246	9.46	0.011	0.91
1397	BIS8	62.8713	9.6467	39.2666	86.4759	6.52	0.0006	44.2353	6.0323	18.2804	70.1901	7.33	0.0181	0.0135	0.0016	0.00661	0.0204	8.44	0.0138	0.87
1491	PAL12	54.727	4.7677	43.061	66.3931	11.48	<.0001	641	43758.4	-187636	188918	0.01	0.9896	2.3054	978.9	-4209.8	4214.4	0	0.9983	0.90
1491	PAL16	68.3053	10.2966	43.1105	93.5001	6.63	0.0006	56.3319	2.7939	44.3107	68.3532	20.16	0.0025	0.0185	0.000712	0.0155	0.0216	26.02	0.0015	0.99
1538	VIF3	72.867	7.1009	55.4918	90.2472	10.26	<.0001	63.1073	4.7186	42.8046	83.41	13.37	0.0055	0.0224	0.00114	0.0175	0.0273	19.67	0.0026	0.99
1538	VIF6	77.0915	10.6615	51.0038	103.2	7.23	0.0004	63.9801	12.4544	10.3933	117.6	5.14	0.0359	0.0237	0.00316	0.0101	0.0373	7.49	0.0174	0.93
1664	PAN1	65.1424	7.5971	46.553	83.7319	8.57	0.0001	537.6	45316.9	-194445	195521	0.01	0.9916	9.2553	5997.9	-25798	25816	0	0.9989	0.92
1664	PAN5	63.0502	4.6954	51.5611	74.5393	13.43	<.0001	63.9604	2.0648	55.0763	72.8444	30.98	0.001	0.0275	0.000626	0.0248	0.0302	43.92	0.0005	1.00

Table 3.4: Continued from previous page.

SPRING GERMINATED COHORT														
		Alpha						Beta						
Elevation	Geno	Estimate	Std. Error	95% Confidence		t Value	Approx Pr > t	Estimate	Std. Error	95% Confidence		t Value	Approx Pr > t	Pseudo r-square
				Lower	Upper					Lower	Upper			
110	RAB17	0.00393	0.000602	0.00201	0.00584	6.53	0.0073	0.00905	0.00128	0.00498	0.0131	7.09	0.0058	0.95
110	RAB4	0.00574	0.000847	0.00305	0.00844	6.78	0.0066	0.0082	0.00125	0.00422	0.0122	6.55	0.0072	0.94
340	BAR4	0.00915	0.000853	0.00644	0.0119	10.73	0.0017	0.00288	0.000917	-3E-05	0.0058	3.15	0.0515	0.77
519	COC7	0.00866	0.00148	0.00394	0.0134	5.83	0.01	0.0038	0.00164	-0.0014	0.00901	2.32	0.1027	0.64
912	VDM17	0.0041	0.000914	0.00119	0.00701	4.48	0.0207	0.0121	0.00176	0.00654	0.0178	6.89	0.0063	0.95
1491	PAL12	0.00382	0.000971	0.00073	0.00692	3.94	0.0292	0.00994	0.00208	0.00333	0.0166	4.78	0.0174	0.90
1664	PAN1	0.00381	0.00154	-0.0011	0.0087	2.48	0.0892	0.0145	0.0031	0.00462	0.0243	4.67	0.0185	0.92

Table 3.5: Results from two parameter logistic nonlinear regression models fit to each genotype in both germination cohort are provided here for the proportion of living rosette leaves versus time. In addition to the parameter estimates, standard errors, 95% confidence intervals, and significance tests are provided for each parameter. Pseudo r-squares are provided as a measure of each model's fit.

FALL GERMINATED COHORT														
		Alpha						Beta						Pseudo r-square
Elevation	Geno	Estimate	Std. Error	95% Confidence		t Value	Approx Pr > t	Estimate	Std. Error	95% Confidence		t Value	Approx Pr > t	
				Lower	Upper					Lower	Upper			
109	PIN6	-0.1392	0.0115	-0.1665	-0.1119	-12.05	<.0001	91.0941	0.7562	89.3061	92.8821	120.47	<.0001	1.00
109	PIN9	-0.0418	0.00692	-0.0581	-0.0254	-6.03	0.0005	120.9	5.1894	108.6	133.1	23.29	<.0001	0.98
110	RAB17	-0.1295	0.039	-0.2217	-0.0372	-3.32	0.0128	111	4.2048	101	120.9	26.39	<.0001	0.99
110	RAB4	-0.0548	0.0089	-0.0758	-0.0337	-6.15	0.0005	83.1968	2.9435	76.2365	90.1571	28.26	<.0001	0.98
332	SPE5	-0.0497	0.00335	-0.0576	-0.0418	-14.83	<.0001	120.9	1.8381	116.6	125.2	65.78	<.0001	1.00
332	SPE6	-0.0424	0.00443	-0.0529	-0.0319	-9.56	<.0001	129.3	3.207	121.7	136.8	40.31	<.0001	0.99
340	BAR4	-0.0507	0.00325	-0.0584	-0.043	-15.6	<.0001	133.5	1.5349	129.8	137.1	86.96	<.0001	1.00
340	BAR9	-0.0638	0.00284	-0.0705	-0.0571	-22.46	<.0001	119.3	1.0555	116.8	121.8	113.03	<.0001	1.00
351	HOR16	-0.0436	0.00408	-0.0533	-0.034	-10.7	<.0001	107.1	2.598	100.9	113.2	41.21	<.0001	0.99
351	HOR6	-0.0401	0.0041	-0.0498	-0.0304	-9.79	<.0001	116.7	3.2596	109	124.4	35.79	<.0001	0.99
440	ARB10	-0.0485	0.00501	-0.0604	-0.0367	-9.69	<.0001	158	2.8129	151.3	164.6	56.16	<.0001	0.99
440	ARB8	-0.0891	0.0147	-0.124	-0.0542	-6.04	0.0005	109.8	2.6666	103.5	116.1	41.18	<.0001	0.99
519	COC14	-0.0401	0.00356	-0.0485	-0.0317	-11.25	<.0001	111.9	2.7589	105.4	118.4	40.55	<.0001	0.99
519	COC7	-0.068	0.00986	-0.0913	-0.0447	-6.9	0.0002	100.6	2.276	95.2192	106	44.2	<.0001	0.99
597	POB10	-0.0447	0.0121	-0.0732	-0.0161	-3.7	0.0077	141.8	7.5523	123.9	159.6	18.77	<.0001	0.95
597	POB7	-0.0275	0.00671	-0.0434	-0.0116	-4.1	0.0046	158.2	11.2588	131.5	184.8	14.05	<.0001	0.91
719	BOS5	-0.2044	0.0292	-0.2733	-0.1354	-7.01	0.0002	75.8382	0.2869	75.1599	76.5166	264.36	<.0001	1.00
719	BOS6	-0.1404	0.00216	-0.1455	-0.1352	-64.93	<.0001	86.9688	0.1633	86.5826	87.355	532.47	<.0001	1.00
836	MUR15	-0.078	0.0228	-0.1319	-0.024	-3.42	0.0112	154.4	5.4121	141.6	167.2	28.53	<.0001	0.97
836	MUR17	-0.0251	0.00819	-0.0445	-0.0058	-3.07	0.0181	203.5	11.5926	176.1	230.9	17.56	<.0001	0.83
912	VDM17	-0.0519	0.00726	-0.0691	-0.0348	-7.15	0.0002	185.9	3.0905	178.6	193.2	60.15	<.0001	0.99
912	VDM9	-0.0335	0.00345	-0.0417	-0.0254	-9.72	<.0001	148.1	4.0601	138.5	157.7	36.48	<.0001	0.99
1163	ALE10	-0.0385	0.00666	-0.0543	-0.0228	-5.79	0.0007	145.1	5.8603	131.2	159	24.76	<.0001	0.97
1163	ALE12	-0.0605	0.0196	-0.1069	-0.0141	-3.08	0.0177	160.5	7.6565	142.4	178.6	20.96	<.0001	0.94
1397	BIS11	-0.0352	0.0028	-0.0418	-0.0286	-12.55	<.0001	129	2.9543	122	136	43.65	<.0001	0.99
1397	BIS8	-0.0575	0.00732	-0.0748	-0.0402	-7.86	0.0001	143.2	2.3521	137.7	148.8	60.9	<.0001	0.99
1491	PAL12	-0.0567	0.00335	-0.0646	-0.0488	-16.93	<.0001	110.5	1.3913	107.2	113.8	79.44	<.0001	1.00
1491	PAL16	-0.0415	0.00485	-0.053	-0.03	-8.56	<.0001	137.3	3.6134	128.8	145.9	38.01	<.0001	0.99
1538	VIE3	-0.0317	0.00418	-0.0416	-0.0219	-7.59	0.0001	151	5.468	138.1	163.9	27.62	<.0001	0.98
1538	VIE6	-0.0605	0.0103	-0.0848	-0.0361	-5.88	0.0006	155.9	3.8161	146.8	164.9	40.84	<.0001	0.99
1664	PAN1	-0.0443	0.0115	-0.0716	-0.017	-3.84	0.0064	170	7.5486	152.1	187.8	22.51	<.0001	0.95
1664	PAN5	-0.0486	0.00812	-0.0678	-0.0294	-5.99	0.0005	160.8	4.5857	149.9	171.6	35.06	<.0001	0.98

Table 3.5: Continued from previous page.

SPRING GERMINATED COHORT														
Elevation	Geno	Alpha						Beta						Pseudo r-square
		Estimate	Std. Error	95% Confidence		t Value	Approx Pr > t	Estimate	Std. Error	95% Confidence		t Value	Approx Pr > t	
				Lower	Upper					Lower	Upper			
109	PIN6	-1.4066	1.78E-07	-1.4066	-1.4066	-8E+06	<.0001	61.2664						1.00
109	PIN9	-1.1921	3.22E-08	-1.1921	-1.1921	-4E+07	<.0001	62.2922						1.00
110	RAB17	-0.8213	0.0453	-0.9654	-0.6772	-18.14	0.0004	63.8916	0.1594	63.3842	64.399	400.74	<.0001	1.00
110	RAB4	-1.4859	2.9746	-9.7447	6.7728	-0.5	0.6436	61.0499						0.99
332	SPE5	-0.0554	0.0105	-0.0888	-0.0219	-5.27	0.0133	91.1925	6.1559	71.6016	110.8	14.81	0.0007	0.98
332	SPE6	-0.867	0.0434	-1.0051	-0.7289	-19.98	0.0003	62.9545	0.0978	62.6432	63.2658	643.55	<.0001	1.00
340	BAR4	-0.8607	0.0436	-0.9995	-0.722	-19.74	0.0003	63.0572	0.1042	62.7255	63.3889	604.98	<.0001	1.00
340	BAR9	-0.8558	0.0436	-0.9947	-0.7169	-19.61	0.0003	63.1567	0.11	62.8067	63.5067	574.26	<.0001	1.00
351	HOR16	-0.0674	0.00787	-0.0925	-0.0424	-8.57	0.0033	97.1144	3.0636	87.3647	106.9	31.7	<.0001	1.00
351	HOR6	-0.8663	0.0434	-1.0044	-0.7282	-19.96	0.0003	62.9678	0.0986	62.6541	63.2816	638.74	<.0001	1.00
440	ARB10	-0.7752	0.054	-0.9472	-0.6033	-14.35	0.0007	65.1522	0.2894	64.2313	66.073	225.16	<.0001	1.00
440	ARB8	-0.0836	0.00503	-0.0996	-0.0676	-16.61	0.0005	93.3205	1.6393	88.1036	98.5373	56.93	<.0001	1.00
519	COC14	-0.0744	0.00698	-0.0967	-0.0522	-10.66	0.0018	89.5223	2.8212	80.5439	98.5007	31.73	<.0001	1.00
519	COC7	-1.1533	2.95E-08	-1.1533	-1.1533	-4E+07	<.0001	62.9965						1.00
597	POB10	-0.0937	0.011	-0.1286	-0.0588	-8.54	0.0034	82.6592	2.9277	73.3419	91.9766	28.23	<.0001	1.00
597	POB7	-0.0903	0.00435	-0.1042	-0.0765	-20.75	0.0002	92.7938	1.308	88.6312	96.9564	70.94	<.0001	1.00
719	BOS5	-0.0597	0.00985	-0.091	-0.0283	-6.06	0.009	89.7555	5.2589	73.0195	106.5	17.07	0.0004	0.99
719	BOS6	-0.8142	0.0461	-0.9608	-0.6676	-17.67	0.0004	64.052	0.1727	63.5023	64.6016	370.87	<.0001	1.00
836	MUR15	-0.7193	0.3112	-1.5834	0.1447	-2.31	0.0819	117.5						0.99
836	MUR17	-0.6741	1.33E-07	-0.6741	-0.6741	-5E+06	<.0001	116.4						1.00
912	VDM17	-0.1084	0.00422	-0.1219	-0.095	-25.7	0.0001	87.8157	1.1052	84.2985	91.3329	79.46	<.0001	1.00
912	VDM9	-0.0807	0.00554	-0.0984	-0.0631	-14.57	0.0007	95.337	1.7545	89.7533	100.9	54.34	<.0001	1.00
1163	ALE10	-0.8074	0.0467	-0.9559	-0.6589	-17.3	0.0004	64.2388	0.1872	63.643	64.8346	343.13	<.0001	1.00
1163	ALE12	-1.2302	0.0482	-1.364	-1.0963	-25.52	<.0001	62.2713						1.00
1397	BIS11	-0.6109	1.43E-06	-0.6109	-0.6109	-4E+05	<.0001	114.9						1.00
1397	BIS8	-0.115	0.00821	-0.1411	-0.0889	-14	0.0008	101.8	1.1121	98.2993	105.4	91.57	<.0001	1.00
1491	PAL12	-0.7765	0.054	-0.9483	-0.6047	-14.38	0.0007	65.0928	0.2845	64.1873	65.9983	228.77	<.0001	1.00
1491	PAL16	-0.078	0.00604	-0.0972	-0.0587	-12.9	0.001	90.8079	2.2812	83.5482	98.0676	39.81	<.0001	1.00
1538	VIE3	-0.0778	0.00728	-0.1009	-0.0546	-10.68	0.0018	87.8693	2.788	78.9968	96.7419	31.52	<.0001	1.00
1538	VIE6	-0.0744	0.00707	-0.0969	-0.0519	-10.51	0.0018	89.3227	2.8638	80.2088	98.4367	31.19	<.0001	1.00
1664	PAN1	-0.7438	4.9627	-14.523	13.0349	-0.15	0.8881	116.9						0.92
1664	PAN5	-0.0589	0.0149	-0.1064	-0.0114	-3.95	0.029	104.7	5.6466	86.692	122.6	18.54	0.0003	0.98

Table 3.6: Basic descriptive statistics within and across cohorts for rosette per-mass photosynthetic rate and rosette mass per area at bolting, rosette lifespan, age at bolting and summed fruit length.

Across Cohorts					
	Rosette				
	Photosynthetic Rate at Bolting (nM CO₂ g⁻¹ s⁻¹)	Rosette Mass Per Area at Bolting (g cm⁻²)	Rosette Lifespan (Days Since Sowing)	Age at Bolting (Days Since Sowing)	Summed Fruit Length (mm)
Mean	41.8	0.01510	146.7	85.2	375.6
Min	1.1	0.00610	63.0	47.0	7.2
Max	144.6	0.03110	320.7	167.8	962.4
Std. Dev.	37.3	0.00547	61.2	27.7	265.1

Fall Germinated Cohort					
	Rosette				
	Photosynthetic Rate at Bolting (nM CO₂ g⁻¹ s⁻¹)	Rosette Mass Per Area at Bolting (g cm⁻²)	Rosette Lifespan (Days Since Sowing)	Age at Bolting (Days Since Sowing)	Summed Fruit Length (mm)
Mean	35.1	0.01741	192.0	98.5	601.7
Min	2.1	0.00830	90.2	59.6	369.4
Max	144.6	0.02430	320.7	167.8	962.4
Std. Dev.	38.7	0.00405	48.2	27.5	160.5

Spring Germinated Cohort					
	Rosette				
	Photosynthetic Rate at Bolting (nM CO₂ g⁻¹ s⁻¹)	Rosette Mass Per Area at Bolting (g cm⁻²)	Rosette Lifespan (Days Since Sowing)	Age at Bolting (Days Since Sowing)	Summed Fruit Length (mm)
Mean	48.8	0.01279	101.4	71.8	142.3
Min	1.1	0.00610	63.0	47.0	7.2
Max	129.4	0.03110	154.6	145.0	404.4
Std. Dev.	35.0	0.00579	32.4	20.7	88.7

Table 3.7: Genotype mean trait values within each cohort for rosette per-mass photosynthetic rate and rosette mass per area at bolting, rosette lifespan, age at bolting, summed fruit length and score on rosette economy PC1.

Germination Cohort	Genotype	Elevation of Origin (m.a.s.l.)	Climate PC1 Score	Rosette Photosynthetic Rate at Bolting (nM CO ₂ g ⁻¹ s ⁻¹)	Rosette Mass Per Area at Bolting (g cm ⁻²)	Rosette Lifespan (Days Since Sowing)	Age at Bolting (Days Since Sowing)	Summed Fruit Length (mm)	Rosette Economy PC1 Score
Fall	BAR4	340	-4.58	35.6	0.0150	191.6	83.6	863.9	0.259
Fall	BAR9	340	-4.58	29.5	0.0163	165.4	87.2	823.1	0.258
Fall	RAB17	110	-4.48	113.4	0.0083	133.7	62.4	622.0	-1.613
Fall	RAB4	110	-4.48	65.3	0.0116	137.0	59.9	528.4	-0.930
Fall	PIN6	109	-3.65	79.1	0.0113	112.3	67.9	762.1	-1.286
Fall	PIN9	109	-3.65	14.7	0.0154	191.4	79.8	550.6	0.751
Fall	COC14	519	-3.28	47.4	0.0150	185.4	82.3	577.6	0.062
Fall	COC7	519	-3.28	112.9	0.0125	143.9	69.6	900.8	-1.044
Fall	SPE5	332	-2.92	10.9	0.0195	180.1	107.9	663.6	1.260
Fall	SPE6	332	-2.92	16.5	0.0177	198.7	86.8	962.4	1.020
Fall	HOR16	351	-2.71	25.0	0.0194	174.6	84.8	490.0	0.778
Fall	HOR6	351	-2.71	14.1	0.0178	190.1	82.8	824.5	1.025
Fall	ARB10	440	-2.19	38.8	0.0155	218.6	92.3	541.2	0.518
Fall	ARB8	440	-2.19	33.7	0.0145	142.9	78.6	778.9	-0.214
Fall	MUR15	836	-2.00	3.3	0.0208	192.2	117.1	619.6	2.119
Fall	MUR17	836	-2.00	4.5	0.0192	320.7	129.4	439.9	2.953
Fall	POB10	597	-2.00	10.3	0.0207	207.7	106.6	492.2	1.673
Fall	POB7	597	-2.00	9.8	0.0216	265.2	121.1	596.2	2.333
Fall	VDM17	912	1.29	21.3	0.0208	242.6	116.4	572.4	1.642
Fall	VDM9	912	1.29	23.5	0.0167	235.9	120.7	482.4	1.062
Fall	ALE10	1163	2.31	16.4	0.0192	221.5	115.0	560.2	1.399
Fall	ALE12	1163	2.31	26.1	0.0165	209.2	99.4	450.6	0.747
Fall	BOS5	719	2.61	144.6	0.0127	90.2	61.7	725.8	-1.634
Fall	BOS6	719	2.61	118.2	0.0130	107.9	59.6	553.0	-1.337
Fall	PAL12	1491	4.26	61.4	0.0133	162.5	75.6	787.9	-0.476
Fall	PAL16	1491	4.26	10.1	0.0165	208.3	109.8	495.8	1.217
Fall	VIE3	1538	5.73	13.8	0.0243	243.8	121.5	446.4	2.263
Fall	VIE6	1538	5.73	9.8	0.0222	204.6	116.3	445.2	1.846
Fall	PAN1	1664	5.79	2.1	0.0214	236.4	164.4	386.4	2.828
Fall	PAN5	1664	5.79	3.2	0.0240	221.4	167.8	460.5	2.762
Fall	BIS11	1397	5.82	4.0	0.0227	212.6	107.6	369.4	2.434
Fall	BIS8	1397	5.82	3.3	0.0216	194.5	117.2	480.1	2.233

Table 3.7: Continued from previous page.

Germination		Elevation of	Climate PC1	Rosette Photosynth etic Rate at	Rosette Mass Per Area at	Rosette Lifespan	Age at Bolting	Summed	Rosette
Cohort	Genotype	Origin {m.a.s.l.}	Score	Bolting (nM CO ² g ⁻¹ s ⁻¹)	Bolting (g cm ⁻²)	{Days Since Sowing}	{Days Since Sowing}	Fruit Length {mm}	Economy PC1 Score
Spring	BAR4	340	-4.58	22.3	0.0110	66.5	64.3	111.9	-1.101
Spring	BAR9	340	-4.58	42.8	0.0102	66.6	67.3	182.7	-1.526
Spring	RAB17	110	-4.48	111.9	0.0061	67.5	49.0	105.6	-2.460
Spring	RAB4	110	-4.48	129.4	0.0084	63.0	47.0	118.0	-2.311
Spring	PIN6	109	-3.65	100.4	0.0079	63.4	47.0	275.4	-2.241
Spring	PIN9	109	-3.65	42.2	0.0104	64.8	60.0	159.2	-1.510
Spring	COC14	519	-3.28	24.2	0.0115	129.1	65.4	120.0	-0.515
Spring	COC7	519	-3.28	38.7	0.0106	65.5	53.2	108.1	-1.434
Spring	SPE5	332	-2.92	41.4	0.0139	144.4	82.3	36.6	-0.371
Spring	SPE6	332	-2.92	14.9	0.0120	66.4	67.6	77.1	-0.786
Spring	HOR16	351	-2.71	48.8	0.0100	140.8	62.2	87.2	-0.929
Spring	HOR6	351	-2.71	34.2	0.0091	66.4	57.4	337.7	-1.532
Spring	ARB10	440	-2.19	83.2	0.0107	69.0	59.4	293.1	-1.782
Spring	ARB8	440	-2.19	23.2	0.0086	128.6	60.8	151.0	-0.820
Spring	MUR15	836	-2.00	39.6	0.0197	121.6	81.0	121.3	0.101
Spring	MUR17	836	-2.00	1.1	0.0175	120.7	99.8	37.3	1.645
Spring	POB10	597	-2.00	69.0	0.0119	114.1	70.0	133.4	-1.130
Spring	POB7	597	-2.00	26.5	0.0207	125.4	89.0	36.8	0.453
Spring	VDM17	912	1.29	13.9	0.0106	115.0	78.3	141.0	-0.463
Spring	VDM9	912	1.29	7.0	0.0118	131.8	78.3	108.4	0.178
Spring	ALE10	1163	2.31	66.4	0.0069	67.9	63.6	404.4	-2.107
Spring	ALE12	1163	2.31	33.1	0.0083	64.7	63.3	177.5	-1.621
Spring	BOS5	719	2.61	127.0	0.0070	139.1	50.5	132.2	-1.773
Spring	BOS6	719	2.61	82.0	0.0092	67.7	49.0	112.8	-1.955
Spring	PAL12	1491	4.26	78.9	0.0071	68.9	62.3	84.3	-2.159
Spring	PAL16	1491	4.26	14.6	0.0155	128.6	81.4	195.4	0.187
Spring	VIE3	1538	5.73	22.1	0.0198	125.7	98.3	7.2	0.447
Spring	VIE6	1538	5.73	47.8	0.0181	128.9	82.3	114.6	-0.115
Spring	PAN1	1664	5.79	6.7	0.0311	120.9	145.0		2.277
Spring	PAN5	1664	5.79		0.0265	154.6	110.3	235.3	
Spring	BIS11	1397	5.82	66.8	0.0142	119.7	76.0	87.3	-0.806
Spring	BIS8	1397	5.82	51.7	0.0130	127.4	77.5	118.2	-0.747

Table 3.8: Population mean trait values within each cohort for rosette per-mass photosynthetic rate and rosette mass per area at bolting, rosette lifespan, age at bolting, summed fruit length and score on rosette economy PC1.

Germination Cohort	Population	Elevation of Origin (m.a.s.l.)	Climate PCI Score	Rosette Photosynthetic Rate at Bolting (nM CO ₂ g ⁻¹ s ⁻¹)	Rosette Mass Per Area at Bolting (g cm ⁻²)	Rosette Lifespan (Days Since Sowing)	Age at Bolting (Days Since Sowing)	Summed Fruit Length (mm)	Rosette Economy PCI Score
Fall	ALE	1163	2.31	21.2	0.0178	215.3	107.2	505.4	1.073
Fall	ARB	440	-2.19	36.2	0.0150	180.7	85.4	660.0	0.152
Fall	BAR	340	-4.58	32.5	0.0156	178.5	85.4	843.5	0.258
Fall	BIS	1397	5.82	3.7	0.0222	203.5	112.4	424.7	2.333
Fall	BOS	719	2.61	131.4	0.0129	99.1	60.7	639.4	-1.486
Fall	COC	519	-3.28	80.1	0.0138	164.6	76.0	739.2	-0.491
Fall	HOR	351	-2.71	19.6	0.0186	182.3	83.8	657.2	0.902
Fall	MUR	836	-2.00	3.9	0.0200	256.4	123.3	529.7	2.536
Fall	PAL	1491	4.26	35.8	0.0149	185.4	92.7	641.8	0.371
Fall	PAN	1664	5.79	2.6	0.0227	228.9	166.1	423.5	2.795
Fall	PIN	109	-3.65	46.9	0.0134	151.8	73.9	656.3	-0.267
Fall	POB	597	-2.00	10.1	0.0212	236.4	113.8	544.2	2.003
Fall	RAB	110	-4.48	89.3	0.0100	135.3	61.1	575.2	-1.271
Fall	SPE	332	-2.92	13.7	0.0186	189.4	97.3	813.0	1.140
Fall	VDM	912	1.29	22.4	0.0187	239.2	118.6	527.4	1.352
Fall	VIE	1538	5.73	11.8	0.0232	224.2	118.9	445.8	2.055
Spring	ALE	1163	2.31	49.7	0.0076	66.3	63.5	291.0	-1.864
Spring	ARB	440	-2.19	53.2	0.0097	98.8	60.1	222.0	-1.301
Spring	BAR	340	-4.58	32.6	0.0106	66.5	65.8	147.3	-1.314
Spring	BIS	1397	5.82	59.3	0.0136	123.6	76.8	102.7	-0.777
Spring	BOS	719	2.61	104.5	0.0081	103.4	49.8	122.5	-1.864
Spring	COC	519	-3.28	31.5	0.0110	97.3	59.3	114.1	-0.975
Spring	HOR	351	-2.71	41.5	0.0096	103.6	59.8	212.4	-1.231
Spring	MUR	836	-2.00	20.4	0.0186	121.2	90.4	79.3	0.873
Spring	PAL	1491	4.26	46.8	0.0113	98.7	71.9	139.8	-0.986
Spring	PAN	1664	5.79	6.7	0.0288	137.7	127.7	235.3	2.277
Spring	PIN	109	-3.65	71.3	0.0091	64.1	53.5	217.3	-1.876
Spring	POB	597	-2.00	47.8	0.0163	119.7	79.5	85.1	-0.338
Spring	RAB	110	-4.48	120.6	0.0073	65.3	48.0	111.8	-2.386
Spring	SPE	332	-2.92	28.1	0.0130	105.4	74.9	56.8	-0.578
Spring	VDM	912	1.29	10.4	0.0112	123.4	78.3	124.7	-0.143
Spring	VIE	1538	5.73	34.9	0.0190	127.3	90.3	60.9	0.166

Table 3.9: Genotype mean correlation matrix for rosette per-mass photosynthetic rate and rosette mass per area at bolting, rosette lifespan, age at bolting and summed fruit length. In each cell, the top row represents the pearson product-moment correlation coefficient, the middle row includes the p-value for the two-tailed test of the hypothesis that the correlation is zero and the bottom contains the sample size.

Pearson Correlation Coefficients Prob > r under H0: Rho=0 Number of Observations					
	SummedFruitLength	log10Photo	RMA	Lifespan	Days2Bolt
SummedFruitLength	1.00000	-0.04840	0.28213	0.50610	0.27176
		0.7087	0.0251	<.0001	0.0312
	63	62	63	63	63
log10Photo	-0.04840	1.00000	-0.69528	-0.56094	-0.78603
	0.7087		<.0001	<.0001	<.0001
	62	63	63	63	63
RMA	0.28213	-0.69528	1.00000	0.67247	0.87096
	0.0251	<.0001		<.0001	<.0001
	63	63	64	64	64
Lifespan	0.50610	-0.56094	0.67247	1.00000	0.77540
	<.0001	<.0001	<.0001		<.0001
	63	63	64	64	64
Days2Bolt	0.27176	-0.78603	0.87096	0.77540	1.00000
	0.0312	<.0001	<.0001	<.0001	
	63	63	64	64	64

Table 3.10: Rosette economy PCA results. Each column contains information for one of the three principal components. Each row of the first subsection contains the loading for an individual variable onto each of the three PCs. The second subsection contains eigenvalues, 99% significance thresholds and variance explained for each PC.

Variable	Loadings		
	PC1	PC2	PC3
Rosette Photosynthetic Rate (log10)	-0.56	0.70	0.43
Rosette Mass Per Area (RMA)	0.60	-0.01	0.80
Rosette Lifespan	0.56	0.71	-0.42
	PC1	PC2	PC3
Eigenvalue	2.30	0.44	0.26
Upper 99% PC Significance Threshold	1.48	1.12	0.97
Prop. of Variance Explained by PC	0.77	0.15	0.09

Table 3.11: Daily high and low temperatures, day length, water table height and total daily water supply (in grams) per pot for each week of the experiment. Standard errors are given for temperature data as they represent averages from multiple sites and years based on data logger data. The actual growth chamber program did not incorporate the temperature variance reported below.

Weekly Chamber Program	Daily High Temperature (\pmSE, °C)		Daily Low Temperature (\pmSE, °C)		Day Length (hours)	Water Table Height (inches)	Grams of Water Per Day
1	18.0		12.0		12.0		
2	18.0		12.0		12.0		
3	19.8 \pm 0.7		9.2 \pm 0.3		10.7	7	2.8
4	21.2 \pm 0.6		10.2 \pm 0.2		10.4	4	1.6
5	19.3 \pm 0.9		7.6 \pm 0.7		10.1	4	1.6
6	17.2 \pm 0.5		7.3 \pm 0.6		9.8	4	1.6
7	15.7 \pm 0.3		7.3 \pm 0.6		9.6	4	1.6
8	13.3 \pm 0.4		4.2 \pm 0.2		9.4	4	1.6
9	14.8 \pm 0.7		6.2 \pm 0.8		9.3	4	1.6
10	12.7 \pm 1.3		4.0 \pm 1.0		9.2	4	1.6
11	9.2 \pm 0.7		4.0 \pm 1.0		9.1	4	1.6
12	10.9 \pm 0.4		4.0 \pm 0.8		9.1	4	1.6
13	10.7 \pm 0.7		4.1 \pm 0.8		9.2	4	1.6
14	12.1 \pm 0.4		4.6 \pm 0.5		9.3	4	1.6
15	13.6 \pm 0.4		5.3 \pm 0.3		9.5	4	1.6
16	12.5 \pm 0.2		4.0 \pm 0.5		9.7	4	1.6
17	12.4 \pm 0.7		4.0 \pm 0.4		9.9	4	1.6
18	15.9 \pm 1.0		4.1 \pm 0.2		10.2	4	1.6
19	12.7 \pm 0.8		4.0 \pm 0.2		10.5	4	1.6
20	16.0 \pm 1.0		5.4 \pm 0.4		10.8	4	1.6
21	19.9 \pm 0.7		7.7 \pm 0.3		11.1	4	1.6
22	16.6 \pm 1.2		4.2 \pm 0.7		11.4	4	1.6
23	16.7 \pm 1.1		5.1 \pm 0.8		11.8	4	1.6
24	20.8 \pm 0.8		6.4 \pm 0.4		12.1	4	1.6
25	21.3 \pm 0.7		6.0 \pm 0.6		12.4	4	1.6
26	24.9 \pm 0.6		7.8 \pm 0.3		12.8	4	1.6
27	25.7 \pm 1.5		9.8 \pm 0.6		13.1	4	1.6
28	22.6 \pm 0.9		7.3 \pm 0.1		13.4	4	1.6
29	25.7 \pm 1.5		10.4 \pm 0.6		13.7	4	1.6
30	25.9 \pm 0.9		10.4 \pm 0.4		14.0	4	1.6
31	26.4 \pm 0.6		11.5 \pm 0.2		14.3	4	1.6
32	27.0 \pm 0.5		11.5 \pm 0.4		14.6	4	1.6
33	33.3 \pm 0.9		14.0 \pm 0.7		14.8	4	1.6
34	31.9 \pm 1.1		14.0 \pm 0.6		15.0	3.5	1.4
35	30.1 \pm 0.5		13.9 \pm 0.4		15.1	3	1.2
36	35.8 \pm 0.9		16.4 \pm 0.3		15.2	2.5	1
37	36.1 \pm 0.6		16.2 \pm 0.4		15.3	2	0.8
38	36.9 \pm 0.8		16.1 \pm 0.5		15.3	1.5	0.6
39	38.7 \pm 1.0		18.8 \pm 0.4		15.2	0	0
40	36.8 \pm 0.9		18.0 \pm 0.4		15.1	0	0

Table 3.12: The week, plant age and growth chamber conditions for each sampling time point is shown for both fall and spring germinated cohorts. Additionally, the pot types sampled at each time point are listed (see Appendix A.3 in Supporting Information for details).

Fall Germinating Cohort							
Harvest #	Week of Experiment	Age At Harvest (Days)	Daily High Temp (°C)	Daily Low Temp (°C)	Day Length (hours)	Water supply (g pot⁻¹ day⁻¹)	Pot Types
1	4	35	21.2	10.2	10.4	1.6	RLC3
2	7	56	15.7	7.3	9.6	1.6	RLC3
3	10	77	12.7	4.0	9.2	1.6	SC10
4	13	98	10.7	4.1	9.2	1.6	SC10
5	19	140	12.7	4.0	10.5	1.6	SC10
6	25	182	21.3	6.0	12.4	1.6	SC10
7	29	210	25.7	10.4	13.7	1.6	SC10
8	32	231	27.0	11.5	14.6	1.6	SC10
9	34	244	31.9	14.0	15.0	1.4	SC10

Spring Germinating Cohort							
Harvest #	Week of Experiment	Age At Harvest (Days)	Daily High Temp (°C)	Daily Low Temp (°C)	Day Length (hours)	Water supply (g pot⁻¹ day⁻¹)	Sample Size (Pot Type)
1	24	33	20.8	6.4	12.1	1.6	RLC3 & SC10
2	26	47	24.9	7.8	12.8	1.6	RLC3 & SC10
3	28	61	22.6	7.3	13.4	1.6	RLC3 & SC10
4	36	117	35.8	16.4	15.2	1	SC10
5	40	145	36.8	18.0	15.1	0	SC10

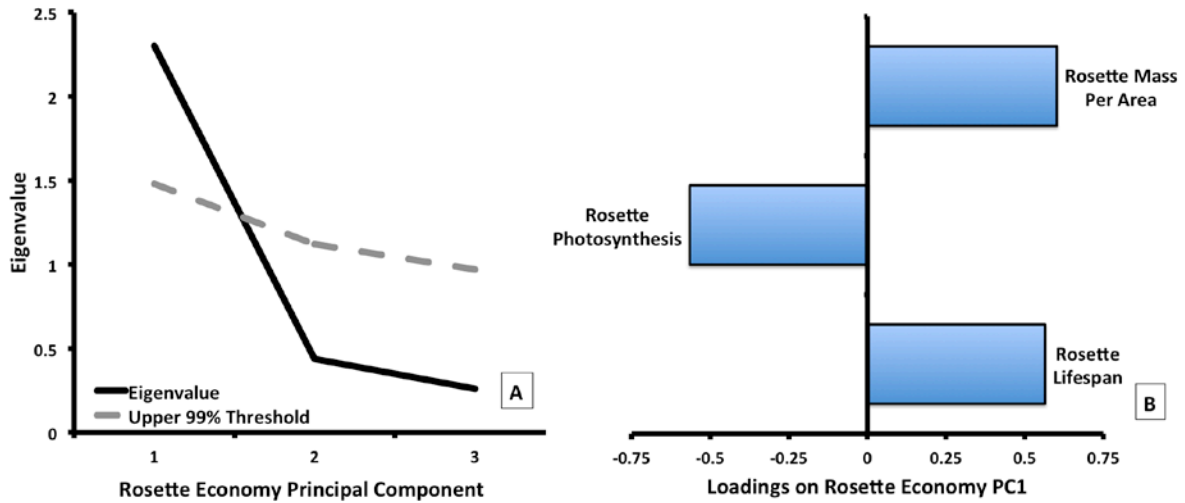


Figure 3.1: Rosette economy PCA results. Eigenvalues for a PCA of three rosette economic traits (AM, RMA and RL) are plotted against the upper 99% limit of the distribution of eigenvalues under the null hypothesis of random correlation structure (A). Eigenvector coefficients (loadings) of the 3 rosette economic variables onto the first PC of trait space (B). The sign of each loading indicates whether trait values increase or decrease with increasing scores on rosette economy PC1 and also indicates the relationship between each trait pair.

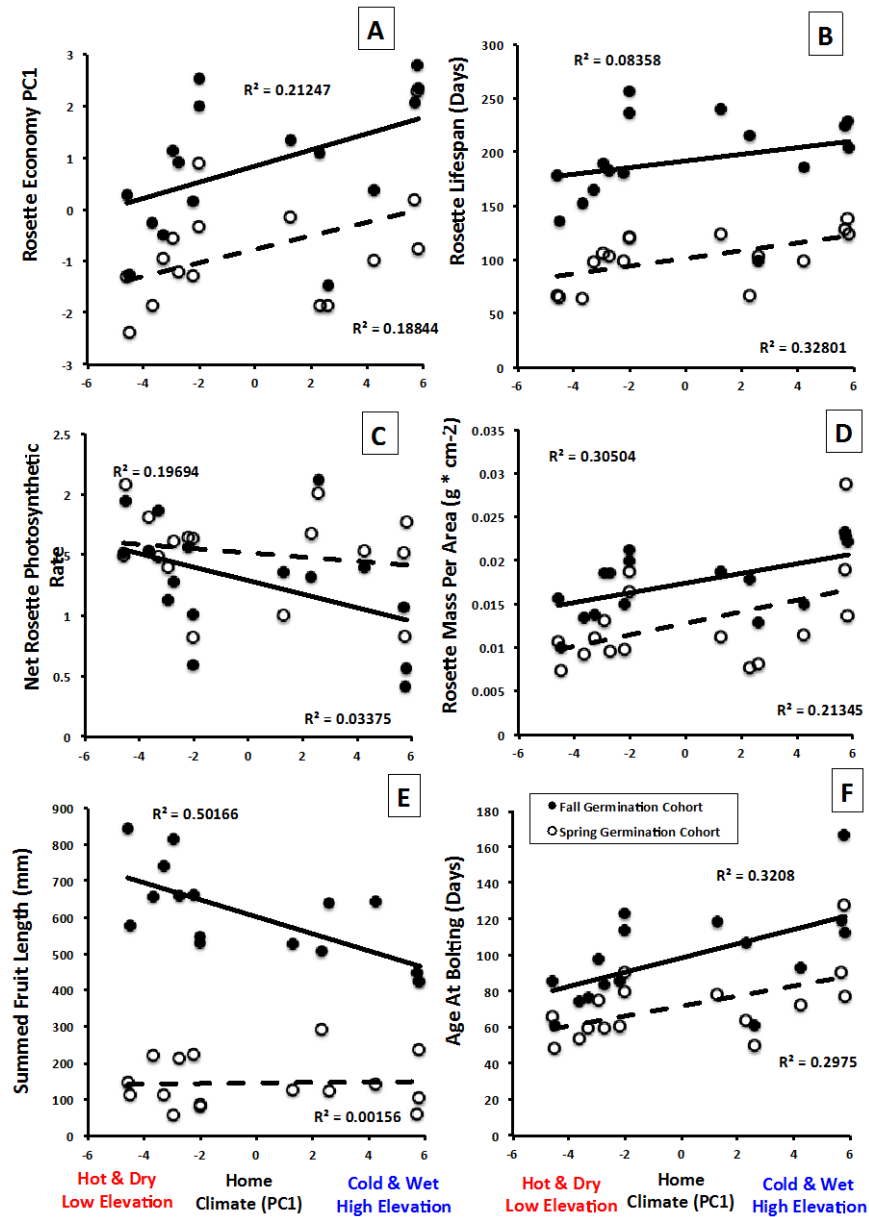


Figure 3.2: Trait vs. Climate Plots. Scatter plot and least squares regressions of population-means for each trait (vertical axis) on the climate PC1 score for that population (horizontal axis). Filled circles and solid regression lines represent the results for the Fall germinated cohort while open circles and dashed regression lines are for the Spring germinated cohort. R-squares are presented for each individual regression line within each plot. Climate PC1 is the result of a PCA of population values of 19 BIOCLIM variables and Elevation originally published in Wolfe & Tonsor *in press*. High values of climate PC1 represent high elevation sites that are cold and wet overall while low values are low elevation sites with hot, dry climatic conditions.

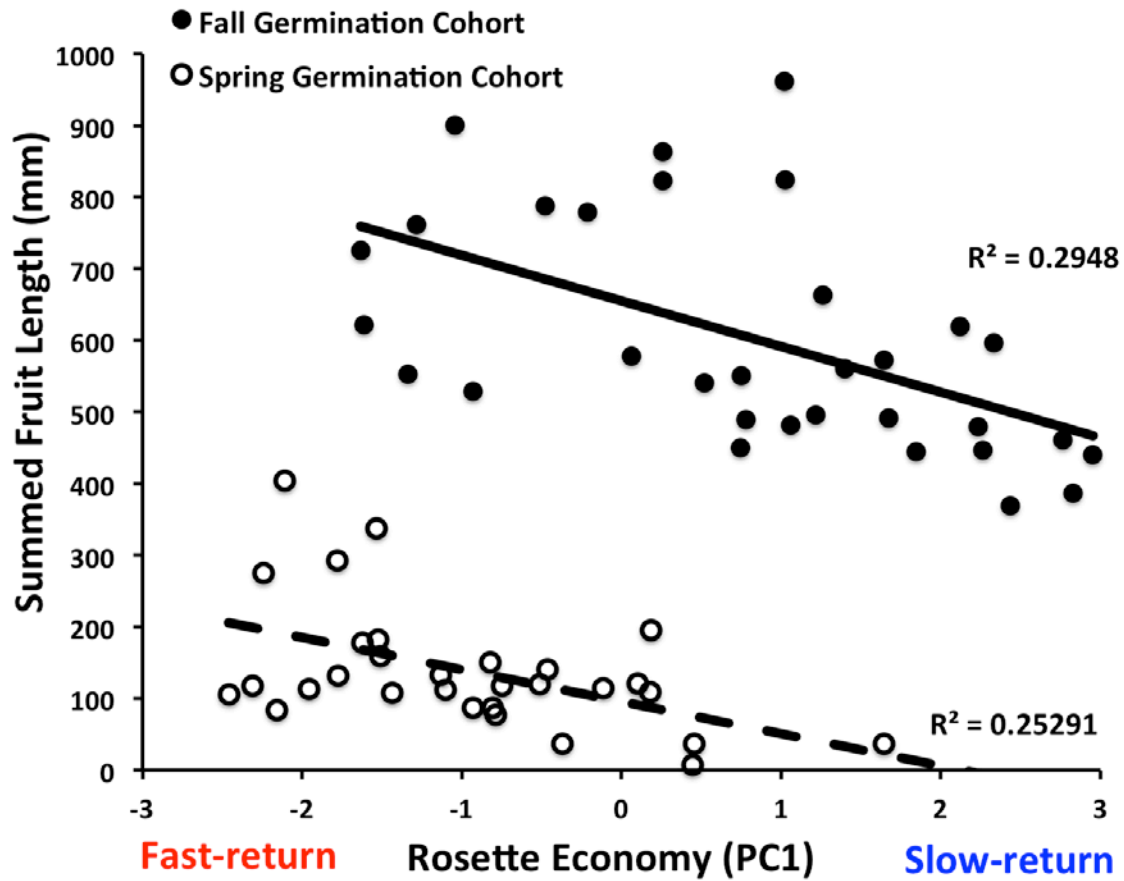


Figure 3.3: Rosette economy predicts fitness (summed fruit length). Scatter plot and least squares regressions of genotype-means within the spring (open circles, dashed regression lines) and fall (closed circles, solid regression lines) germinated cohorts. The vertical axis represents a fitness component related to total seed number (summed fruit length) while the horizontal axis represents each genotype's score on rosette economy PC1. High values of the predictor variable represent "slow-type" economics; long rosette lifespan, high rosette mass per area and low rosette photosynthetic rate at bolting. Low values of rosette economy PC1 represent "fast-type" rosette economies. R-squares are presented for each individual regression line within each plot.

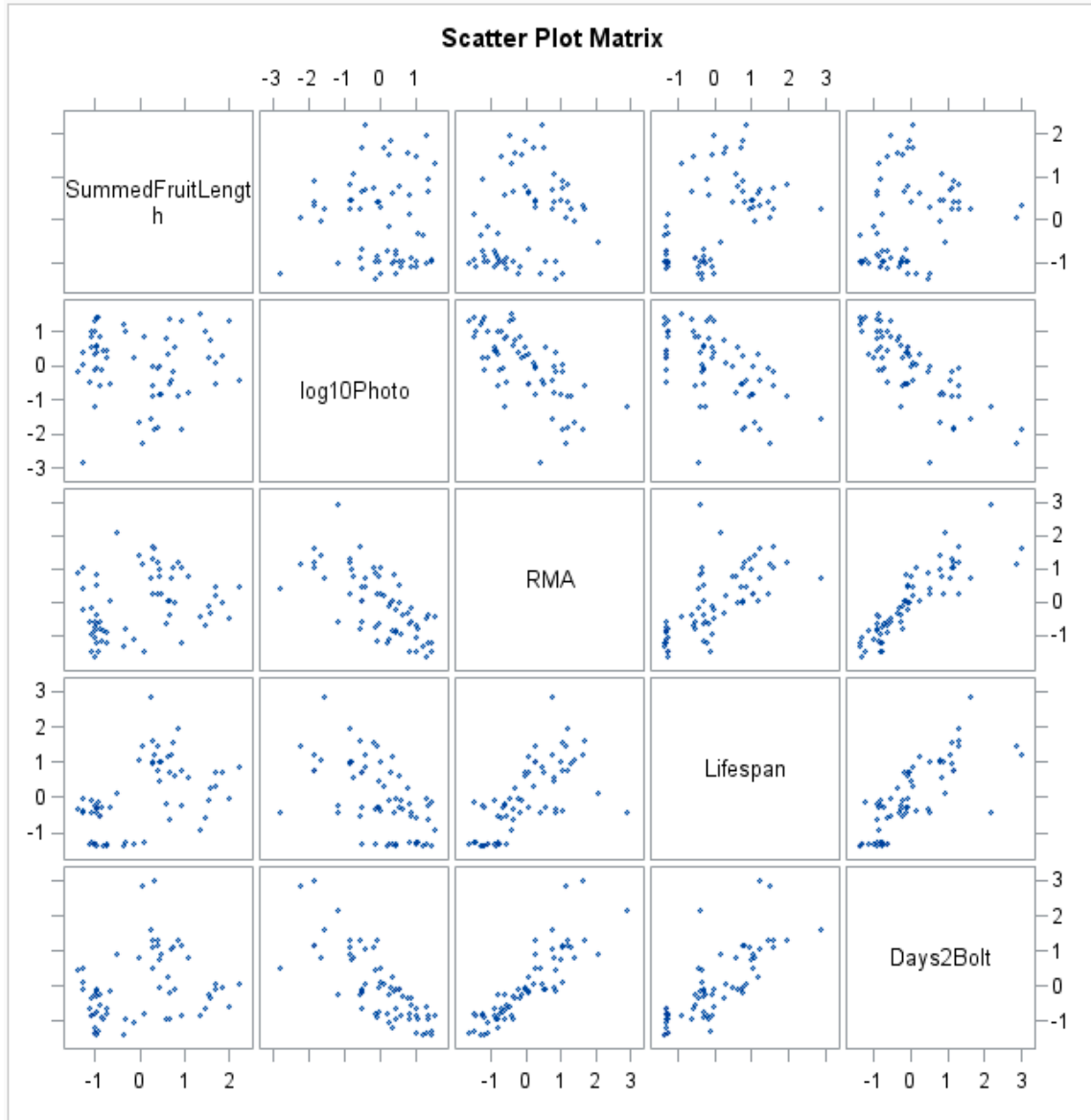


Figure 3.4: Genotype mean scatterplot matrix for rosette per-mass photosynthetic rate and rosette mass per area at bolting, rosette lifespan, age at bolting and summed fruit length.

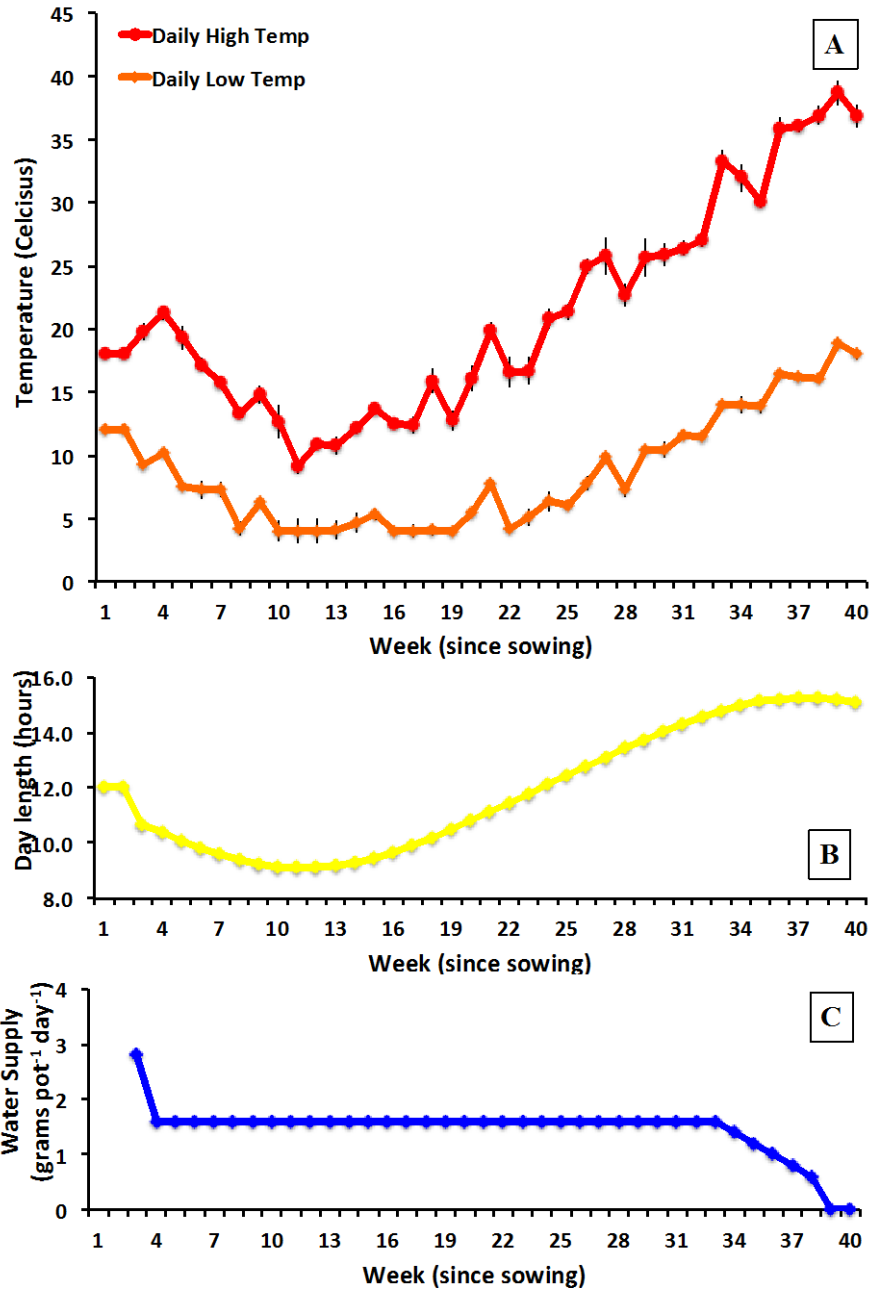


Figure 3.5: The dynamic growth chamber cycle simulating a low elevation N.E. Spanish seasonal climate is shown here. Daily high and low temperatures in centigrade (A), day lengths in hours (B) and daily water supply in grams per pot (C) are plotted by week. Standard errors bars for the temperature cycle represent variance in field temperature data (averaged across sites and years) and do not represent thermal variance in growth chamber conditions.

4.0 ADAPTIVE SHIFTS IN WHOLE PLANT ECONOMY FROM ROSETTE TO INFLORESCENCE ACROSS A CLIMATE GRADIENT IN *ARABIDOPSIS THALIANA*

4.1 INTRODUCTION

Plant leaves generally experience a lifespan-associated trade off between carbon income and investment. Leaves fall along a continuum between short lives with rapid photosynthesis and long lives with slow photosynthesis; a pattern known as the worldwide leaf economic spectrum (LES). This apparent trade off has recently been extended from single leaves to whole rosettes in the winter annual *Arabidopsis thaliana* and implicated in adaptation to climate. We hypothesized that photosynthetic inflorescences might also play a role in adaptation to climate and vary along a similar economic spectrum to that of leaves and rosettes. In this study, we tested for economic spectra in the form of single principal component axes that describe the economic strategies of N.E. Spanish *A. thaliana* from across a climate gradient. We tested for trade offs analogous to those observed at the single leaf level among rosettes, inflorescences, and at the whole plant level of organization. We found that rosette and whole plant economies exhibited a trade-off similar to the LES. Inflorescence economies match leaf and rosette level patterns except that lifespan and photosynthetic rate are not traded off. Slow rosette economy was associated with a long-life and slow economy overall, but also with a short-lived, slowly photosynthesizing inflorescence. In this experiment faster plants from hotter, drier low elevation sites that gained

most of their carbon income from their inflorescences were most fit. The adaptive value of inflorescence-centric life cycle under the relatively hot and dry conditions of this experiment suggests a role for this strategy in heat and drought avoidance. The key contribution of this study, therefore, is to provide evidence of the integrative changes to whole plant economy that are involved in climatic adaptation and the potential importance of photosynthetic stems and fruits in this process.

4.2 INTRODUCTION

The limitations on plant form and function can be fruitfully understood through economic analogy (Bloom et al. 1985). For example, leaves across the plant kingdom appear to trade a long life for a high photosynthetic rate. Corresponding to this trade off is a shift from high carbon and low nutrient cost to high nutrient and low carbon cost (Wright et al. 2004; Shipley et al. 2006). This trade-off is known as the worldwide leaf economic spectrum (LES hereafter) and represents a shift in the balance of resources investment over a time period that hypothetically optimizes the lifetime profitability in carbon gain of the leaf. Species tend to fall along the spectrum between slow leaves optimized for conservation and leaves optimized for fast acquisition of resources.

The economic indicators describing the LES have generally been applied at the interspecific level (but see Donovan et al. 2011) and relate to everything from post-fire regenerative ability (Saura-Mas et al. 2009) to litter decomposition rates (Cornwell et al. 2008) to the parameterization of global vegetation models (Wright et al. 2005a; Shipley et al. 2006). Recently, examination of this leaf-level trade off has been simultaneously extended to a higher level of biological organization (whole rosettes) and focused on within species variation

(Vasseur et al. 2012; Chapter 2). Vasseur et al. (2012) demonstrated that recombinant inbred lines of the plant model organism *Arabidopsis thaliana* exhibited a rosette economic spectrum (RES hereafter) ranging from slow rosettes with long lives but slow photosynthesis to fast rosettes with short lives and fast assimilation. These will be referred to as “slow” and “fast” economies henceforth.

In Wolfe & Tonsor (Chapter 3) we showed that rosette carbon economies were adaptively differentiated according to their climate of origin. Specifically, we showed that hot, dry climates of the N.E. Spanish coastal lowlands produced rosettes with relatively fast economies while *A. thaliana* from high elevation sites where cold, wet montane climates prevail produced slow rosettes. The age at bolting, a critical life-history trait for annual species has also been shown to increase with elevation and thus covary with climate in this system (Montesinos-Navarro et al. 2011; Wolfe & Tonsor *in press*). Age at bolting is typically highly correlated with and causally related to vegetative lifespan in *A. thaliana* (Levey & Wingler 2005; Balazadeh et al. 2008; Vasseur et al. 2012). Thus bolting age is necessarily a strong determinant of overall rosette carbon economy. However, a potentially significant and largely unexplored contributor to whole plant carbon economy in many species is the time and resource economics of photosynthetic inflorescences.

Numerous plant species have green stems and reproductive structures. These non-foliar photosynthetic structures can range from carbon sink to net carbon source (Watson & Casper 1984; Nilsen 1995; Aschan & Pfanz 2003). In the Brassicaceae, *Brassica napus* fruits (siliques) have been shown to exhibit net photosynthetic rates in the late growing season that are higher than in the basal leaves (Gammelvind et al. 1996; Bennett et al. 2011). In fact, among five ecotypes of *A. thaliana* the inflorescence on average contributes the majority of lifetime carbon

gained in rapid cycling laboratory conditions (Earely et al. 2009). Photosynthesis from the upright branches held above the still ground air layer may be advantageous when temperature and irradiance are high (Nilsen 1995). We therefore hypothesize that inflorescence photosynthesis may be an important and adaptive alternative (or complement) to the rosette's contribution to whole plant economy.

For monocarpic plants, especially annuals, the correct timing of reproduction is an essential step in adaptation to the local environment (Cohen 1976; Metcalf & Mitchell-Olds 2009). Given contribution to photosynthesis by inflorescences, variation in age at bolting may have added significance to whole plant economy because bolting initiates the formation of the inflorescence. Thus the seasonal timing of bolting determines the environmental context but not necessarily economics and lifespan of the inflorescence. Indeed in the monocarpic annual *A. thaliana* loci influencing bolting time generally have extensive pleiotropic effects on other vegetative and reproductive traits (Van Tienderen 1996; Scarcelli et al. 2007; Atwell et al. 2010). Therefore, we hypothesize that variation in age at bolting will be strongly associated not just with the timing of reproduction, but also with the overall carbon economy of the plant.

In N.E. Spain *A. thaliana* rosette economics go from fast to slow with increasing elevation and with the change from hot, dry low elevation to cold, wet high elevation sites (Chapter 3). Given the potential role bolting time plays in determining inflorescence growth, it is hypothesized that inflorescence economy will be correlated with rosette economy and vary with climate-of-origin in this system. Alternatively, the inflorescence economy may be independent of (uncorrelated with) bolting time and rosette economy, providing an alternative dimension to whole plant economics. Thus adaptive shifts in rosette economy associated with the climate gradient may or may not coincide with adaptive shifts in inflorescence economy.

The conceptual model for carbon economy (Figure 4.1) involves balancing resource investment (cost), and return on investment (income). Investment can be measured as either the absolute or per unit area dry mass (cost of a functional unit) allocated to a given plant module. Return on investment can also be measured in absolute terms as the total lifetime carbon gained or as a function of the rate of return (photosynthesis) and duration, or lifetime, of the structure in question. This model can in theory be applied to leaves, rosettes, inflorescences and whole plants. Whole plant economy is the sum of rosette and inflorescence economies. The whole plant might be expected to balance total investment with total return as well as the apportioning of investment and duration between rosette and inflorescence. In this paper we test for spectra in inflorescence as well as whole plant and rosette level carbon economies. We compare these spectra not only to each other but to the LES to understand how carbon economic trade-offs change at different levels of organization.

Ultimately, both rosette and inflorescence economies contribute to the whole plant economy, determining the whole plant's fitness. Previous studies of whole plant carbon and nutrient economics address correlations between above and below ground traits among species, but rarely include physiological and lifespan measurements (reviewed in Freshet et al. 2010). Briefly, our approach to whole plant carbon economy subdivides resource investment between rosette and inflorescence over the course of the plant's lifespan. Figure 4.1 illustrates the rise and fall of rosette photosynthesis, peaking at approximately the time of bolting. Figure 4.1 also illustrates that upon bolting, photosynthetic carbon gain by the inflorescence and the process of rosette senescence both begin. Inflorescence photosynthesis terminates with the end of the plant's lifespan. The whole plant's lifespan is therefore allocated between rosette and inflorescence photosynthesis with a period of functional overlap between the two, hinging on the

timing of bolting and other unknown factors. If the costs and/or benefits of carbon gain via the rosette differs from that of the inflorescence, then variation in age at bolting will have an important impact on whole plant economy. This would mean that, whole plant economy and fitness may modified by the effect that variation in age at bolting may have on rosette and/or inflorescence economy.

In this study, we address adaptive functional variation in the photosynthetic roles of rosette and inflorescence for semelparous annuals by focusing on the whole plant carbon economy of N.E. Spanish *A.thaliana* from 16 sites along a climate gradient. We present a growth chamber study of rosette and inflorescence photosynthesis as well as biomass allocation over time under seasonally varying conditions. We accomplish the following specific aims: First, we quantify variation in carbon economy at the rosette, inflorescence and whole plant organization levels, testing for evidence of an inflorescence economic spectrum for the first time and comparing to the LES. Second we examine how rosette and inflorescence economic spectra are related to each other and how they contribute to variation in whole plant economy. Third, we examine the way in which variation in the age at bolting alters whole plant, rosette and inflorescence economic spectra as well as the correlation among modules. Fourth, we test for adaptive variation in rosette, inflorescence and whole plant economic spectra according to climate of origin. Finally, we assess the functional significance of plant economic variation by testing whether and how such variation predicts fitness under a simulated low elevation climatic regime.

4.3 MATERIALS & METHODS

4.3.1 Collection

The data presented in this paper were generated as part of a larger experiment designed to measure key aspects of seasonal growth curves for a number of ecologically important traits. Two genotypes were randomly selected from available seed stores from each of 16 different populations along a climate gradient in N.E. Spain (Figure 3.2). The genotypes have been donated to the Arabidopsis Biological Resource Center (ABRC). Information about the climate gradient and field collections is published elsewhere (Montesinos et al. 2009; Montesinos-Navarro et al. 2011; Montesinos-Navarro et al. 2012; Wolfe & Tonsor in press). Each genotype has experienced at least two generations of propagation by single seed descent in laboratory-controlled environments to minimize any possible maternal effects.

4.3.2 Planting

We planted two sets of replicates of the 32 experimental genotypes, designated as fall and spring cohorts. There were 18 replicate pots per genotype. Four replicate pots per genotype were planted for early-age destructive sampling in Ray Leach RLC3 49 mL Cone-tainers. The remaining replicates were planted in Ray Leach SC10 164 mL Supercell Cone-tainers (hereafter pots, regardless of size) (<http://www.stuewe.com/products/rayleach.php>).

We filled all pots with Turface MVP fritted clay (<http://www.turface.com>) with 0.21-0.24 grams of Nutricote pellets added, for release of equal daily quantities of nutrients for 100 days (NPK 13-13-13, Type 100, Arysta Life Science NA Co., New York, NY). Central plugs 1 cm

wide by 2 cm deep of Sunshine germination-mix (<http://www.sungro.com>) in each pot provided a safe site for germination and early growth. RLC3 and SC10 pots were placed in RL200 and RL98 racks (<http://www.stuewe.com/products/rayleach.php>) respectively.

Seeds were surface sterilized through exposure to chlorine gas for three hours prior to planting. We planted 10-20 seeds per pot and at 15 days post-sowing we thinned seedlings to one per pot. We planted half of the replicates for each genotype on each of two consecutive days. After planting racks were placed in the dark at 4°C and 100% relative humidity for seven days to induce germination competency. After the cold treatment, racks were transferred to a Conviron PGW36 growth chamber for the remainder of the experiment.

4.3.3 Dynamic Growth Chamber Cycle

We imposed a dynamic growth chamber cycle in which temperature, day length and water availability varied over a 34-week period. Growth chamber seasonal cues, combined with heating and drying stress in the reproductive phase, result in variable fitness among N.E. Spanish populations such that low elevation plants are favored and fecundity scales with climate of origin (Wolfe & Tonsor *in press*). We based the seasonal temperature cycle on field plant-height temperature obtained from Hobo pendant temperature loggers (www.onsetcomp.com) placed in four low elevation sites, logging every 60 or 90 minutes. The number of years of temperature data and the number of loggers per site varied as follows: population BAR (2007-2010, 1 logger), population COC (2007, 1 logger and 2010, 3 loggers), population HOR (2007-2010, 1 logger) and population RAB (2010, 2 loggers). We extracted daily high and low temperatures from the raw logger data (Dryad doi:(to be posted at time of acceptance)). We averaged by day across years and sites separately for daily high and low temperature. We then averaged daily

high and low temperatures in seven-day intervals. This created an archetype of a low elevation Mediterranean temperature regime, not representing any specific site or year. Growth chamber temperature ramped linearly between the weekly mean minimums at lights on and weekly mean maximums at lights off (Figure 3.5).

Day length was also varied on a weekly basis (Figure 3.5) based on US Navy sunset/sunrise table calculator (http://aa.usno.navy.mil/data/docs/RS_OneYear.php) for the mean latitude and longitude (42.1539° Lat, 1.5738° Lon) of the study populations' sites of origin.

Plants were germinated under mild conditions that continued for two weeks: 12 hour day length, $150 \pm 50 \mu\text{mol photons m}^{-2} \text{ s}^{-1}$, 18°C maximum and 12°C minimum daily temperatures. At the third week post-sowing, light increased to $350 \pm 50 \mu\text{mol photons m}^{-2} \text{ s}^{-1}$ and the seasonal day length and temperature regimes were begun for the fall cohort (Figure 2.8). Lighting increased a final time to $550 \pm 50 \mu\text{mol photons m}^{-2} \text{ s}^{-1}$ at the start of week four. Based on observations of field germination timing (Montesinos et al. 2009), we began our growth chamber temperature and day length cycle to correspond with conditions in the field at the beginning of October.

For the first 20 days of life standpipe height is 7" with constant water supply. From day 21 to 27 bins are drained each day and filled in the morning for one hour providing approximately 2.8 grams of water per pot per day (Tonsor, unpublished). On day 28, standpipe height was reduced to 4" or 1.6 grams of water per pot per day and remained at this supply for the remainder of the life cycle (Figure 3.5).

Because building CO₂ concentration varied both daily and seasonally, we controlled CO₂ concentration by keeping it just above the building max at 530 ppm.

After ebb-and-flood watering regime began, rack rotations were conducted on a twice-weekly basis and continued for the duration of the experiment.

4.3.4 Sampling Design

We conducted trait measurement through destructive harvests of individual plants on nine dates during the growing season (35, 56, 77, 98, 140, 182, 210, 231 and 244 days after sowing, Table 3.11). On each harvest date we sampled one of two replicates of each genotype on each of two consecutive planting days (n=32 plants per day). This sampling protocol resulted in a gradual reduction in plant density in the growth chamber. This process maximized the number of sampling days possible while largely avoiding light-competition and overcrowding. We analyze growth and plant economy in terms of genotype and population means (see below).

The first two sampling dates used only the smaller RLC3 pots. This design increased the number of plants we could grow at one time and thus the number of time points we could sample. We randomly and evenly assigned and distributed pots across racks within each sampling date / planting day combination.

4.3.5 Trait measurements at each sampling point

At all except the final sampling date, at which point plants had completely senesced, we measured whole plant photosynthesis. For plants with inflorescences, we first measured whole plant gas exchange, then also measured gas exchange of the inflorescence only by excluding the rosette from our cuvette (see Earley et al. 2009). By doing this we were able to measure rosette

gas exchange non-destructively on a flowering plant by subtracting inflorescence from whole plant rates.

We begin physiological measurements one hour after lights turned on, in a separate growth chamber whose temperature and lighting matched that of the primary growth chamber. We used a LI-6400 XT infrared gas analyzer (IRGA; LI-COR Biosciences, Inc., Lincoln NE) to measure net photosynthetic rates in conjunction with a custom built four-cuvette array (Tonsor & Scheiner 2007; Earley et al. 2009; Tonsor et al. 2013). We allowed all plant parts to adjust to conditions in the cuvette for 15 minutes before we recorded net carbon assimilation rate ($\text{nM CO}_2 \text{ s}^{-1}$) five times over one minute. We averaged across the five records of each plant part for a single measurement of instantaneous gas exchange.

Following gas exchange measurement, we counted the total number of rosette leaves (TLN) and partitioned leaf counts into the number of live (TLLN) and dead (TDLN) leaves. We also counted the number of inflorescence branches arising from rosette leaf axils (basal branches hereafter). After removing inflorescences, we flattened rosettes under glass and photographed them with 1cm^2 area standards providing a top down, projected rosette area measurement, which was made using a custom pixel-counting macro (<http://www.tonsorlab.pitt.edu/>) in NIH ImageJ 64-bit version 1.47k (<http://rsbweb.nih.gov/ij/>). We then calculated the ratio of rosette dried mass to projected area (rosette mass per area or RMA hereafter). We washed the planting medium from the roots and separated rosettes from inflorescences. We dried plant parts for a week at 70°C before weighing. We express inflorescence and rosette dry mass in both absolute terms and proportional to the total mass of root, rosette and inflorescence.

4.3.6 Other traits measured

We estimated the summed fruit length, a proxy for the total seed number (Tonsor et al. 2013; Wolfe & Tonsor in press), by counting the number of ripened fruits (siliques) on the final harvest. We separated, spread out and photographed all inflorescence branches, then used the random grid overlay function of NIH ImageJ to generate digital transects across the inflorescence branches of a plant. We used the NIH ImageJ line tool to measure the length of each fruit that intersected a transect line. The average fruit length times the total fruit number equaled the summed fruit length.

On the final harvest, we excised the basal most 10 cm of the primary inflorescence branch and dried it for a week at 70°C. We express the mass of the basal 10 cm as mass per length, a measurement of cost per functional unit analogous to leaf mass per area because we expect branch length to be proportional to branch surface area.

Finally, we conducted weekly censuses, recording age in days since sowing at bolting.

4.3.7 Estimating Return on Investment (Relative Lifetime Carbon Gain)

One important measure of whole plant carbon economy is the gross lifetime carbon gained by the plant (lifetime return on investment). We followed the approach of Earley et al. (2009) and constructed line plots describing the change over time in net photosynthetic rate for the whole plant, the rosette and the inflorescence separately (Figure 3a, b). By determining the area under these plots we obtain an estimate of the relative net carbon gain over the lifespan of the plant. This approach does not accurately estimate absolute lifetime carbon gain since we cannot account for variation in carbon balance over the course of a day, between sampling dates. As

such, we consider our measures to provide only relative lifetime carbon gain by each part, and lifetime absolute net carbon gain by the whole and individual plant parts to be a latent variable. Our estimates of area under the photosynthesis vs. time curve represent indicators of that latent variable. We express the relative lifetime carbon contributions of the individual plant parts as the individual areas under the curve. We further assume that, while not measuring absolute differences between genotypes in absolute carbon gain by a given structure, the differences between genotypes in areas under the carbon gain curve are roughly proportional to the unmeasured absolute differences and can therefore be used to test for differences in total lifetime carbon gain.

The day 56 gas exchange measures, all conducted on plants in RLC3 pots (see above), did not match the overall shape of lifetime photosynthetic growth curves. Subsequent comparisons of growth in 49 mL RLC3 pots compared to 134 mL SC10 pots reveal that growth is accelerated in 49 mL pots so that while measures taken on the first harvest (35 days post-sowing) fit the overall growth curve, photosynthetic rates were higher than the rest of the growth curve for the day 56 harvest (data not shown). Because of this effect, we excluded day 56 measures from subsequent analyses of gas exchange and mass data. The dataset used to calculate relative lifetime carbon contributions is available through DRYAD (to be uploaded upon acceptance of manuscript)).

4.3.8 Estimating Functional Lifespan

Defining the age at death for a plant or plant part can be difficult yet lifespan is a critical component of plant economy. Any measure of time or age at death sets an arbitrary point in a progression of events that lead to complete loss of biological activity. We were most interested

in death defined in terms of loss of photosynthetic carbon gain. We estimated effective photosynthetic lifespan using non-linear regression fitting the following Gaussian function to the age-specific photosynthetic measures for each genotype: $\text{Net Photosynthetic Rate} = \alpha * \text{EXP}(-0.5 * ((\text{Age} - \mu)/\sigma)^2)$. In this model, α estimates the peak age-specific photosynthetic rate for the genotype. The parameter μ is the first moment of the Gaussian, describing the point on the age axis where the distribution of photosynthetic rates is centered (i.e. the age at which peak photosynthetic rate α occurs). Finally, the parameter σ is the second moment of the Gaussian (e.g. the standard deviation of the normal Gaussian) and describes the spread of the curve around the peak on the age axis. We took advantage of these properties of the Gaussian function and defined $\mu + 1.96 * \sigma$ (the upper 95th percentile of a normal Gaussian distribution) as the end of the functional lifespan. We model whole plant, rosette and inflorescence functional lifespans separately for each genotype. We defined the functional lifespan of the inflorescence by subtracting genotype mean ages at bolting from $\mu + 1.96 * \sigma$, providing a standardized estimate of the time of death for each genotype.

Nonlinear regressions were conducted using PROC NLIN in SAS (version 9.3, SAS Institute 2011). For all nonlinear regressions, we use the pseudo r^2 (pseudo $r^2 = 1 - (\text{SS}_{\text{Error}} / \text{Corrected SS}_{\text{Total}})$) to quantify model fit.

4.3.9 Rosette Economic Spectrum Traits from Chapter 3

In Chapter 3, we quantified the carbon economic spectrum of the rosette with three key traits. In that study, rosette lifespan was measured as the number of days from germination until 95% of rosette leaves had died (See Chapter 3 for details). We include this measurement in addition to the photosynthetic functional lifespan described above. In addition, in Chapter 3, we used non-

linear regression models similar to those described above to estimate the rosette cost (RMA) and photosynthetic gain rate (per gram) at the time of bolting. We did this rather than examining RMA and photosynthesis per gram at any directly observed time point because bolting is approximately when we expect rosette function to peak and because it represents a consistent developmental time point at which to compare genotypes with varying developmental rates. However, there was no apparent developmental age analogous to bolting time for inflorescence measurements in this study. Instead we used the maximum observed rate of photosynthesis and the end-of-life mass per length of inflorescences in this study. We include the maximum observed RMA and photosynthetic rate per gram for rosettes in addition to estimated values at bolting, providing two measures of RMA and two of carbon gain rate for rosettes.

4.3.10 Statistical Analysis

From the measurements and models described above, we extracted a total of 26 variables that describe aspects of rosette, inflorescence and whole plant carbon economy (Table 4.1). We divide them up into 12 rosette, nine inflorescence traits and five whole plant indicators. Thus our primary dataset had n=32 genotypes each with measures of 26 plant characters plus fitness and the age at bolting (Appendix A.1).

4.3.10.1 Test for rosette, inflorescence and whole plant economic spectra

Our first aim was to quantify the extent to which the carbon economies of rosettes, inflorescences and the whole plant varied along “spectra” or principal components (PCs). We used separate principal components analysis (PCA) to describe the multivariate correlation structure of rosette, inflorescence and the whole plant. The variables representing carbon

economy for each analysis (rosette, inflorescence and whole plant) are listed in Table 4.1. In order to determine the number of meaningful PCs (spectra), we tested whether each principal component explained more variation than a threshold determined by iterative randomization of the data. This approach is described in detail elsewhere (Perez-Neto et al. 2003; Wolfe & Tonsor *in press*; Chapter 3). Briefly, variable IDs are randomly assigned and a PCA conducted 3,000 times. The upper 99th percentile of the distribution of eigenvalues is then computed and compared to the true eigenvalue (SAS macro program available at <http://www.tonsorlab.pitt.edu>). We therefore define the principal components (PCs) whose eigenvalues exceed the threshold as significant and label them as economic spectra (e.g. Inflorescence Economy PC1)

The scores for each genotype on each economy PC represent indicators of rosette, inflorescence and whole plant economy and are used in further analyses. We interpret the nature of detected economic spectra based on the loadings of each original variable onto the PC. We ask whether the variable loadings onto rosette, inflorescence and whole plant economic PCs show a correlation structure analogous to the worldwide LES. In each PCA (rosette, inflorescence and whole plant) we include variables above and beyond the three critical traits for quantifying carbon economy (i.e. lifespan, mass per area and photosynthetic rate). We do this because carbon economies represent latent (un-measurable) variables; as we have laid them out above, the traits we include in each analysis represent indicators of particular properties of the latent economic spectrum being measured.

Loadings here are defined as the correlation between the original variable and each PC score. PCA was conducted with PROC PRINCOMP in SAS (version 9.3, SAS Institute 2011).

4.3.10.2 Relationships among rosette, inflorescence and whole plant economic spectra

Our second aim in this study was to examine the relationship between rosette and inflorescence economics and the manner in which they contribute (are associated with) whole plant economic variation. We used PROC CORR in SAS (version 9.3, SAS Institute 2011) to determine the Pearson product-moment correlations between significant whole plant, rosette and inflorescence economic PCs.

4.3.10.3 The association between plant economics and bolting time

Our third aim was to assess the relationship between age at bolting and whole plant, rosette and inflorescence economic variation. We chose a univariate regression model, positing a causal relationship between age at bolting (independent variable) and whole plant, rosette and inflorescence economic PCs (dependent variables). In order to summarize the relationships between age at bolting, rosette, inflorescence, and whole plant economic PCs, we conducted an additional PCA on those variables. Lastly, we show how variation in the age at bolting actually accounts for 3-way correlation structure between rosette, inflorescence and whole plant PCs, we calculated partial correlations between them, controlling for the age at bolting. We compare partial correlations with the effect of bolting time removed to the raw correlations.

We used PROC CORR to calculate partial correlation coefficients and PROC REG to conduct univariate regressions (SAS version 9.3, SAS Institute 2011).

4.3.10.4 Test for climate associated adaptive variation.

Our fourth aim was to test for adaptive divergence in plant economic spectra according to climate of origin. We tested for adaptive divergence in rosette, inflorescence and whole plant economic PCs by regressing population mean scores against the scores each population had on a

principal component describing the climate gradient (see below). In order to make the magnitude of association between traits and climate comparable among traits, we standardized all dependent variables to a mean of zero and a variance of one. We also present results for univariate regressions of the age at bolting and summed fruit length on climate (see below).

Our predictor variable in the regression analyses described above is the first PC of a PCA with 19 bioclimatic variables and elevation (called Climate PC1 hereafter) that explained 75% of the among site variation in climate. In Wolfe & Tonsor (2013, in press) we found that as climate PC1 increases elevation increases and conditions become wetter but colder. There is high variability in precipitation at low climate PC1 sites, which is traded for high variability in temperature at high climate PC1 sites.

4.3.10.5 Assessing the fitness effects of plant economic variation.

Our final aim was to assess the potential adaptive significance of plant economic variation under the experiment's growing conditions by testing whether and how such variation is related to fitness under a simulated low elevation climatic regime.

We test the fitness effects of rosette, inflorescence and whole plant economic PCs with univariate regressions using summed fruit length as the dependent variable. We also compared the independent effects of rosette and inflorescence economic spectra on fitness with multiple regression; basically a genotypic selection analysis. We standardized genotype mean summed fruit length (mean of zero, variance of one) and all independent variables (economic PCs) prior to regression. We used genotype means (n=32) for all tests of fitness effects, which were conducted using PROC REG in SAS (version 9.3, SAS Institute 2011).

4.4 RESULTS

4.4.1 Functional lifespan model results

Gaussian function estimation procedures for rosettes, inflorescences and whole plants successfully converged for all genotypes (Figure 3c,d). All parameters were significant for whole plant photosynthesis models, and model pseudo r^2 averaged 0.88 ranging from 0.53 to 0.98 (Table 4.2). Models of rosette photosynthesis generally fit well (mean pseudo $r^2 = 0.91$ ranging from 0.65 to 1.00) (Table 4.3). There was a significant negative rosette photosynthetic rate at age 98 days for genotype RAB17 that did not fit the overall growth curve and was thus judged to be an outlier. We had to remove this outlier data point to achieve model convergence. For inflorescence models, pseudo r^2 ranged from 0.64 to 1.00 and averaged 0.92 (Table 4.4).

However, there were several genotypes for whom inflorescence parameters were either not significant and/or where statistical tests could not be conducted by PROC NLIN. For genotypes SPE5 and VIE6 the α and σ were not well estimated. Our goal was to estimate the approximate date when inflorescence function ceased (thus death). Plotting SPE5 and VIE6 functions versus the data indicated that inflorescence age at death was reasonably estimated by the parameter estimates for these two genotypes, despite lack of convergence. PROC NLIN could not provide statistical tests of the σ parameter for genotypes PAN5 and PAN1. Here as in the models for SPE5 and VIE6, plotting the estimated Gaussian function indicated that the age at inflorescence death was likely well estimated by these models and they are therefore used as is.

Unlike the other genotypes mentioned, the inflorescence model for genotype PIN6 did not fit a Gaussian function well (pseudo $r^2 = 0.67$) and both the μ and σ parameters were not statistically testable. Overlaying the PIN6 inflorescence data against the estimated Gaussian

function indicated that inflorescence age at death was strongly underestimated. Photosynthesis for this genotype's inflorescence peaks early and then displays a linear and gradual decline. While we report the parameter estimates for PIN6's Gaussian function, we used an alternative approach to estimating the age at death for this inflorescence and use that value in subsequent analyses. Basically, there were four dates where inflorescence photosynthesis was observed for genotype PIN6 and the decline in photosynthesis was linear. We therefore used a linear regression of photosynthesis versus plant age based on the last four sampling ages. This regression had an r^2 of 0.94. We used the regression to predict the age when inflorescence photosynthesis reached zero (i.e. intercepted the age axis).

Mean whole plant functional lifespan was 209 days (range 146-247). Rosette lifespan averaged 159 days (73-238). Inflorescences lived an average of 108 days (37-153).

4.3.2 Whole plant economic spectra

In each of the three PCAs of plant carbon economy, the first principal components were the only ones with eigenvalues above the null hypothesis threshold (Figure 4.3D, Table 4.5). Carbon investment (e.g. RMA), lifespan and lifetime carbon gain loaded positively on Rosette Economy PC1 while Rosette Photosynthetic Rate per Gram (maximum and at bolting) loaded negatively (Figure 4.3A, Table 4.6), explaining 58% of the variance in rosette economy (Table 4.5). Loadings on Inflorescence Economy PC1 were all positive except for the Branch Mass per Length, the carbon cost per functional unit of inflorescence (Figure 4.3B, Table 4.6). Inflorescence Economy PC1 explained 45% of the total variance in inflorescence economic trait space (Table 4.5). Whole Plant Economy PC1 explained 43% of the variation in the five traits analyzed (Table 4.5). Plants with high values along that PC had long lifespans, achieved greater

lifetime carbon income and thus large total mass but tended to photosynthesize more slowly (Figure 4.3C, Table 4.6).

4.4.3 Relationships among rosette, inflorescence and whole plant economic spectra

Rosette, inflorescence and whole plant economy PC1 are all significantly correlated (Figure 4.4). Rosette-inflorescence and whole plant-inflorescence correlations are negative, $r=-0.85$ and -0.64 respectively with $p < 0.0001$, $n=32$ (Figure 4.4). Rosette economy PC1 is positively correlated with whole plant economy PC1, $r=0.76$, $p < 0.0001$ (Figure 4.4).

4.4.4 The association between plant economics and bolting time

The age at bolting explained 81%, 82% and 57% of the variation in rosette, inflorescence and whole plant economy PC1 respectively. Later age at bolting corresponded with higher values of rosette and whole plant economy but lower values of inflorescence economy PC1 (Figure 4.5). Principal component analysis of scores on rosette, inflorescence and whole plant economy PC1 plus age at bolting revealed a single axis explaining 85% of the variance in the four variables analyzed. Age at bolting (loading = 0.96), whole plant economy PC1 (loading = 0.85) and rosette economy PC1 (loading = 0.95) load positively while inflorescence economy PC1 loads negatively (loading = -0.92).

Our partial correlation analysis testing whether rosette-inflorescence, rosette-whole plant and inflorescence-whole plant associations are accounted for by bolting age revealed no significant correlations. However, each individual partial correlation was in the same direction

only smaller than the raw correlation, with partial $r=-0.23$, 0.29 and 0.15 for rosette-inflorescence, rosette-whole plant and inflorescence-whole plant respectively.

4.4.5 Test for climate associated adaptive variation

Climate PC1 was a significant predictor of population mean trait values in 16 out of 31 univariate regressions (Table 4.7). In particular, rosette economy PC1 ($r^2 = 0.24$, $p=0.06$), whole plant economy PC1 ($r^2 = 0.30$, $p=0.03$) and age at bolting ($r^2 = 0.32$, $p=0.02$) increased with climate PC1 (Figure 4.6A, 7C, 7D). Inflorescence economy PC1 ($r^2 = 0.52$, $p=0.002$) and summed fruit length ($r^2 = 0.50$, $p=0.002$) both decreased with increasing climate PC1 (Figure 4.6B, 7E).

Of the significant plant carbon economic trait-climate associations, there were five rosette traits, five inflorescence traits and two whole plant traits. In addition, inflorescence economy PC1, whole plant economy PC1, summed fruit length and age at bolting were also significantly associated with climate PC1 (Table 4.7).

4.4.6 Assessing the fitness effects of plant economic variation

Multiple regression analysis of standardized summed fruit length our measure of plant fecundity, as the dependent variable predicted by rosette economy PC1 and inflorescence economy PC1 explained 32% of the variation in fitness (Table 4.8). However, in that analysis, neither predictor was significant. We note that the correlation between rosette and inflorescence economy PC1 was $r=-0.85$ ($p < 0.0001$, $n=32$). In univariate regressions, fitness increased significantly with decreasing whole plant economy PC1 (Figure 4.7A), rosette economy PC1 (Figure 4.7C), and

age at bolting (Figure 4.7D) and increasing inflorescence economy PC1 (Figure 4.7B). We note that in the multiple regression, even though not significant, rosette economy PC1 is negative and inflorescence economy PC1 is positively associated with fitness (Table 4.8).

4.5 DISCUSSION

The carbon economies of photosynthetic structures appear to exhibit a trade off to which almost all plant life conforms (Wright et al. 2004). Fast photosynthetic carbon gain is typically associated with a short lifespan and low carbon investment while long lifespans are associated with a greater carbon investment and generally also have lower photosynthetic rates. This apparent trade off has recently been extended from single leaves (Wright et al. 2004, Donovan et al. 2011) to whole rosettes in the winter annual *Arabidopsis thaliana* (Vasseur et al. 2012; Chapter 3). Rosette economy in *A. thaliana* appears to play a role in adaptation along a climate gradient in N.E. Spain (Chapter 3). However, inflorescences play a major role in lifetime carbon gain in *A. thaliana* (Earley et al. 2009) and other species (Nilsen 1995). Therefore, we hypothesized that inflorescences potentially provide a dimension of economic variation that is independent of rosette economics, and may be involved in adaptation.

In this study, we tested for economic spectra in the form of single principal component axis that describe the economic strategies of N.E. Spanish *A. thaliana* from across a climate gradient as a study system. We tested for trade offs analogous to those observed at the single leaf level (Wright et al. 2004) among rosettes, inflorescences and at the whole plant level of organization. We found that rosette and whole plant economies exhibited a trade-off similar to the LES. Plants with high values of whole plant economy PC1 and rosette economy PC1 lived

longer, required greater investment overall and per unit area, but photosynthesized more slowly. Further rosette-whole plant economic spectra are positively correlated (Figure 4.4) indicating a potentially strong contribution of rosette economy to the overall whole plant spectrum observed. Thus, rosettes and whole plants exhibit a trade-off between fast- and slow-return carbon economics.

In contrast, while inflorescence economies were confined along a spectrum described by a single principal component, the trait combinations observed did not conform to the expectations of the LES. Instead, inflorescences with high values on inflorescence economy PC1 were not only longer lived with greater carbon investment, they also had a higher rate of income (photosynthesis) and lifetime carbon incomes were greater (Figure 4.3B). We note that inflorescences with faster photosynthetic rates (higher PC1) did cost somewhat less per unit length (lower mass per length), which we use as a proxy for the photosynthetic surface area of branches. Below, we consider one possible explanation for the apparent lack of a trade-off between lifespan, cost and income rate.

Plant economic theory would predict the senescence of a vegetative organ when the costs of maintaining photosynthesis outweigh the benefits (Chabot & Hicks 1982; Bloom et al. 1985). For the rosette, most vegetative growth is tied to a single meristem and spiral phyllotaxy means that self-shading occurs as new leaves are produced. This appears to mean that the plant experiences diminishing photosynthetic returns on the investment of new leaves and mass into the rosette as they age (Chapter 3). When the plant bolts, the time of investment in the rosette generally ends and leaves senescence. In the inflorescence, biomass accumulation, photosynthetic income and reproductive activity are divided among potentially multiple meristems (Bonser & Aarssen 2001). This may mean that inflorescence lifespan can be extended

by activation of additional axillary meristems. It may also be that the vertical architecture of the inflorescence means that accumulation of additional inflorescence biomass does not result in the same diminishing photosynthetic rates per gram observed for the rosette. Thus, at least for the inflorescences we observed, longer lifespan and additional biomass appear to yield faster rates of acquisition and overall greater contribution of the inflorescence to lifetime carbon income of the whole plant.

Whether and to what degree the above explanation accounts for the economic spectra observed for inflorescences in this study remains to be seen. In addition, other factors may enable greater photosynthetic rate per unit investment in inflorescences. Firstly, inflorescence assimilation rates may be influenced by nutrients from xylem and photosynthate in the phloem that are more accessible in stems versus leaves due to proximity (Watson & Casper 1984; Bennett et al. 2011; Blonder et al. 2011). In addition, significant quantities of nutrients and biomass ultimately deposited in the inflorescence originate from the rosette, meaning that the rosette to some extent covers the cost of construction and operation of inflorescences (Watson & Casper 1984; Hörtensteiner et al. 2002; Balazadeh et al. 2008; Bennet et al. 2011; Masclaux-Daubresse et al. 2011). Lastly, stems of some species re-fix carbon dioxide from leaves via internal gas transport (Nilsen 1995; Aschan & Pfanz 2003) although it is unclear whether this is the case in *A. thaliana*.

The rosette and inflorescence carbon economies exhibited a strong, negative correlation ($r = -0.85$, $p < 0.0001$; Figure 4.4) indicating a trade-off. Plants with slower-type rosette economy tended to have faster, more productive (high PC1) inflorescence economies (Figure 4.3A, 4B). Indeed, the whole plant and subsidiary economies of the rosette and inflorescence were all highly integrated around the age at bolting (Figure 4.5). Plants that bolted later had more productive but

slower-type overall economies, corresponding to the slower economies of their rosettes and despite the less productive, shorter-lived inflorescences they typically produce.

Negative correlations between vegetative and reproductive structures have long been known (Cohen 1976, Grime 1977, Geber 1990). Shifts between strictly vegetative and reproductive tissues have been hypothesized to result from trade-offs between current and future survival and reproduction, but reproductive tissues that photosynthesize are expected to change the economics of this trade-off (Cohen 1976, Watson & Casper 1984). That is, *A. thaliana* that in this experiment simultaneously achieve the greatest fecundity (Figure 4.7A) and earliest time of reproduction appear to do so by allocating to dual-purpose reproductive and photosynthetic tissues. This hypothesis potentially explains how *A. thaliana* and other annuals (Nilsen 1995; Aschan & Pfanz 2003; Earley et al. 2009) cover the carbon cost of accelerating the age at flowering, which is important for ensuring completion of the life cycle when growing seasons are short (Grime 1977; e.g. Chaves et al. 2002; McKay et al. 2003; Griffith & Watson 2005; Heschel & Riginos 2005).

The trade off between rosette and inflorescence photosynthetic function that we observed may also stem from the nutrient costs of the inflorescence being covered by re-mobilization from the senescing rosette (Hörtensteiner et al. 2002; Masclaux-Daubresse et al. 2011). Another possibility is that the rosette-inflorescence trade-off may result partially from shading of the rosette by the inflorescence. In addition, vertically oriented photosynthetic structures may be at an advantage in hotter and/or brighter environments (Nilsen 1995; Gammelvind et al. 1996;). The water conditions of the growing season, given potentially higher water use efficiency (Earley et al. 2009) of the inflorescence, may contribute to the observed trade off. Lastly, however, the apparent trade off that we observed might in fact be the result of some combination

of natural selection and genetic constraint (Antonovics 1976; Pigliucci 2003; Blows & Hoffman 2005) given the particular climate gradient from which we have drawn our experimental population, rather than a physiological or morphological constraint. Thus other samples and alternative growing conditions e.g. a more favorable environment with cooler more consistent temperature and additional soil nutrients might alter the rosette-inflorescence relationship we have observed. One could most readily test for pleiotropic constraints vs. trade-offs resulting from selection by measuring the same traits used here in an advanced generation recombinant population in which non-pleiotropic linkage disequilibrium, caused by selection, has been removed.

In N.E. Spain, mean annual temperature gets about 11°C cooler and mean annual precipitation is about 550 mm greater as you move from the lowest elevation population (PIN, 109 m.a.s.l.) near the Mediterranean to the highest elevation site (PAN, 1664 m.a.s.l.) in the Pyrenees Mountains (Wolfe & Tonsor 2013. *in press*). In this study we asked whether whole plant, rosette, and inflorescence carbon economic spectra were adaptively differentiated according to home climate. Under the conditions of this experiment, plants from hotter, drier low climate PC1 sites were favored (Table 4.7). Indeed, fitness decreased monotonically with increasing climate PC1 (Figure 4.6E). Ultimately climate PC1 explained 50% of among-site variation in fitness. The more fit, low climate PC1 populations in this study bolted earlier, had faster-type rosette and whole plant economies and longer-lived, more productive type inflorescence economic strategies (Figure 4.6). Thus the adaptive strategy observed under the experimental conditions, corresponding to the carbon economic strategy of low elevation populations involved trading-off a longer, more productive life centered on carbon gain from the rosette, for a faster, cheaper existence dependent on the inflorescence for carbon uptake.

The adaptive value of inflorescence-centric life cycle under the relatively hot and dry conditions of this experiment suggests a role for this strategy in heat and drought avoidance. The experimental conditions favored plants from low elevation sites where spring heat and drought are thought to be important selective agents (Wolfe & Tonsor 2013. *in press*). This also makes sense given that stems tend to be more water use efficient than leaves (Nilsen 1995; Earley et al. 2009). Additionally, since near-ground climate is generally warmer than at inflorescence height (Geiger 1950) inflorescence-centric low elevation life may also represent an adaptive mechanism for escaping heat stress (Nilsen 1995). Thus the overall strategy that appears to be favored at the low elevation extreme in this system is akin to the ruderal strategy of Grime (1977), in which vegetative allocation (basal leaves in this case) is traded for accelerated allocation to reproduction. The key contribution of this study, therefore, is to provide evidence of the integrative changes to whole plant economy that are involved in evolving such a strategy and the potential importance of photosynthetic stems and fruits in this process.

Future studies must determine whether genetic constraints (i.e. pleiotropy), natural selection or both (Antonovics 1976; Blows & Hoffman 2005) maintain the economic trade-off we observe varying across this climate gradient. The age at bolting appears to be the nexus of a genetically based trade off between inflorescence and rosette, which has significant implications for adaptation. Specifically, the first principal component of the G-matrix (G_{\max}), has been termed the evolutionary line of least resistance (Schluter 1996). Selection on any of the traits that align with G_{\max} will tend to drag the other traits with it in the direction of the principal component. This would explain why adaptation to climate in *A. thaliana* tends to always involve variation in age at bolting, and why in turn age at bolting tends to be highly correlated with other plant traits (van Tienderen et al. 1996; Scarcelli et al. 2007; Atwell et al. 2010).

Remaining questions therefore include whether inflorescence structure and function is independent genetically from age at bolting? Addressing this question will potentially reveal an alternative (additional) dimension in multivariate trait space that may be explored during adaptation. Would it therefore be possible to have a long-lived, high investment rosette (i.e. late bolting age) plant with a highly productive, highly branched inflorescence? If the genetic correlations between rosette, inflorescence and bolting time could indeed be broken, we could then ask under what conditions might selection favor rosette-inflorescence dissociation?

Table 4.1: Carbon economy variable list by plant module. Details on the measurement or calculation of traits are provided. Carbon economy traits are grouped based on the plant module they represent rosette, inflorescence and the whole plant. Within each plant module traits are further grouped based on the aspect of plant carbon economy they describe; either resource investment (cost) or return on investment (income). Return on Investment is subdivided into traits measuring the lifetime return, the duration of return (lifespan) and the rate of return.

Rosette Economic Indicators (12 total)		
Type of Measurement	Trait	Details
Resource Investment (Cost)	Rosette Mass Per Area at Bolting	The estimated RMA at bolting.
	Max Rosette Mass Per Area	Max RMA
	Proportion Rosette	Proportion of total mass
	Rosette Dry Mass	The maximum observed rosette dry mass.
	Rosette Area	The maximum observed rosette area.
	Total Leaf Number	The maximum observed number of rosette leaves.
Return on Investment (Income)	<u>Lifetime Return</u>	
	Rosette Lifetime Carbon Gain	Area under a line plot of photosynthesis vs. age.
	<u>Duration of Return</u>	
	Rosette Functional Lifespan	Age corresponding to the upper 95th percentile of the gaussian curve fit to a photosynthesis vs. age curve.
	Rosette Leaf Lifespan	Age at which 95% of rosette leaves had died.
	<u>Rate of Return</u>	
	Rosette Photo per Gram at Bolting	The estimated photosynthetic rate per gram at bolting.
Max Rosette Photo per Gram	The maximum observed (per gram) photosynthetic rate	
	Rosette Total Photo	The maximum observed photosynthetic rate (per rosette)

Inflorescence Measurements (9 total)		
Type of Measurement	Trait	Description
Resource Investment (Cost)	Mass Per Length	The mass per basal 10 cm of the primary inflorescence branch.
	Proportion Inflorescence	Proportion of total mass
	Inflorescence Dry Mass	The maximum observed inflorescence dry mass.
	# Basal Inflorescence Branches	The maximum observed number of inflorescence branches arises basally from the rosette leaf axils.
Return on Investment (Income)	<u>Lifetime Return</u>	
	Inflorescence Lifetime Carbon Gain	Area under a line plot of photosynthesis vs. age.
	<u>Duration of Return</u>	
	Inflorescence Functional Lifespan	Age corresponding to the upper 95th percentile of the gaussian curve fit to a photosynthesis vs. age curve.
	Post-bolting Plant Functional Lifespan	Whole Plant Functional Lifespan - Age At Bolting
	<u>Rate of Return</u>	
	Inflorescence Photo per Gram	The maximum observed (per gram) photosynthetic rate
	Inflorescence Total Photo	The maximum observed (per inflorescence) photosynthetic rate

Table 4.1: Continued from previous page.

Whole Plant Measurements (5 total)		
Type of Measurement	Trait	Description
Resource Investment (Cost)	Total Mass	
	<u>Lifetime Return</u>	
Return on Investment (Income)	Whole Plant Lifetime Carbon Gain	Area under a line plot of photosynthesis vs. age.
	<u>Duration of Return</u>	
	Whole Plant Functional Lifespan	Age corresponding to the upper 95th percentile of the gaussian curve fit to a photosynthesis vs. age curve.
	<u>Rate of Return</u>	
	Whole Plant Photo per Gram	The maximum observed (per gram) photosynthetic rate
	Whole Plant Total Photo	The maximum observed (per plant) photosynthetic rate

Table 4.2: Results from 3-parameter Gaussian function regression of whole plant net photosynthesis on plant age for each genotype. In addition to the parameter estimates, standard errors, 95% confidence intervals, and significance tests are provided for each parameter. Pseudo r-squares are provided as a measure of each models fit.

Geno	Parameter: α						Parameter: μ						Parameter: σ							
	Estimate	SE	95% Confidence		t Value	Approx Pr > t	Estimate	SE	95% Confidence		t Value	Approx Pr > t	Estimate	SE	95% Confidence		t Value	Approx Pr > t	Pseudo r-square	Convergence Method
			Lower	Upper					Lower	Upper					Lower	Upper				
ALE10	23.2	2.0	18.3	28.2	11.5	<0001	118.4	5.1	105.8	131.0	23.0	<0001	52.6	5.0	40.3	64.9	10.5	<0001	0.93	Marquardt
ALE12	30.5	2.8	23.7	37.3	11.0	<0001	134.2	3.5	125.5	142.8	38.0	<0001	37.0	3.3	29.0	45.0	11.3	<0001	0.94	Marquardt
ARB10	25.9	3.2	18.0	33.8	8.0	0.0002	124.3	7.6	105.7	142.9	16.4	<0001	56.7	7.6	38.1	75.2	7.5	0.0003	0.86	Marquardt
ARB8	15.6	1.9	10.9	20.3	8.1	0.0002	109.6	8.0	90.1	129.1	13.8	<0001	53.3	7.5	34.9	71.6	7.1	0.0004	0.87	Marquardt
BAR4	16.4	2.9	9.3	23.5	5.6	0.0013	109.4	11.9	80.4	138.4	9.2	<0001	55.4	11.1	28.1	82.6	5.0	0.0025	0.77	Marquardt
BAR9	17.4	2.4	11.6	23.2	7.4	0.0003	104.1	8.1	84.3	123.9	12.9	<0001	46.8	7.6	28.2	65.5	6.1	0.0009	0.85	Marquardt
BIS11	24.7	2.2	19.3	30.0	11.3	<0001	122.7	5.0	110.5	134.9	24.6	<0001	52.0	5.0	39.9	64.1	10.5	<0001	0.93	Marquardt
BIS8	22.0	1.6	18.1	25.9	13.8	<0001	114.8	4.7	103.4	126.2	24.6	<0001	55.9	4.5	44.9	66.8	12.5	<0001	0.95	Marquardt
BOS5	26.8	1.4	23.5	30.2	19.9	<0001	90.4	2.8	83.6	97.2	32.5	<0001	34.6	2.3	29.0	40.2	15.1	<0001	0.98	Marquardt
BOS6	25.6	3.6	16.7	34.4	7.1	0.0004	98.6	7.6	80.0	117.2	13.0	<0001	38.9	7.1	21.7	56.2	5.5	0.0015	0.86	Marquardt
COC14	28.0	2.9	20.8	35.2	9.5	<0001	129.0	4.9	117.0	141.0	26.3	<0001	45.7	5.0	33.5	57.9	9.2	<0001	0.92	Marquardt
COC7	23.9	2.6	17.5	30.4	9.1	0.0001	103.5	6.5	87.6	119.4	15.9	<0001	45.8	6.1	30.8	60.8	7.5	0.0003	0.91	Marquardt
HOR16	19.3	3.1	11.8	26.8	6.3	0.0008	118.6	9.7	95.0	142.2	12.3	<0001	54.0	9.4	30.9	77.0	5.7	0.0012	0.81	Marquardt
HOR6	28.8	7.5	10.3	47.2	3.8	0.0088	106.7	5.8	92.4	120.9	18.3	<0001	19.8	4.3	9.4	30.3	4.6	0.0036	0.72	Marquardt
MUR15	22.2	2.1	17.1	27.3	10.6	<0001	120.6	5.4	107.4	133.9	22.2	<0001	52.4	5.4	39.3	65.5	9.8	<0001	0.93	Marquardt
MUR17	22.4	1.4	18.9	25.9	15.8	<0001	125.4	3.5	117.0	133.9	36.3	<0001	51.7	3.5	43.2	60.1	14.9	<0001	0.97	Marquardt
PAL12	22.8	1.8	18.4	27.2	12.7	<0001	112.5	4.5	101.6	123.4	25.3	<0001	48.1	4.4	37.4	58.7	11.0	<0001	0.95	Marquardt
PAL16	23.1	3.0	15.7	30.5	7.6	0.0003	133.2	5.7	119.4	147.1	23.5	<0001	43.1	5.6	29.3	56.8	7.7	0.0003	0.89	Marquardt
PAN1	21.4	6.4	5.7	37.2	3.3	0.0159	138.5	16.3	98.6	178.4	8.5	0.0001	55.3	17.1	13.4	97.1	3.2	0.0179	0.53	Marquardt
PAN5	24.9	4.0	15.1	34.7	6.2	0.0008	127.7	9.3	105.0	150.3	13.8	<0001	55.0	9.4	32.0	77.9	5.9	0.0011	0.81	Marquardt
PIN6	31.9	5.9	17.5	46.4	5.4	0.0017	104.0	5.2	91.4	116.6	20.2	<0001	23.2	4.4	12.5	33.9	5.3	0.0018	0.82	Marquardt
PIN9	14.6	2.5	8.6	20.7	5.9	0.001	108.8	10.4	83.5	134.2	10.5	<0001	50.4	9.8	26.4	74.5	5.1	0.0021	0.79	Marquardt
POB10	22.7	2.1	17.5	27.9	10.7	<0001	121.2	5.4	108.0	134.3	22.6	<0001	52.6	5.3	39.6	65.6	9.9	<0001	0.93	Marquardt
POB7	20.6	1.9	16.0	25.3	10.8	<0001	120.0	5.5	106.5	133.6	21.7	<0001	54.1	5.4	40.8	67.4	10.0	<0001	0.93	Marquardt
RAB17	22.4	3.0	15.0	29.8	7.4	0.0003	95.4	8.5	74.6	116.1	11.3	<0001	46.0	7.6	27.2	64.7	6.0	0.001	0.86	Marquardt
RAB4	25.2	1.4	21.6	28.7	17.4	<0001	90.8	3.6	82.0	99.6	25.3	<0001	44.4	3.2	36.6	52.2	13.9	<0001	0.97	Marquardt
SPE5	26.3	2.2	20.9	31.8	11.8	<0001	119.8	4.1	109.9	129.8	29.5	<0001	44.5	4.2	34.2	54.8	10.6	<0001	0.95	Marquardt
SPE6	22.3	2.1	17.1	27.6	10.4	<0001	111.0	5.2	98.2	123.8	21.2	<0001	46.0	5.2	33.3	58.7	8.9	0.0001	0.93	Marquardt
VDM17	23.8	1.9	19.3	28.4	12.8	<0001	122.3	4.4	111.6	133.0	28.1	<0001	51.6	4.3	41.0	62.1	11.9	<0001	0.95	Marquardt
VDM9	23.5	4.0	13.8	33.2	5.9	0.001	126.9	8.9	105.1	148.7	14.2	<0001	50.7	9.0	28.7	72.7	5.6	0.0013	0.80	Marquardt
VIE3	22.9	1.5	19.2	26.5	15.3	<0001	122.0	3.8	112.6	131.4	31.8	<0001	53.8	3.8	44.5	63.1	14.2	<0001	0.96	Marquardt
VIE6	21.0	1.3	17.7	24.2	15.7	<0001	132.8	3.0	125.5	140.0	44.8	<0001	46.5	3.0	39.2	53.8	15.5	<0001	0.97	Marquardt

Table 4.3: Results from 3-parameter Gaussian function regression of rosette net photosynthesis on plant age for each genotype. In addition to the parameter estimates, standard errors, 95% confidence intervals, and significance tests are provided for each parameter. Pseudo r-squares are provided as a measure of each models fit.

Geno	Parameter: α					Approx Pr > t	Parameter: μ					Approx Pr > t	Parameter: σ					Pseudo r-square	Convergence Method	
	Estimate	SE	95% Confidence		t Value		Estimate	SE	95% Confidence		t Value		Estimate	SE	95% Confidence		t Value			
			Lower	Upper				Lower	Upper				Lower	Upper						
ALE10	22.8	1.3	19.6	26.0	17.6	<.0001	102.6	2.7	95.9	109.3	37.3	<.0001	37.7	2.7	30.9	44.4	13.7	<.0001	0.98	Marquardt
ALE12	29.4	6.3	14.0	44.9	4.7	0.0034	118.3	2.7	111.8	124.9	44.1	<.0001	23.5	4.9	11.6	35.5	4.8	0.003	0.91	Marquardt
ARB10	20.8	2.5	14.7	26.8	8.4	0.0002	96.5	6.6	80.3	112.8	14.6	<.0001	39.5	6.0	24.8	54.1	6.6	0.001	0.89	Marquardt
ARB8	12.5	3.1	4.9	20.1	4.0	0.0071	67.0	6.5	51.1	82.9	10.3	<.0001	27.4	7.5	9.1	45.7	3.7	0.011	0.82	Marquardt
BAR4	14.6	3.2	6.8	22.3	4.6	0.0037	74.1	9.3	51.4	96.7	8.0	0.0002	32.4	9.0	10.5	54.3	3.6	0.011	0.80	Marquardt
BAR9	15.3	1.6	11.4	19.2	9.7	<.0001	81.1	4.9	69.2	93.0	16.7	<.0001	28.0	4.1	17.9	38.0	6.8	0.001	0.94	Marquardt
BIS11	19.9	1.5	16.2	23.5	13.3	<.0001	104.3	4.8	92.6	116.0	21.8	<.0001	50.3	4.5	39.4	61.2	11.3	<.0001	0.95	Marquardt
BIS8	20.6	1.7	16.4	24.7	12.2	<.0001	99.7	5.2	87.1	112.4	19.4	<.0001	47.4	4.7	35.8	59.0	10.0	<.0001	0.94	Marquardt
BOS5	9.9	2.1	4.8	14.9	4.8	0.0031	70.6	8.7	49.3	92.0	8.1	0.0002	34.9	9.1	12.5	57.3	3.8	0.009	0.81	Marquardt
BOS6	16.4	0.4	15.4	17.4	40.0	<.0001	63.3	0.4	62.4	64.2	168.9	<.0001	20.8	0.4	19.8	21.8	49.9	<.0001	1.00	Marquardt
COC14	15.5	1.3	12.4	18.6	12.2	<.0001	85.1	5.0	72.9	97.3	17.1	<.0001	42.5	4.4	31.7	53.2	9.7	<.0001	0.95	Marquardt
COC7	15.5	1.6	11.7	19.3	9.9	<.0001	75.9	4.2	65.5	86.2	17.9	<.0001	29.8	3.9	20.3	39.3	7.7	0.000	0.94	Marquardt
HOR16	14.3	2.1	9.0	19.5	6.7	0.0005	82.7	7.8	63.6	101.8	10.6	<.0001	31.4	6.4	15.8	47.0	4.9	0.003	0.86	Marquardt
HOR6	12.7	2.7	6.1	19.2	4.7	0.0032	66.3	6.2	51.1	81.5	10.7	<.0001	30.5	7.5	12.1	48.9	4.1	0.007	0.85	Marquardt
MUR15	21.5	2.3	15.9	27.2	9.3	<.0001	105.6	5.1	93.2	118.0	20.9	<.0001	38.6	5.3	25.6	51.5	7.3	0.000	0.93	Marquardt
MUR17	21.9	2.0	16.9	27.0	10.7	<.0001	112.2	4.1	102.2	122.3	27.3	<.0001	39.8	4.5	28.8	50.9	8.8	0.000	0.95	Marquardt
PAL12	18.7	2.9	11.8	25.7	6.6	0.0006	81.2	7.3	63.2	99.2	11.1	<.0001	28.9	6.2	13.8	44.0	4.7	0.003	0.88	Marquardt
PAL16	24.3	5.5	10.8	37.7	4.4	0.0045	110.5	3.7	101.5	119.4	30.2	<.0001	20.0	3.5	11.4	28.6	5.7	0.001	0.84	Marquardt
PAN1	17.9	3.7	8.9	26.9	4.9	0.0028	123.6	12.9	92.0	155.2	9.6	<.0001	58.1	12.9	26.6	89.7	4.5	0.004	0.70	Marquardt
PAN5	23.7	0.8	21.7	25.7	28.4	<.0001	108.9	1.8	104.6	113.2	61.6	<.0001	42.1	1.8	37.7	46.6	23.3	<.0001	0.99	Marquardt
PIN6	17.0	1.4	13.7	20.4	12.5	<.0001	65.6	2.1	60.4	70.7	31.1	<.0001	28.9	2.6	22.6	35.3	11.1	<.0001	0.98	Marquardt
PIN9	10.1	3.1	2.5	17.6	3.25	0.0174	69.9	13.0	38.1	101.8	5.37	0.0017	35.9	13.8	2.0	69.7	2.600	0.04	0.65	Marquardt
POB10	24.5	4.0	14.7	34.2	6.1	0.0009	111.2	5.6	97.5	124.8	19.9	<.0001	34.3	7.0	17.3	51.4	4.9	0.003	0.88	Marquardt
POB7	18.1	1.1	15.3	20.9	15.8	<.0001	102.7	3.9	93.2	112.2	26.5	<.0001	47.6	3.6	38.7	56.4	13.2	<.0001	0.97	Marquardt
RAB17	234.9	23.2	178.1	291.8	10.11	<.0001	56.8	0.3	56.0	57.6	166.19	<.0001	8.5						0.93	Marquardt
RAB4	65.7	137.6	-270.9	402.3	0.5	0.65	55.9	0.2	55.3	56.5	232.9	<.0001	11.6	7.3	-6.4	29.5	1.6	0.167	0.99	Marquardt
SPE5	20.6	1.7	16.3	24.8	11.9	<.0001	97.7	4.7	86.3	109.2	21.0	<.0001	40.0	4.3	29.5	50.5	9.4	<.0001	0.95	Marquardt
SPE6	14.3	0.6	12.8	15.7	24.3	<.0001	70.2	1.5	66.6	73.9	47.3	<.0001	31.6	1.6	27.6	35.5	19.8	<.0001	0.99	Marquardt
VDM17	23.2	1.6	19.3	27.1	14.5	<.0001	112.4	3.5	103.9	120.9	32.3	<.0001	43.8	3.6	35.0	52.5	12.3	<.0001	0.97	Marquardt
VDM9	23.1	3.8	13.9	32.4	6.1	0.0009	116.4	7.3	98.5	134.3	15.9	<.0001	41.6	7.9	22.2	60.9	5.3	0.002	0.84	Marquardt
VIE3	20.5	1.4	16.9	24.0	14.2	<.0001	106.7	4.2	96.5	117.0	25.6	<.0001	47.4	4.0	37.7	57.1	11.9	<.0001	0.96	Marquardt
VIE6	21.4	1.7	17.3	25.5	12.7	<.0001	124.9	3.0	117.6	132.3	41.6	<.0001	37.9	3.2	30.1	45.8	11.8	<.0001	0.96	Marquardt

Table 4.4: Results from 3-parameter Gaussian function regression of inflorescence net photosynthesis on plant age for each genotype. In addition to the parameter estimates, standard errors, 95% confidence intervals, and significance tests are provided for each parameter. Pseudo r-squares are provided as a measure of each models fit.

Geno	Parameter: α						Parameter: μ						Parameter: σ							
	Estimate	SE	95% Confidence		t Value	Approx Pr > t	Estimate	SE	95% Confidence		t Value	Approx Pr > t	Estimate	SE	95% Confidence		t Value	Approx Pr > t	Pseudo r-square	Convergence Method
			Lower	Upper					Lower	Upper					Lower	Upper				
ALE10	12.2	1.9	7.6	16.8	6.3	0.0004	168.2	5.6	154.9	181.4	30.0	<.0001	35.0	5.6	21.7	48.3	6.2	0.0004	0.86	Gauss
ALE12	17.5	0.6	16.0	19.1	27.6	<.0001	168.1	0.8	166.2	170.1	205.4	<.0001	26.1	0.9	23.9	28.3	28.0	<.0001	0.99	Gauss
ARB10	15.5	3.6	7.0	23.9	4.3	0.0035	159.7	9.7	136.6	182.7	16.4	<.0001	42.5	9.2	20.7	64.3	4.6	0.003	0.70	Gauss
ARB8	16.1	1.7	12.1	20.1	9.5	<.0001	141.0	4.1	131.4	150.7	34.7	<.0001	35.9	3.4	27.8	43.9	10.5	<.0001	0.92	Gauss
BAR4	17.7	2.2	12.5	22.8	8.1	<.0001	157.1	2.9	150.3	163.9	54.5	<.0001	26.9	3.7	18.1	35.7	7.2	0.000	0.94	Gauss
BAR9	10.9	1.2	8.0	13.7	9.0	<.0001	149.4	4.4	139.0	159.8	33.9	<.0001	38.8	3.9	29.6	48.1	9.9	<.0001	0.91	Gauss
BIS11	10.9	1.1	8.3	13.4	10.2	<.0001	159.9	2.7	153.6	166.2	59.9	<.0001	29.6	3.1	22.2	37.1	9.4	<.0001	0.95	Gauss
BIS8	9.9	0.2	9.5	10.3	58.3	<.0001	167.7	0.3	167.0	168.4	539.7	<.0001	23.2	0.4	22.3	24.0	62.3	<.0001	1.00	Gauss
BOS5	18.9	3.5	10.7	27.2	5.4	0.001	106.1	5.9	92.1	120.2	17.9	<.0001	31.1	6.1	16.8	45.5	5.2	0.001	0.82	Gauss
BOS6	31.1	8.2	11.6	50.6	3.8	0.007	110.2	4.2	100.3	120.1	26.3	<.0001	19.0	3.7	10.3	27.7	5.2	0.001	0.79	Gauss
COC14	22.9	2.8	16.3	29.4	8.2	<.0001	152.7	4.1	142.9	162.5	36.8	<.0001	31.4	3.9	22.2	40.6	8.1	<.0001	0.92	Gauss
COC7	15.9	1.4	12.5	19.2	11.3	<.0001	130.0	3.4	121.9	138.2	37.8	<.0001	38.3	3.2	30.7	45.9	11.9	<.0001	0.94	Gauss
HOR16	16.2	1.5	12.6	19.7	10.7	<.0001	154.7	3.5	146.4	163.1	43.8	<.0001	36.8	3.3	29.1	44.5	11.3	<.0001	0.94	Gauss
HOR6	14.5	4.4	3.8	25.2	3.3	0.016	134.5	12.0	105.2	163.9	11.2	<.0001	38.7	11.4	10.9	66.6	3.4	0.014	0.64	Gauss
MUR15	12.5	0.3	11.9	13.2	44.7	<.0001	174.2	0.6	172.8	175.7	285.1	<.0001	22.8	0.5	21.7	23.9	49.4	<.0001	1.00	Gauss
MUR17	12.2	0.7	10.5	13.9	17.2	<.0001	188.1	2.1	183.1	193.1	88.9	<.0001	20.0	2.0	15.2	24.7	10.0	<.0001	0.98	Gauss
PAL12	19.8	1.5	16.2	23.4	13.0	<.0001	154.2	2.8	147.7	160.8	55.6	<.0001	34.3	2.6	28.2	40.5	13.3	<.0001	0.96	Gauss
PAL16	16.9	0.7	15.2	18.6	23.5	<.0001	158.9	0.6	157.4	160.3	262.8	<.0001	23.9	1.1	21.3	26.5	21.7	<.0001	1.00	Gauss
PAN1	154.1	0.0	154.1	154.1	7.65E+08	<.0001	194.4	0.0	194.4	194.4	6.40E+10	<.0001	5.4						1.00	Gauss
PAN5	286.1	0.0	286.1	286.1	7.09E+08	<.0001	194.5	0.0	194.5	194.5	5.99E+10	<.0001	5.4						1.00	Gauss
PIN6	52.3	9.9	29.9	74.8	5.3	0.0005	100.0						1.5						0.67	Gauss
PIN9	13.9	0.6	12.6	15.3	24.2	<.0001	137.4	1.6	133.7	141.1	87.5	<.0001	30.0	1.2	27.2	32.7	25.6	<.0001	0.99	Gauss
POB10	13.3	0.5	12.2	14.4	28.3	<.0001	181.2	1.3	178.2	184.2	141.5	<.0001	22.2	0.9	20.2	24.3	25.8	<.0001	0.99	Gauss
POB7	10.6	0.2	10.1	11.1	51.4	<.0001	167.2	0.4	166.4	168.0	474.3	<.0001	23.7	0.4	22.6	24.7	53.9	<.0001	1.00	Gauss
RAB17	31.7	4.9	20.2	43.2	6.5	0.0003	108.2	3.0	101.1	115.4	35.7	<.0001	19.8	2.4	14.2	25.4	8.4	<.0001	0.90	Gauss
RAB4	27.9	3.3	20.1	35.7	8.4	<.0001	108.9	2.5	103.0	114.8	43.9	<.0001	23.1	2.4	17.5	28.7	9.7	<.0001	0.94	Gauss
SPE5	330	2.5E-05	330	330	1.33E+07	<.0001	160.7	0.0	160.7	160.7	6.73E+08	<.0001	8.1						1.00	Gauss
SPE6	18.9	2.9	12.0	25.7	6.5	0.0003	130.6	5.4	117.8	143.4	24.1	<.0001	30.9	4.7	19.7	42.2	6.5	0.0003	0.85	Gauss
VDM17	8.0	0.5	6.8	9.1	16.2	<.0001	173.0	1.8	168.8	177.1	98.4	<.0001	27.6	1.6	23.7	31.5	16.9	<.0001	0.98	Gauss
VDM9	9.4	0.1	9.0	9.7	70.7	<.0001	180.0	0.6	178.7	181.3	322.0	<.0001	19.6	0.3	18.8	20.4	59.6	<.0001	1.00	Gauss
VIE3	12.2	0.1	11.9	12.5	96.9	<.0001	170.9	0.2	170.4	171.4	783.7	<.0001	21.0	0.2	20.5	21.4	111.0	<.0001	1.00	Gauss
VIE6	126.9	0.0	126.9	126.9	2.98E+07	<.0001	194.6	9.16E-08	194.6	194.6	2.12E+09	<.0001	5.9						1.00	Gauss

Table 4.5: Eigenvalues, proportion variance explained and significance threshold for rosette, inflorescence and whole plant carbon economy PCAs. * denotes PC's with eigenvalues > threshold.

Rosette Economy PCA			
Principal Component	Eigenvalue	Proportion of Variance Explained	Upper 99% Threshold
1	6.97	58.1	2.74 *
2	1.55	12.9	2.15
3	0.84	7.0	1.83
4	0.74	6.2	1.57
5	0.63	5.2	1.34
6	0.48	4.0	1.16
7	0.24	2.0	0.99
8	0.18	1.5	0.85
9	0.15	1.3	0.72
10	0.10	0.8	0.6
11	0.07	0.6	0.48
12	0.05	0.4	0.35

Inflorescence Economy PCA			
Principal Component	Eigenvalue	Proportion of Variance Explained	Upper 99% Threshold
1	4.05	45.0	2.44 *
2	1.73	19.2	1.9
3	1.21	13.4	1.6
4	0.74	8.2	1.31
5	0.56	6.2	1.12
6	0.34	3.8	0.96
7	0.19	2.2	0.8
8	0.14	1.6	0.64
9	0.05	0.5	0.5

Inflorescence Economy PCA			
Principal Component	Eigenvalue	Proportion of Variance Explained	Upper 99% Threshold
1	2.17	43.4	1.98 *
2	1.27	25.5	1.48
3	0.81	16.3	1.16
4	0.47	9.5	0.96
5	0.27	5.4	0.78

Table 4.6: Loadings onto PC1 from three separate PCAs of rosette, inflorescence and whole plant economic traits.

Rosette Economy PC1 (58%)	
Rosette Photo per Gram at Bolting	-0.84919
Max Rosette Photo per Gram	-0.25663
Max Rosette Total Photo	0.37331
Rosette Area	0.55543
Proportion Rosette	0.62587
Max Rosette Mass Per Area	0.71436
Rosette Leaf Lifespan	0.81566
Rosette Lifetime Carbon Gain	0.88812
Rosette Functional Lifespan	0.905
Rosette Mass	0.9091
Total Leaf Number	0.92831
Rosette Mas per Area at Bolting	0.93434
Inflorescence Economy PC1 (45%)	
Branch Mass per Length	-0.32442
Inflorescence Mass	0.44691
Post-bolting Plant Functional Lifespan	0.49727
Inflorescence Functional Lifespan	0.62606
Max Inflorescence Photo per Gram	0.64214
Max Inflorescence Total Photo	0.67268
# Basal Inflorescence Branches	0.7714
Inflorescence Lifetime Carbon Gain	0.89346
Proportion Inflorescence	0.91905
Whole Plant Economy PC1 (43%)	
Whole Plant Photo per Gram	-0.54804
Whole Plant Total Photo	-0.36888
Whole Plant Lifetime Carbon Gain	0.55694
Total Mass	0.80372
Whole Plant Functional Lifespan	0.88138

Table 4.7: Results from univariate regressions of plant carbon economy traits onto home climate PC1 scores. Each regression was conducted independently on the population means for the traits listed on each row. Dependent variables were standardized (mean = 0, standard deviation = 1). Regressions are sorted by the economy measured (i.e. rosette, inflorescence, whole plant). For each regression, the parameter estimates \pm the standard error are provided followed by the t-test, p-value and r^2 describing the model fit. Descriptive statistics (mean, standard deviation, minimum and maximum values) for each dependent variable are also provided. Significant models are in bold.

Trait	Parameter			Approx			Trait Descriptive Statistics			
	Estimate	\pm SE	t Value	Pr > t	r^2	Mean	Std Dev	Min	Max	
Summed Fruit Length	-0.71	\pm 0.19	-3.75	0.0021	0.50	601.66	160.50	369.40	962.40	
Age at Bolting	0.57	\pm 0.22	2.57	0.0222	0.32	98.53	27.55	59.60	167.80	
Rosette Economy PC1	0.49	\pm 0.23	2.09	0.0552	0.24	0.00	2.64	-5.85	3.82	
Inflorescence Economy PC1	-0.72	\pm 0.19	-3.90	0.0016	0.52	0.00	2.01	-4.07	2.90	
Whole Plant Economy PC1	0.55	\pm 0.22	2.47	0.0268	0.30	0.00	1.47	-2.91	2.33	

Table 4.8: Analysis of fitness effects. Standardized (mean = 0, std. dev. = 1) summed fruit length was regressed on genotype mean scores for rosette and inflorescence economy PC1. Parameter estimates $\beta \pm$ one standard error is provided with significance tests. Overall model F-value, p-value and r^2 are also presented. N=32.

Traits	$\beta \pm$ SE	t-value	P	F-value	Overall P	r^2
Rosette Economy PC1	-0.22	0.3	-0.75	0.46	6.77	0.004
Inflorescence Economy PC1	0.36	0.3	1.24	0.23		0.32

Note: Correlation between predictors was $r = -0.85$ ($p < 0.0001$, $n=32$).

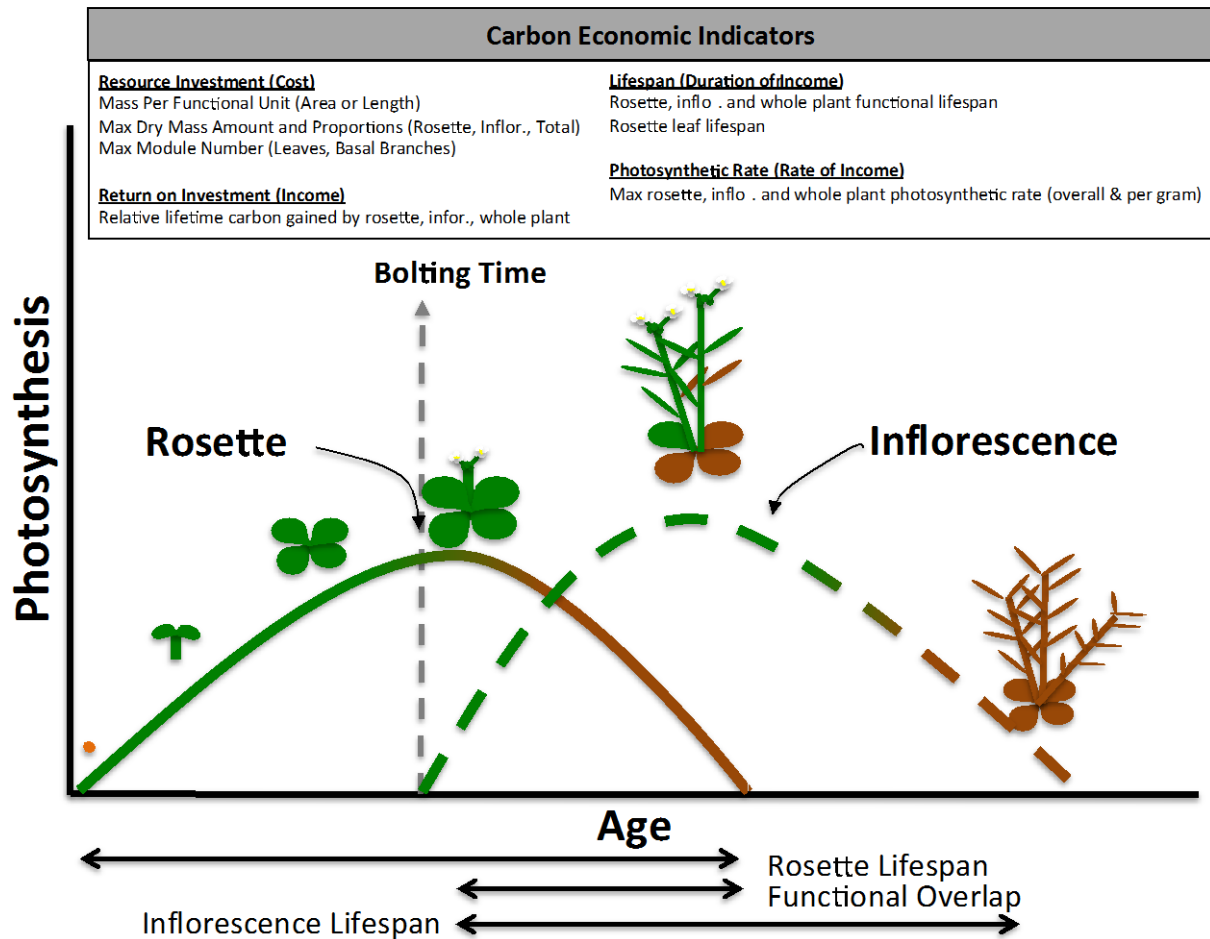


Figure 4.1: Conceptual model of rosette and inflorescence carbon economy. Illustrated here is our conceptual framework for understanding whole plant carbon economy. Plant carbon economy is determined by the balance between resource investment (cost) and return on investment (income), which is a function of rate and duration of income. Total rosette photosynthesis rises until a peak near the time of bolting. Upon bolting, a period of photosynthetic carbon gain by the inflorescence begins and the plants life ends when the inflorescence has fully senesced. In this scheme, the whole plant's lifespan is allocated between rosette and inflorescence with a period of functional overlap, which hinges on the age at bolting. The inset lists carbon economic indicators quantified in this study according to the aspect of economy they measure (i.e. resource investment).

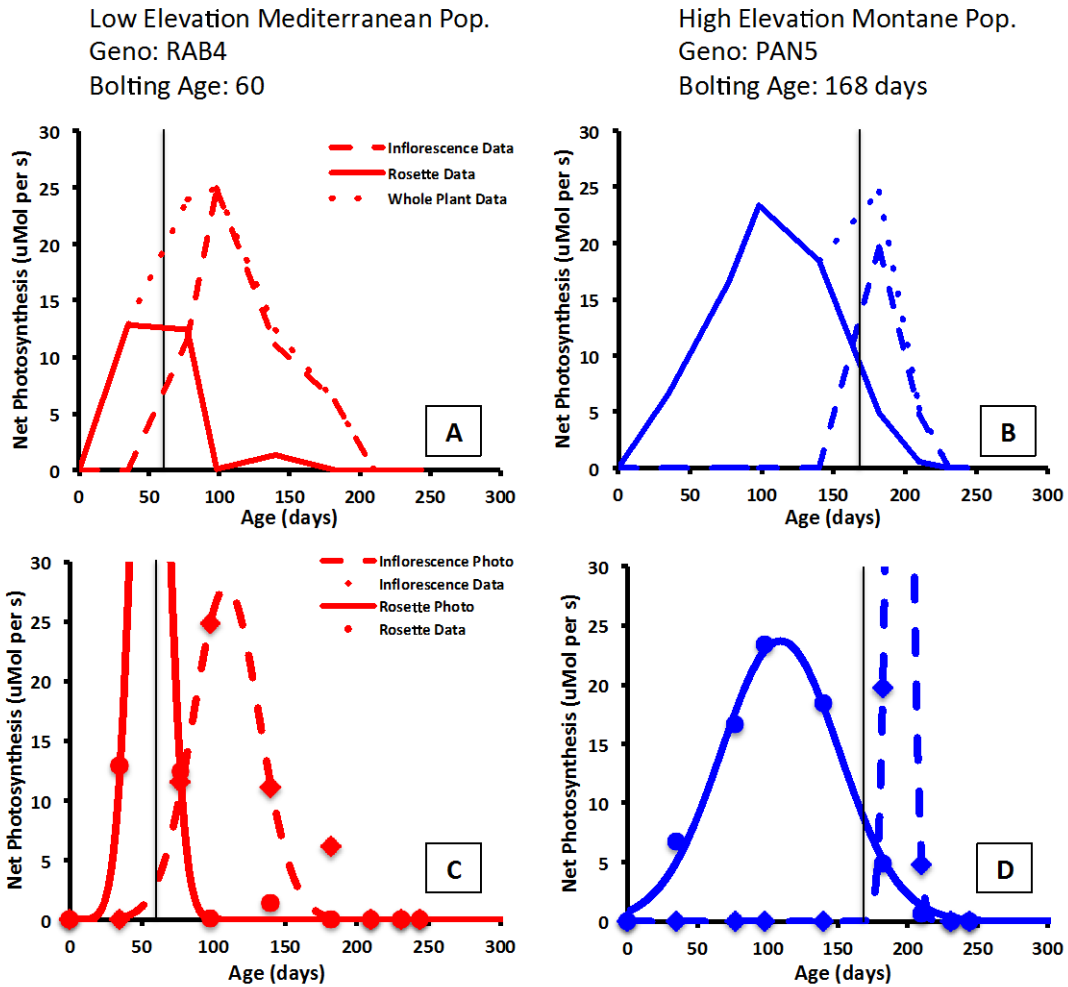


Figure 4.2: Examples of lifetime photosynthetic carbon gain data and models. Here we compare line plots of lifetime carbon gain for an early bolting, low elevation genotype RAB4 (A) to the high elevation, late bolting genotype PAN5 (B). We also compare Gaussian functions fit to each genotypes carbon gain curve for the rosette and the inflorescence separately (C, D). We place a narrow vertical bar through the age at bolting in each plot.

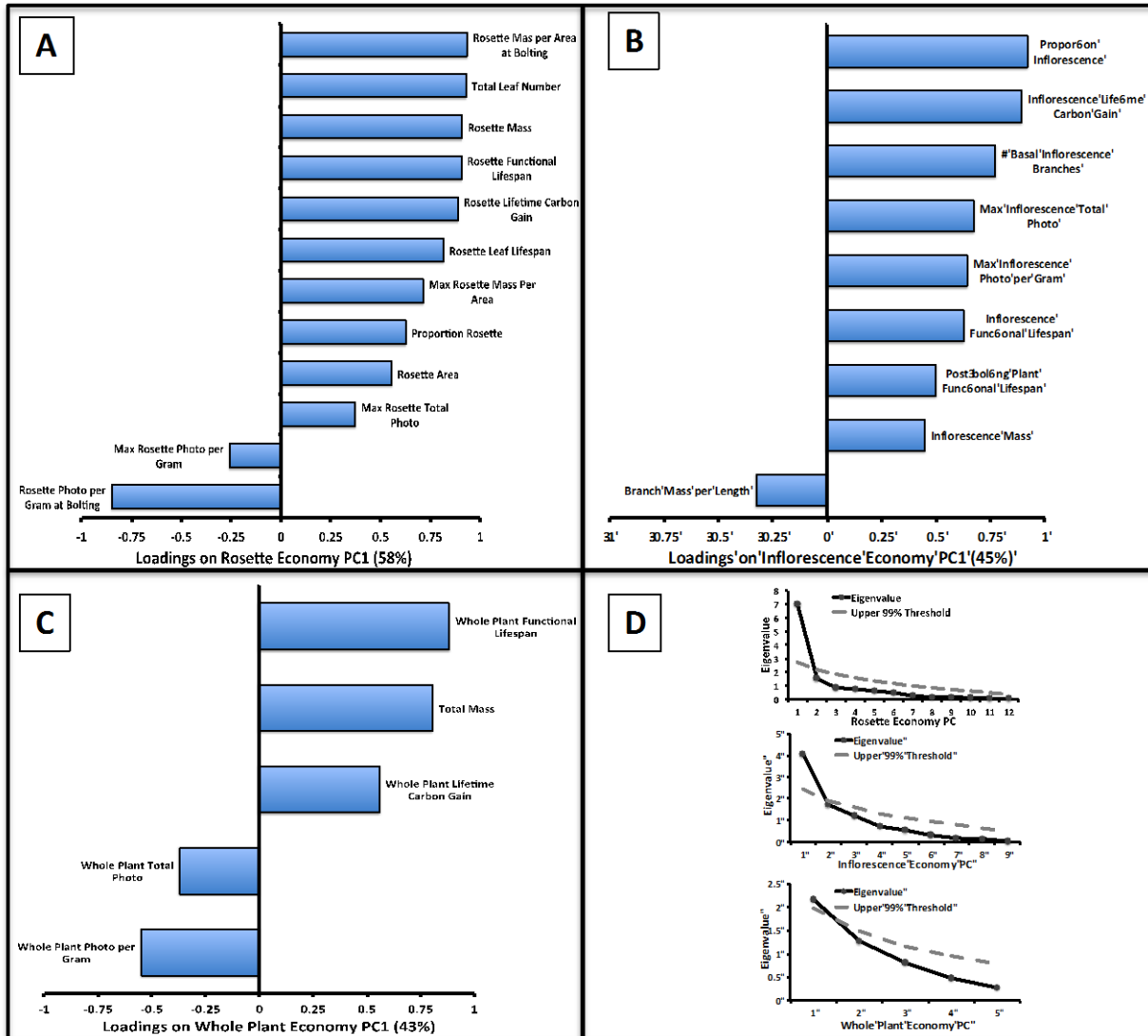


Figure 4.3: Rosette, inflorescence and whole plant carbon economy PCA results. Correlating between PC scores and the original variables (loadings) are presented in this horizontal bar plot. Panels A-C show loadings for rosette, inflorescence and whole plant economy PC1 respectively. The sign of each loading indicates whether trait values increase or decrease with increasing scores on the corresponding PC and also indicates the relationship among the traits in each analysis. Panel D shows scree plots for the analyses summarized in panels A-C. In each scree plot, eigenvalues are plotted against the upper 99% limit of the distribution of eigenvalues under the null hypothesis of random correlation structure. Eigenvalues that are greater than the threshold represent meaningful axes for summarizing carbon economy.

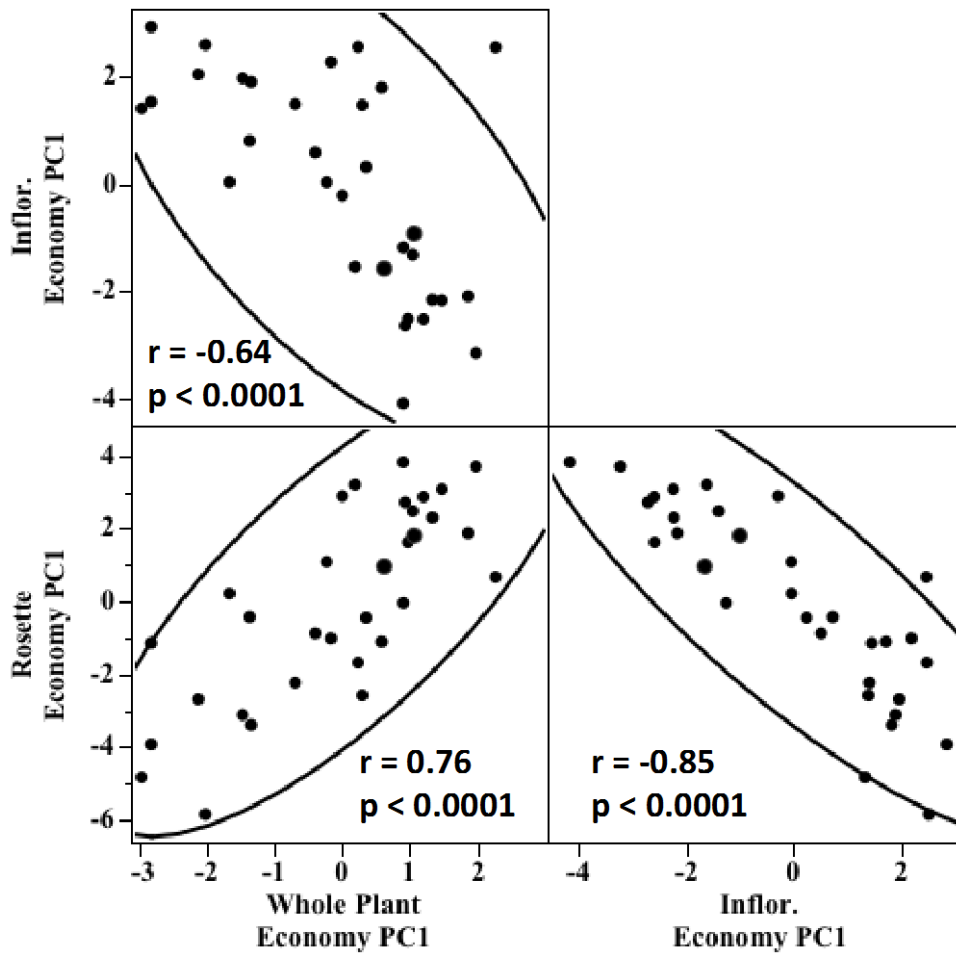


Figure 4.4: Scatterplot matrix for whole plant, rosette and inflorescence economy PC1 scores. 95% confidence ellipses are shown and pearson product-moment correlation coefficients and corresponding p-values are inset in each panel. N = 32.

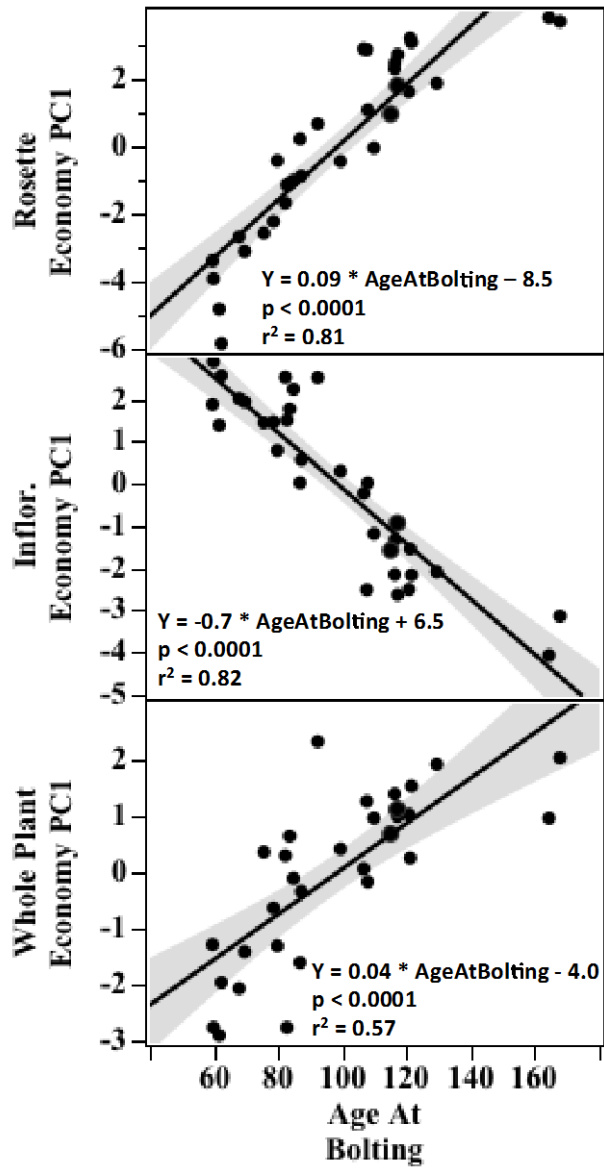


Figure 4.5: Regression of rosette, inflorescence and whole plant economy PCI scores on age at bolting (days since sowing). The equation for the best fit line along with corresponding p-value and r^2 are inset in each panel. $N = 32$.

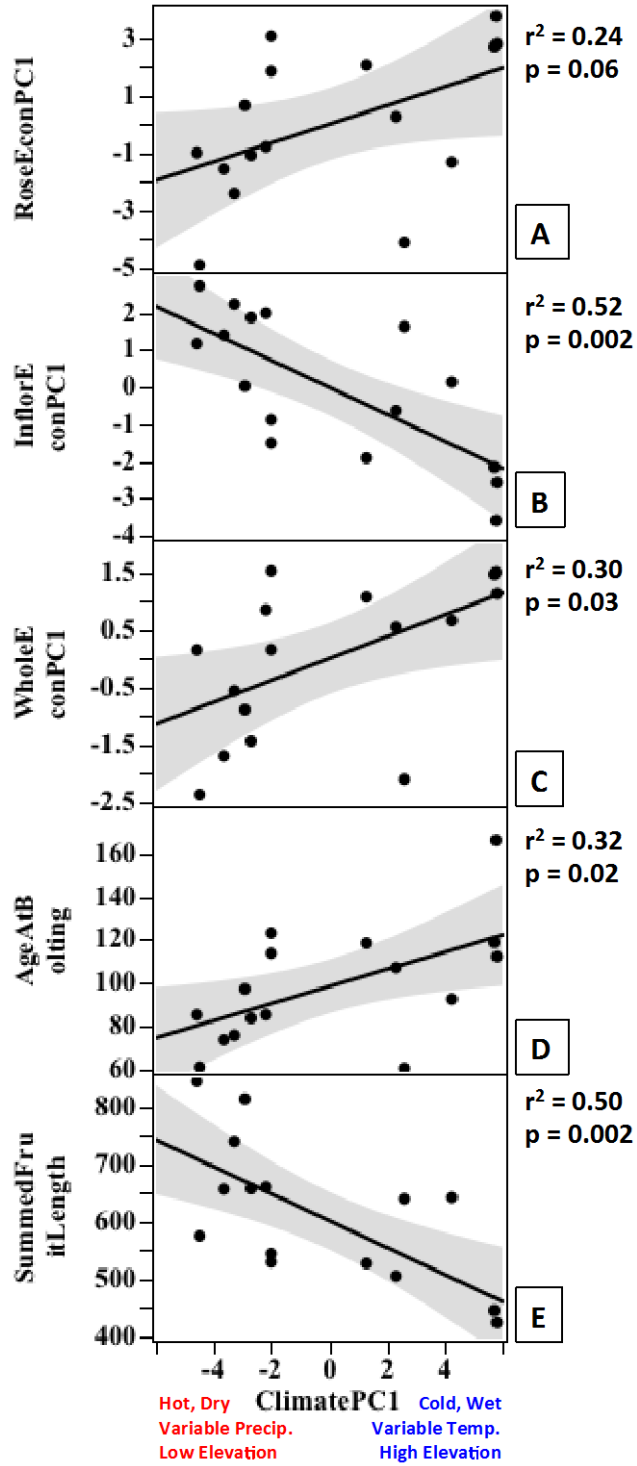


Figure 4.6: Associations between carbon economic spectra (A-C) plus age at bolting (D) and summed fruit length (E) and home climate PC1 scores. r^2 and p-value are provided at right.

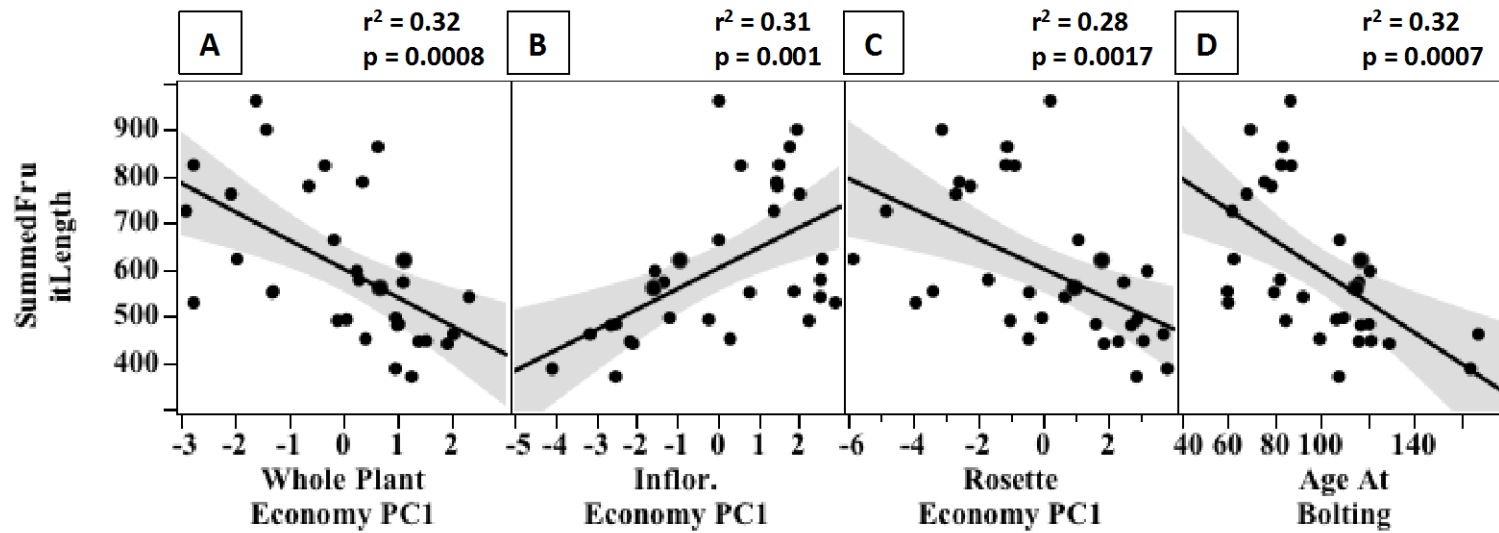


Figure 4.7: Regression of summed fruit length on whole plant (A), inflorescence (B) and rosette economy PC1 (C) plus age at bolting (D). r^2 and p-value are presented, $n = 32$.

5.0 CONCLUSION

In this dissertation I set out to improve understanding of the functional ecology and adaptive evolution of annual plants. I began with the idea that life is difficult and all species are constrained in the conditions in which they can succeed. Adaptive differentiation is a prevalent phenomenon in the plant kingdom, yet the nature of natural selection and genetic constraint that result in this differentiation is rarely understood (Linhart & Grant 1996; Hereford 2009; Leimu & Fischer 2008). Recognizing that successful adaptation to any environment likely requires close integration of numerous plant characters (Grime 1977; Murren 2002); I examined suites of traits describing key aspects of plant form and function. I used the annual plant and genetic model organism *Arabidopsis thaliana* collected across a climate gradient as a case study of adaptive trait divergence.

I found that almost every trait investigated covaries with variables describing the climate of origin. Association between environmental variables and plant traits are a classic approach and provide a key piece of evidence indicating that those traits are under divergent selection in different environments (Clausen et al. 1940; Antonovics 1976; Endler 1986). I therefore combined trait-environment associations with analyses of the fitness effects of those traits under controlled conditions to develop functional hypotheses about adaptation across my focal climate gradient.

In *A. thaliana* and other annual plants, the correct timing of reproduction is critical for success (Cohen 1976; Metcalf & Mitchell-Olds 2009) and has thus become one of the most investigated plant traits. One of my major contributions therefore, is showing that fitness depends not just on the age of reproductive onset, but on the rate and magnitude of other physiological processes like carbon acquisition and fruit ripening (Chapter 2). However, I found, as others have (Van Tienderen et al. 1996; Scarcelli et al. 2007; Atwell et al. 2010) that the age at bolting is highly correlated and potentially causally related to variation in many other plant traits. In subsequent studies, I found evidence that *A. thaliana* rosettes experience a trade-off between fast- and slow-return carbon economics and that the trade-off is strongly associated with the age at bolting (Chapter 3). In fact, I found that even inflorescence traits are highly integrated with bolting time, even though because inflorescence development plays out after bolting, this was not necessarily true (Chapter 4).

Ultimately, from this dissertation, I generate hypotheses about the selective agents and subsequent selection responses that led to the trait-climate associations observed in chapters two through four. Low elevation sites along my focal, N.E. Spanish climate gradient are generally hot and dry, but are particularly so during the transition from spring into summer. I hypothesize that as a result of stochastic (or even consistent) heat waves and droughts during the reproductive season (spring), populations become have evolved ruderal, or avoidance characteristics. That is, I hypothesize that plants at low elevations must complete their life cycle before being killed off by unsuitable conditions during the spring. Thus these plants have reduced investment in vegetative rosettes, earlier bolting, faster fruit ripening rates and an overall cheaper construction (thinner stems and rosettes) and greater mass use efficiency overall (fruits per mass).

In contrast to the adaptive strategy I have hypothesized for low elevation plants, at high elevations conditions are cold and wet. During the winter in particular, high elevation N.E. Spanish sites experience snow cover and extended periods of freezing or sub-zero temperatures. However, high elevation reproductive seasons (springs) are longer and hypothetically milder in terms of temperature and water availability. The plants from these montane sites have longer, more carbon intensive lives in which they spend a significant amount of time as a vegetative rosette. Thus, while low elevation plants move quickly and cheaply to the finish line (seed production), high elevation plants are hypothesized to succeed by going slowly and investing in mechanisms of cold, or freezing tolerance. These hypotheses, if further studies (see below) should support them, suggest the differences in the selective regime at opposite extremes of the climate gradient place conflict demands on plant form and function leading to a trade off in fitness (local adaptation) across the gradient.

This work is significant because it provides insight into the trade offs that at least annual plant species experience in adapting to variation in climate regime. Further, the strong genetic correlation structure, particularly the rosette-inflorescence economy trade-off revealed in Chapter 4 is valuable for understanding adaptive divergence in general. Schluter (1996) famously referred to the first principal component of the G -matrix as an evolutionary line of least resistance. Thus in N.E. Spanish *A. thaliana* at least, such strong correlation structure associated with variation in bolting age might either constrain or else facilitate adaptation. If selection favors plants with late bolting and a long-lived, productive inflorescence for instance, evolutionary response may be slow. However, if selection is in the same direction as the correlation structure (late bolting, short-lived, unproductive inflorescence) than adaptation may occur quickly.

There are two major avenues for advancing the work presented in my dissertation. Firstly, advanced generation crosses of genotypes from across the climate gradient can break apart combinations of alleles across multiple loci. This will allow association-mapping studies to reveal the number of effect of loci underlying traits implicated in adaptive evolution by my dissertation. This will help determine whether and to what extent the correlations observed in my thesis work are due to natural selection and subsequent genetic linkage or else antagonistic pleiotropy. Secondly, field studies to better understand the true selective agents operating across my focal climate gradient are needed. In the field, it should now be possible to take advantage of the data I have generated on genetic correlations among traits in the lab. Instead of attempting to measure plant physiology in the field, we can make interpretations of functional significance in the field in part based on results generated in the lab.

This is an exciting time in evolutionary ecology. Studies like the ones presented here provide evolutionary context and hypotheses for explaining the origin and maintenance of genetic and phenotypic diversity within and among species. It is my hope that as we improve our understanding historical adaptive evolution, like the kind I have shown occurred in N.E. Spain, we will also enhance our appreciation of the consequences of current and future changes to the climate.

APPENDIX A

A.1 DETAILED DESCRIPTION OF PLANTING DESIGN AND SET-UP

We planted two sets of replicates of the 32 experimental genotypes designated as the fall and spring cohorts (see below). We prepared 18 replicate pots per genotype for the fall cohort and 10 replicates for the spring. Four replicate pots per genotype were planted for the fall cohort and three replicates for the spring cohort were planted for early-age destructive sampling in Ray Leach RLC3 49 mL Cone-tainers. The remaining replicates were planted in Ray Leach SC10 164 mL Supercell Cone-tainers (hereafter pots, regardless of size) (<http://www.stuewe.com/products/rayleach.php>).

We filled all pots with Turface MVP fritted clay (<http://www.turface.com>) including with 0.21-0.24 grams of Nutricote pellets that released equal daily quantities of nutrients for 100 days (NPK 13-13-13, Type 100, Arysta Life Science NA Co., New York, NY). Central plugs 1 cm wide by 2 cm deep of Sunshine germination-mix (<http://www.sungro.com>) in each pot provided a safe site for germination and early growth. RLC3 and SC10 pots were placed in RL200 and RL98 racks (<http://www.stuewe.com/products/rayleach.php>) respectively.

Seeds were surface sterilized through exposure to chlorine gas for three hours prior to planting. We planted 10-20 seeds per pot and at 15 days post-sowing we thinned seedlings to one per pot. During each round of planting (fall and spring) we planted half of the replicates of each genotype on each of two consecutive days. The spring planting took place 20 weeks after the fall cohort was planted.

After planting racks were placed in the dark at 4°C and 100% relative humidity for seven days to induce germination competency. After the cold treatment, racks were transferred into a Conviron PGW36 growth chamber for the remainder of the experiment.

A.2 CREATING A DYNAMIC GROWTH CHAMBER CYCLE SIMULATING LOW ELEVATION GROWING SEASON IN N.E. SPAIN.

We imposed a dynamic growth chamber cycle in which temperature, day length and water availability varied over a 40-week period. Growth chamber seasonal cues, combined with heating and drying stress in the reproductive phase, result in variable fitness among N.E. Spanish populations such that low elevation plants are favored and fecundity scales with climate of origin (**Wolfe & Tonsor in press**). We based the seasonal temperature cycle on field plant-height temperature obtained from Hobo pendant temperature loggers (www.onsetcomp.com) placed in four low elevation sites, logging every 60 or 90 minutes. The number of years of temperature data and the number of loggers per population site varied as follows: BAR (2007-2010: 1 logger), COC (2007: 1, 2010: 3), population HOR (2007-2010: 1) and RAB (2010,:2). We extracted daily high and low temperatures from the raw logger data (Dryad doi:(to be posted at time of acceptance)). We averaged by day across years and sites separately for daily high and low temperature. We then averaged daily high and low temperatures in seven-day intervals. This created an archetype of a low elevation Mediterranean temperature regime, not representing any specific site or year. Growth chamber temperature ramped linearly between the weekly mean minimums at the time lights turned on and weekly mean maximums at the time lights turned off (**Figure 3.5a, Table 3.11**).

Day length was also varied on a weekly basis (**Figure 3.5b, Table 3.11**) based on US Navy sunset/sunrise table calculator (http://aa.usno.navy.mil/data/docs/RS_OneYear.php) for the mean latitude and longitude (42.1539° Lat, 1.5738° Lon) of the study populations' sites of origin.

Fall cohort plants were germinated under mild conditions that continued for two weeks: 12 hour day length, $150 \pm 50 \mu\text{mol photons m}^{-2} \text{ s}^{-1}$, 18°C maximum and 12°C minimum daily temperatures. At the third week post-sowing, light increased to $350 \pm 50 \mu\text{mol photons m}^{-2} \text{ s}^{-1}$ and the seasonal day length and temperature regimes were begun for the fall cohort (**Figure 3.5**). Lighting increased a final time to $550 \pm 50 \mu\text{mol photons m}^{-2} \text{ s}^{-1}$ at the start of week four. Based on observations of field germination timing (Montesinos et al. 2009), we began our growth chamber temperature and daylength cycle to correspond with conditions in the field at the beginning of October.

The spring cohort plants were sown 20 weeks after the fall cohort and were moved to the growth chamber at the start of week 21. Conditions for germination for spring cohort plants therefore corresponded to field logger data between 2/24 and 3/02. Unlike the fall germination cohort, the spring germinating plants had to share a growth chamber with the now mature fall germinated cohort growing in $550 \pm 50 \mu\text{mol photons m}^{-2} \text{ s}^{-1}$. To match conditions for the fall germinating cohort shade screens were placed over the spring cohort. Seedlings were started with two layers of fiberglass window screen, reducing light intensity to $150 \pm 50 \mu\text{mol photons m}^{-2} \text{ s}^{-1}$. Three weeks after sowing one layer was removed raising light to $350 \pm 50 \mu\text{mol photons m}^{-2} \text{ s}^{-1}$. At four weeks all shade screen was removed.

We simulated the low elevation spring dry-down (Montesinos et al. 2009) between weeks 34 and 40 under thermal conditions corresponding to field logger data for 5/30 to 7/12. Water

availability was controlled by varying standpipe and thus water table height in growth bins such that water table declined by 0.5” (0.2 grams of water per pot per day) every week during the dry down. For the first 20 days of life standpipe height is 7” with constant water supply. From day 21 to 27 bins are drained each day and filled in the morning for one hour providing approximately 2.8 grams of water per pot per day (**Tonsor, unpublished**). On day 28, standpipe height was reduced to 4” or 1.6 grams of water per pot per day and remained at this supply rate until the week 34 dry down (**Figure 3.5c, Table 3.11**).

Because CO₂ concentration the building that housed the growth chambers varied both daily and seasonally, we controlled CO₂ concentration by keeping it just above the building maximum at 530 ppm.

After ebb-and-flood watering regime began, rack rotations were conducted on a twice-weekly basis and continued for the duration of the experiment.

A.3 DETAILED DESCRIPTION OF SAMPLING DESIGN AND TRAIT MEASUREMENTS.

The nine fall and five spring cohort measurement periods (**Table 3.12**) involved destructive sampling. At each time point two replicates of each genotype, one on each of two consecutive days, were sampled from the growth chamber (n=32 plants per day). This had the effect of thinning out growth chamber space as plants grew, minimizing light-competition. All examinations of trait changes over time are done at the genotype means level.

For the fall cohort on the first two sampling dates we used only the smaller RLC3 type pots in order to avoid pot size effecting development. This design increased the number of plants

we could grow at one time and thus the number of time points we could sample. For the spring cohort, we planted one replicate per sample date per genotype in RLC3 and one in SC10 for the first three of the five sampling dates. In all cases, we randomly and evenly assigned and distributed pots across racks within each sampling date / planting day combination.

At all except each cohort's final sampling date we measured whole plant photosynthesis. When inflorescences were present, we also measured inflorescence gas exchange excluding the rosette. Measurements commenced one hour after lights on in a separate growth chamber whose temperature matched that of the primary growth chamber. Gas exchange measures were made with a LI-6400 XT infrared gas analyzer (IRGA; LI-COR Biosciences, Inc., Lincoln NE) connected to a custom built four-cuvette array (Tonsor & Scheiner 2007; Earley et al. 2009; Tonsor et al. 2013).

In order to interface plants with the whole plant cuvette array, we increased the height of SC10 pots by approximately 0.25" by fitting the pots with removable collars consisting of a 6" strip of rubber splicing tape (Scotch 130C 1" Linerless Rubber Splicing Tape, 3M, Austin, TX). We used thoroughly washed bicycle tire inner tubes cut into approximate 1 cm sections to increase the height of the smaller RLC3 pots. By extending the height of each pot with a removable collar we were able to non-destructively expose the top 0.5 cm of the primary root, which was crucial for interfacing the plant with our whole plant gas exchange system.

For plants with inflorescences, after whole plant measures were conducted, a measurement of inflorescences only was taken (see Earley et al. 2009). This allowed rosette gas exchange rates to be estimated by subtracting inflorescence rates from whole plant rates. Measures from plants with fully senescent rosettes were not used in this study and rosette gas exchange was set to zero in the dataset. For all measures, plants were allowed to equilibrate in

the open-system cuvette for 15 minutes before we recorded net carbon assimilation ($\text{nM CO}_2 \text{ s}^{-1}$) rate five times over one minute. For each plant, we averaged across the five records for a single measurement of instantaneous gas exchange. After additional measurements (see below) rosettes were collected, dried for a week at 70°C and massed, allowing us to express rosette gas exchange rates on a dry mass basis.

After physiological measurements, we recorded the total number of live (TLLN and dead (TDLN) leaves. Rosette status was then calculated as the ratio ($\text{TLLN} / (\text{TLLN} + \text{TDLN})$), or the proportion of rosette leaves that are alive (Proportion Live Leaves). After leaf counting, we severed each rosette from the root system at the soil surface, flattened it under a pane of glass and photographed it with a 1cm^2 area standard obtaining a top down, projected rosette area using a pixel-counting macro (available upon request) in NIH ImageJ 64-bit version 1.47k (<http://rsbweb.nih.gov/ij/>). We then calculated the ratio of rosette dried mass to projected area (rosette mass per area hereafter).

We also estimated the summed fruit length, a proxy for the total seed number (Tonsor et al. 2013; Wolfe & Tonsor in press, by counting the number of ripened fruits (siliques) on the final harvest. We separated, spread out and photographed all inflorescence branches, then used the random grid overlay function of NIH ImageJ to generate digital transects across the inflorescence branches of a plant. We used the NIH ImageJ line tool to measure the length of each fruit that intersected a transect line. The average fruit length times the total fruit number equaled the summed fruit length.

We also conducted weekly censuses, recording age at bolting. Age at bolting is expressed as the number of days since sowing.

APPENDIX B

EXPERIMENT TO DETERMINE THE EFFECT OF FERTILIZER REDUCTION ON TRAIT-ELEVATION ASSOCIATIONS

B.1 BACKGROUND

Plants grown in growth chambers in nutrient saturated environments grow to sizes much larger than those observed in the field (Wolfe, personal observation). The focal species *A. thaliana* grows across a broad range of environmental conditions (Hoffmann 2002) including at least nitrate supplies ranging from 1-56 ppm (Diane Byers, personal communication; see also Tonsor et al. 2013). In the dynamic seasonal growth chamber experiment described above, I sought to grow plants under nutrient limiting conditions in order to produce plants that were closer to field-observed sizes. However, I was concerned that reducing nutrient availability might alter the trait-elevation relationships I intended to test for as evidence of adaptive differentiation.

Statistical association between plant traits expressed in a growth chamber and environmental characteristics found at their place of collection is evidence of adaptive divergence. However, it does not prove that the specific predictor variable examined was the selective agent. Elevation- or climate-correlated factors like nitrogen supply, herbivory and the

phenology of plant communities could also be selecting the measure plant traits differentially across the climate gradient.

While there is no experiment we can do in the lab that would identify the actual selective agent(s), it was important that we determine whether our results depended on nutrient supply. My goal with reducing nutrient supply is to produce smaller plants but without altering the trait-elevation relationship. I conducted a short preliminary experiment with the following specific aims:

Aim 1: Determine a dosage of fertilizer suitable for reducing the plants to a more “field-like” stature. This will enable us to grow plants at a greater density and thus obtain a greater sample size.

Aim 2: Determine whether the ranking for measures of size and growth rate varies among populations as a result of fertilizer reduction. If populations respond differently to the treatments, then our future comparisons of populations will be contingent on fertilizer supply.

B.2 METHODS

B.2.1 Plant Material

One genotype from each of sixteen NE Spanish populations was selected. Selection was made at random from a collection of 48 (three per population) used in a previous study.

B.2.2 Planting Design

Three replicates were planted for each of 16 genotypes in each of three fertilizer treatments for a total of 144 plants. Plants were planted in three separate racks at a density of 48 each. Each fertilizer-genotype combination was replicated once in each tray. This means that there are three replicates per genotype per tray but each replicate is at a different fertilizer level. Additionally, the ordering of each pot within each tray was randomized.

Plants were grown in Ray Leach SC10 Supercell Conetainer 164 mL pots (www.stuewe.com/products/rayleach.html). Pots were filled with Metromix-grade Turface (<http://www.turface.com>). A 1 cm wide, 2 cm deep plug of Sunshine germination mix (<http://www.sungro.com>) was inserted at the surface of each pot. Four to ten seeds were planted per pot.

B.2.3 Fertilizer Treatments

Nutricote, an encapsulated fertilizer that releases nearly equal daily quantities of nutrients for up to 100 days (NPK 13-13-13, Type 100, Arysta Life Science NA Co., Cary NC) was screened through a colander to remove abnormally large pellets. The standard supply of Nutricote used in the lab is 1.5 mL. This volume was previously determined to provide a saturating supply of nutrients. For this experiment, ten aliquots of 1.5 mL of sieved Nutricote were weighed. Based on the mean weight ($\mu=1.62$ g) a saturating fertilizer treatment ($1.0 \text{ NUT}_{\text{saturating}}$) was created using per pot fertilizer mass of between 1.62 and 1.66 grams. Two additional treatments ($0.50 \text{ NUT}_{\text{saturating}}$ and $0.25 \text{ NUT}_{\text{saturating}}$) were created with fertilizer aliquots of 0.81-0.85g and 0.41-0.45g respectively per pot.

B.2.4 Growth Conditions

Plants were grown in a Conviron PGW36 with a daily temperature cycle of 20°C maximum at lights off and 12°C minimum at lights on each day. Twelve hours of 350 $\mu\text{M}/\text{m}^2 \cdot \text{s}$ photosynthetically active radiation were supplied per day. Plants were watered via an automated ebb-and-flood system supply a 7" water table for twenty minutes daily.

Following planting, bins were placed in the dark at 4°C and 100% relative humidity for five days to induce germination competency. After cold treatment, bins were transferred to a Conviron PGW36 with a daily temperature cycle of 20°C maximum at lights off and 12°C minimum at lights on each day. Twelve hours of 150 $\mu\text{M}/\text{m}^2 \cdot \text{s}$ photosynthetically active radiation (PAR) were supplied for seven days. On day seven after cold treatment ended the lights increased to 250 $\mu\text{M}/\text{m}^2 \cdot \text{s}$ PAR and were again increased to 350 $\mu\text{M}/\text{m}^2 \cdot \text{s}$ PAR on day nine.

B.2.5 Leaf Initiation Rate

Three counts of the total leaf number (TLN) were conducted on eight (TLN8), 13 (TLN13) and 19 (TLN19) days after germination. Counts including all true leaves at least 1 mm in length along the midrib. Leaf initiation rate (LIR) was calculated as: $\text{LIR} = (\text{TLN}_{t2} - \text{TLN}_{t1}) / (t2 - t1)$. LIR was calculated between one and eight (LIR1to8), eight and 13 (LIR8to13), 13 and 19 (LIR13to19) days after germination. The average leaf initiation rate was also calculated (AvgLIR).

B.2.6 Rosette Expansion Rate

Two methods were employed and compared for measuring project two-dimensional area of the rosette: whole-bin and individual photographs. Whole-bin photographs are taken by fixing an aluminum frame over a fiberglass bin in which one rack of 48 plants is situated. An 12 megapixel Stylus-7010 digital camera was centered over the bin. Two 1.0 cm² area standards were placed in each photograph. Silhouettes of each rosette in a photograph were selected using Photoshop CS5 Extended Edition (v12.1x64, Adobe Systems, Inc.). The background was then removed and the image converted to black and white. Pixels for each rosette and area standard were counted in NIH ImageJ 64-bit version 1.45m (<http://rsbweb.nih.gov/ij/>). Rosette area (cm²) was calculated as the number of pixels in the rosette divided by the number of pixels in the area standard. Whole-bin photographs of were taken on 21 and 24 days after germination.

Individual rosettes were also photographed for area measurements. Black construction paper was fitted between the soil surface and the rosette leaves, flattening the rosette into an approximately two-dimensional configuration. The camera was centered over the rosette with a copy stand. Area standards (1.0 cm²) were placed in each photograph. The procedure for obtaining an area measurement is essentially identical to whole-bin photographs. Individual rosette photographs have the advantage of greater magnification and focus for each rosette, but the disadvantage of being considerably more invasive and slow. Individual rosette photographs were taken on 24 and 30 days post-germination.

Relative rosette expansion rate (RoseRER) was calculated between 1 and 21, 21 and 24, 24 and 30 days after germination. The average RoseRER (AvgRoseRER) was also calculated. Whole-bin rosette area on days 21 and 24 (WBArea21 and WBArea24) as well as individual rosette area on days 24 and 30 (RosetteArea24 and RosetteArea30) were also analyzed. Relative

expansion rates are calculated as follows: $RER = (\log(\text{RoseArea})_{t2} - \log(\text{RoseArea})_{t1}) / (t2 - t1)$.

B.2.7 Leaf Expansion Rate

Leaf area was measured photographically. Leaves were fixed at a right angle to the camera and gently pressed into a two-dimensional pane between a black construction paper background and a standard microscope slide. Care was taken to non-destructively move non-focal leaves that obscured the view of the leaf-of-interest. Area standards (1.0 cm²) were placed in each photograph. The procedure for obtaining an area measurement is essentially identical to whole-bin and individual-rosette photographs. Two leaves were measured on each plant.

First, the fifth rosette leaf was photographed on day 30 after germination. This represents a group of leaves of varying age but equal position in the rosette. The age on day 30 of the fifth rosette leaf will be used as a covariate in analysis and was determined by recording the number of leaves initiated daily for the 19th day after germination.

Next, a cohort of leaves was designated as the most recently initiated (expanded to >1mm along the midrib) leaf on day 19 after germination. Leaves were marked with a spot of 3D puffy paint on the leaf tip. This represents a group of leaves all of the same age but of potentially different positions in the rosette.

The cohort of leaves was then photographed at age 21 (after leaf initiation, 40 days after germination) and again at age 26 (45 days after germination). Relative expansion rate of the cohort leaf (CohortRER) was calculated between days 1 and 21 as well as between days 21 and 26 after leaf initiation. The average cohort expansion rate (CohortAvgRER) was also calculated. Cohort leaf position in the rosette (TLN19) will be used as a covariate in analysis. Cohort leaf

area at age 21 (CohortArea21) and age 26 (CohortArea26) were also analyzed. Cohort leaf relative expansion rate was calculated as: $\text{CohortRER} = (\log(\text{CohortArea})_{t2} - \log(\text{CohortArea})_{t1}) / (t2 - t1)$.

B.2.8 Dry Mass

Aboveground plant parts were cut-off at the base of the stem 47 days after germination and dried at 65°C and weighed. Roots were washed from the soil medium, and also dried at 65°C and weighed. The dry mass of aboveground parts, roots, proportion of total mass invested in roots and total mass of the plant are all analyzed.

B.2.9 Analyses

There were 28 measures of growth and size. For each I used an ANCOVA model, tested in PROC GLM (SAS version 9.3). The model included the fertilizer treatment (FERT) as a fixed effect and elevation-of-origin (ELEVATION) as a covariate plus the interaction and a fixed effect for rack (RACK). The key factor of interest is ELEVATION x FERT as it would indicate a significant change in trait expression relative to the elevation gradient and potentially make our results contingent upon fertilizer application.

B.3 RESULTS AND CONCLUSION

Fertilizer reduction altered almost every trait that I measured in the manner that I expected, reducing plant size and growth rate. Elevation significantly explained differences in plant traits for 11 of the 28 traits measured. There was no significant ELEVATION x FERT interaction for any trait measured (Table B.1). I concluded the 0.25 of saturating nutrient treatment was ideal for future experiments because it reduced plant stature (Figure B.1) while the rank-order of plants relative to elevation did not change.

Table B1: Results for 28 response variable of a general linear model testing the fixed effect of fertilizer treatment, the covariate effect of elevation-of=origin and the interaction of the two. Factor F- and P-values are provided as well as the model r-square and p-value.

Variable	FERT		ELEVATION		ELEVATION X FERT		RACK		MODEL	
	FValue	ProbF	FValue	ProbF	FValue	ProbF	FValue	ProbF	RSquare	ProbF
Age of Plant When 5 True Leaves	2.75	0.0675	1.33	0.2517	0.46	0.6325	0.90	0.410	0.09	0.1053
Average Rate of Leaf Initiation	2.93	0.0570	6.45	0.0122	1.92	0.1507	0.68	0.507	0.09	0.0796
Average Rosette Expansion Rate	10.36	0.0001	6.48	0.0121	0.59	0.5576	42.24	<0.0001	0.52	<0.0001
Cohort Leaf Average Relative Expansion Rate	20.53	<0.0001	2.08	0.1514	1.15	0.3209	4.86	0.009	0.45	<0.0001
Cohort Leaf Area - Day 21	8.58	0.0003	7.03	0.0090	1.31	0.2729	12.75	<0.0001	0.43	<0.0001
Cohort Leaf Area Day 26	17.87	<0.0001	7.10	0.0087	0.16	0.8542	16.63	<0.0001	0.55	<0.0001
CohortRER1to21	16.01	<0.0001	7.80	0.0060	1.37	0.2577	14.56	<0.0001	0.50	<0.0001
CohortRER21to26	12.64	<0.0001	0.49	0.4871	1.22	0.2985	1.51	0.225	0.30	<0.0001
Leaf 5 Age - Day 30	2.89	0.0590	0.46	0.4989	0.65	0.5214	2.34	0.100	0.10	0.0603
Leaf 5 Area - Day 30	1.10	0.3371	0.09	0.7648	0.24	0.7879	1.32	0.271	0.05	0.4851
Leaf 5 Relative Expansion Rate	0.62	0.5416	0.03	0.8579	0.03	0.9716	0.82	0.445	0.04	0.6894
Leaf Initiation Rate - Days 13 to 19	0.31	0.7373	7.21	0.0082	1.82	0.1655	0.36	0.695	0.10	0.0602
Leaf Initiation Rate - Days 1 to 8	0.29	0.7459	1.33	0.2505	0.20	0.8168	1.46	0.236	0.04	0.6529
Leaf Initiation Rate - Days 8 to 13	3.80	0.0247	0.52	0.4704	0.44	0.6423	2.31	0.103	0.13	0.0099
N Leaves - Day 13	4.73	0.0104	1.99	0.1609	0.76	0.4711	1.09	0.339	0.13	0.0097
N Leaves - Day 19	3.16	0.0455	6.16	0.0144	1.83	0.1644	0.72	0.490	0.09	0.0713
N Leaves - Day 8	0.29	0.7459	1.33	0.2505	0.20	0.8168	1.46	0.236	0.04	0.6529
Proportion Root Mass	8.13	0.0005	1.00	0.3180	2.25	0.1096	22.24	<0.0001	0.56	<0.0001
RER1to21	4.65	0.0112	4.61	0.0336	1.40	0.2493	6.06	0.003	0.18	0.0005
RER21to24	10.17	0.0001	8.92	0.0034	1.86	0.1599	52.05	<0.0001	0.53	<0.0001
RER24to30	4.68	0.0109	3.19	0.0766	0.17	0.8443	6.07	0.003	0.25	<0.0001
Root Mass	1.44	0.2402	0.36	0.5493	0.22	0.8050	11.87	<0.0001	0.18	0.0003
Rosette Area 24	2.27	0.1069	2.74	0.1000	0.88	0.4191	1.59	0.208	0.08	0.1442
Rosette Area 30	2.77	0.0665	1.65	0.2010	1.98	0.1417	0.46	0.632	0.08	0.1526
Rosette Mass	6.56	0.0019	0.83	0.3649	1.37	0.2568	0.13	0.882	0.38	<0.0001
Total Mass	3.83	0.0242	0.79	0.3749	0.99	0.3747	1.38	0.254	0.25	<0.0001
Whole Bin Measure of Rosette Area - Day 21	3.58	0.0307	3.72	0.0560	0.98	0.3764	5.47	0.005	0.15	0.0022
Whole Bin Measure of Rosette Area - Day 24	2.53	0.0836	1.67	0.1987	1.11	0.3339	0.62	0.539	0.06	0.3170

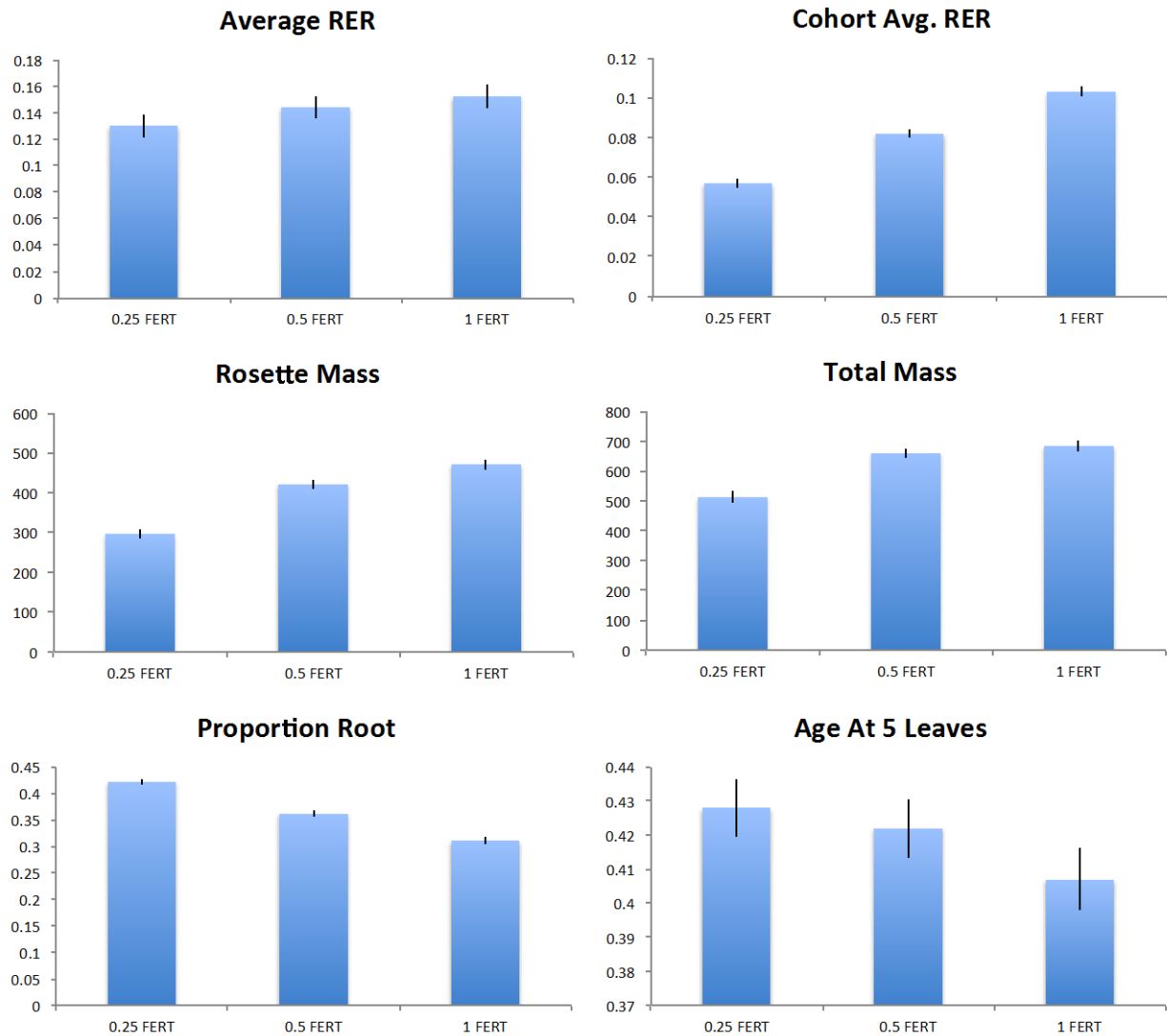


Figure B1: Least squares means for the fertilizer effect estimated from a GLM with the model Trait = FERT + ELEVATION + FERT x ELEVATION + RACK. One standard error is shown above and below each LS mean.

APPENDIX C

COMPARISON OF EURASIAN CLIMATE GRADIENT TO N.E. SPANISH GRADIENT

In the various analyses I conduct in the dissertation above, I use population scores on a principal component describing climate differences between the 16 study sites. This variable describes 75% of the climate variation between the populations I studied but leaves the reader without a broader understanding of the relationship between the climate in N.E. Spain and the climate variation across *A. thaliana*'s Eurasian range.

I used the same 19 BIOCLIM variables that form the N.E. Spanish Climate PC1 in a Eurasia wide analysis. To do this, I randomly sampled 10,000 locations across *A. thaliana*'s Eurasian range (Figure C.1). I conducted a PCA on the resulting dataset, the scores on climate PC1 were translated into a raster map of Eurasia showing a broad latitudinal gradient from cold, wet high latitude and altitude to hot, dry low latitude and altitude (Figure C.1). There is a strong significant correlation ($r = -0.86$, $n = 19$, $p < 0.0001$) between the loadings of the BIOCLIM variables on the Eurasian climate PC1 and the loadings on N.E. Spanish climate PC1 (Table C.1). There is an even stronger correlation ($r = -0.99$, $n = 16$, $p < 0.0001$) between the scores for each population along Eurasian and N.E. Spanish climate PC1s (Table C.2). These two results taken together indicate that the N.E. Spanish climate gradient is a portion of a larger, latitudinal

climate gradient covering most of *A. thaliana*'s native distribution. Scores along Eurasian climate PC1 range from -14 to 4.6, with a standard deviation of 2.97 across the 10,000 randomly sampled points used in the Eurasian climate PC1. The scores for the 16 N.E. Spanish sites along the Eurasian climate PC1 range from -4.3 to 1.19 or about 1.84 standard deviations. This amounts to about 29% of the total variation in climate encompassed by the Eurasian PCA I conducted. While the Eurasian PC1 does not specifically describe climates where *A. thaliana* occurs, the species is known to occur throughout the entire region of Eurasia analyzed. The key point here is that in the portion of the lower end of *A. thaliana*'s climate distribution that I examined (N.E. Spain), I have identified a great deal of variation in ecologically important plant traits. Future research examining a broader climatic range is therefore likely to reveal stronger patterns of trait-climate variation and generalize our understanding of climatic adaptation in plants.

Table C1: Loadings for each of 19 bioclimatic variables and elevation onto the first principal component from two separate analyses. In the first analysis, 10,000 locations across Eurasia were randomly sampled for the variables listed. In the second analyses as is explained in Chapter 2, the values from each variable at 16 *A. thaliana* collection sites are analyzed. The percentage of multivariate variance accounted for by the first PC is also listed.

		Loadings on Climate PC1	
BIOCLIM # Trait		Eurasian	N.E. Spanish
BIO1	Annual Mean Temp.	0.27	-0.26
BIO2	Mean Diurnal Range	0.18	0.14
BIO3	Isothermality (BIO2/BIO7)*100	-0.02	0.14
BIO4	Temp. Seasonality (Std Dev*100)	0.17	0.05
BIO5	Max. Temp. of the Warmest Month	0.32	-0.25
BIO6	Min. Temp. of Coldest Month	0.16	-0.25
BIO7	Annual Temp. Range	0.19	0.10
BIO8	Mean Temp. of Wettest Quarter	0.13	-0.24
BIO9	Mean Temp. of Driest Quarter	0.23	-0.20
BIO10	Mean Temp. of the Warmest Quarter	0.31	-0.26
BIO11	Mean Temp. of Coldest Quarter	0.20	-0.26
BIO12	Annual Precip.	-0.27	0.25
BIO13	Precip. Of Wettest Month	-0.20	0.21
BIO14	Precip. Of Driest Month	-0.31	0.25
BIO15	Precip. Seasonality (Coeff. Of Var.)	0.21	-0.25
BIO16	Precip. Of Wettest Quarter	-0.19	0.24
BIO17	Precip. Of Driest Quarter	-0.31	0.25
BIO18	Precip. Of Warmest Quarter	-0.31	0.24
BIO19	Precip. Of Coldest Quarter	-0.15	0.24
n/a	Elevation	-	0.24
Percent Variance Explained		65%	75%

Table C2: Scores along the first PC of climate space from two separate analyses are present here. Scores along PC1 for the Eurasian and N.E. Spanish climate were calculated based on the loadings as described in the text.

ABBREV	Elevation (m.a.s.l.)	Climate PC1 Scores	
		Eurasian	N.E. Spanish
ALE	1163	-2.037	2.3142534
ARB	440	-0.46997	-2.188414
BAR	340	0.892144	-4.579997
BIS	1397	-4.13302	5.8196446
BOS	719	-2.02303	2.6055719
COC	519	0.571206	-3.276053
HOR	351	-0.16214	-2.708289
MUR	836	-0.3109	-2.003312
PAL	1491	-2.91474	4.257865
PAN	1664	-3.65118	5.7899011
PIN	109	0.303286	-3.645752
POB	597	0.233353	-2.002803
RAB	110	1.187491	-4.480331
SPE	332	0.045909	-2.921276
VDM	912	-1.39319	1.293321
VIE	1538	-3.88066	5.7256693

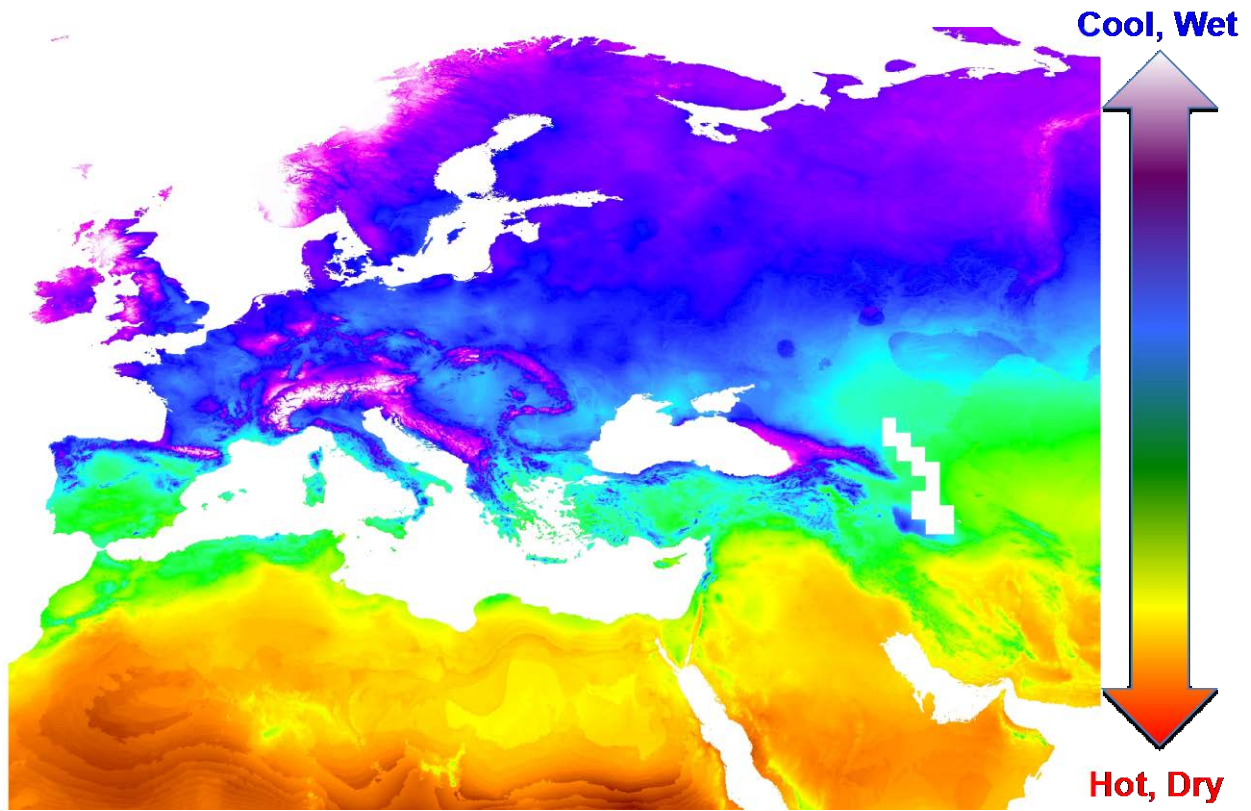


Figure C1: Map of Eurasian climate PC1 generated in ArcGIS 9.0 based on the loadings from a PCA conducted on a random sample of 10,000 locations across the region indicated. Warmer colors denote hotter, drier climates corresponding to the positive end of Eurasian climate PC1 while cooler colors indicate colder, wetter high latitude / altitude locations on the negative size of climate PC1.

APPENDIX D

SAS CODE

D.1 SAS CODE USED IN CHAPTER 2

```
%GLOBAL Prefix;
%LET prefix= /*INSERT FILE PATH HERE */ ;

data Master;
  infile "&prefix.HD Adapt - Master Dataset - 8'26'12.csv "
  delimiter=',' firstobs=2 truncover lrecl=1200;
  input Pot Pop $   Geno $ Chamber $ Rack $ PlantDate $
        RootMass RosetteMass InflorMass TotMass
        FvFm
        Days2FitMeas Nbranches RepBranchLength SilDense SilNumb
MeanSilLength TotSilLength
        Germ2Bolt Bolt2Ripe
        PhotoPerM2 TotalPhoto TransPerM2 TotalTrans WUE TimeofDay
CO2Ref H2ORef RHRef
        LeafArea LeafMass SLA;
run;
proc sort data=Master; by pot; run;
proc print data=Master; titlel 'Master Dataset'; run;

data SpanishPopData; set gecko.SpanishPopData; run;
proc print data=SpanishPopData; titlel 'Spanish Population Climate Data';
run;

OPTIONS MPRINT;
%MACRO RemoveDesignRelatedVariance;
proc glimmix data=Master plots = all;
  titlel "&Trait - Test for Chamber, Rack and PlantDate Effects";
  class Chamber PlantDate Rack;
  model &Trait = Chamber PlantDate Chamber*PlantDate;
  random Rack(PlantDate) / solution ;
  output out=&Trait Resid=R Pred=P;
run;
```

```

Proc Sort data=Master; by Pot; run;
Proc Sort data=&Trait; by Pot; run;
data &Trait; set &Trait; KEEP Pot R; RENAME R=R&Trait; run;
data Master; merge Master &Trait; by Pot; run;
%MEND RemoveDesignRelatedVariance;

/* REMOVE DESIGN RELATED VARIANCE */
%LET Trait = TotSillLength; %RemoveDesignRelatedVariance;
%LET Trait = FvFm; %RemoveDesignRelatedVariance;
%LET Trait = PhotoPerM2; %RemoveDesignRelatedVariance;
%LET Trait = TransPerM2; %RemoveDesignRelatedVariance;
%LET Trait = WUE; %RemoveDesignRelatedVariance;
%LET Trait = SLA; %RemoveDesignRelatedVariance;
%LET Trait = RootMass; %RemoveDesignRelatedVariance;
%LET Trait = RosetteMass; %RemoveDesignRelatedVariance;
%LET Trait = InflorMass; %RemoveDesignRelatedVariance;
%LET Trait = Germ2Bolt; %RemoveDesignRelatedVariance;
%LET Trait = Bolt2Ripe; %RemoveDesignRelatedVariance;
%LET Trait = NBranches; %RemoveDesignRelatedVariance;

proc corr data=Master;
    title 'Correlations Among Phenotypes - AFTER Removing Design
Variance';
    var RTotSillLength RFvFm RPhotoPerM2 RTransPerM2 RWUE RSLA RRootMass
RRosetteMass RInflorMass RGerm2Bolt RBolt2Ripe RNBranches;
run;
proc print data=p; title 'Correlation Coeffs and P-values After GLIMMIX';
run;

/* CALCULATE STANDARDIZED GENOTYPE MEANS FOR EACH PHENOTYPE */
proc sort data=Master; BY Pop; run;
proc means data=Master Mean StdErr NOPRINT;
    title 'Pop Means';
    var RTotSillLength RFvFm RPhotoPerM2 RTransPerM2 RWUE RSLA RRootMass
RRosetteMass RInflorMass RGerm2Bolt RBolt2Ripe RNBranches;
    output out=PopMeans Mean =
                                StdErr = / AUTONAME;
    by POP;
run;
proc sort data=PopMeans; by Pop; run;
proc sort data=SpanishPopData; by Pop; run;
data PopMeans; merge PopMeans SpanishPopData; by Pop; drop _TYPE_ _FREQ_;
run;
proc print data=PopMeans; title 'Standardized Pop Mean and Standard Error
for Each Phenotype PLUS Climate Data'; run;

/* STANDARDIZE POP MEANS DATASET */
proc standard
    data=PopMeans
    out=StdPopMeans
    mean=0 std=1;
VAR
RTotSillLength_Mean
RFvFm_Mean
RPhotoPerM2_Mean
RTransPerM2_Mean
RWUE_Mean

```

```

RSLA_Mean
RRootMass_Mean
RRosetteMass_Mean
RInflorMass_Mean
RGerm2Bolt_Mean
RBolt2Ripe_Mean
RNBranches_Mean
BIO1-BIO19 Elevation;
run;
proc print data=StdPopMeans; title1 "Standardized POP MEANS Dataset"; run;

/* TRAIT PCA */
proc princomp data=StdPopMeans plots=all
  Prefix = TraitPC
  Outstat = PCStats
  Out = TraitPCScores;
  title1 'Pop Mean Trait PCA';
  var RFvFm_Mean RPhotoPerM2_Mean RTransPerM2_Mean RWUE_Mean RSLA_Mean
RRootMass_Mean RRosetteMass_Mean RInflorMass_Mean RGerm2Bolt_Mean
RBolt2Ripe_Mean
  RNBranches_Mean RTotSilLength_Mean;
run;
data TraitPCScores; set TraitPCScores; Keep Pop Geno TraitPC1 TraitPC2; run;
proc print data=traitpcscores; title1 'Trait PCA Scores'; run;

/* CLIMATE PCA */
proc princomp data=StdPopMeans plots=all
  Prefix = ClimatePC
  Outstat = PCStats
  Out = ClimatePCScores;
  title1 'Climate PCA';
  var BIO1-BIO19 Elevation;
run;
data ClimatePCScores; set ClimatePCScores; Keep Pop ClimatePC1 ClimatePC2;
run;
proc print data=ClimatePCScores; title1 'Climate PCA Scores'; run;

/* MERGE TRAIT AND CLIMATE PC SCORES TO STANDARDIZED GENO MEANS DATASET */
proc sort data=StdPopMeans; by pop; run;
proc sort data=traitpcscores; by pop; run;
proc sort data=ClimatePCScores; by pop; run;
data StdPopMeans; merge StdPopMeans TraitPCScores ClimatePCScores; by Pop;
run;
proc print data=StdPopMeans; title1 'Std Pop Means - With PCA Scores'; run;

/* REGRESS TRAIT PC'S ON CLIMATE PC'S */
proc reg data=StdPopMeans plots=all;
  title1 'Trait PC1 vs. Climate PC1 & PC2';
  MODEL TraitPC1 = ClimatePC1 ClimatePC2;
run;
proc reg data=StdPopMeans plots=all;
  title1 'Trait PC2 vs. Climate PC1 & PC2';
  MODEL TraitPC2 = ClimatePC1 ClimatePC2;
run;

proc reg data=StdPopMeans plots=all;
  title1 'Trait PC1 vs. Climate PC1';

```

```

MODEL TraitPC1 = ClimatePC1;
run;
proc reg data=StdPopMeans plots=all;
  title 'Trait PC2 vs. Climate PC2';
  MODEL TraitPC2 = ClimatePC2;
run;

data NoBossost;
  set StdPopMeans;
  if Pop = 'BOS' then DELETE;
run;
proc princomp data=NoBossost plots=all
  Prefix = TraitPC
  Outstat = PCStats
  Out = NoBossostPCA;
  title 'No Bossost Trait PCA';
  var RFvFm_Mean RPhotoPerM2_Mean RTransPerM2_Mean RWUE_Mean RSLA_Mean
  RRootMass_Mean RRosetteMass_Mean RInflorMass_Mean RGerm2Bolt_Mean
  RBolt2Ripe_Mean
  RNBranches_Mean RTotSilLength_Mean;
run;
proc reg data=NoBossost plots=all;
  title 'Trait PC1 vs. Climate PC1 & PC2';
  MODEL TraitPC1 = ClimatePC1 ClimatePC2;
run;

proc sort data=PopMeans; by Pop; run;
data PopMeans; merge PopMeans ClimatePCScores; by pop; run;

/* UNIVARAITE REGRESSIONS - POPULATION MEAN PHENOTYPE ON ELEVATION-OF-ORIGIN
*/
OPTIONS MPRINT;
%MACRO TraitElevationRegression;
proc reg data=PopMeans plots=all;
  title "Regress &Trait on ClimatePC1";
  MODEL &Trait._Mean = ClimatePC1;
run;
run;
%MEND TraitElevationRegression;
%LET Trait = RTotSilLength; %TraitElevationRegression;
%LET Trait = RFvFm; %TraitElevationRegression;
%LET Trait = RPhotoPerM2; %TraitElevationRegression;
%LET Trait = RTransPerM2; %TraitElevationRegression;
%LET Trait = RWUE; %TraitElevationRegression;
%LET Trait = RSLA; %TraitElevationRegression;
%LET Trait = RRootMass; %TraitElevationRegression;
%LET Trait = RRosetteMass; %TraitElevationRegression;
%LET Trait = RInflorMass; %TraitElevationRegression;
%LET Trait = RGerm2Bolt; %TraitElevationRegression;
%LET Trait = RBolt2Ripe; %TraitElevationRegression;
%LET Trait = RNBranches; %TraitElevationRegression;

%MACRO TraitElevationRegression;
proc reg data=PopMeans plots=all;
  title "Regress &Trait on ClimatePC2";
  MODEL &Trait._Mean = ClimatePC2;

```

```

run;
run;
%MEND TraitElevationRegression;
%LET Trait = RTotSilLength; %TraitElevationRegression;
%LET Trait = RFvFm; %TraitElevationRegression;
%LET Trait = RPhotoPerM2; %TraitElevationRegression;
%LET Trait = RTransPerM2; %TraitElevationRegression;
%LET Trait = RWUE; %TraitElevationRegression;
%LET Trait = RSLA; %TraitElevationRegression;
%LET Trait = RRootMass; %TraitElevationRegression;
%LET Trait = RRosetteMass; %TraitElevationRegression;
%LET Trait = RInflorMass; %TraitElevationRegression;
%LET Trait = RGerm2Bolt; %TraitElevationRegression;
%LET Trait = RBolt2Ripe; %TraitElevationRegression;
%LET Trait = RNBranches; %TraitElevationRegression;

/* SELECTION ANALYSIS - FULL MODEL */
proc reg data=stdmaster plots=all;
    title 'TotSilLength - LINEAR Selection';
    MODEL RTotSilLength = RFvFm RPhotoPerM2 RTransPerM2 RWUE RSLA RRootMass
RRosetteMass RInflorMass RGerm2Bolt RBolt2Ripe RNBranches / VIF COLLIN AIC;
    OUTPUT Out = Residual1 R=R;
run;
proc univariate data=Residual1 normal plots; var R; run;
data StdMaster; set StdMaster; logRTotSilLength = log( RTotSilLength + 10);
run;
proc reg data=stdmaster plots=all;
    title 'logTotSilLength - LINEAR Selection';
    MODEL logRTotSilLength = RFvFm RPhotoPerM2 RTransPerM2 RWUE RSLA
RRootMass RRosetteMass RInflorMass RGerm2Bolt RBolt2Ripe RNBranches / VIF
COLLIN AIC;
    OUTPUT Out = Residual2 R=R;
run;
proc univariate data=Residual2 normal plots; var R; run;

/* SELECTION ANALYSIS - AIC MODEL */
proc reg data=stdmaster outest=est;
    model logRTotSilLength= RFvFm RPhotoPerM2 RTransPerM2 RWUE RSLA
RRootMass RRosetteMass RInflorMass RGerm2Bolt RBolt2Ripe /
selection=adjrsq sse aic ;
run;
proc sort data=est; by _aic_; run;
proc print data=est; title 'AIC Model Selection'; run;
proc reg data=stdmaster plots=all;
    title 'logTotSilLength - AIC BEST MODEL';
    MODEL logRTotSilLength = RTransPerM2 RSLA RRootMass RInflorMass
RGerm2Bolt RBolt2Ripe;
    OUTPUT Out = Residual3 R=R;
run;
proc univariate data=Residual3 normal plots; var R; run;
proc reg data=stdmaster;
    title 'TotSilLength - AIC BEST MODEL';
    MODEL RTotSilLength = RTransPerM2 RSLA RRootMass RInflorMass RGerm2Bolt
RBolt2Ripe;

```

D.2 SAS CODE USED IN CHAPTER 3

D.2.1 SAS code modeling photosynthesis over time and calculating photosynthetic rate at bolting.

```
/* RUN THE START-UP MASTER DATASET SAS PROGRAM FIRST */
/* There is a CSV format Master dataset with the raw data used in all
subsequent analyses.
   This file is located on the Tonsor laboratory DROPBOX.
   The file is paired with a SAS program that processes it and calculates the
genotype mean dataset "CGC_GenoMeans".
   Please contact me (Marnin Wolfe, wolfemd@gmail.com) or Dr. Stephen J.
Tonsor (tonsor@pitt.edu) for these files.
   Alternatively, when this dissertation is published, the related datasets
and SAS code will be uploaded to DRYAD for public access.
*/
DATA CGC_GenoMeans1; SET CGC_GenoMeans;
    WHERE Env = 'Mediterr';
    RENAME Elevation_Mean = Elevation;
RUN;
PROC PRINT DATA=CGC_GenoMeans1; RUN;

PROC SORT DATA=CGC_GenoMeans1; BY Env Cohort Elevation Geno; RUN;
%MACRO EXPO2P;
PROC NLIN DATA=&Data Plots=all METHOD=Marquardt TOTALSS MAXITER=500;
    title1 "&ID";
    PARAMETERS ALPHA = 1000 BETA = 0.05;
    MODEL &Trait = ALPHA * EXP(BETA*AgeAtHarvest);
    BY Env Cohort Elevation Geno;
    ODS OUTPUT ParameterEstimates=&ID.PARMS ANOVA=&ID.ANOVA;
RUN;
PROC PRINT DATA=&ID.PARMS; RUN;
/*The following code calculates pseudo r-square for each model */
PROC SORT DATA=&ID.ANOVA; BY Source Env Cohort Elevation Geno; RUN;
DATA &ID.SSE; SET &ID.ANOVA; WHERE Source = "Error"; RENAME SS=SSE; KEEP Env
Cohort Elevation Geno SS; RUN;
DATA &ID.SSCT; SET &ID.ANOVA; WHERE Source = "Corrected Total"; RENAME
SS=SSCT; KEEP Env Cohort Elevation Geno SS; RUN;
DATA &ID.SSUCT; SET &ID.ANOVA; WHERE Source = "Uncorrected Total"; RENAME
SS=SSUCT; KEEP Env Cohort Elevation Geno SS; RUN;
PROC SORT DATA=&ID.SSE; BY Env Cohort Elevation Geno; RUN;
PROC SORT DATA=&ID.SSCT; BY Env Cohort Elevation Geno; RUN;
PROC SORT DATA=&ID.SSUCT; BY Env Cohort Elevation Geno; RUN;
DATA &ID.PSEUDORSQ; MERGE &ID.SSCT &ID.SSE &ID.SSUCT; BY Env Cohort Elevation
Geno;
    CtPseudoRsq = 1 - (SSE/SSCT);
    UnCtPseudoRsq = 1 - (SSE/SSUCT);
RUN;
PROC PRINT DATA=&ID.PSEUDORSQ; TITLE1 "&ID - PseudoRsq by Env-Cohort-
```

```

Elevation-Geno"; RUN;

/* The following code extracts the parameter estimates from each model,
merges it with
    population (or genotype) mean bolting ages and calculates the predicted
photosynthetic rate per gram at the age of bolting */
DATA &ID.ALPHA; SET &ID.PARMS; WHERE Parameter = "ALPHA"; RENAME
Estimate=ALPHA; KEEP Env Cohort Elevation Geno Estimate; RUN;
DATA &ID.BETA; SET &ID.PARMS; WHERE Parameter = "BETA"; RENAME Estimate=BETA;
KEEP Env Cohort Elevation Geno Estimate; RUN;
PROC SORT DATA=&ID.ALPHA; BY Env Cohort Elevation Geno; RUN;
PROC SORT DATA=&ID.BETA; BY Env Cohort Elevation Geno; RUN;
PROC SORT DATA=GenoMeansDays2Climate; BY Env Cohort Elevation Geno; RUN;
PROC PRINT DATA=&ID.ALPHA; TITLE1 "&ID - ALPHA"; RUN;
PROC PRINT DATA=&ID.BETA; TITLE1 "&ID - BETA"; RUN;
DATA &ID.PHOTOATBOLTING; MERGE &ID.ALPHA &ID.BETA GenoMeansDays2Climate; BY
Env Cohort Elevation Geno; RUN;
DATA &ID.PHOTOATBOLTING; SET &ID.PHOTOATBOLTING;
    PhotoAtBolting = ALPHA * EXP(BETA*Days2Bolt_Mean);
    PhotoAt7days = ALPHA * EXP(BETA*7);
    PhotoAt14days = ALPHA * EXP(BETA*14);
    PhotoAt28days = ALPHA * EXP(BETA*28);
    PhotoAt56days = ALPHA * EXP(BETA*56);
RUN;
PROC PRINT DATA=&ID.PHOTOATBOLTING; TITLE1 "&ID - Calculated Photo Per Gram @
Bolting"; RUN;
%MEND EXPO2P;
%LET Data = CGC_GenoMeans1; %LET ID = PhotoExpo2P; %LET Trait =
RosePhotoPerGram1_Mean; %EXPO2P;

```

D.2.2 SAS code modeling rosette mass per area (RMA) over time and calculating photosynthetic rate at bolting.

```

/* DEVELOPING AND TESTING MODELS THAT WORK */
/*
PROC NLIN DATA=CGC_GenoMeans1 Plots=all METHOD=Marquardt TOTALSS MAXITER=1000
MAXSUBIT=75;
    TITLE1 'GRID SEARCH 1';
    PARAMETERS ALPHA = 0.001 to 0.10 by 0.01 BETA = 50 to 1500 by 200 GAMMA
= 0.02 to 1000 by 100;
    MODEL RMA_Mean = ( GAMMA / (1 + EXP(-ALPHA*(AgeAtHarvest-BETA)))));
    BY Cohort Elevation Geno;
RUN;
PROC NLIN DATA=CGC_GenoMeans1 Plots=all METHOD=Marquardt TOTALSS MAXITER=500
MAXSUBIT=75;
    TITLE1 'GRID SEARCH 2';
    PARAMETERS ALPHA = 0.001 to 0.10 by 0.01 BETA = 50 to 1500 by 200 GAMMA
= 0.02 to 1000 by 100;
    MODEL RMA_Mean = ( GAMMA / (1 + EXP(-ALPHA*(AgeAtHarvest-BETA)))));
    BY Cohort Elevation Geno;

```

```

RUN;
PROC NLIN DATA=CGC_GenoMeans1 Plots=all METHOD=Marquardt TOTALSS;
  TITLE1 'GRID SEARCH 3';
  PARAMETERS ALPHA = 0.001 to 0.10 by 0.01 BETA = 50 to 1500 by 200 GAMMA
= 0.02 to 1000 by 100;
  MODEL RMA_Mean = ( GAMMA / (1 + EXP(-ALPHA*(AgeAtHarvest-BETA)))));
  BY Cohort Elevation Geno;
RUN;
PROC NLIN DATA=CGC_GenoMeans1 Plots=all METHOD=Marquardt TOTALSS;
  TITLE1 'GRID SEARCH 4';
  PARAMETERS ALPHA = 0.05 0.10 BETA = 50 100 GAMMA = 0.02 0.08;
  MODEL RMA_Mean = ( GAMMA / (1 + EXP(-ALPHA*(AgeAtHarvest-BETA)))));
  BY Cohort Elevation Geno;
RUN;

DATA CGC_GenoMeans2; set CGC_GenoMeans1; WHERE Cohort='Spring'; RUN;
PROC SORT DATA=CGC_GenoMeans2; BY Elevation Geno; RUN;
PROC NLIN DATA=CGC_GenoMeans2 Plots=all METHOD=Marquardt TOTALSS;
  TITLE1 'Test Exponential';
  WHERE Geno = 'RAB17' or Geno = 'RAB4' or Geno = 'BAR4' or Geno = 'COC7'
or Geno = 'VDM17' or Geno = 'PAL12' or Geno = 'PAN1';
  PARAMETERS ALPHA = 0.001 to 0.02 by 0.001 BETA = 0.001 to 0.02 by 0.001
;
  MODEL RMA_Mean = ALPHA * EXP(BETA*AgeAtHarvest);
  BY Elevation Geno;
RUN;
*/

PROC SORT DATA=CGC_GenoMeans1; BY Cohort Elevation Geno; RUN;
%MACRO LOGISTIC3P;
PROC NLIN DATA=&Data Plots=all METHOD=Marquardt TOTALSS;
  title1 "&ID";
  PARAMETERS ALPHA = 0.05 0.10 BETA = 50 100 700 GAMMA = 0.02 0.08;
  MODEL &Trait = ( GAMMA / (1 + EXP(-ALPHA*(AgeAtHarvest-BETA)))));
  BY Cohort Elevation Geno;
  ODS OUTPUT ParameterEstimates=&ID.PARMS ANOVA=&ID.ANOVA;
RUN;
PROC PRINT DATA=&ID.PARMS; RUN;
/*The following code calculates pseudo r-square for each model */
PROC SORT DATA=&ID.ANOVA; BY Source Cohort Elevation Geno; RUN;
DATA &ID.SSE; SET &ID.ANOVA; WHERE Source = "Error"; RENAME SS=SSE; KEEP
Cohort Elevation Geno SS; RUN;
DATA &ID.SSCT; SET &ID.ANOVA; WHERE Source = "Corrected Total"; RENAME
SS=SSCT; KEEP Cohort Elevation Geno SS; RUN;
DATA &ID.SSUCT; SET &ID.ANOVA; WHERE Source = "Uncorrected Total"; RENAME
SS=SSUCT; KEEP Cohort Elevation Geno SS; RUN;
PROC SORT DATA=&ID.SSE; BY Cohort Elevation Geno; RUN;
PROC SORT DATA=&ID.SSCT; BY Cohort Elevation Geno; RUN;
PROC SORT DATA=&ID.SSUCT; BY Cohort Elevation Geno; RUN;
DATA &ID.PSEUDORSQ; MERGE &ID.SSCT &ID.SSE &ID.SSUCT; BY Cohort Elevation
Geno;
  CtPseudoRsqr = 1 - (SSE/SSCT);
  UnCtPseudoRsqr = 1 - (SSE/SSUCT);
RUN;
PROC PRINT DATA=&ID.PSEUDORSQ; TITLE1 "&ID - PseudoRsqr by Cohort-Elevation-
Geno"; RUN;

```

```

/* The following code extracts the parameter estimates from each model,
merges it with
    population (or genotype) mean bolting ages and calculates the predicted
photosynthetic rate per gram at the age of bolting */
DATA &ID.ALPHA; SET &ID.PARMS; WHERE Parameter = "ALPHA"; RENAME
Estimate=ALPHA; KEEP Cohort Elevation Geno Estimate; RUN;
DATA &ID.BETA; SET &ID.PARMS; WHERE Parameter = "BETA"; RENAME Estimate=BETA;
KEEP Cohort Elevation Geno Estimate; RUN;
DATA &ID.GAMMA; SET &ID.PARMS; WHERE Parameter = "GAMMA"; RENAME
Estimate=GAMMA; KEEP Cohort Elevation Geno Estimate; RUN;
PROC SORT DATA=&ID.ALPHA; BY Cohort Elevation Geno; RUN;
PROC SORT DATA=&ID.BETA; BY Cohort Elevation Geno; RUN;
PROC SORT DATA=&ID.GAMMA; BY Cohort Elevation Geno; RUN;
DATA GenoMeansDays2Climate1; SET GenoMeansDays2Climate; WHERE Env =
"Mediterr"; RUN;
PROC SORT DATA=GenoMeansDays2Climate1; BY Cohort Elevation Geno; RUN;
PROC PRINT DATA=&ID.ALPHA; TITLE1 "&ID - ALPHA"; RUN;
PROC PRINT DATA=&ID.BETA; TITLE1 "&ID - BETA"; RUN;
PROC PRINT DATA=&ID.GAMMA; TITLE1 "&ID - GAMMA"; RUN;
DATA &ID.RMAATBOLTING; MERGE &ID.ALPHA &ID.BETA &ID.GAMMA
GenoMeansDays2Climate1; BY Cohort Elevation Geno; RUN;
DATA &ID.RMAATBOLTING; SET &ID.RMAATBOLTING;
    RMAatBolting = ( GAMMA / (1 + EXP(-ALPHA*(Days2Bolt_Mean-BETA)))));
    RMAat7days = ( GAMMA / (1 + EXP(-ALPHA*(7-BETA)))));
    RMAat14days = ( GAMMA / (1 + EXP(-ALPHA*(14-BETA)))));
    RMAat28days = ( GAMMA / (1 + EXP(-ALPHA*(28-BETA)))));
    RMAat56days = ( GAMMA / (1 + EXP(-ALPHA*(56-BETA)))));
RUN;
PROC PRINT DATA=&ID.RMAATBOLTING; TITLE1 "&ID - Calculated RMA @ Bolting";
RUN;
%MEND LOGISTIC3P;
%LET Data = CGC_GenoMeans1; %LET ID = RMALogistic; %LET Trait = RMA_Mean;
%LOGISTIC3P;

DATA CGC_GenoMeans2; set CGC_GenoMeans1; WHERE Cohort='Spring'; RUN;
PROC SORT DATA=CGC_GenoMeans2; BY Env Cohort Elevation Geno; RUN;
%MACRO EXPONENTIAL;
PROC NLIN DATA=&Data Plots=all METHOD=Marquardt TOTALSS;
    title1 "&ID";
    WHERE Geno = "RAB17" or Geno = "RAB4" or Geno = "BAR4" or Geno = "COC7"
or Geno = "VDM17" or Geno = "PAL12" or Geno = "PAN1";
    PARAMETERS ALPHA = 0.001 to 0.02 by 0.001 BETA = 0.001 to 0.02 by 0.001
;
    MODEL &Trait = ALPHA * EXP(BETA*AgeAtHarvest);
    BY Env Cohort Elevation Geno;
    ODS OUTPUT ParameterEstimates=&ID.PARMS ANOVA=&ID.ANOVA;
RUN;
PROC PRINT DATA=&ID.PARMS; RUN;
/*The following code calculates pseudo r-square for each model */
PROC SORT DATA=&ID.ANOVA; BY Source Env Cohort Elevation Geno; RUN;
DATA &ID.SSE; SET &ID.ANOVA; WHERE Source = "Error"; RENAME SS=SSE; KEEP Env
Cohort Elevation Geno SS; RUN;
DATA &ID.SSCT; SET &ID.ANOVA; WHERE Source = "Corrected Total"; RENAME
SS=SSCT; KEEP Env Cohort Elevation Geno SS; RUN;
DATA &ID.SSUCT; SET &ID.ANOVA; WHERE Source = "Uncorrected Total"; RENAME
SS=SSUCT; KEEP Env Cohort Elevation Geno SS; RUN;

```

```

PROC SORT DATA=&ID.SSE; BY Env Cohort Elevation Geno; RUN;
PROC SORT DATA=&ID.SSCT; BY Env Cohort Elevation Geno; RUN;
PROC SORT DATA=&ID.SSUCT; BY Env Cohort Elevation Geno; RUN;
DATA &ID.PSEUDORSQ; MERGE &ID.SSCT &ID.SSE &ID.SSUCT; BY Env Cohort Elevation
Geno;
      CtPseudoRsqr = 1 - (SSE/SSCT);
      UnCtPseudoRsqr = 1 - (SSE/SSUCT);
RUN;
PROC PRINT DATA=&ID.PSEUDORSQ; TITLE1 "&ID - PseudoRsqr by Elevation-Geno";
RUN;

/* The following code extracts the parameter estimates from each model,
merges it with
      population (or genotype) mean bolting ages and calculates the predicted
photosynthetic rate per gram at the age of bolting */
DATA &ID.ALPHA; SET &ID.PARMS; WHERE Parameter = "ALPHA"; RENAME
Estimate=ALPHA; KEEP Env Cohort Elevation Geno Estimate; RUN;
DATA &ID.BETA; SET &ID.PARMS; WHERE Parameter = "BETA"; RENAME Estimate=BETA;
KEEP Env Cohort Elevation Geno Estimate; RUN;
PROC SORT DATA=&ID.ALPHA; BY Env Cohort Elevation Geno; RUN;
PROC SORT DATA=&ID.BETA; BY Env Cohort Elevation Geno; RUN;
DATA GenoMeansDays2Climate1; SET GenoMeansDays2Climate; WHERE Env =
"Mediterr" and Cohort = "Spring"; RUN;
DATA GenoMeansDays2Climate1; SET GenoMeansDays2Climate1; WHERE Geno = "RAB17"
or Geno = "RAB4" or Geno = "BAR4" or Geno = "COC7" or Geno = "VDM17" or Geno
= "PAL12" or Geno = "PAN1"; RUN;
PROC SORT DATA=GenoMeansDays2Climate1; BY Env Cohort Elevation Geno; RUN;
PROC PRINT DATA=&ID.ALPHA; TITLE1 "&ID - ALPHA"; RUN;
PROC PRINT DATA=&ID.BETA; TITLE1 "&ID - BETA"; RUN;
DATA &ID.RMAATBOLTING; MERGE &ID.ALPHA &ID.BETA GenoMeansDays2Climate1; BY
Env Cohort Elevation Geno; RUN;
DATA &ID.RMAATBOLTING; SET &ID.RMAATBOLTING;
      RMAatBolting = ALPHA * EXP(BETA*Days2Bolt_Mean);
      RMAat7days = ALPHA * EXP(BETA*7);
      RMAat14days = ALPHA * EXP(BETA*14);
      RMAat28days = ALPHA * EXP(BETA*28);
      RMAat56days = ALPHA * EXP(BETA*56);
RUN;
PROC PRINT DATA=&ID.RMAATBOLTING; TITLE1 "&ID - Calculated RMA @ Bolting -
Exponential Model Subset"; RUN;
%MEND EXPONENTIAL;
%LET Data = CGC_GenoMeans2; %LET ID = SubsetExpo2P; %LET Trait = RMA_Mean;
%EXPONENTIAL;

```

D.2.3 SAS code modeling the proportion live rosette leaves over time and calculating the age at 95% rosette mortality.

```

/* RUN THE START-UP MASTER DATASET SAS PROGRAM FIRST */
/* PROC PRINT DATA=PopMeans; RUN; */
DATA CGC_GenoMeans1; SET CGC_GenoMeans;
      WHERE Env = 'Mediterr';
      RENAME Elevation_Mean = Elevation;

```

```

PropLiveLeaves = PctLiveLeaves / 100;
RUN;

PROC SORT DATA=CGC_GenoMeans1; BY Env Cohort Elevation Geno; RUN;
%MACRO LOGISTIC2P;
PROC NLIN DATA=&Data Plots=all METHOD=Marquardt TOTALSS;
  title "&ID";
  PARAMETERS ALPHA = -0.1 to -0.02 by 0.02 BETA = 70, 80, 90, 120, 140,
160, 180, 200;
  MODEL &Trait = 1 / ( 1 + EXP(-ALPHA *(AgeAtHarvest - BETA) ) );
  BY Env Cohort Elevation Geno;
  ODS OUTPUT ParameterEstimates=&ID.PARMS ANOVA=&ID.ANOVA;
RUN;
PROC PRINT DATA=&ID.PARMS; RUN;
/*The following code calculates pseudo r-square for each model */
PROC SORT DATA=&ID.ANOVA; BY Source Env Cohort Elevation Geno; RUN;
DATA &ID.SSE; SET &ID.ANOVA; WHERE Source = "Error"; RENAME SS=SSE; KEEP Env
Cohort Elevation Geno SS; RUN;
DATA &ID.SSCT; SET &ID.ANOVA; WHERE Source = "Corrected Total"; RENAME
SS=SSCT; KEEP Env Cohort Elevation Geno SS; RUN;
DATA &ID.SSUCT; SET &ID.ANOVA; WHERE Source = "Uncorrected Total"; RENAME
SS=SSUCT; KEEP Env Cohort Elevation Geno SS; RUN;
PROC SORT DATA=&ID.SSE; BY Env Cohort Elevation Geno; RUN;
PROC SORT DATA=&ID.SSCT; BY Env Cohort Elevation Geno; RUN;
PROC SORT DATA=&ID.SSUCT; BY Env Cohort Elevation Geno; RUN;
DATA &ID.PSEUDORSQ; MERGE &ID.SSCT &ID.SSE &ID.SSUCT; BY Env Cohort Elevation
Geno;
  CtPseudoRsqr = 1 - (SSE/SSCT);
  UnCtPseudoRsqr = 1 - (SSE/SSUCT);
RUN;
PROC PRINT DATA=&ID.PSEUDORSQ; TITLE1 "&ID - PseudoRsqr by Env-Cohort-
Elevation-Geno"; RUN;

/* The following code extracts the parameter estimates from each model,
merges it with
  population (or genotype) mean bolting ages and calculates the predicted
photosynthetic rate per gram at the age of bolting */
DATA &ID.ALPHA; SET &ID.PARMS; WHERE Parameter = "ALPHA"; RENAME
Estimate=ALPHA; KEEP Env Cohort Elevation Estimate Geno; RUN;
DATA &ID.BETA; SET &ID.PARMS; WHERE Parameter = "BETA"; RENAME Estimate=BETA;
KEEP Env Cohort Elevation Estimate Geno; RUN;
PROC SORT DATA=&ID.ALPHA; BY Env Cohort Elevation Geno; RUN;
PROC SORT DATA=&ID.BETA; BY Env Cohort Elevation Geno; RUN;
PROC SORT DATA=GenoMeansDays2Climate; BY Env Cohort Elevation Geno; RUN;
PROC PRINT DATA=&ID.ALPHA; TITLE1 "&ID - ALPHA"; RUN;
PROC PRINT DATA=&ID.BETA; TITLE1 "&ID - BETA"; RUN;
DATA &ID.TimeOfDeath; MERGE &ID.ALPHA &ID.BETA GenoMeansDays2Climate; BY Env
Cohort Elevation Geno; RUN;
DATA &ID.TimeOfDeath; SET &ID.TimeOfDeath;
  TimeAt1PctLive = ( log(-(.01/((.01-1))) + ALPHA*BETA ) / ALPHA;
  TimeAt5PctLive = ( log(-(.05/((.05-1))) + ALPHA*BETA ) / ALPHA;
  TimeAt10PctLive = ( log(-(.1/((.1-1))) + ALPHA*BETA ) / ALPHA;
  TimeAt50PctLive = ( log(-(.5/((.5-1))) + ALPHA*BETA ) / ALPHA;
  PropLiveLeavesAtBolting = 1 / ( 1 + EXP(-ALPHA *(Days2Bolt_Mean - BETA)
) );
RUN;
PROC PRINT DATA=&ID.TimeOfDeath; TITLE1 "&ID - Calculated Days to Death and

```

```

PropLiveLeaves @ Bolting"; RUN;
%MEND LOGISTIC2P;
%LET Data = CGC_GenoMeans1; %LET ID = Logistic2P; %LET Trait =
PropLiveLeaves; %LOGISTIC2P;

```

D.2.4 SAS code used in all analyses subsequent to the nonlinear models of RMA, Photosynthetic Rate and Proportion live Leaves.

```

/* RUN START-UP MASTER DATASET SAS PROGRAM LOCATED ON TONSOR LAB DROPBOX
BEFORE RUNNING THIS CODE */
DATA Master;
    SET CGC_GenoMeans;
    WHERE Env = 'Mediterr' AND Cohort = 'Fall';
    PropRose = RosetteMass_Mean / TotMass_Mean;
    PropRoot = RootMass_Mean / TotMass_Mean;
    PropInflor = InflorMass_Mean / TotMass_Mean;
RUN;
PROC PRINT DATA=Master; TITLE1 'Mediterranean Fall Geno Means Dataset'; RUN;

proc sort data=Master; by Geno Harvest AgeAtHarvest CGDD3 CGDD4; run;
PROC MEANS DATA=Master Max NOPRINT;
    VAR NBasalBranches_Mean RosetteMass_Mean RootMass_Mean InflorMass_Mean
Totmass_Mean
    RosetteArea_Mean RMA_Mean LeafArea_Mean LeafMassMG_Mean TLN_Mean;
    OUTPUT OUT = MaxValues
        MAX = / AUTONAME;
    BY Geno Harvest AgeAtHarvest CGDD3 CGDD4;
RUN;
PROC PRINT DATA=MaxValues; TITLE1 'Max Trait Values by Genotype'; RUN;

%LET prefix = /* INSERT FILE PATH HERE */;

DATA LES;
    INFILE "&prefix.LES Project - GENO MEANS - Raw Rosette Economic Traits
- 5.13.13.csv" DLM = ',' FIRSTOBS = 2 TRUNCOVER LRECL = 2000 ;
    INPUT Env $ Cohort $ Pop $ Geno $ Elevation
        Days2Bolt Lifespan Photo RMA SummedFruitLength;
RUN;
DATA LES; SET LES; log10Photo = log10(Photo); RUN;
proc print data=LES; title1 'Rosette Economics Dataset'; run;

DATA PopClimateData;
    INFILE "&prefix.Spanish Population Climate Data - 11.19.12.csv" DLM =
',' FIRSTOBS = 2 TRUNCOVER LRECL = 2000 ;
    INPUT POP $ POPELEV $ Longitude Latitude Elevation
        BIO1 BIO2 BIO3 BIO4 BIO5 BIO6 BIO7 BIO8 BIO9 BIO10 BIO11 BIO12
BIO13 BIO14 BIO15 BIO16 BIO17 BIO18 BIO19
        IberianClimatePC1 IberianClimatePC2 MintSeptoFeb MaxTMartoJun

```

```

MinPreMarttoJun MinPreSeptoFeb
      ClimatePC1 ClimatePC2 ShortestDistanceToCoast DistanceToMedit
DistanceToAtlantic;
      KEEP Pop Elevation ClimatePC1;
RUN;
PROC PRINT DATA=PopClimateData; TITLE1 'Spanish Population Climate Data';
RUN;

PROC SORT DATA=PopClimateData; BY Pop; RUN;
PROC SORT DATA=LES; BY Pop; RUN;
DATA LES; MERGE LES PopClimateData; BY Pop; RUN;
PROC PRINT DATA=LES; TITLE1 'Rosette Economics Dataset + Climate Data'; RUN;

PROC PRINCOMP DATA=LES PLOTS=All PREFIX = RoseEconPC OUTSTAT = PCStats OUT =
GenoMeanRoseEcon;
      TITLE1 'PCA of Rosette Economic Variables';
      VAR Lifespan log10Photo RMA;
RUN;
PROC PRINT DATA=GenoMeanRoseEcon; TITLE1 'Geno Means - Rosette Economy
Dataset'; run;

PROC SORT DATA=GenoMeanRoseEcon; BY Env Cohort Pop Elevation ClimatePC1; RUN;
PROC MEANS DATA=GenoMeanRoseEcon MEAN NOPRINT;
      VAR Days2Bolt Lifespan Photo RMA SummedFruitLength log10Photo
RoseEconPC1;
      OUTPUT OUT = PopMeanRoseEcon
      MEAN (Days2Bolt Lifespan Photo RMA SummedFruitLength log10Photo
RoseEconPC1) =
      Days2Bolt Lifespan Photo RMA SummedFruitLength log10Photo
RoseEconPC1;
      BY Env Cohort Pop Elevation ClimatePC1;
RUN;
PROC PRINT DATA=PopMeanRoseEcon; TITLE1 'Pop Means - Rosette Economy
Dataset'; RUN;

%MACRO ANCOVA_ClimatePC1;
PROC GLM DATA=PopMeanRoseEcon PLOTS = All;
      TITLE1 "&Trait - ClimatePC1";
      CLASS Cohort;
      MODEL &Trait = Cohort ClimatePC1 Cohort*ClimatePC1 / SS3 SOLUTION;
      LSMEANS Cohort / PDIFF;
RUN;
%MEND ANCOVA_ClimatePC1;

%LET Trait = RoseEconPC1; %ANCOVA_ClimatePC1;
%LET Trait = log10Photo; %ANCOVA_ClimatePC1;
%LET Trait = Photo; %ANCOVA_ClimatePC1;
%LET Trait = RMA; %ANCOVA_ClimatePC1;
%LET Trait = Lifespan; %ANCOVA_ClimatePC1;
%LET Trait = SummedFruitLength; %ANCOVA_ClimatePC1;
%LET Trait = Days2Bolt; %ANCOVA_ClimatePC1;

PROC STANDARD
      DATA=GenoMeanRoseEcon
      out=StdGenoMeanRoseEcon
      mean=0 std=1;

```

```

VAR SummedFruitLength log10Photo RMA Lifespan Days2Bolt RoseEconPC1
Days2Bolt;
run;
proc print data=StdGenoMeanRoseEcon; title1 "Standardized Rosette Econ
Dataset"; run;

%MACRO DirectSelection;
PROC REG DATA=StdGenoMeanRoseEcon PLOTS = All;
    TITLE1 "Direct Selection - &Trait";
    MODEL SummedFruitLength = &Trait;
RUN;
PROC REG DATA=StdGenoMeanRoseEcon PLOTS = All;
    TITLE1 "Direct Selection - &Trait - By Cohort";
    MODEL SummedFruitLength = &Trait;
    BY Cohort;
RUN;
%MEND DirectSelection;
%LET Trait = RoseEconPC1; %DirectSelection;
%LET Trait = log10Photo; %DirectSelection;
%LET Trait = Photo; %DirectSelection;
%LET Trait = RMA; %DirectSelection;
%LET Trait = Lifespan; %DirectSelection;
%LET Trait = Days2Bolt; %DirectSelection;

PROC CORR DATA=StdGenoMeanRoseEcon PLOTS=All;
    TITLE1 "Trait Correlations";
    VAR SummedFruitLength log10Photo RMA Lifespan Days2Bolt RoseEconPC1;
RUN;

PROC GLM DATA=StdGenoMeanRoseEcon;
    TITLE1 "Comparing Fitness-Economy Relationships Among Cohorts";
    CLASS Cohort;
    MODEL SummedFruitLength = RoseEconPC1 Cohort RoseEconPC1*Cohort / SS3
SOLUTION;
RUN;

```

D.3 SAS CODE USED IN CHAPTER 4

D.3.1 Modeling whole plant photosynthesis over time.

```

PROC SORT DATA=Master; BY Geno; RUN;
PROC NLIN DATA=Master Plots=fit METHOD=Marquardt TOTALSS;
    TITLE1 'Whole Plant - GAUSSIAN';
    *PARAMETERS ALPHA = 0.01 0.5 0.75 1.5 3 5 10 15 20 50 75 100 200 300
400 BETA = 0.001 0.01 0.5 0.75 1.5 3 5 10 50 100 150 200 400 500 800 GAMMA =

```

```

0.001 0.01 0.5 0.75 1.5 3 5 15 25 35 45 55 75 100 150 500;
PARAMETERS ALPHA = 0.5 1.5 3 5 10 15 20 50 75 100 BETA = 0.001 0.01 0.1
1 10 50 100 150 200 GAMMA = 0.001 0.01 0.5 0.75 1.5 3 5 15 25;
MODEL WholeTotalPhoto = ALPHA * EXP( - ( 0.5 * ( ( AgeAtHarvest - BETA
) / GAMMA )**2 ) );
BY Geno;
RUN;

PROC SORT DATA=Master; BY Geno; RUN;
%MACRO GAUSSIAN;
PROC NLIN DATA=&Data Plots=Fit METHOD=Marquardt TOTALSS;
    title1 "&ID";
    PARAMETERS ALPHA = 0.5 1.5 3 5 10 15 20 50 75 100 BETA = 0.001 0.01 0.1
1 10 50 100 150 200 GAMMA = 0.001 0.01 0.5 0.75 1.5 3 5 15 25;
    MODEL &Trait = ALPHA * EXP( - ( 0.5 * ( ( AgeAtHarvest - BETA ) / GAMMA
)**2 ) );
    BY Geno;
    ODS OUTPUT ParameterEstimates=&ID.PARMS ANOVA=&ID.ANOVA;
RUN;
PROC PRINT DATA=&ID.PARMS; TITLE1 "&ID - Parameters"; RUN;
/* The following code calculates pseudo r-square for each model */
PROC SORT DATA=&ID.ANOVA; BY Source Geno; RUN;
DATA &ID.SSE; SET &ID.ANOVA; WHERE Source = "Error"; RENAME SS=SSE; KEEP Geno
SS; RUN;
DATA &ID.SSCT; SET &ID.ANOVA; WHERE Source = "Corrected Total"; RENAME
SS=SSCT; KEEP Geno SS; RUN;
DATA &ID.SSUCT; SET &ID.ANOVA; WHERE Source = "Uncorrected Total"; RENAME
SS=SSUCT; KEEP Geno SS; RUN;
PROC SORT DATA=&ID.SSE; BY Geno; RUN;
PROC SORT DATA=&ID.SSCT; BY Geno; RUN;
PROC SORT DATA=&ID.SSUCT; BY Geno; RUN;
DATA &ID.PSEUDORSQ; MERGE &ID.SSCT &ID.SSE &ID.SSUCT; BY Geno;
    CtPseudoRsqr = 1 - (SSE/SSCT);
    UnCtPseudoRsqr = 1 - (SSE/SSUCT);
RUN;
PROC PRINT DATA=&ID.PSEUDORSQ; TITLE1 "&ID - PseudoRsqr by Geno"; RUN;

/* The following code extracts the parameter estimates from each model,
merges it with
    population (or genotype) mean bolting ages and calculates the predicted
photosynthetic rate per gram at the age of bolting */
/*
DATA &ID.ALPHA; SET &ID.PARMS; WHERE Parameter = "ALPHA"; RENAME
Estimate=ALPHA; KEEP Geno Estimate; RUN;
DATA &ID.BETA; SET &ID.PARMS; WHERE Parameter = "BETA"; RENAME Estimate=BETA;
KEEP Geno Estimate; RUN;
DATA &ID.GAMMA; SET &ID.PARMS; WHERE Parameter = "GAMMA"; RENAME
Estimate=GAMMA; KEEP Geno Estimate; RUN;
PROC SORT DATA=&ID.ALPHA; BY Geno; RUN;
PROC SORT DATA=&ID.BETA; BY Geno; RUN;
PROC SORT DATA=&ID.GAMMA; BY Geno; RUN;
PROC PRINT DATA=&ID.ALPHA; TITLE1 "&ID - ALPHA"; RUN;
PROC PRINT DATA=&ID.BETA; TITLE1 "&ID - BETA"; RUN;
PROC PRINT DATA=&ID.GAMMA; TITLE1 "&ID - GAMMA"; RUN;
DATA &ID.GAUSSIANPARMS; MERGE &ID.ALPHA &ID.BETA &ID.GAMMA; BY Geno; RUN;
RUN;

```

```

PROC PRINT DATA=&ID.GAUSSIANPARMS; TITLE1 "&ID - Gaussian Parameters"; RUN;
*/
%MEND GAUSSIAN;
  %LET Data = Master; %LET ID = WholeCGain; %LET Trait = WholeTotalPhoto;
%GAUSSIAN;

```

D.3.2 Modeling rosette photosynthesis over time.

```

PROC SORT DATA=Master; BY Geno; RUN;
%MACRO GAUSSIAN;
PROC NLIN DATA=&Data Plots=Fit METHOD=Marquardt TOTALSS;
  where geno = "&ID";
  title1 "&ID";
  PARAMETERS ALPHA = 9.77 15 235 BETA = 56.79 70.59 GAMMA = 8.45 16 24
37.84 48;
  *PARAMETERS ALPHA = 0.5 1.5 3 5 10 15 20 50 75 100 BETA = 0.001 0.01
0.1 1 10 50 100 150 200 GAMMA = 0.001 0.01 0.5 0.75 1.5 3 5 15 25;
  MODEL &Trait = ALPHA * EXP( - ( 0.5 * ( ( AgeAtHarvest - BETA ) / GAMMA
)**2 ) );
  BY Geno;
  ODS OUTPUT ParameterEstimates=&ID.PARMS ANOVA=&ID.ANOVA;
RUN;
PROC PRINT DATA=&ID.PARMS; TITLE1 "&ID - Parameters"; RUN;
/* The following code calculates pseudo r-square for each model */
PROC SORT DATA=&ID.ANOVA; BY Source Geno; RUN;
DATA &ID.SSE; SET &ID.ANOVA; WHERE Source = "Error"; RENAME SS=SSE; KEEP Geno
SS; RUN;
DATA &ID.SSCT; SET &ID.ANOVA; WHERE Source = "Corrected Total"; RENAME
SS=SSCT; KEEP Geno SS; RUN;
DATA &ID.SSUCT; SET &ID.ANOVA; WHERE Source = "Uncorrected Total"; RENAME
SS=SSUCT; KEEP Geno SS; RUN;
PROC SORT DATA=&ID.SSE; BY Geno; RUN;
PROC SORT DATA=&ID.SSCT; BY Geno; RUN;
PROC SORT DATA=&ID.SSUCT; BY Geno; RUN;
DATA &ID.PSEUDORSQ; MERGE &ID.SSCT &ID.SSE &ID.SSUCT; BY Geno;
  CtPseudoRsqr = 1 - (SSE/SSCT);
  UnCtPseudoRsqr = 1 - (SSE/SSUCT);
RUN;
PROC PRINT DATA=&ID.PSEUDORSQ; TITLE1 "&ID - PseudoRsqr by Geno"; RUN;
%MEND GAUSSIAN;

%LET Data = Master; %LET ID = PIN9; %LET Trait = RoseTotalPhoto; %GAUSSIAN;
DATA Master; SET Master;
  if AgeAtHarvest = 98 and Geno = 'RAB17' then RoseTotalPhoto = .;
RUN;
%LET Data = Master; %LET ID = RAB17; %LET Trait = RoseTotalPhoto; %GAUSSIAN;

```

D.3.3 Modeling inflorescence photosynthesis over time.

```
PROC SORT DATA=Master; BY Geno; RUN;
%MACRO GAUSSIAN;
PROC NLIN DATA=&Data Plots=Fit METHOD=Gauss TOTALSS;
  where geno = "&ID";
  title1 "&ID";
  PARAMETERS ALPHA = 14.61 8 4 BETA = 135.24 175 194.8 GAMMA = 5.45 7 10
12 14 16 18 20 37.92;
  *PARAMETERS ALPHA = 0.5 1.5 3 5 10 15 20 50 75 100 BETA = 0.001 0.01
0.1 1 10 50 100 150 200 GAMMA = 0.001 0.01 0.5 0.75 1.5 3 5 15 25;
  MODEL &Trait = ALPHA * EXP( - ( 0.5 * ( ( AgeAtHarvest - BETA ) / GAMMA
)**2 ) );
  BY Geno;
  ODS OUTPUT ParameterEstimates=&ID.PARMS ANOVA=&ID.ANOVA;
RUN;
PROC PRINT DATA=&ID.PARMS; TITLE1 "&ID - Parameters"; RUN;
/* The following code calculates pseudo r-square for each model */
PROC SORT DATA=&ID.ANOVA; BY Source Geno; RUN;
DATA &ID.SSE; SET &ID.ANOVA; WHERE Source = "Error"; RENAME SS=SSE; KEEP Geno
SS; RUN;
DATA &ID.SSCT; SET &ID.ANOVA; WHERE Source = "Corrected Total"; RENAME
SS=SSCT; KEEP Geno SS; RUN;
DATA &ID.SSUCT; SET &ID.ANOVA; WHERE Source = "Uncorrected Total"; RENAME
SS=SSUCT; KEEP Geno SS; RUN;
PROC SORT DATA=&ID.SSE; BY Geno; RUN;
PROC SORT DATA=&ID.SSCT; BY Geno; RUN;
PROC SORT DATA=&ID.SSUCT; BY Geno; RUN;
DATA &ID.PSEUDORSQ; MERGE &ID.SSCT &ID.SSE &ID.SSUCT; BY Geno;
  CtPseudoRsq = 1 - (SSE/SSCT);
  UnCtPseudoRsq = 1 - (SSE/SSUCT);
RUN;
PROC PRINT DATA=&ID.PSEUDORSQ; TITLE1 "&ID - PseudoRsq by Geno"; RUN;
%MEND GAUSSIAN;

%LET Data = Master; %LET ID = HOR6; %LET Trait = InflorTotalPhoto; %GAUSSIAN;

PROC SORT DATA=Master; BY Geno; RUN;
%MACRO GAUSSIAN;
PROC NLIN DATA=&Data Plots=Fit METHOD=Gauss TOTALSS;
  where geno = "&ID";
  title1 "&ID";
  PARAMETERS ALPHA = 6 12 15 20 133.77 284.62 BETA = 194.36 194.51 GAMMA
= 5.41 10 15 20 22 24 26 ;
  *PARAMETERS ALPHA = 0.5 1.5 3 5 10 15 20 50 75 100 BETA = 0.001 0.01
0.1 1 10 50 100 150 200 GAMMA = 0.001 0.01 0.5 0.75 1.5 3 5 15 25;
  MODEL &Trait = ALPHA * EXP( - ( 0.5 * ( ( AgeAtHarvest - BETA ) / GAMMA
)**2 ) );
  BY Geno;
  ODS OUTPUT ParameterEstimates=&ID.PARMS ANOVA=&ID.ANOVA;
RUN;
PROC PRINT DATA=&ID.PARMS; TITLE1 "&ID - Parameters"; RUN;
/* The following code calculates pseudo r-square for each model */
PROC SORT DATA=&ID.ANOVA; BY Source Geno; RUN;
```

```

DATA &ID.SSE; SET &ID.ANOVA; WHERE Source = "Error"; RENAME SS=SSE; KEEP Geno
SS; RUN;
DATA &ID.SSCT; SET &ID.ANOVA; WHERE Source = "Corrected Total"; RENAME
SS=SSCT; KEEP Geno SS; RUN;
DATA &ID.SSUCT; SET &ID.ANOVA; WHERE Source = "Uncorrected Total"; RENAME
SS=SSUCT; KEEP Geno SS; RUN;
PROC SORT DATA=&ID.SSE; BY Geno; RUN;
PROC SORT DATA=&ID.SSCT; BY Geno; RUN;
PROC SORT DATA=&ID.SSUCT; BY Geno; RUN;
DATA &ID.PSEUDORSQ; MERGE &ID.SSCT &ID.SSE &ID.SSUCT; BY Geno;
    CtPseudoRsqr = 1 - (SSE/SSCT);
    UnCtPseudoRsqr = 1 - (SSE/SSUCT);
RUN;
PROC PRINT DATA=&ID.PSEUDORSQ; TITLE1 "&ID - PseudoRsqr by Geno"; RUN;
%MEND GAUSSIAN;
%LET Data = Master; %LET ID = PAN1; %LET Trait = InflorTotalPhoto; %GAUSSIAN;
%LET Data = Master; %LET ID = PAN5; %LET Trait = InflorTotalPhoto; %GAUSSIAN;

```

D.3.4 Principal component and all subsequent analyses.

```

PROC PRINCOMP DATA=GenoMeans PLOTS=All PREFIX = WholeEconPC OUTSTAT = PCStats
OUT = GenoMeanWholeEcon;
    TITLE1 'PCA of Whole Plant Economic Variables';
    VAR WholeFunctionalLifespan MaxTotMass MaxWholePhotoPerGram
MaxWholeTotalPhoto WholeCarbonGain;
RUN;
PROC PRINCOMP DATA=GenoMeans PLOTS=All PREFIX = RoseEconPC OUTSTAT = PCStats
OUT = GenoMeanRoseEcon;
    TITLE1 'PCA of Whole Plant Economic Variables';
    VAR RosetteLeafLifespan RosetteFunctionalLifespan MaxRoseMass
MaxRoseArea MaxTLN MaxRosePhotoPerGram MaxRoseTotalPhoto MaxRMA
RosePhotoAtBolting RMAAtBolting RoseCarbonGain MaxPropRose;
RUN;
PROC PRINCOMP DATA=GenoMeans PLOTS=All PREFIX = InflorEconPC OUTSTAT =
PCStats OUT = GenoMeanInflorEcon;
    TITLE1 'PCA of Whole Plant Economic Variables';
    VAR InflorFunctionalLifespan PostBoltWholeFunctionalLifespan
MaxInflorMass MaxBasalBranches MaxInflorPhotoPerGram MaxInflorTotalPhoto
MassPerLength InflorCarbonGain MaxPropInflor;
RUN;
DATA GenoMeans;
INPUT POP $ Genotype $ Elevation ClimatePC1 AgeAtBolting
RosetteLeafLifespan RosetteFunctionalLifespan InflorFunctionalLifespan
WholeFunctionalLifespan PostBoltRoseFunctionalLifespan
PostBoltRoseLeafLifespan PostBoltWholeFunctionalLifespan
PropLifePostBolt MaxBasalBranches MaxRoseMass MaxInflorMass
MaxTotMass RoseArea MaxRMA MaxTLN MaxWholePhotoPerGram
MaxWholeTotalPhoto MaxInflorPhotoPerGram MaxInflorTotalPhoto
MaxRosePhotoPerGram MaxRoseTotalPhoto WholeCarbonGain
RoseCarbonGain InflorCarbonGain PercentInflorContribution
MaxPropRose MaxPropInflor MassPerLength

```

RosePhotoPerGramAtBolting RMAAtBolting SummedFruitLength
 WholeEconPC1 WholeEconPC2 InflorEconPC1 InflorEconPC2
 RoseEconPC1 RoseEconPC2;

DATALINES;

ALE	ALE10	1163	2.31	115	221.5	176.444568	121.8	221.534612	61.4	106.5
		106.5	0.481	6	0.475	0.5865	1.246	21.47743336	0.023399799	60.5
		364.9792841	24.50162924	44.27816956	9.896727591	364.9792841	24.21382114			
		2927.081912	2160.910332	996.7850745	31.56685324	0.647912886	0.47070626			
		0.03775	16.40622439	0.01919453	560.2	0.680634228	-0.047336505			
		-1.57264092	-0.087180479		0.962361065	-0.767892161				
ALE	ALE12	1163	2.31	99.4	209.2	164.388224	119.9	206.669236	65	109.8
		107.3	0.519	10.5	0.369	0.7045	1.3255	21.51604583	0.020246281	
		50.5	312.9339765	30.3012046	96.97403925	15.06794915	312.9339765			
		20.7890443	2947.553526	1897.361146	1078.073567	36.23247259	0.654188948			
		0.560183257	0.033	26.08475909	0.016498154	450.6	0.411915533	1.278121839		
		0.308418176	-0.099334178		-0.44282047	-1.520598795				
ARB	ARB10	440	-2.19	92.3	218.6	173.901592	150.7	235.36928	81.6	126.3
		143.1	0.608	9	0.4365	1.0095	1.408	24.01054022	0.021927806	
		57	276.2424013	26.48486837	89.06150919	17.19059094	276.2424013			
		23.62205112	3475.908299	2101.405557	1568.161068	42.73423073	0.704610951			
		0.716974432	0.04275	38.75073796	0.015472558	541.2	2.327540724			
		1.232263211	2.525055406	2.013926885	0.67191018	-0.879917167				
ARB	ARB8	440	-2.19	78.6	142.9	120.787516	132.7	214.019784	42.2	64.3
		135.4	0.633	8.5	0.2775	0.692	1.055	24.9252161	0.018886306	46
		355.564831	21.96814167	95.19708446	15.31823955	355.564831	21.96814167			
		1998.797618	747.3389482	1363.483423	64.59489162	0.671383648	0.717880086			
		0.04175	33.73519972	0.014514967	778.9	-0.635016198	-			
		2.049192341	1.473322695	0.690462755	-2.232920594	0.373242779				
BAR	BAR4	340	-4.58	83.6	191.6	137.490956	126.3	217.896192	53.9	108
		134.3	0.616	19	0.3515	1.019	1.5115	24.29124271	0.022173966	
		49.5	372.1016968	22.93368496	80.17902906	13.57431314	372.1016968			
		22.93368496	2176.356202	1103.568802	1147.945554	50.98548678	0.668863262			
		0.710590137	0.05475	35.57654347	0.014992331	863.9	0.641584387	-		
		1.789640298	1.778537462	1.943884987	-1.106839446	0.157408385				
BAR	BAR9	340	-4.58	87.2	165.4	135.893588	138.3	195.881508	48.7	78.2
		108.7	0.555	17.5	0.3255	0.9615	1.404	29.0569261	0.019886607	
		51	328.8752034	26.59780133	52.57969559	10.28182207	328.8752034			
		26.59780133	2022.296009	1061.374583	993.9579441	48.35995786	0.654822335			
		0.687378641	0.0585	29.4671413	0.01625521	823.1	-0.338915609			
		-1.142550479	0.576299107	1.868558595	-0.877322614	1.242742732				
BIS	BIS11	1397	5.82	107.6	212.6	202.885452	110.4	224.57296	95.3	105
		117	0.521	6.5	0.4905	0.4795	1.447	24.35858053	0.026604825	
		67	400.6646334	25.33379077	21.1460246	9.2831048	400.6646334			
		24.08868765	3198.398141	2450.181785	748.2163556	23.39347144	0.767728674			
		0.424336283	0.04275	3.965336647	0.02271605	369.4	1.261570616			
		0.475744878	-2.51023873	-0.357468238	2.87067145	0.333697406				
BIS	BIS8	1397	5.82	117.2	194.5	192.589356	95.9	224.323428	75.4	77.3
		107.1	0.478	5.5	0.6	0.6075	1.433	22.88626236	0.027665676	67
		402.3590555	25.19113671	43.25175536	8.162715748	402.3590555	25.19113671			
		2958.123105	2420.781541	537.341564	18.16494936	0.73857868	0.439712389			
		0.0455	3.334771251	0.021639594	480.1	0.989960245	0.056672262	-		
		2.628956635	0.144367533	2.719621215	0.284732371					
BOS	BOS5	719	2.61	61.7	90.2	139.009528	105.4	158.250836	77.3	28.5
		96.6	0.61	17.5	0.201	0.5585	0.8145	17.66718193	0.017834737	
		29.5	389.44669	28.96866697	72.11695289	18.05040853	389.44669			
		25.35257912	2440.881401	800.112015	1671.860378	67.63264763	0.606557377			
		0.782212885	0.04125	144.5692822	0.012720079	725.8	-2.906121569			

		0.3984266	1.391736498	-1.567627633		-4.824189025		-	
0.153124347									
BOS	BOS6	719	2.61	59.6	107.9	104.10568	87.8	174.922488	44.5 48.3
		115.3	0.659	20.5	0.2775	0.6635	0.915	21.9375179	0.021978043
		34.5	254.0100616	29.36974102	43.04654602	25.28147499	254.0100616		
		26.97744827	2642.750958	817.6562006	1825.094757	69.06041418	0.652173913		
		0.766318538	0.04725	118.1659217	0.013004951	553	-1.287717718		
		0.783463793	1.885323864	-1.864263722		-3.393021923		-	
0.084114999									
COC	COC14	519	-3.28	82.3	185.4	168.312756	132	218.534172	86 103.1
		136.2	0.623	16	0.2315	0.8275	1.2215	20.92171626	
		0.020776808	45	415.4851783	28.3030419	72.34836527	21.50030124		
		415.4851783	24.35476502	3278.308086	1591.346579	1710.410914	51.80304481		
		0.625407166	0.70046729	0.03675	47.36641044	0.015031027	577.6		
		0.293526407	1.414086635	2.532706839	0.050496183	-1.680630385		-	
0.174728307									
COC	COC7	519	-3.28	69.6	143.9	134.211864	135.4	193.285836	64.6 74.3
		123.7	0.64	21	0.1985	0.616	0.8595	19.02062131	0.024308254
		37.5	366.4956044	26.96543354	83.33107545	13.78951146	366.4956044		
		23.71580169	2698.772399	1130.292959	1494.404514	56.9362576	0.672881356		
		0.716695753	0.027	112.8691335	0.012486253	900.8	-1.415250228		
		0.350496031	1.953441446	-0.608844279		-3.116966428		-	
0.478017956									
HOR	HOR16	351	-2.71	84.8	174.6	144.294948	142.1	224.387276	59.5 89.8
		139.6	0.622	18	0.3195	0.748	1.091	18.50756321	0.030687262 44
		380.3263601	23.74259922	120.5652468	13.59864146	380.3263601	21.59418423		
		2486.738434	1094.982347	1406.959455	56.23469954	0.630799605	0.685609533		
		0.0505	24.96046172	0.019376608	490	-0.107423773		-	
		0.857569275	2.249212209	1.296071815	-1.014733489		-1.199180677		
HOR	HOR6	351	-2.71	82.8	190.1	125.998004	127.6	145.592672	43.2 107.3
		62.8	0.431	23.5	0.265	0.8965	1.281	28.12712949	0.023124975 43
		493.7703676	26.23967134	97.97864721	16.41117567	493.7703676	24.72062823		
		2060.129543	798.1247794	1313.585533	62.20481688	0.671736375	0.711403097		
		0.0525	14.14534436	0.017765267	824.5	-2.766854554		-	
		1.129220941	1.514365653	0.061048601	-1.144269186		2.219344771		
MUR	MUR15	836	-2	117.1	192.2	181.198768	101.7	223.224032	64.1 75.1
		106.1	0.475	13.5	0.448	0.8035	1.4335	21.82003764	0.025954546
		62.5	374.9878567	23.55770919	54.83960386	11.75989648	374.9878567		
		23.55770919	2824.218569	2147.417233	676.8013357	23.96419821	0.765100671		
		0.615214507	0.06975	3.290052416	0.02075764	619.6	1.122729604		-
		0.538410419	-0.92416768	1.176022947	1.807262137	-0.072412069			
MUR	MUR17	836	-2	129.4	320.7	190.290908	97.8	226.63988	60.9 191.3
		97.2	0.429	3.5	0.4415	0.7665	1.423	22.46747574	0.022663426
		57	273.5168046	21.52790944	50.20160666	11.41397177	273.5168046		
		20.03794306	2816.899589	2178.814607	638.0849821	22.6520315	0.69591528		
		0.538650738	0.069	4.533850118	0.019162779	439.9	1.922156955		-
		1.003717756	-2.085253464		1.178550083	1.876305875	-2.211928449		
PAL	PAL12	1491	4.26	75.6	162.5	137.822248	145.9	206.762672	62.2 86.9
		131.2	0.634	10	0.256	0.9255	1.3645	20.20648945	0.019753388
		46.5	364.695492	25.03927392	60.86333789	18.20065892	364.695492		
		20.91673769	2677.892625	1183.793562	1604.476802	57.54380287	0.640625		
		0.68877551	0.08	61.41508238	0.013291809	787.9	0.356321439		-
		0.404053807	1.454960018	2.333580382	-2.578500809		-0.93289159		
PAL	PAL16	1491	4.26	109.8	208.3	149.665896	95.9	217.596032	39.9 98.5
		107.8	0.495	7	0.338	0.7395	1.29	21.40222877	0.025173519 68
		299.9152229	20.53738452	50.2809156	12.4890364	299.9152229	20.05531944		
		2485.46401	1542.314573	943.1494378	37.94661415	0.646271511	0.600247525		

		0.06575	10.13644215	0.01650948	495.8	0.963707589	-1.707221951			
		-1.179142101	0.793027609	-0.042908127			-1.866093174			
PAN	PAN1	1664	5.79	164.4	236.4	237.55538	40.6	246.823908	73.2	72
		82.4	0.334	1	0.533	0.5695	1.2805	26.35088841	0.025084558	
		77	352.1159649	31.4725813	25.03307085	11.01455117	352.1159649			
		31.4725813	2973.867184	2544.481372	445.4540049	14.89844925	0.72005772			
		0.460714286	0.059	2.075575548	0.021389632	386.4	0.96116011	1.631113378		
		-4.069424107	-0.930225338		3.822262984	1.060397957				
PAN	PAN5	1664	5.79	167.8	221.4	191.48362	37.3	235.403372	23.7	53.6
		67.6	0.287	6.5	0.55	0.579	1.5285	25.70546537	0.025898514	79.5
		290.7169038	30.82526935	34.64513682	19.70403575	290.7169038	30.82526935			
		3282.168192	2475.950756	806.2174357	24.56356252	0.725	0.416696654			
		0.0595	3.219285967	0.023981927	460.5	2.037500931	1.848336368	-		
		3.136321377	-2.081742751	3.704945543	0.596196028					
PIN	PIN6	109	-3.65	67.9	112.3	122.279148	152.6	149.517472	54.4	44.4
		81.6	0.546	24.5	0.234	0.836	1.1275	22.70107677	0.023207528	52
		328.9946245	31.62415019	40.31424659	21.51478881	328.9946245	21.98057118			
		2526.184811	1162.450394	1390.0049	54.45756105	0.666666667	0.773311897			
		0.044	79.09637254	0.011323553	762.1	-2.069357467	0.97743985			
		2.023874731	-0.509007438	-2.682820783	-0.450508705					
PIN	PIN9	109	-3.65	79.8	191.4	140.217464	116.3	207.677884	60.4	111.6
		127.9	0.616	9	0.373	0.7845	1.077	25.56849391	0.022649711	46.5
		385.1443434	25.1355436	85.49623843	13.76345711	385.1443434	25.1355436			
		1828.015567	879.7071494	1003.682394	53.29127993	0.739742087	0.728412256			
		0.0455	14.74103677	0.015431867	550.6	-1.310098143	-			
		1.615245134	0.793549326	0.962178167	-0.42424297	1.355202026				
POB	POB10	597	-2	106.6	207.7	178.525216	118.2	224.347156	71.9	101.1
		117.7	0.525	17	0.6635	0.7505	1.2815	26.47823553		
		0.030662797	66	457.2504763	27.72179441	42.99278587	13.1146442			
		457.2504763	27.72179441	2937.177191	2233.510962	720.1742425	24.38222738			
		0.71450858	0.585641826	0.035	10.33999033	0.020674803	492.2	0.0605723		
		0.686754698	-0.21900166	0.024058516	2.891660337	1.567606872				
POB	POB7	597	-2	121.1	265.2	195.908388	92.5	226.091076	74.8	144.1
		105	0.464	7.5	0.551	0.5875	1.176	23.69597265	0.033921023	70
		358.8361296	26.8625015	97.52084372	8.694564632	358.8361296	26.8625015			
		2704.559967	2116.071319	588.4886482	21.75912737	0.682648402	0.49957483			
		0.0375	9.847786505	0.021636162	596.2	0.249744798	0.174488291	-		
		1.538134461	-0.089399291	3.208274331	-0.330713347					
RAB	RAB17	110	-4.48	62.4	133.7	73.3536	84.7	185.44138	11	71.3
		123	0.664	20	0.163	0.675	0.9315	15.36437	0.017299275	28
		491.8907887	22.83966743	61.56129917	27.73749725	491.8907887	19.92987656			
		2566.986557	739.266821	1821.688731	71.13316472	0.636363636	0.769156159			
		0.02675	113.3665534	0.00830416	622	-1.962838022	-			
		0.871070231	2.57042713	-2.460583249	-5.848256221	-0.258954338				
RAB	RAB4	110	-4.48	59.9	137	78.557612	94.3	177.881944	18.7	77.1
		118	0.663	29	0.238	0.5055	0.726	21.14482844	0.02197675	20.5
		410.4473307	32.76387645	89.44058866	24.84123338	410.4473307	25.60862935			
		2769.457904	944.4835492	1824.974355	65.89644682	0.639175258	0.706293706			
		0.013333333	65.30003226	0.011617622	528.4	-2.765617443	1.869118759			
		2.902049896	-3.372142195	-3.924496267	0.911416545					
SPE	SPE5	332	-2.92	107.9	180.1	176.184676	68.8	206.973156	68.3	72.2
		99.1	0.479	20.5	0.2955	0.8295	1.247	27.41917384	0.02760195	
		62.5	424.7167107	26.74689886	55.59257168	13.00640453	424.7167107			
		26.74689886	2947.710476	2025.819096	921.8913797	31.27482795	0.680399501			
		0.681594084	0.0345	10.929846	0.019494964	663.6	-0.168696106			
		0.493214993	0.027547403	-0.865080355	1.085001004	1.248936232				
SPE	SPE6	332	-2.92	86.8	198.7	132.080608	104.5	201.147848	45.3	111.9

```

114.3 0.568 6.5 0.3615 0.6245 1.074 31.15789367 0.022158428
48.5 465.9937942 29.93563516 68.51056517 16.96597282 465.9937942
29.93563516 2568.139512 1110.436523 1459.104557 56.7846363 0.729695432
0.639006663 0.0595 16.46441757 0.017701684 962.4 -1.608039773
0.698065416 0.031643117 -0.003893534 0.219831593 3.578581865
VDM VDM17 912 1.29 116.4 242.6 198.16764 110.7 223.353288 81.8 126.2
107 0.479 7.5 0.468 0.6725 1.3125 26.49568824 0.02625134
62 309.9206287 26.62136233 61.9877679 7.344030022 309.9206287
26.62136233 2975.559784 2538.734511 521.4385758 17.0395125 0.684491979
0.609700816 0.03575 21.34932243 0.020807522 572.4 1.104198037
0.489345884 -1.317183954 0.429886752 2.479374715 -0.211474883
VDM VDM9 912 1.29 120.7 235.9 197.872496 97.8 226.261808 77.2 115.2
105.6 0.467 6.5 0.412 0.68 1.413 27.1027713 0.029731621 64
364.8483843 26.86883105 25.16121458 9.286472824 364.8483843 26.86883105
2910.339574 2461.620986 448.7185879 15.41808358 0.599690881 0.481245577
0.04275 23.48431345 0.016652222 482.4 1.03039432 0.380533734 -
2.503768388 0.153412623 1.625941937 -0.17816265
VIE VIE3 1538 5.73 121.5 243.8 199.629088 90.5 227.406448 78.1 122.3
105.9 0.466 6.5 0.4705 0.5895 1.2445 26.10742837
0.031134095 65 290.4658186 21.66608605 61.85205217 10.57254847
290.4658186 21.66608605 2990.223374 2398.354197 595.9117778 19.90176501
0.708211144 0.473684211 0.05025 13.79415537 0.024256089 446.4
1.533108498 -0.589217723 -2.159546198 -0.009788936
3.082795317 -1.30596515
VIE VIE6 1538 5.73 116.3 204.6 199.243584 89.9 223.890412 82.9 88.3
107.6 0.481 9 0.416 0.682 1.4025 22.60308588 0.033290952 68.5
274.3725513 22.05803402 18.60366697 13.33882922 274.3725513 22.05803402
2437.268719 2096.791128 573.9071021 21.48902844 0.685459941 0.494202899
0.049 9.800809141 0.0222126 445.2 1.393619879 -1.493239762 -
2.1486913 -0.212952819 2.306719053 -1.852827208

```

```

;
RUN;

/* CORRELATION MATRIX */
ODS OUTPUT PearsonCorr=Correlations;
PROC CORR DATA=GenoMeans plots=all;
    TITLE1 'Correlation Matrix';
    VAR SummedFruitLength AgeAtBolting WholeEconPC1 InflorEconPC1
RoseEconPC1;
RUN;
PROC PRINT DATA=Correlations; RUN;

/* STANDARDIZE GENOMEANS DATASET */
proc standard
    data=GenoMeans
    out=StdGenoMeans
    mean=0 std=1;
    VAR SummedFruitLength AgeAtBolting PostBoltRoseFunctionalLifespan
PercentInflorContribution MassPerLength RosePhotoPerGramAtBolting
RMAAtBolting WholeEconPC1 InflorEconPC1 RoseEconPC1;
run;
proc print data=StdGenoMeans; title1 "Standardized Dataset"; run;

/* STANDARDIZE POP MEANS DATASET */
proc standard
    data=PopMeans
    out=StdPopMeans

```

```

        mean=0 std=1;
        VAR ClimatePC1      SummedFruitLength AgeAtBolting
PostBoltRoseFunctionalLifespan PercentInflorContribution      MassPerLength
RosePhotoPerGramAtBolting RMAAtBolting WholeEconPC1 InflorEconPC1
RoseEconPC1;
run;
proc print data=StdPopMeans; title1 "Standardized Dataset"; run;

/* SPECIFIC AIM 2: ROSETTE AND WHOLE PLANT CONTRIBUTION TO WHOLE PLANT
ECONOMY */
PROC REG DATA=StdGenoMeans PLOTS=All;
        TITLE1 'Std Whole = Rose + Inflor';
        MODEL WholeEconPC1 = RoseEconPC1 InflorEconPC1;
RUN;
PROC REG DATA=StdGenoMeans PLOTS=All;
        TITLE1 'Std Whole = Rose';
        MODEL WholeEconPC1 = RoseEconPC1;
RUN;
PROC REG DATA=StdGenoMeans PLOTS=All;
        TITLE1 'Std Whole = Inflor';
        MODEL WholeEconPC1 = InflorEconPC1;
RUN;

/* SPECIFIC AIM 3: ECONOMY PREDICTED BY BOLTING AGE? */
PROC REG DATA=GenoMeans PLOTS=All;
        TITLE1 'Rose = AgeAtBolting';
        MODEL RoseEconPC1 = AgeAtBolting;
RUN;
PROC REG DATA=GenoMeans PLOTS=All;
        TITLE1 'Inflor = AgeAtBolting';
        MODEL InflorEconPC1 = AgeAtBolting;
RUN;
PROC REG DATA=GenoMeans PLOTS=All;
        TITLE1 'Whole = AgeAtBolting';
        MODEL WholeEconPC1 = AgeAtBolting;
RUN;
PROC PRINCOMP DATA=GenoMeans PLOTS=All PREFIX = PC1;
        TITLE1 'AgeAtBolting, Whole, Rose and Inflor Economies are highly
integrated';
        VAR WholeEconPC1 RoseEconPC1 InflorEconPC1 AgeAtBolting;
RUN;

/* SPECIFIC AIM 4: ECONOMY VS. CLIMATE */
PROC REG DATA=PopMeans Outest=TraitsvsClimate TABLEOUT RSQUARE;
        TITLE1 "Traits vs Climate";
        MODEL SummedFruitLength AgeAtBolting WholeEconPC1 InflorEconPC1
RoseEconPC1 = ClimatePC1;
RUN;

/* SPECIFIC AIM 5: FITNESS VS. ECONOMY */
PROC REG DATA=StdGenoMeans PLOTS=All Outest=SelectionAnalysis TABLEOUT
RSQUARE;
        TITLE1 'STD Fitness = WholeEconPC1';
        MODEL SummedFruitLength = WholeEconPC1;
RUN;

```

```

PROC PRINT DATA=SELECTIONANALYSIS; RUN;
PROC REG DATA=StdGenoMeans PLOTS=All Outest=SelectionAnalysis TABLEOUT
RSQUARE;
    TITLE1 'STD Fitness = RoseEconPC1';
    MODEL SummedFruitLength = RoseEconPC1;
RUN;
PROC PRINT DATA=SELECTIONANALYSIS; RUN;
PROC REG DATA=StdGenoMeans PLOTS=All Outest=SelectionAnalysis TABLEOUT
RSQUARE;
    TITLE1 'STD Fitness = InflorEconPC1';
    MODEL SummedFruitLength = InflorEconPC1;
RUN;
PROC PRINT DATA=SELECTIONANALYSIS; RUN;
PROC REG DATA=StdGenoMeans PLOTS=All Outest=SelectionAnalysis TABLEOUT
RSQUARE;
    TITLE1 'STD Fitness = AgeAtBolting';
    MODEL SummedFruitLength = AgeAtBolting;
RUN;
PROC PRINT DATA=SELECTIONANALYSIS; RUN;
PROC REG DATA=StdGenoMeans PLOTS=All Outest=SelectionAnalysis TABLEOUT
RSQUARE;
    TITLE1 'STD Fitness = RoseEconPC1 + InflorEconPC1';
    MODEL SummedFruitLength = RoseEconPC1 InflorEconPC1;
RUN;
PROC PRINT DATA=SELECTIONANALYSIS; RUN;
PROC REG DATA=StdGenoMeans PLOTS=All Outest=SelectionAnalysis TABLEOUT
RSQUARE;
    TITLE1 'STD Fitness = RoseEconPC1 + InflorEconPC1 + AgeAtBolting';
    MODEL SummedFruitLength = RoseEconPC1 InflorEconPC1 AgeAtBolting;
RUN;
PROC PRINT DATA=SELECTIONANALYSIS; RUN;

```

BIBLIOGRAPHY

- Ackerly DD. 2003.** Community Assembly, Niche Conservatism, and Adaptive Evolution in Changing Environments. *International Journal of Plant Sciences* **164**: S165–S184.
- Agren J, Schemske DW. 2012.** Reciprocal transplants demonstrate strong adaptive differentiation of the model organism *Arabidopsis thaliana* in its native range. *The New Phytologist* **194**: 1112–22.
- Alonso-Blanco C, Blankestijn-de Vries H, Hanhart CJ, Koornneef M. 1999.** Natural allelic variation at seed size loci in relation to other life history traits of *Arabidopsis thaliana*. *Proceedings of the National Academy of Sciences of the United States of America* **96**: 4710–7.
- Anderson JT, Panetta AM, Mitchell-Olds T. 2012.** Evolutionary and ecological responses to anthropogenic climate change: update on anthropogenic climate change. *Plant Physiology* **160**: 1728–40.
- Anderson JT, Willis JH, Mitchell-Olds T. 2011.** Evolutionary genetics of plant adaptation. *Trends in Genetics* **27**.
- Antonovics J. 1976.** The Nature of Limits to Natural Selection. *Annals of the Missouri Botanical Garden* **63**: 224–247.
- Arntz M, Delph L. 2001.** Pattern and process: evidence for the evolution of photosynthetic traits in natural populations. *Oecologia* **127**: 455–467.
- Aschan G, Pfanz H, Vodnik D, Batič F. 2005.** Photosynthetic performance of vegetative and reproductive structures of green hellebore (*Helleborus viridis* L. agg.). *Photosynthetica* **43**: 55–64.
- Atkin OK, Loveys BR, Atkinson LJ, Pons TL. 2006.** Phenotypic plasticity and growth temperature: understanding interspecific variability. *Journal of Experimental Botany* **57**: 267–81.
- Atwell S, Huang YS, Vilhjálmsson BJ, Willems G, Horton M, Li Y, Meng D, Platt A, Tarone AM, Hu TT, et al. 2010.** Genome-wide association study of 107 phenotypes in *Arabidopsis thaliana* inbred lines. *Nature* **465**: 627–31.

- Baker NR. 2008.** Chlorophyll fluorescence: a probe of photosynthesis in vivo. *Annual Review of Plant Biology* **59**: 89–113.
- Balazadeh S, Parlitz S, Mueller-Roeber B, Meyer RC. 2008.** Natural developmental variations in leaf and plant senescence in *Arabidopsis thaliana*. *Plant Biology* **10 Suppl 1**: 136–47.
- Bennett EJ, Roberts J a, Wagstaff C. 2011.** The role of the pod in seed development: strategies for manipulating yield. *The New phytologist* **190**: 838–53.
- Blonder B, Violle C, Bentley LP, Enquist BJ. 2011.** Venation networks and the origin of the leaf economics spectrum. *Ecology letters* **14**: 91–100.
- Bloom A, Chapin F, Mooney H. 1985.** RESOURCE LIMITATION IN PLANTS-AN ECONOMIC ANALOGY. *Annual review of Ecology and ...* **16**: 363–92.
- Blows M, Hoffmann A. 2005.** A reassessment of genetic limits to evolutionary change. *Ecology* **86**: 1371–1384.
- Bolle C, Schneider a, Leister D. 2011.** Perspectives on Systematic Analyses of Gene Function in *Arabidopsis thaliana*: New Tools, Topics and Trends. *Current genomics* **12**: 1–14.
- Bonser S, Aarssen L. 1996.** Meristem allocation: a new classification theory for adaptive strategies in herbaceous plants. *Oikos* **77**: 347–352.
- Bonser SP, Aarssen LW. 2001.** Allometry and plasticity of meristem allocation throughout development in *Arabidopsis thaliana*. *Journal of Ecology* **89**: 72–79.
- Bonser SP, Aarssen LW. 2006.** Meristem allocation and life-history evolution in herbaceous plants. *Botany* **84**: 143–150.
- Bradshaw WE, Holzapfel CM, Crowder R. 2006.** Evolutionary Response to Rapid Climate Change. *Science* **312**: 1477–1478.
- Caicedo AL, Stinchcombe JR, Olsen KM, Schmitt J, Purugganan MD. 2004.** Epistatic interaction between *Arabidopsis* FRI and FLC flowering time genes generates a latitudinal cline in a life history trait. *Proceedings of the National Academy of Sciences of the United States of America* **101**: 15670–5.
- Chabot BF, Hicks DJ. 1982.** The Ecology of Leaf Life Spans. *Annual Review of Ecology and Systematics* **13**: 229–259.
- Chase JM, Leibold MA. 2003.** *Ecological niches: linking classical and contemporary approaches.*
- Chaves M, Pereira J, Maroco J, Rodrigues M, Ricardo C, Osorio M, Carvalho I, Faria T, Pinheiro C. 2002.** How plants cope with water stress in the field? Photosynthesis and growth. *Annals of Botany* **89**: 907.

- Clausen J, Keck DD HW. 1940.** *Experimental studies on the nature of species. I. Effect of varied environment on Western North American plants.* Washington, D.C.: Carnegie Institution of Washington.
- Cohen D. 1976.** The Optimal Timing of Reproduction. *American Naturalist* **110**: 801–807.
- Cornelissen JHC, Lavorel S, Garnier E, Díaz S, Buchmann N, Gurvich DE, Reich PB, Steege H Ter, Morgan HD, Heijden MG a. Van Der, et al. 2003.** A handbook of protocols for standardised and easy measurement of plant functional traits worldwide. *Australian Journal of Botany* **51**: 335.
- Cornwell WK, Cornelissen JHC, Amatangelo K, Dorrepaal E, Eviner VT, Godoy O, Hobbie SE, Hoorens B, Kurokawa H, Pérez-Harguindeguy N, et al. 2008.** Plant species traits are the predominant control on litter decomposition rates within biomes worldwide. *Ecology letters* **11**: 1065–71.
- Cronin JP, Tonsor SJ, Carson WP. 2010.** A simultaneous test of trophic interaction models: which vegetation characteristic explains herbivore control over plant community mass? *Ecology letters* **13**: 202–12.
- Diemer M, Korner C. 1996.** Lifetime Leaf Carbon Balances of Herbaceous Perennial Plants from Low and High Altitudes in the Central Alps. *Functional Ecology* **10**: 33.
- Donohue K. 2005.** Niche construction through phenological plasticity: life history dynamics and ecological consequences. *The New phytologist* **166**: 83–92.
- Donohue K, Dorn L, Griffith C, Kim E, Aguilera A, Polisetty CR, Schmitt J. 2005.** The evolutionary ecology of seed germination of *Arabidopsis thaliana*: variable natural selection on germination timing. *Evolution; international journal of organic evolution* **59**: 758–70.
- Donovan L a., Maherali H, Caruso CM, Huber H, de Kroon H. 2011.** The evolution of the worldwide leaf economics spectrum. *Trends in Ecology & Evolution* **26**.
- Earley EJ, Ingle B, Winkler J, Tonsor SJ. 2009.** Inflorescences contribute more than rosettes to lifetime carbon gain in *Arabidopsis thaliana* (Brassicaceae). *American Journal of Botany* **96**: 786–792.
- Endler JA. 1986.** *Natural Selection in the Wild.* Princeton: Princeton University Press.
- Farnsworth EJ, Ellison AM. 2007.** Prey availability directly affects physiology, growth, nutrient allocation and scaling relationships among leaf traits in 10 carnivorous plant species. *Journal of Ecology*: 071106211313002–???
- Farquhar GD, Sharkey TD. 1982.** Stomatal Conductance and Photosynthesis. *Annual Review of Plant Physiology* **33**: 317–345.

- Feder ME. 2007.** Evolvability of physiological and biochemical traits: evolutionary mechanisms including and beyond single-nucleotide mutation. *The Journal of Experimental Biology* **210**: 1653–60.
- Feder M, Mitchell-Olds T. 2003.** Evolutionary and ecological functional genomics. *Nature Reviews Genetics* **100**: 101–2.
- Fournier-Level A, Korte A, Cooper MD, Nordborg M, Schmitt J, Wilczek a. M. 2011.** A Map of Local Adaptation in *Arabidopsis thaliana*. *Science* **334**: 86–89.
- Fournier-Level A, Wilczek AM, Cooper MD, Roe JL, Anderson J, Eaton D, Moyers BT, Petipas RH, Schaeffer RN, Pieper B, et al. 2013.** Paths to selection on life history loci in different natural environments across the native range of *Arabidopsis thaliana*. *Molecular Ecology*: n/a–n/a.
- Freschet G, Cornelissen JHC, van Logtestijn RSP, Aerts R. 2010.** Evidence of the “plant economics spectrum” in a subarctic flora. *Journal of Ecology* **98**: 362–373.
- Gammelvind LH, Schjoerring JK, Mogensen VO, Jensen CR, Bock JGH. 1996.** Photosynthesis in leaves and siliques of winter oilseed rape (*Brassica napus* L.). *Hydrobiologia* **186**: 227–236.
- Geber MA. 1990.** The Cost of Meristem Limitation in *Polygonum arenastrum*: Negative Genetic Correlations between Fecundity and Growth. *Evolution* **44**: 799–819.
- Geiger R. 1950.** *The Climate Near the Ground*. Cambridge, MA.: Harvard University Press.
- Griffith TM, Watson M a. 2005.** Stress avoidance in a common annual: reproductive timing is important for local adaptation and geographic distribution. *Journal of Evolutionary Biology* **18**: 1601–12.
- Grillo M a, Li C, Hammond M, Wang L, Schemske DW. 2013.** Genetic architecture of flowering time differentiation between locally adapted populations of *Arabidopsis thaliana*. *The New Phytologist* **197**: 1321–31.
- Grime J. 1977.** Evidence for the Existence of Three Primary Strategies in Plants and Its Relevance to Ecological and Evolutionary Theory. *The American Naturalist* **111**: 1169–1194.
- Hannah M a, Wiese D, Freund S, Fiehn O, Heyer AG, Hinch DK. 2006.** Natural genetic variation of freezing tolerance in *Arabidopsis*. *Plant Physiology* **142**: 98–112.
- Havaux M. 1992.** Stress Tolerance of Photosystem II in Vivo: Antagonistic Effects of Water, Heat, and Photoinhibition Stresses. *Plant Physiology* **100**: 424–32.
- Heberling JM, Fridley JD. 2012.** Biogeographic constraints on the world-wide leaf economics spectrum. *Global Ecology and Biogeography* **21**: 1137–1146.

- Hereford J. 2009.** A quantitative survey of local adaptation and fitness trade-offs. *The American naturalist* **173**: 579–88.
- Heschel MS, Riginos C. 2005.** MECHANISMS OF SELECTION FOR DROUGHT STRESS TOLERANCE AND AVOIDANCE IN *IMPATIENS CAPENSIS* (BALSAMINACEAE). *American Journal of Botany* **92**: 37.
- Hijmans RJ, Cameron SE, Parra JL, Jones PG, Jarvis A. 2005.** Very high resolution interpolated climate surfaces for global land areas. *International Journal of Climatology* **25**: 1965–1978.
- Hoffmann MH. 2002.** Biogeography of *Arabidopsis thaliana* (L.) Heynh. (Brassicaceae). *Journal of Biogeography* **29**: 125–134.
- Hoffmann MH. 2005.** Evolution of the realized climatic niche in the genus *Arabidopsis* (Brassicaceae). *Evolution* **59**: 1425–36.
- Hoffmann A a, Sgrò CM. 2011.** Climate change and evolutionary adaptation. *Nature* **470**: 479–85.
- Hopkins R, Schmitt J, Stinchcombe JR. 2008.** A latitudinal cline and response to vernalization in leaf angle and morphology in *Arabidopsis thaliana* (Brassicaceae). *The New Phytologist* **179**: 155–64.
- Hörtensteiner S, Feller U. 2002.** Nitrogen metabolism and remobilization during senescence. *Journal of experimental botany* **53**: 927–37.
- Hudson ME. 2008.** Sequencing breakthroughs for genomic ecology and evolutionary biology. *Molecular ecology resources* **8**: 3–17.
- Hutchinson GE. 1957.** Concluding Remarks. *Population Studies: Animal Ecology and Demography. Cold Spring Harbor Symposia on Quantitative Biology* **22**: 415–427.
- Jagtap V. 1998.** Comparative effect of water, heat and light stresses on photosynthetic reactions in *Sorghum bicolor*(L.) Moench. *Journal of Experimental Botany* **49**: 1715–1721.
- Kalisz S, Teeri JA. 1986.** POPULATION-LEVEL VARIATION IN PHOTOSYNTHETIC METABOLISM AND GROWTH IN *SEDUM-WRIGHTII*. *Ecology* **67**: 20–26.
- Kawecki TJ, Ebert D. 2004.** Conceptual issues in local adaptation. *Ecology Letters* **7**: 1225–1241.
- Kirkpatrick M, Barton NH. 1997.** Evolution of a species' range. *The American naturalist* **150**: 1–23.
- Korves TM, Schmid KJ, Caicedo AL, Mays C, Stinchcombe JR, Purugganan MD, Schmitt J. 2007.** Fitness effects associated with the major flowering time gene *FRIGIDA* in *Arabidopsis thaliana* in the field. *The American naturalist* **169**: E141–57.

- Kronholm I, Picó FX, Alonso-Blanco C, Goudet J, de Meaux J. 2012.** Genetic basis of adaptation in *Arabidopsis thaliana*: local adaptation at the seed dormancy QTL DOG1. *Evolution* **66**: 2287–302.
- Lake J. 2004.** Gas exchange: new challenges with *Arabidopsis*. *New Phytologist* **162**: 1–3.
- Lande R, Arnold SJ. 1983.** The Measurement of Selection on Correlated Characters. *Evolution* **37**: 1210–1226.
- Leimu R, Fischer M. 2008.** A meta-analysis of local adaptation in plants. *PLoS One* **3**: e4010.
- Lempe J, Balasubramanian S, Sureshkumar S, Singh A, Schmid M, Weigel D. 2005.** Diversity of flowering responses in wild *Arabidopsis thaliana* strains. *PLoS Genetics* **1**: 109–18.
- Levey S, Wingler a. 2005.** Natural variation in the regulation of leaf senescence and relation to other traits in *Arabidopsis*. *Plant, Cell and Environment* **28**: 223–231.
- Li B, Suzuki JI, Hara T. 1998.** Latitudinal variation in plant size and relative growth rate in *Arabidopsis thaliana*. *Oecologia* **115**: 293–301.
- Lim PO, Kim HJ, Nam HG. 2007.** Leaf senescence. *Annual review of plant biology* **58**: 115–36.
- Linhart YB, Grant MC. 1996.** Evolutionary Significance of Local Genetic Differentiation in Plants. *Annual Review of Ecology and Systematics* **27**: 237–277.
- Lusk CH, Reich PB, Montgomery R a, Ackerly DD, Cavender-Bares J. 2008.** Why are evergreen leaves so contrary about shade? *Trends in ecology & evolution* **23**: 299–303.
- MacColl ADC. 2011.** The ecological causes of evolution. *Trends in ecology & evolution* **26**: 514–22.
- Martin RE, Asner GP, Sack L. 2007.** Genetic variation in leaf pigment, optical and photosynthetic function among diverse phenotypes of *Metrosideros polymorpha* grown in a common garden. *Oecologia* **151**: 387–400.
- Masclaux-Daubresse C, Chardon F. 2011.** Exploring nitrogen remobilization for seed filling using natural variation in *Arabidopsis thaliana*. *Journal of experimental botany* **62**: 2131–42.
- Mauricio R, Rausher M. 1997.** Experimental Manipulation of Putative Selective Agents Provides Evidence for the Role of Natural Enemies in the Evolution of Plant Defense. *Evolution* **51**: 1435–1444.
- Mayr E. 1947.** Ecological Factors in Speciation. *Evolution* **1**: 263–288.

- McKay JK, Richards JH, Mitchell-Olds T. 2003.** Genetics of drought adaptation in *Arabidopsis thaliana*: I. Pleiotropy contributes to genetic correlations among ecological traits. *Molecular Ecology* **12**: 1137–51.
- Metcalf CJE, Mitchell-Olds T. 2009.** Life history in a model system: opening the black box with *Arabidopsis thaliana*. *Ecology letters* **12**: 593–600.
- Mitchell-Olds T. 2001.** *Arabidopsis thaliana* and its wild relatives: a model system for ecology and evolution. *Trends in Ecology & Evolution* **16**: 693–700.
- Mitchell-Olds T, Feder M, Wray G. 2008.** Evolutionary and ecological functional genomics. *Heredity* **100**: 101–2.
- Mitchell-olds T, Schmitt J. 2006.** Genetic mechanisms and evolutionary significance of natural variation in *Arabidopsis*. *Nature* **441**: 947–952.
- Mitchell-Olds T, Shaw RG. 1987.** Regression Analysis of Natural Selection: Statistical Inference and Biological Interpretation. *Evolution* **41**: 1149–1161.
- Montesinos A, Tonsor SJ, Alonso-Blanco C, Picó FX. 2009.** Demographic and genetic patterns of variation among populations of *Arabidopsis thaliana* from contrasting native environments. *PLoS One* **4**: e7213.
- Montesinos-Navarro A, Wig J, Xavier Pico F, Tonsor SJ. 2011.** *Arabidopsis thaliana* populations show clinal variation in a climatic gradient associated with altitude. *New Phytologist*: no–no.
- Montesinos-Navarro A, Picó F, Tonsor S. 2012.** Clinal variation in seed traits influencing life cycle timing in *Arabidopsis thaliana*. *Evolution*: 1–15.
- Murren CJ. 2002.** Phenotypic integration in plants. *Plant Species Biology* **17**: 89–99.
- Noordwijk A Van, Jong G De. 1986.** Acquisition and Allocation of Resources : Their Influence on Variation in Life History Tactics. *American Naturalist* **128**: 137–142.
- Parmesan C. 2006.** Ecological and Evolutionary Responses to Recent Climate Change. *Annual Review of Ecology, Evolution, and Systematics* **37**: 637–669.
- Paul JR, Morton C, Taylor CM, Tonsor SJ. 2009.** Evolutionary time for dispersal limits the extent but not the occupancy of species' potential ranges in the tropical plant genus *Psychotria* (Rubiaceae). *The American naturalist* **173**: 188–99.
- Pensa M, Karu H, Luud A, Kund K. 2009.** Within-species correlations in leaf traits of three boreal plant species along a latitudinal gradient. *Plant Ecology* **208**: 155–166.
- Penuelas J, Sardans J, Llusà J, Owen SM, Carnicer J, Giambelluca TW, Rezende EL, Waite M, Niinemets Ü. 2009.** Faster returns on “leaf economics” and different

- biogeochemical niche in invasive compared with native plant species. *Global Change Biology* **16**: 2171–2185.
- Peres-Neto P, Jackson D, Somers K. 2003.** Giving Meaningful Interpretation to Ordination Axes: Assessing Loading Significance in Principal Component Analysis. *Ecology* **84**: 2347–2363.
- Petrů M, Tielbörger K, Belkin R. 2006.** Life history variation in an annual plant under two opposing environmental constraints along an aridity gradient. *Ecography* **0**: 1–9.
- Phillips PC, Arnold SJ. 1999.** Hierarchical Comparison of Genetic Variance-Covariance Matrices. I. Using the Flury Hierarchy. *Evolution* **53**: 1506.
- Picó FX. 2012.** Demographic fate of *Arabidopsis thaliana* cohorts of autumn- and spring-germinated plants along an altitudinal gradient. *Journal of Ecology* **100**: 1009–1018.
- Pico FX, Méndez-Vigo B, Martínez-Zapater JM, Alonso-Blanco C. 2008.** Natural genetic variation of *Arabidopsis thaliana* is geographically structured in the Iberian peninsula. *Genetics* **180**: 1009.
- Pigliucci M. 2003.** Phenotypic integration: studying the ecology and evolution of complex phenotypes. *Ecology Letters* **6**: 265–272.
- Poorter H, Remkes C. 1990.** Leaf area ratio and net assimilation rate of 24 wild species differing in relative growth rate. *Oecologia* **83**: 553–559.
- Reich P, Ellsworth D, Walters M. 1999.** Generality of leaf trait relationships: a test across six biomes. *Ecology* **80**: 1955–1969.
- Reich PB, Wright IJ, Lusk CH. 2007.** Predicting leaf physiology from simple plant and climate attributes: a global GLOPNET analysis. *Ecological applications: a publication of the Ecological Society of America* **17**: 1982–8.
- SAS Institute Inc. 2011.** *Base SAS 9.3 Procedures Guide*. Cary, NC.
- Saura-Mas S, Shipley B, Lloret F. 2009.** Relationship between post-fire regeneration and leaf economics spectrum in Mediterranean woody species. *Functional Ecology* **23**: 103–110.
- Scarcelli N, Cheverud JM, Schaal B a, Kover PX. 2007.** Antagonistic pleiotropic effects reduce the potential adaptive value of the FRIGIDA locus. *Proceedings of the National Academy of Sciences of the United States of America* **104**: 16986–91.
- Scarcelli N, Kover PX. 2009.** Standing genetic variation in FRIGIDA mediates experimental evolution of flowering time in *Arabidopsis*. *Molecular ecology* **18**: 2039–49.
- Schluter D. 1996.** Adaptive Radiation Along Genetic Lines of Least Resistance. *Evolution* **50**: 1766.

- Sexton JP, McIntyre PJ, Angert AL, Rice KJ. 2009.** Evolution and Ecology of Species Range Limits. *Annual Review of Ecology, Evolution, and Systematics* **40**: 415–436.
- Shaw RG, Geyer CJ. 2010.** Inferring fitness landscapes. *Evolution* **64**: 2510–20.
- Shipley B. 2006.** Net assimilation rate, specific leaf area and leaf mass ratio: which is most closely correlated with relative growth rate? A meta-analysis. *Functional Ecology* **20**: 565–574.
- Shipley B, Lechowicz MJ, Wright I, Reich PB. 2006a.** Fundamental trade-offs generating the worldwide leaf economics spectrum. *Ecology* **87**: 535–41.
- Shipley B, Vile D, Garnier E. 2006b.** From plant traits to plant communities: a statistical mechanistic approach to biodiversity. *Science (New York, N.Y.)* **314**: 812–4.
- Smith J, Burian R, Kauffman S. 1985.** Developmental Constraints and Evolution: A Perspective from the Mountain Lake Conference on Development and Evolution. *Quarterly Review of ...* **60**: 265–287.
- Stearns SC. 1989.** Trade-offs in life-history evolution. *Functional ecology* **3**: 259–268.
- Stearns S, Magwene P. 2003.** The Naturalist in a World of Genomics. *The American Naturalist* **161**: 171–180.
- Stenoien HK, Fenster CB, Kuittinen H, Savolainen O. 2002.** Quantifying latitudinal clines to light responses in natural populations of *Arabidopsis thaliana* (Brassicaceae). *American Journal of Botany* **89**: 1604.
- Stinchcombe JR, Weing C, Ungerer M, Olsen KM, Mays C, Halldorsdottir SS, Purugganan MD, Schmitt J. 2004.** A latitudinal cline in flowering time in *Arabidopsis thaliana* modulated by the flowering time gene FRIGIDA. *Proceedings of the National Academy of Sciences of the United States of America* **101**: 4712–7.
- Straalen N Van, Roelofs D. 2006.** *An introduction to Ecological Genomics*. New York: Oxford University Press, USA.
- Tienderen P Van, Hammad I, Zwaal F. 1996.** Pleiotropic effects of flowering time genes in the annual crucifer *Arabidopsis thaliana* (Brassicaceae). *American journal of botany* **83**: 169–174.
- Tonsor SJ, Alonso-Blanco C, Koornneef M. 2005.** Gene function beyond the single trait: natural variation, gene effects, and evolutionary ecology in *Arabidopsis thaliana*. *Plant, Cell and Environment* **28**: 2–20.
- Tonsor SJ, Elnaccash TW, Scheiner SM. 2013.** Developmental Instability Is Genetically Correlated With Phenotypic Plasticity, Constraining Heritability, and Fitness. *Evolution*.

- Tonsor SJ, Scheiner SM. 2007.** Plastic trait integration across a CO₂ gradient in *Arabidopsis thaliana*. *The American naturalist* **169**: E119–40.
- Tonsor SJ, Scott C, Boumaza I, Liss TR, Brodsky JL, Vierling E. 2008.** Heat shock protein 101 effects in *A. thaliana*: genetic variation, fitness and pleiotropy in controlled temperature conditions. *Molecular Ecology* **17**: 1614–26.
- Ungerer MC, Johnson LC, Herman M a. 2008.** Ecological genomics: understanding gene and genome function in the natural environment. *Heredity* **100**: 178–83.
- Vasseur F, Violle C, Enquist BJ, Granier C, Vile D, Maherali H. 2012.** A common genetic basis to the origin of the leaf economics spectrum and metabolic scaling allometry. *Ecology letters* **15**: 1149–57.
- Vile D, Garnier E, Shipley B, Laurent G, Navas M-L, Roumet C, Lavorel S, Díaz S, Hodgson JG, Lloret F, et al. 2005.** Specific leaf area and dry matter content estimate thickness in laminar leaves. *Annals of botany* **96**: 1129–36.
- Visser ME. 2008.** Keeping up with a warming world; assessing the rate of adaptation to climate change. *Proceedings. Biological sciences / The Royal Society* **275**: 649–59.
- Wade MJ, Kalisz S. 1990.** The Causes of Natural Selection. *Evolution* **44**: 1947–1955.
- Wahid a, Gelani S, Ashraf M, Foolad M. 2007.** Heat tolerance in plants: An overview. *Environmental and Experimental Botany* **61**: 199–223.
- Watson DJ. 1958.** The dependence of net assimilation rate on leaf-area index. *Annals of Botany* **22**: 37–54.
- Watson M, Casper B. 1984.** Morphogenetic constraints on patterns of carbon distribution in plants. *Annual Review of Ecology and Systematics* **15**: 233–258.
- Weiner J. 2004.** Allocation, plasticity and allometry in plants. *Perspectives in Plant Ecology, Evolution and Systematics* **6**: 207–215.
- Westoby M, Wright IJ. 2006.** Land-plant ecology on the basis of functional traits. *Trends in ecology & evolution (Personal edition)* **21**: 261–8.
- Wilczek AM, Roe JL, Knapp MC, Cooper MD, Lopez-Gallego C, Martin LJ, Muir CD, Sim S, Walker A, Anderson J, et al. 2009.** Effects of genetic perturbation on seasonal life history plasticity. *Science* **323**: 930–4.
- Wright IJ, Reich PB, Cornelissen JHC, Falster DS, Garnier E, Hikosaka K, Lamont BB, Lee W, Oleksyn J, Osada N, et al. 2005a.** Assessing the generality of global leaf trait relationships. *The New phytologist* **166**: 485–96.

- Wright IJ, Reich PB, Cornelissen JHC, Falster DS, Groom PK, Hikosaka K, Lee W, Lusk CH, Niinemets Ü, Oleksyn J, et al. 2005b.** Modulation of leaf economic traits and trait relationships by climate. *Global Ecology and Biogeography* **14**: 411–421.
- Wright IJ, Reich PB, Westoby M, Ackerly DD, Baruch Z, Bongers F, Cavender-Bares J, Chapin T, Cornelissen JHC, Diemer M, et al. 2004.** The worldwide leaf economics spectrum. *Nature* **428**: 821–7.
- Wright JP, Sutton-Grier A. 2012.** Does the leaf economic spectrum hold within local species pools across varying environmental conditions? (C Stevens, Ed.). *Functional Ecology* **26**: 1390–1398.
- Zhen Y, Ungerer MC. 2008.** Clinal variation in freezing tolerance among natural accessions of *Arabidopsis thaliana*. *The New Phytologist* **177**: 419–27.
- Zhu C, Gore M, Buckler ES, Yu J. 2008.** Status and Prospects of Association Mapping in Plants. *The Plant Genome Journal* **1**: 5.